INFLUENCE OF WAVE CLIMATE SCHEMATISATION ON THE SIMULATED MORPHOLOGICAL DEVELOPMENT OF THE WESTERN SCHELDT ENTRANCE

ARCADIS & DELFT UNIVERSITY OF TECHNOLOGY

MSC THESIS B.W.F. VAN RIJN

15 August 2012
- Final

INFLUENCE OF WAVE CLIMATE SCHEMATISATION ON THE SIMULATED MORPHOLOGICAL DEVELOPMENT OF THE WESTERN SCHELDT ENTRANCE

THESIS
Submitted to acquire the degree of MASTER OF SCIENCE
To be presented in public
on Wednesday, 22 August 2012 at 16:00 hours
at Delft University of Technology, Delft, The Netherlands

by

Bart Wilhelmus Franciscus van Rijn

Delft University of Technology
Faculty of Civil Engineering and Geosciences
Department of Civil Engineering

Student number 1272071

This thesis has been approved by the supervisors:

Dr. ir. G. Ph. van Vledder
Dr. ir. B.T. Grasmeijer

Members of the thesis committee:

Prof. dr. ir. M.J.F. Stive	Chairman, TU Delft, section of coastal engineering
Dr. ir. G. Ph. van Vledder	Supervisor, TU Delft, section of fluid mechanics
Dr. ir. B.T. Grasmeijer	Supervisor, ARCADIS, section coastal and marine systems
Ir. M. Eelkema	TU Delft, section of coastal engineering
Ir. J. van Overeem	TU Delft / ARCADIS, section of coastal engineering
Prof. dr. ir. H.H.G. Savenije	TU Delft, section of water resource management

Cover image: entrance of the Western Scheldt towards the North Sea. On the right, the contours of Vlissingen and its water defence. To the left the water defence near Breskens and a ship entering the estuary on its way to Antwerpen. Calm wind conditions: 2 Bft, significant wave height 0.2 m

‘cause my friend, how do you roll
where do you come from and where do you go…
…you've been weathering the storm
and it's been blowing hard

boy and bear – the storm

Contents

Abstract

To quantify interventions in the system of the Western Scheldt estuary (The Netherlands), numerical morphological models of the estuary have been and are being developed. The physical processes of hydrodynamics and morphodynamics in the estuary are highly complex. This holds especially for the entrance, where the estuary has an open connection to the North Sea. Numerical models are applied to approximate these processes. For practical application of these models, input of forcing conditions (tides, winds, waves) needs to be reduced, c.q. schematised. This thesis investigates the influence of the way the wave climate is schematised on the simulated morphological development. This is done on the scale of the shoals and ebb and flood channels in the entrance of the Western Scheldt during a period of one year.

In the entrance of the estuary (defined as the area between Vlissingen and Terneuzen), wave conditions are dominated by local wind conditions rather than by wave conditions at the North Sea. This is caused by the presence of the ebb tidal delta in front of the entrance. The dominancy of the wind conditions on the wave conditions increases further into the estuary. At Terneuzen, the influence of wave conditions at the North Sea is almost completely disappeared. Waves influence the simulated morphology by eroding shoals edges and by depositing sediment in the adjacent channels. Waves have the most influence at relative shallow areas where also tidal currents are present. Sediment stirred up by waves is subsequently transported by these currents. Wave breaking at these locations also result in an increase of the local velocity of the current. At these areas, patterns of sedimentation and erosion due to tidal currents are partly enhanced and partly shifted under the influence of waves. These shallow areas are in particular the shoals of Spijkerplaat and the shoals south of the Everingen flood channel.

The way the wave climate is schematised influences the simulated morphological development on the considered time and spatial up to 20% to 25%. This means that the simulated local bottom change (referred to as sedimentation and erosion pattern) due to currents and waves can deviate 20% to 25% between simulations which are based on different wave climate schematisations. The amount of wind and wave classes within the climate schematisation has the most influence on the simulated morphology. Other influences within the schematisation are subordinate to the influence of the amount of classes. When ten classes are included in the schematisation, the simulated pattern of sedimentation and erosion deviates 3% to 7% of the benchmark simulation. When five classes are included in the schematisation, this deviation is 4% to 8%. When one class is included in the schematisation, this deviation is around 20% to 25%. The range in deviation is caused by other influences within the climate schematisation, such as the quantity (bottom change or sediment transport) and considered location on which the schematisation is based. The deviations occur mainly at the locations where waves have the most influence; i.e. the shoals of Spijkerplaat and the shoals south of the Everingen flood channel.

Including a storm event within the wave climate schematisation, has limited influence on the considered time and spatial scale. On the short time scale of the event itself, the impact of a storm on the morphology can be significant, but does not result in irreversible changes in the morphology. On the time scale of one year, the influence of the storm is to a large extent redone by more occurring, moderate conditions.

For the simulation of the morphological development in the entrance of the Western Scheldt at the considered time and spatial scale, it is recommended to apply a wave climate schematisation of five wind and wave classes at most. The schematisation should be based on the reproduction of the bottom changes in the estuary, seasonality and storm event don’t need to be taken into account.

Samenvatting

Om ingrepen in het systeem van het Westerschelde estuarium (Nederland) te kunnen kwantificeren, zijn numerieke morfologische modellen van het estuarium ontwikkeld en in ontwikkeling. De fysieke processen van de hydro- en morfodynamica in het estuarium zijn zeer complex. Dit geldt zeker voor de monding, waar het estuarium een open verbinding met de Noordzee heeft. Numerieke modellen worden toegepast om deze processen te benaderen. Voor praktische toepassing van deze modellen moeten de opgelegde randvoorwaarden (getij, wind, golven) worden gereduceerd, c.q. geschematiseerd. Deze scriptie onderzoekt de invloed van de wijze waarop het golfklimaat wordt geschematiseerd op de gesimuleerde morfologische ontwikkeling. Dit is gedaan op een ruimteschaal van de platen en eb- en vloedgeulen in de monding van de Westerschelde en een tijdschaal van één jaar.

In de monding van het estuarium (gedefinieerd als het gebied tussen Vlissingen en Terneuzen) zijn de golfcondities gedomineerd door lokale windcondities, niet zozeer door de golfcondities op de Noordzee. Dit wordt veroorzaakt door de aanwezigheid van de buitendelta voor de monding. De dominantie van de windcondities op de golfcondities neemt verderop in het estuarium toe. Bij Terneuzen is de invloed van de golfcondities op de Noordzee bijna geheel verdwenen. Golven beïnvloeden de gesimuleerde morfologie door het eroderen van de plaatranden en het sedimenteren van naastgelegen geulen. Golven hebben de grootste invloed in de laaggelegen gebieden waar ook getij gedreven stromingen aanwezig zijn. Door golven opgewoeld sediment wordt getransporteerd door deze stromingen. Het breken van golven op deze locatie zorgt ook voor een lokale toename van de stroomsnelheid. Bij deze gebieden worden de patronen van sedimentatie en erosie als gevolg van de stroming deels versterkt en verschoven onder de invloed van golven. Deze gebieden zijn met name de Spijkerplaat en platen ten zuiden van de Everingen vloedgeul.

De manier waarop het golfklimaat wordt geschematiseerd beïnvloed de gesimuleerde morfologische ontwikkeling op de beschouwde tijd en ruimteschaal met 20% tot 25%. Dit betekent dat de gesimuleerde lokale bodem veranderingen 20% tot 25% kunnen verschillen als gevolg van verschillende schematisaties van het golfklimaat. De hoeveelheid wind en golfklassen in een geschematiseerd klimaat heeft de meeste invloed op de gesimuleerde morfologie. Andere invloeden binnen de schematisatie zijn ondergeschikt. Wanneer tien klassen zijn opgenomen in de schematisatie kunnen de gesimuleerde patronen van sedimentatie en erosie 3% tot 7% afwijken van de referentie simulatie, bij vijf klassen is deze afwijking 4% tot 8%. Wanneer één klasse is opgenomen ligt de afwijking rond 20% tot 25%. De bandbreedte in afwijking wordt veroorzaakt door andere invloeden binnen de schematisatie van het klimaat, zoals de grootheid (bodemverandering of sediment transport) en beschouwd gebied waarop de schematisatie is gebaseerd. De afwijkingen komen voornamelijk voor op de locaties waar golven de meeste invloed hebben.

Het meenemen van een storm in de schematisatie van het golfklimaat heeft beperkte invloed op de beschouwde tijd en ruimteschaal. Tijdens de storm zelf is de invloed op de morfologie significant, maar leidt niet tot onomkeerbare veranderingen in de morfologie. Op de tijdschaal van één jaar is de invloed van de storm tenietgedaan door vaker voorkomende, gematigde condities.

Voor de simulatie van de morfologische ontwikkeling in de monding van de Westerscheld op de beschouwde tijd en ruimteschaal wordt het aanbevolen een schematisatie van het golfklimaat met maximaal vijf wind en golfklassen toe te passen. De schematisatie moet worden gebaseerd op de reproductie van de bodemveranderingen in het estuarium. Het is niet nodig storm en seizoensinvloeden mee te nemen.

Preface

This MSc thesis investigates and describes the influence of the way the wave climate is schematised on the simulated morphological development in the entrance of the Western Scheldt. The need for this research stems from the need to predict human interventions in this natural system and base decisions on those predictions. The natural environment of the entrance of the Western Scheldt is however a complex environment in terms of bathymetry, occurring currents, wind and wave conditions. To obtain a better understanding of such an environment is however not only useful in terms of decision making. It is, in my opinion, above all fascinating to understand these elements of nature. It is fascinating to understand wind and wave environments, how they come about and what their influence is on the ocean and on the coastline. It is interesting to understand the origin of a coast and to know what the driving forces behind coastal development are. When working in such an environment, awareness of the natural system in terms of its origin and present forces of nature are therefore essential.

The objective and ambition of this thesis are in line with my personal interest in winds and waves and their impact on the coastline. It was therefore a pleasure to work on this thesis. Some of the photos in this thesis I made myself; it are those with the flat water surface. I prefer storm waves and swell, but calm seas can be nice as well, occasionally.

Bart van Rijn

Anna Paulowna, 15 August 2012

Acknowledgements

With this thesis, a period of seven years is completed. I followed my education to master of science in part time, next to my profession as a coastal engineer. It has been seven very interesting years. Sometimes long years, but always interesting. Within those seven years, I met a lot of different, often also interesting, people, from Hoorn to Sydney. I like to thank many people from those seven years and the years before that.

First of all, I like to thank my parents, Wim and Els van Rijn, my brother Jeroen and his wife Annemarie for their support and patience during these seven years and the many years before. I like to thank my friends, who kept curious but also helped me to keep perspective on important things in life. There's probably a bet on whether or not I'll succeed. I thank the family Van Duin for their support and curiosity as well. I like to thank my colleagues at ARCADIS. Thanks to them I was able to follow this education next to my profession (and thanks for bringing me coffee). Dimitri van Meir, thank you for the years that we worked together at TU Delft.

I like to thank Gerbrant van Vledder and Bart Grasmeijer for their support during this thesis. Also thanks to the other members in the committee. I know now that there's always more to know. Bart, thanks for your time and enthusiasm. Gerbrant, thanks for your enthusiasm and readiness to share knowledge.

Almost finally I thank Ellen. Thank you, for your endless support, patience, understanding and not understanding. Thank you Noortje, for your smile.

Thanks.

Bart

1 Introduction

1.1 BACKGROUND

As part of the project on the long term vision on the Scheldt estuary (*Dutch:* Lange termijnvisie Schelde-estuarium), morphological models have been developed in the recent past. The final objective within that project was to develop one or more operational morphological models. In potential, these models can be used to address and judge interventions within the natural system of the Scheldt estuary. This especially holds for interventions with possible influence on the three main functions of the Scheldt estuary; accessibility, safety and the natural state. Currently (2012), within the framework of the project Safety and Accessibility Western Scheldt, the morphological model of the Western Scheldt is being further developed.

Need for schematisation of the wave climate

Within the developed morphological models, hydrodynamic (motion of water, i.e. currents and waves) and morphodynamic processes (the interaction between morphology and hydrodynamics) are included. In a tidal estuary, here the Western Scheldt, these processes are highly complex. Simulation of this complexity requires a numerical model which is based on these processes. The application of all relevant physical processes within the numerical model results in relative long run times of the simulation of these processes. Because of constraints on computational capacity, the amount of imposed forcing conditions (tides, wind and waves) needs to be reduced in some way in order to maintain a reasonable run time of the simulations. Simulations based on full time series of water levels, wind and waves (i.e. non-reduced forces) for all hydrodynamic and morphodynamic processes would be too time consuming in a large area as the Western Scheldt from a practical point of view. This especially holds when multiple years of morphological development are considered. The reduction of the imposed forces can be obtained by schematising the forces. With schematisation is meant here the selection of certain conditions (e.g. water levels, wind, waves) to represent all conditions within an certain range of accuracy. This thesis focusses on the schematisation of the wave climate and the influence of the way this climate is schematised on the simulated morphological development. This new understanding supports the further development of the morphological model of the Western Scheldt.

Previous studies

In 2004 and 2006, research was done on the applicability and shortcomings of the morphological model of the Western Scheldt. From these studies followed to the recommendation to investigate the influence of the wave climate schematisation.

Study 2004

Kuijper et al. (2004) set up a morphological model of the Western Scheldt and calibrated the model on morphological changes over the period 1998 up to and including 2002. Based on that research, a number of recommendations on the improvements on the model were stated. One of these recommendations refers to the wave climate that was used in the project.

In the morphological model (set-up in the Delft3D numerical model, (Deltares, formerly WL | Delft Hydraulics)), the influence of wind driven waves is taken into account. Waves are calculated with the SWAN wave model (SWAN, Delft University of Technology). Based on the influence of wind driven waves, one representative wind and wave class was derived, which was assumed to result in more or less the same initial bottom change (sedimentation and erosion pattern) as the full wind and wave climate (within which 52 wind and wave classes are distinguished). This one wind and wave condition was derived with the method of correlation, where the correlation of the results of the individual classes is compared to the result of all conditions combined. The individual class with the highest correlation was selected as the one representative wind and wave class. However, a larger amount of wind and wave classes, in general, results in a better reproduction of the morphological development of the full wind and wave climate. This one wind and wave condition was used in conjunction with a morphological acceleration factor. With this factor, morphodynamic processes are up-scaled. The reason for this upscaling is the difference in time scale on which the hydrodynamics act (seconds to hours) and the time scale on which the morphodynamics act (months to years). By upscaling, the results of the hydrodynamics on the morphology are multiplied by the acceleration factor to apply for the longer time scale of the morphodynamics. This upscaling reduces the runtime of a morphological simulation on medium-term time scale considerably. Because of the use of the morphological acceleration factor, it was considered to be difficult to make simulations with more than one wind and wave condition. Consequently, variations in wind and wave conditions were not taken into account. The used wind and wave class is presented in Table 1.

Wind speed (m/s)	Wind direction (°N)	Wave height (H_s) (m)	Wave period (T_p) (s)	Wave direction (°N)
6.8	258	0.9	5.0	263

Table 1. Representative wind and wave class in the 2004 research (Kuijper et al., 2004).

Furthermore, Van der Kaaij et al. (2004) assumed that the input of wave action on the morphology of the Western Scheldt is limited compared to the influence of the tide. Based on this assumption and given the extra effort to include more wind and wave conditions, it was decided to use only one wind and wave class. At the end of the study, it was recommended to further investigate the influence of a wind and wave climate with more included wind and wave classes. This recommendation was based on the insight that a schematisation of the climate with more wind and wave classes can result in a better approximation of the simulated morphological development based on the full climate. This especially holds for the entrance of the Western Scheldt (defined as the area of the Western Scheldt between Vlissingen and Terneuzen), where the relative influence of waves on the morphology is assumed to be larger than further on in the estuary.

The wave conditions as presented in Table 1 are indicated as the morphological wave. According to Kuijper et al. (2006), the calculated wave height reduces further on in the estuary. Due to this, the influence of waves on the transport of sediment in the channels is assumed to be ‘limited’ or absent. On the tidal flats some influence is expected. Finally, it was recommended to further investigate the influence of a more extensive wave climate, in which also the influence of set up (wind driven surge) should be taken into account. It was expected that more severe conditions can be important for the morphology of the tidal flat areas. This holds specifically for the ebb tidal delta and the western part of the Western Scheldt. For the remaining (vast) parts of the estuary, it was assumed that influence of waves is less important compared to influence of currents.

Study 2006

In a more recent research by Kuijper et al. (2006), the model as it was set up in 2004, was further calibrated. In the 2006 study however, the same wind and wave conditions were used as in the study of 2004. The recommendation from the 2004 study to take a more extensive climate into account was not yet followed. In the 2006 study, it was stated that wind driven waves have a relative large influence on the bottom change in the entrance of the Western Scheldt. Furthermore, it was stated that the used wind and wave climate (Table 1) is probably too much schematised to reproduce the real influence of wind and waves. Analysis of simulations shows that waves possibly contribute to the steepening of the cross shore profiles and consequently influence the hypsometric curves (the ratio between wet and dry area as a function of the tidal phase) and the patterns of sedimentation and erosion. It is expected that especially waves during storm conditions can have a large influence on the morphological development. That influence was not explicitly taken into account in the schematisation of the wind and wave conditions. Based on the executed analysis, Kuijper et al. (2006) recommended to investigate the influence of the schematisation of the wave climate on the predicted morphological development.

Study 2012

Currently (2012), within the framework of the project Safety and Accessibility Western Scheldt, the morphological model of the Western Scheldt is being further developed. Within this project the need to investigate the influence of the wave climate schematisation on the simulated morphology occurred. This need stems from the recommendations made in the earlier studies in 2004 and 2006. This thesis contributes to the 2012 study by investigating the influence of the wave climate schematisation on the simulated morphological development.

1.2 PROBLEM AND OBJECTIVE

Based on the before given background, the problem is defined as "the deficit in knowledge of the influence of the wave climate schematisation on predicted medium-term[1] morphological development of the entrance of the Western Scheldt". This stated problem is formulated into a main question and two underlying questions to be answered by this thesis:

Main question

> What is the influence of the way the wave climate is schematised on the predicted medium-term morphological development of the entrance of the Western Scheldt estuary on the scale of shoals and channels.

Underlying questions

> 1. In what manner is the wave climate to be schematised to realistically and efficiently reproduce the total morphological development by the full wave climate:
> 2. To which extent is the influence of waves during storm events taken into account.

The objective of this thesis is to answer the main question and underlying questions. This results in reasoned answers, based on theory, model simulations and analysis of the results of these simulations. With this new knowledge, conclusions can be made on the predictability of the existing morphological model of the Western Scheldt entrance with regards to the influence of waves on the morphological development. Furthermore, the model might be improved by applying a new wave climate schematisation based on the new knowledge. The approach to reach this objective is described in section 1.4.

---

[1] Here, with medium-term, a time period of several months to several years is meant. In this study, one year of morphological development is considered.

It is emphasized that it is not the objective of this study to *calibrate* the morphological model for the influence of waves on the morphological development. The model as applied in this study is run with values for the calibration factors as applied in previous and current studies (Kuijper et al. (2004, 2006) and Grasmeijer (2012)). To address the influence of the way the wave climate is schematised, the different simulations are therefore compared to benchmark *simulations*, not with measurements. For future morphological simulations with a certain wave climate schematisation, further calibration is recommended.

1.3 HYPOTHESES

Based on the studies as described in section 1.1 and the main and underlying questions stated in the previous section, a number of hypotheses are formulated. These hypotheses are used to verify whether certain hydrodynamic processes (section 4.4) and morphological development (sections 5.3 and 6.3) are explainable and expected. In chapter 7, these hypotheses are verified.

1. When waves propagate from the North Sea towards the entrance of the Western Scheldt, a large amount of wave energy is dissipated over the ebb tidal delta. As a result, inside the estuary the wave conditions are mainly locally influenced and the influence of the imposed wave conditions strongly decreases inside the estuary. It is therefore expected that a classification of wave conditions per class of wind speed and wind direction is more useful than to classify wave conditions per wave height bin and wave direction bin.
2. The quality of the reproduction of the morphological development by a schematised wind and wave climate depends on the amount of wind and wave classes within the schematised climate. An increase in the amount of classes results in more variability in wind, wave and surge conditions, which all can have a different morphological impact. Increasing the amount of classes therefore improves the reproduction of the morphological development by the full wind and wave climate.
3. Wind and wave conditions from a westerly direction are expected to have more influence on the morphological development than conditions from a easterly direction. Waves at the North Sea can grow higher and longer compared to waves inside the estuary. Although a lot of the wave energy from westerly directed waves is dissipated over the ebb tidal delta, still some influence is noticeable. Furthermore, wind and wave conditions from a south western direction contributes most to the wind and wave climate.
4. Storms (high wind speeds) have a large influence on the morphological development. This holds specifically for the ebb tidal delta and the western part of the Western Scheldt. High wind speeds result in higher waves and set-up or set-down of the water level. Due to this, waves are expected to break violently at different locations compared to lower waves under milder conditions. Next, since the waves are larger, the wave driven currents are larger as well. Due to the higher water level (during high water and storm surge), waves can travel further into the estuary, where the impact will be larger compared to the situation with lower water levels.
5. Influence of waves on sediment transport and morphology mainly focusses at the edges of shoals (ebb tidal delta, shoals of Spijkerplaat, shoals south of Everingen), since here the highest orbital velocities and wave driven currents occur. At locations where both waves and (tidal) currents are present, the morphological impact is expected to be the highest. There are several places where both waves and currents occur, especially at the shoals of Spijkerplaat and the shoals of Everingen. Due to the influence of waves at the edges, waves contribute to the steepening of the cross shore profiles and consequently influence the hypsometric curves.

1.4 APPROACH AND THESIS STRUCTURE

To address the hypotheses and research questions stated in section 1.2, three traces are followed:

1. Schematisation of the wave climate:
2. Physics of waves at the Western Scheldt entrance:
3. Quantification of influence wave climate schematisation.

Traces 1 and 2 are two independent traces. The two traces combined support the third and final trace. This final trace results in answering the research questions and the confirmation or falsification of the hypotheses. Figure 1. Overview of the three traces within the thesis approach. gives an overview of the traces and included components.

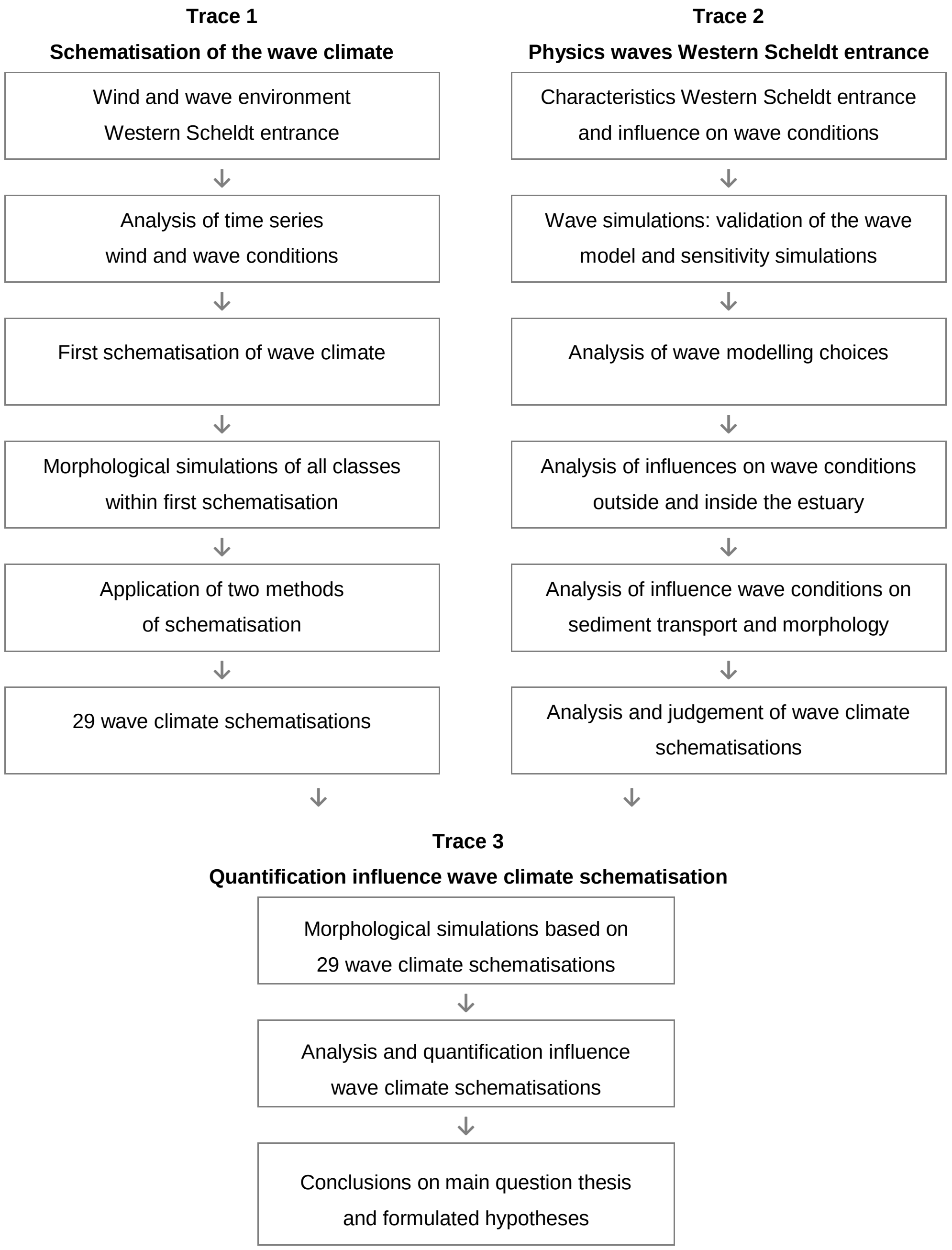

Figure 1. Overview of the three traces within the thesis approach.

1. *Schematisation of the wave climate*

The objective of this trace if to come to founded wave climate schematisations. For the schematisation of wave climate, the Western Scheldt entrance is first described in terms of general wind, wave and tidal environment. For a period of twenty years (1 January 1981 – 1 January 2001), a time series of wind, wave and surge conditions are available. Based on this time series, wave conditions are classified in classes of wind direction and wind speed, thus resulting in a first schematisation of the wave climate. This schematisation hence consists of multiple classes of wind and wave conditions.

A morphological simulation based on this first schematisation takes too much time as a result of the large amount of wind and wave classes [2]. Consequently, the wind and wave climate needs to be reduced to a smaller amount of classes in order to limit the run time of the simulation. This reduction of input is performed by use of two different methods: the so-called optimum method and the method of correlation. To apply these two methods of input reduction, relative short morphological simulations are performed for all classes of the first schematisation of the full wind and wave climate. These morphological simulations are performed with the Delft3D numerical model. The results of these short simulations are input for the mentioned methods.

To investigate the influence of the way the wave climate is schematised (the research question for this thesis), the first schematisation is further reduced in different ways. The way the schematisations differ regards to the amount of remaining classes within a schematisation (15, 10, 5 or 1 class remaining), the quantity on which the schematisation is based (sediment transport or bottom change), the considered area (ebb tidal delta, estuary or whole area), including seasonality and storm event within the schematisation and the method of schematisation. This finally results in 29 different schematisations of the wind and wave climate.

2. *Physics of the waves at the Western Scheldt entrance*

The objective of this trace is to obtain understanding of the physics of the waves in the system and hence be able to review and explain the obtained schematisations of the wave climate by the first trace. The understanding of the physics of the waves regards to propagation, transformation and influence of imposed wind and wave conditions on the wave conditions at the Western Scheldt entrance. Next, the influence of waves on sediment transport and the morphological development is considered.

To obtain understanding in the physics of waves within the Western Scheldt entrance, the Western Scheldt entrance is classified in terms of “tide over wave” influence and is characterised in terms of shape, presence of shallow areas (shoals) and channels. Next, the influence of these characteristics on the physics of the waves is described in a qualitative manner.

To address the quality of the simulated wave conditions within the morphological simulations, the wave model is validated. For this validation, wave simulations are performed for a time period of 14 days. A sensitivity analysis is performed to address the influence of modelling choices. The results of the simulations are compared by measurements at seven locations outside and inside the entrance of the Western Scheldt and described in terms of statistical parameters. Besides the validation, the wave simulations are used to obtain further understanding of the wave physics in the Western Scheldt entrance and to describe these in a quantitative manner. For this, a sensitivity analysis is performed to address the different influences on the wave conditions.

The relative short morphological simulations (as performed for the methods of input reduction) are used to describe the influence of currents and waves on the transport of sediment and the morphological development. Also these simulations are used to obtain understanding of the physics of waves in the Western Scheldt entrance.

---

[2] Depending on choices within the modelling, the simulation based on the first schematisation of the full time series is expected to take a few months up to one year.

3. Quantify influence of wave climate schematisation

The objective of this trace is to answer the research questions for this thesis. After the construction and review of the 29 wave climate schematisations, morphological simulations are performed. These simulations are based on the different wave climate schematisations. Besides these simulations, also simulations are performed without an imposed wave climate. By comparing the simulations with and without imposed wave climates, the influence of the way the wave climate is schematised can be placed in perspective with the general influence of waves.

The considered period of time within the morphological simulations is 1 January 1998 till 1 January 1999, which is one year of morphological development. The reason for this is that the numerical model used for the overall project to which this thesis contributes is calibrated for the time period 1 January 1998 – 1 January 2002, hence including the time period 1 January 1998 – 1 January 1999 (Grasmeijer [3], personal communication).

To quantify the influence of the way the wave climate is schematised, a distinction is made on:

- the influence of the amount of classes:
- the influence of the method of schematisation:
- the influence of the type of the target on which the schematisation is based:
- the influence of the location of the target on which the schematisation is based and location:
- the influence of seasonality and storm event.

The results of the different morphological simulations are compared to benchmark simulations and are compared with each other. The simulations are compared in terms of statistical parameters and physical parameters (patterns of sedimentation and erosion, cross sections, volume changes in ebb and flood channels and hypsometric curves). Based on these results, conclusions are stated on the influence of the way the wave climate is schematised.

[3] Dr. ir. B.T. Grasmeijer is one of the supervisors for this MSc thesis and works at ARCADIS, section Coastal and Marine systems.

Thesis structure

In **chapter 2 (Entrance of the Western Scheldt)**, the entrance of the Western Scheldt is described in a general way. This chapter serves as background information for the schematisation of the wave climate and the understanding of the physics of the waves in the Western Scheldt entrance (the first and second trace within the thesis approach). The general wind, wave and tidal environment is described, together with the characteristics of the system and the influence of these characteristics on the hydro- and morphodynamics. In **chapter 3 (General modelling approach)**, the general modelling approach is briefly described. Also the applied numerical model and the way the hydrodynamic and morphodynamic processes are implemented are briefly described. This chapter serves as background information for the first and second trace of the thesis approach. **Chapter 4 (Wind and wave climate and wave modelling)** serves the first and second trace of the thesis approach. It gives an extensive description of the wind and wave climate at the Western Scheldt entrance and a first schematisation of the wave climate. This first schematisation forms the base for present further schematisation of the wave climate in chapter 5. Wave simulations are performed to validate the wave model and obtain further understanding of the physics of the waves in this area. **Chapter 5 (Schematisation of the wind and wave climate)** also serves the first and second trace of the thesis approach. First, it describes the result of the short morphological simulations of all defined wave classes. These results are the input for the methods of climate schematisation and are used to obtain understanding of the wave physics in the area. Next, the two applied methods of schematisation are described, together with the constructed wave climate schematisations. **Chapter 6 (Modelling of the morphological development)** serves the third and last trace of the thesis approach. First, the results of the benchmark simulations are described. Second, the results of the simulations based on the different wave climate schematisations are described. These are compared to the benchmark simulations and with each other. The comparison is described in terms of statistical and physical parameters. Conclusions on the influence of the way the wave climate is schematised are presented. In **chapter 7 (Final conclusions and recommendations)**, the research questions and hypotheses for this thesis are answered. Recommendations are made on the wave climate schematisation to be used in morphological simulations and on future modelling approach.

2 Entrance of the Western Scheldt

2.1 INTRODUCTION

The Western Scheldt is an estuary which is part of the so-called south-western delta of The Netherlands, where the rivers Rijn, Meuse and Scheldt meet the North Sea. Figure 3 gives an overview of the location of the Western Scheldt (51°27′ N, 03°25′ E). The south-western delta is located in the southern part of the North Sea and consists of multiple estuaria, of which a number are (partly) closed of off the North Sea by water defenses. The Western Scheldt is the most southern estuary of the delta and has a direct connection to the North Sea and is therefore under the direction influence of the North Sea. In terms of morphodynamics, hydrodynamics and water safety (safety against flooding of the low-lying hinterland), the influence from the North Sea consists of the tide and wind driven surges and waves. Furthermore, the Western Scheldt is an important habitat for flora and fauna and forms the main shipping lane towards the Belgian port of Antwerpen. Because of the different functions and values of the Western Scheldt, the estuary is continuously subject to political debat from a local to inter-governamental level [4]. Since this thesis focusses on the hydrodynamic and morphodynamic processes of wind driven waves and the schematisation of the wave climate , the entrance of the Western Scheldt is from here on described from that point of view.

Definition of the entrance of the Western Scheldt

In this study, the entrance of the Western Scheldt is defined as the area between the cities of Vlissingen and Terneuzen. At some locations in this thesis, sometimes reference is made to the entrance as the line between Vlissingen and Breskens. This is indeed the actual entrance. On a larger scale, the ‘entrance’ here is considered the western part of the Western Scheldt up to where waves from the North Sea can propagate into the estuary and influence the local wave conditions (which is up to the city of Terneuzen). The seaward boundary of the estuary is defined by the line between Vlissingen and Breskens. In this study, the focus is also on the ebb tidal delta seawards of this line. The reason for this is that the ebb tidal delta plays an important role in the wave propagation and transformation. The seaward boundary of this area is the line between Westkapelle and Zeebrugge. With respect to the morphological development, the focus is however only on the area between Vlissingen and Terneuzen. Within this area, the focus is on the shoals and ebb and flood channels of the macro cells (as described in section 2.2.3). Figure 3 shows the location of the entrance of the Western Scheldt. Also the names of the cities mentioned here are included.

As mentioned, the entrance of the Western Scheldt is under direct influence of the tide and wind driven surges and waves propagating from the North Sea towards the Western Scheldt. In general, before relevant coastal processes as a result of these influences can be described, it is necessary to classify the coast under consideration in some way. This classification helps to determine which of the coastal

[4] As described in section 1.2, understanding of the natural behaviour of such a system can support decision making on interventions in the system.

processes are dominant and therefore relevant for transport of sediment and morphological development. Moreover, classification of the coast makes one aware of the environment that is looked upon and gives insight in the relative importance of a certain process with respect to morphological development, in this situation wind driven waves. For the classification of the coast, a process-based classification is used. The reason for this is that in this study the physical processes of waves and sediment transport are considered. Other types of classification are e.g. based on the nature and abundance of coastal material or on tectonic control of coasts (e.g. Bosboom and Stive, 2011).

Figure 2. Entrance Western Scheldt with its open connection to the North Sea. On the right the city of Vlissingen. Calm sea during calm wind conditions (2 Bft).

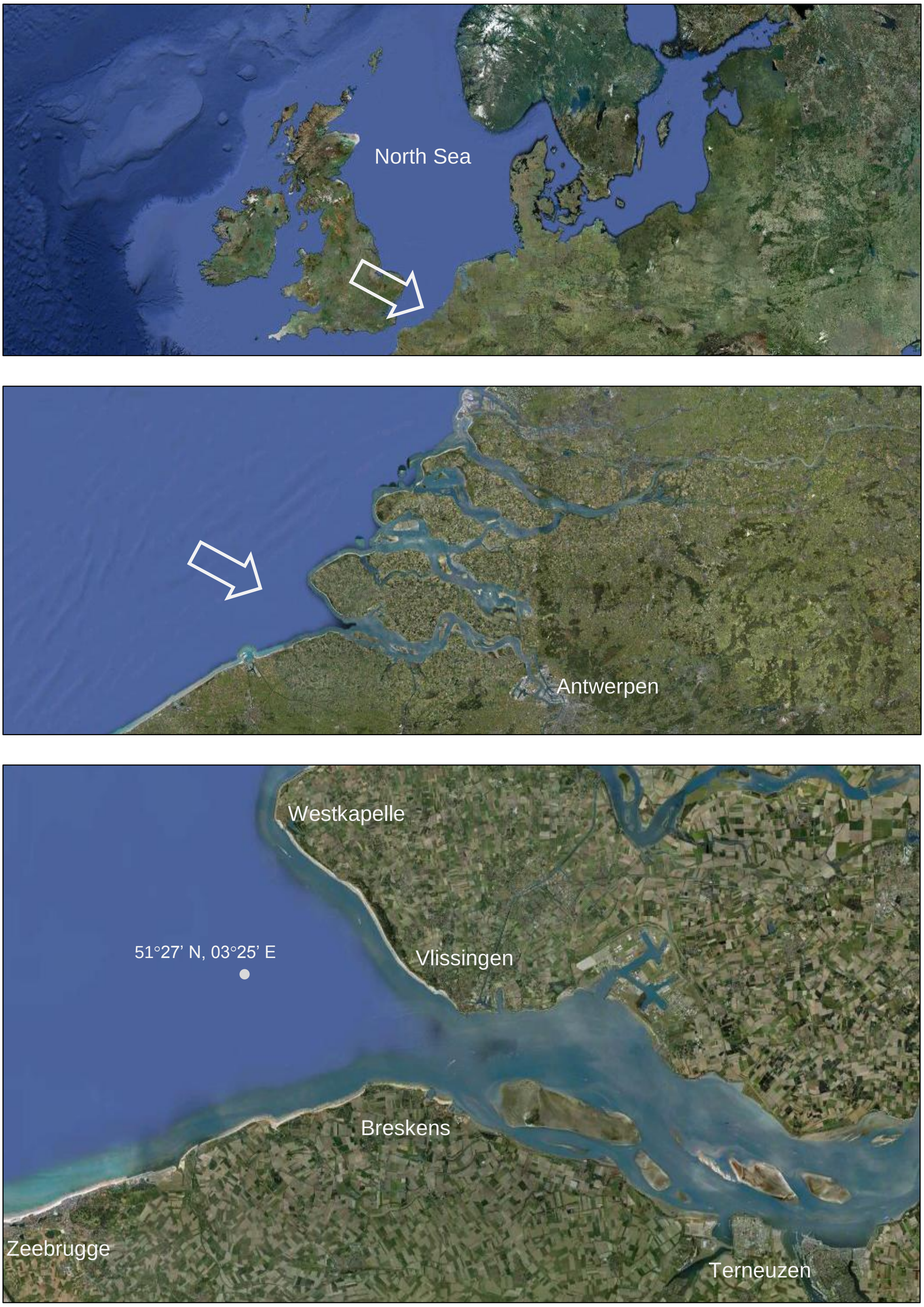

Figure 3. Overview of the location of the Western Scheldt estuary. Top panel: estuary located in the southern part of the North Sea. Middle panel: Western Scheldt as part of the south-western delta in the south of The Netherlands. Bottom panel: area of interest for this study; western part of the Western Scheldt, including the channels and shoals.

Source photos: Google Earth Pro.

2.2 CLASSIFICATION AND CHARACTERISATION OF THE COAST

Most of the *general* description in this section is adopted from Bosboom and Stive (2011). This description is adjusted and applied to classify the specific situation of the coast of the Western Scheldt entrance. First, the general wind, wave and tidal environment are described. After this, the coast is classified and the main characteristics are described. The influences of these characteristics on the coastal processes are discussed in section 2.3.

2.2.1 WIND, WAVE AND TIDAL ENVIRONMENT

Wind system and seasonality

The prevailing wind system determines to a large content the general wave climate. Since the Western Scheldt entrance (51°27′ N, 03°25′ E) is located at the northern hemisphere between latitudes 30°N and 60°N, the area is mainly subject to westerly winds. These westerly winds (‘westerlies’) are the result of the accumulation of air from the equator around 30°N (after travelling from the equator), after which this air sinks from the upper atmosphere to the surface, creating a high pressure area (the subtropical high pressure zone). Since air moves from high surface pressure towards low surface pressure, the air moves from 30°N towards 60°N (and partly back towards the equator). Due to the Coriolis effect, the atmospheric flow deviates to the right on the northern hemisphere. The combination of these two result in (south) westerly winds. The westerlies are considered to be strong and variable winds with the strongest winds occuring between latitudes 50°N and 60°N. The North Sea, to which the Western Scheldt is connected, exactly lies between these latitudes. In the presented wind and wave climate in section 4.2, the large contribution of the south westerly wind directions in the wave climate is indeed shown.

The wind system that prevails at the northen hemisphere is subject to seasonality, i.e. the wind and wave conditions vary with the seasons. Consequently, the North Sea and the Western Scheldt entrance are subject to seasonality as well. This is the result of the large areas of land present at the northern hemisphere. During summer, the temperature differences between land and water are relatively small. During winter these differences increase, since water is more capable of storing heat compared to land. These differences in heat between land and water result in high and low atmospheric pressure areas and consequently result in the movement of air. Large differences in temperature hence result in strong winds. Since the differences in heat between land and water are smaller in the summer season, movement of air is small compared to the winter season. As a result, more and stronger winds occur during winter than during summer. This is also shown in the presented wind climate in section 4.2.2.

Wave environment

The wave environment is to a large extent determined by the prevailing wind climate since waves are generated by wind. Due to the westerlies and the seasonality, the area at the North Sea and Western Scheldt entrance can be identified as a storm wave climate. Waves in a storm wave climate are mainly locally generated. Therefore, in general, waves are steep, short-crested and multi-directional. Due to the westerlies, the dominant wave direction is also west to south-west. The local wave climate can partly consist of swell waves from northern directions as well (generated in wind fields at the northern part of the North Sea). The yearly average significant wave height outside the estuary (at measurement location Schouwenbank [5]) is 1.1 m. During winter, the average significant wave height is higher (1.3 m) and during summer it is lower (0.9 m). Around the entrance (measurement location Wielingen), the average significant wave height is around 0.8 m. Based on these values, the local wave climate can be characterised

[5] The position of the measurement locations is presented in section 4.2.

as a 'medium wave energy' climate (with the significant wave height between 0.6 and 1.5 m). An extensive description of the wind and wave climate is given in section 4.2.

Tidal environment

With an average tidal range of a little less than 4.0 m at the entrance (Vlissingen, www.waternormalen.nl), the tidal environment can be classified as a meso tidal regime (2 m – 4 m). Furthermore, the tide has a semi-diurnal character, meaning that during one day (approximately) two tidal cycles occur.

Figure 4. Tidal range of 4 m visible at the Breskens harbour around low water. The green line marks the high water line.

2.2.2 CLASSIFICATION OF THE COAST

In a process based classification, the coastal character is described based on the relative importance of tide and waves, not the absolute values of tidal range and wave height. With an average tidal range of about 4.0 m at the entrance (Vlissingen) and an average significant wave height in the order of 1.0 m, the coast near the entrance can be classified as a tide dominated coast (Figure 5). According to this, the influence of waves on the morphological development is relatively low compared to the influence of the tide.

The process based classification as a tide dominated coast can be confirmed by considering the shape of the Western Scheldt. The main shape of the Western Scheldt (funnel shaped) is typical for tide dominated alluvial estuaries (Savenije, 2005). At the entrance, the tidal currents has eroded the banks and has consequently widened the estuary entrance. Further into the estuary, the flow velocity decreases, allowing sediment to settle. As a consequence, the estuary narrows from the entrance.

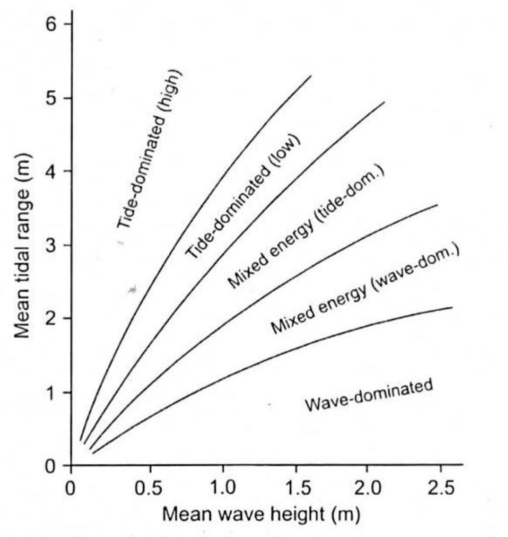

Figure 5. Relationship between tidal range and wave height delineating different fields of wave and tide dominance. From Bosboom and Stive (2011).

2.2.3 CHARACTERISTICS OF THE WESTERN SCHELDT ENTRANCE

The Western Scheldt entrance is mainly characterised as a relative shallow area with spatially varying depths, distinctive shoals and current channels. This characteristic of being a shallow area is extremely important for the hydrodynamic and morphodynamic processes in the entrance. The entrance of the estuary is characterised in more detail by the presence of the flood and ebb channels and the presence of an flood and ebb tidal delta. These are typical characteristics for a tide dominated estuary. Next to the importance of the tide on the estuary shape (existence of the tidal deltas and current channels), the tide is also responsible for the currents and the rise and fall of the water level during a tidal cycle. Hence, one of the characteristics of the Western Scheldt is that it has an large intertidal area, where the water depth strongly varies over one tidal cycle.

Flood and ebb tidal delta, shoals

The tide enters the estuary at the entrance between Vlissingen and Breskens (see Figure 3). Because of the large tidal discharges and hence large flow velocities in the estuary entrance, there is a strong sediment exchange between the estuary and the area outside the estuary. In narrow entrances, such as the Western Scheldt, this results in the formation of extensive sand deposits at both sides of the entrance. These sand deposits are the tidal deltas. When the ebb flow diverges, the flow velocities decrease and sediment is deposited, consequently creating the ebb tidal delta. The flood tidal delta is developed by sediment deposited by the inflowing flood current (adopted from Bosboom and Stive, 2011). As a result, tide dominant estuaries with a large tidal range as the Western Scheldt tend to have well-developed ebb and flood tidal deltas and relative deep entrance channels (such as the Honte channel, with a maximum depth of about 50 m). The ebb tidal delta of the Western Scheldt is called the Vlakte van de Raan [6]. The flood tidal delta is present as the different shoals near the entrance with the names as Hooge Platen and Spijkerplaat. The ebb tidal delta extents relative far seawards (about 20 km) as a result of the tide over waves dominance.

[6] The Vlakte van de Raan (‘plain of the Raan’) is a combination of consecutive shoals in front of the entrance of the Western Scheldt with names as Nolleplaat, Droogte van Schooneveld, Paardenmarkt and Walvischstaart.

Figure 6. Names of the largest shoals in the Western Scheldt entrance. Source photo: Google Earth Pro.

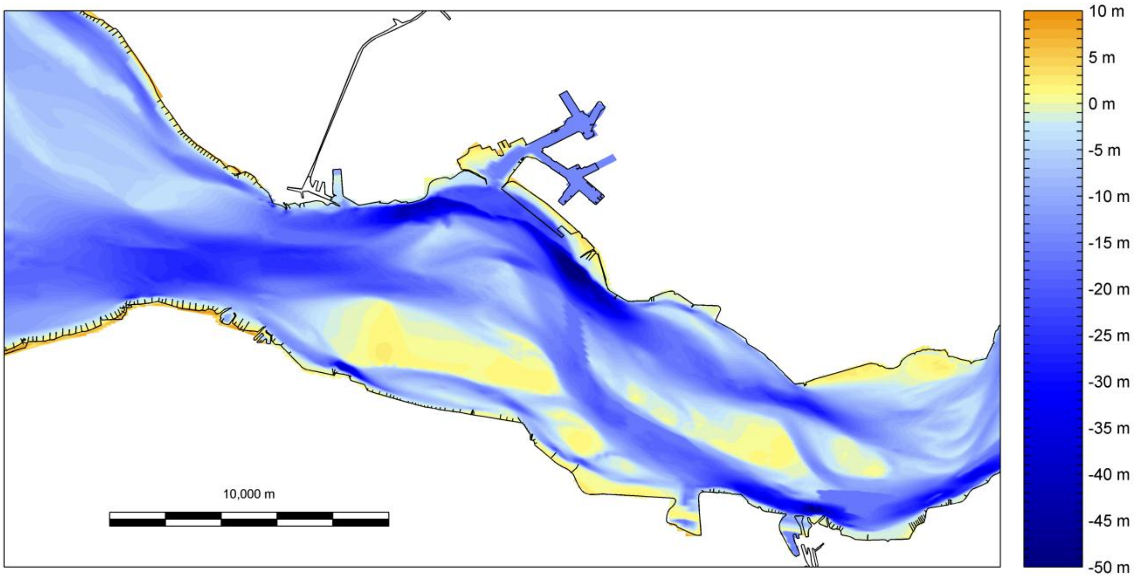

Figure 7. Bottom level in the Western Scheldt entrance. Levels in m related to NAP.

Figure 8. Shoals in the entrance of the Western Scheldt. In the middle the shoals of Hooge Platen, on the left the shoals of Hoofdplaat. In front, a part of the shoals of Lage Springer. Source of photo: beeldbank.rws.nl, Rijkswaterstaat.

Channels

The estuary is laterally bounded by dikes and bank protections. Within these boundaries, the estuary of the Western Scheldt contains a system of ebb and flood channels. Since the Western Scheldt is a relative small estuary, the flood and ebb currents follow to a large extent the same channels (in contrast to wider estuaries, where flood and ebb currents occur in different channels).The estuary has a meandering main channel (the ebb channel) and smaller channels (flood branches) starting in every bend (*Dutch:* vloedscharen) of the main channel. At the beginning of each flood cycle, the water in the main ebb channel continuous to flow seaward as a result of momentum. As a result, water entering the estuary that follows the ebb channel experiences this force and seeks the path of least resistance. In corners, flood currents therefore result in flood branches. According to Van Veen (2005), these flood branches have the function of filling the tidal sand flat in the inner bend of the main channel (resulting in relative shallow parts in the bends, the so-called sills (*Dutch:* drempels) and the function of creating a cut-off channel of the bend. These cut-off channels (*Dutch*: kortsluitgeulen) form a connection between the main channels. Shallow parts are present at the sea side of the ebb channels and the land side of the flood channels.

In Kuijper et al. (2006), the system of channels is defined as a number of macro and meso cells (Figure 9). Macro cells consist of the main ebb and flood channels, the meso cells are formed by the cut-off channels. This schematisation is also presented Table 2 is adopted from Kuijper et al. (2006) and presents the distinctive macro cells in the area of interest for this study.

Macro cel	Ebb channel	Flood channel
1	Honte	Schaar van Spijkerplaat
2	Pas van Terneuzen	Everingen

Table 2. Macro cells in the Western Scheldt entrance (Kuijper at al., 2006).

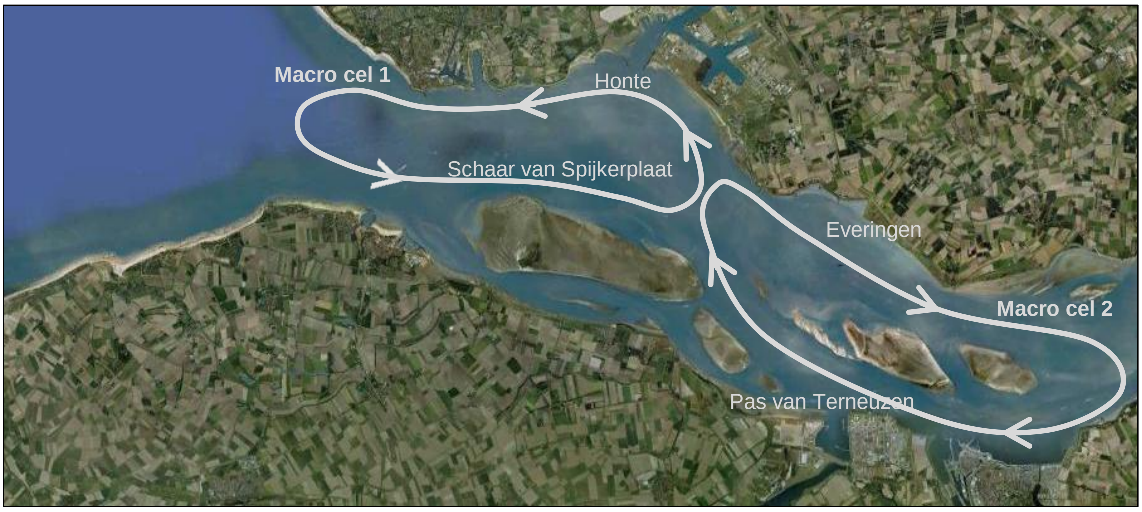

Figure 9. Macro cells with ebb and flood channels in the Western Scheldt entrance. Source photo: Google Earth Pro.

Sediment characteristics

The sediment in the Western Scheldt, in the channels and on the shoals, consists in general of sand with less than 10% silt. However, around the banks and on the shoals, the percentage of silt can be much higher. Characteristic values for the median grain size are (from Kuijper et al. (2006), adopted from Van Eck, 1999):

- Channels: $d_{50} > 150$ µm;
- Shoals: 50 µm < $d_{50} < 150$ µm;
- Along the banks $d_{50} < 125$ µm.

In the western part of the Western Scheldt, the sediment is somewhat more coarse compared to the eastern part. In Kuijper et al. (2006) it is shown that the median grain size in the western part can be larger than 300 µm. Relative coarse sediment is found in the channels, relative fine sediment is found in the inter tidal areas (shoals and banks). In the morphological simulations, one median diameter (d50) of 200 µm is applied (section 0). Next to the areas where sediment is available and thus potentially can be transported, also areas in the Western Scheldt are present where no sediment is available for transport.

2.3 INFLUENCE OF CHARACTERISTICS ON COASTAL PROCESSES

As described in the classification of the coast, the hydrodynamic process of the tide and waves are important for the present morphology and morphological development of the estuary. The morphodynamics are as important, i.e. the transport of sediment and changing morphology due to the hydrodynamics and the way they reinfluence the hydrodynamics. The mentioned characteristics in section 2.2 strongly influence these relevant coastal processes.

Influence of the intertidal area

The funnel shaped morphology of the estuary results in an amplification of the tidal range in the Western Scheldt. While the average tidal range outside the estuary is around 2.0 m to 2.5 m, it increases over the ebb tidal delta (around 3.5 m at Cadzand and Westkapelle) up to 3.9 m at Vlissingen. In the estuary itself the average tidal amplitude increases further up to 4.8 m at Bath, which is about 50 km into the estuary. From there, the amplitude still increases after which the tidal range is damped again. In the area of interest, the average tidal range varies between 3.9 m at Vlissingen and 4.2 m at Terneuzen [7]. Due to the tidal range, an intertidal area is created which is exposed during low water and submerged during high water. In an intertidal area, movement of water near the bed is the result of the present tidal currents and the orbital motion of waves. This motion of water near the bed is an important factor for the entrainment of sediment, after which the sediment can be transported with present currents (tide, wind or wave driven). The exact location where waves focus on the coast and the amount of morphological impact they have depends on the occurring water level and hence changes over a tidal cycle. In general, higher water levels also allow waves to travel further into the estuary (Lesser, 2009), since at a larger water depth wave energy is less dissipated by friction.

Influence of the shoals and other shallow parts

At the shoals of the flood and ebb tidal delta, the water depth strongly decreases and becomes relatively shallow. Here, waves start to interact with the bottom ('feel' the bottom) at a depth equal to half the wave length (approximately; the orbital velocity at a depth of half the wave length is about 4% of the orbital velocity at the surface). Significant wave-bottom interactions however do not occur until a water depth of approximately a quarter of the wave length (Carter, 1988). Since waves are susceptible for changes in shallow water, a lot of wave energy dissipation and wave transformation occurs at the shallow waters

[7] Data on the average tidal amplitudes is obtained from www.rijkswaterstaat.nl, slotgemiddelden 1991.0

around the shoals. This transformation can result in wave driven currents. Furthermore, at shallow water, the orbital velocity of the waves near the bottom increases and consequently more sediment is stirred up. The more the water depth decreases, the more the influence of waves on sediment transport increases. Due to this, the edges of the shoals and other shallow parts in the estuary of the Western Scheldt are most sensitive for sediment transport due to waves. Outside the estuary, the shoals of the ebb tidal delta strongly influences the waves (energy, propagation and transformation), inside the estuary the shoals of Hooge Platen, Spijkerplaat and Middelplaat have the same function.

Figure 10. Breaking waves on the edges of the shoals of Hooge Platen. Small waves during calm wind conditions (2 Bft).

The waves inside the Western Scheldt can't grow unlimited. This is due to the limited fetch over which the wind can blow and the relative small water depths (especially around the shoals), which causes the waves to break (Van Banning et al., 2000). The limited fetch is a result of the presence of the shoals and the meandering of the estuary. In the deeper parts of the estuary (i.e. the channels), the waves can grow to larger heights. In shallow areas, wind also creates currents. The relative influence of wind on these currents increases when the water depth decreases. When such a current is landward directed in a shallow coastal zone as the Western Scheldt, water levels can be increased (set-up). When water levels are set up or set down, waves can have an morphological impact on different levels and locations compared to the situation without set up or set down of the water level.

Influence of the channels
The channel system of the Western Scheldt consist of ebb and flood channels, which have a greater depth than the adjacent shoals. The propagation of the tide into and out of the estuary mainly occurs in these channels and results in a tide driven current. As mentioned before, at these locations the tide driven current can stir up and transport sediment. The currents which are present in the Western Scheldt can also influence the waves. Due to the larger depth at the channels, waves can grow to a larger height. Currents in the channels with an opposite direction of the waves can result in an increase of the wave height (current induced shoaling) and wave period. Currents with the same direction as the waves can result in a decrease of the wave height and wave period. Furthermore, currents can cause waves to refract. The influence of the currents on the waves increases with an increase of the flow velocity and also increases when wave lengths decreases. Consequently, the waves are most influenced by the currents at the channels, especially at the bends and narrows (such as Honte and Everingen, where high flow velocities and large velocity gradients occur) in the estuary and around the ebb tidal delta.

3 General modelling approach

3.1 INTRODUCTION

In this chapter, the general modelling approach is briefly described, together with the applied numerical model. This chapter serves as background information for the first and second trace of the thesis approach (section 1.4). For specific approaches on the wave simulations and morphological simulations reference is made to chapters 4, 5 and 6.

Every model is a schematisation of reality. With a *simulation*, changes of the considered reality in time and space can be approximated by use of that model. Here, the hydrodynamic and morphodynamic processes in the Western Scheldt entrance are approximated by use of a *numerical* model. Within this numerical model, the physical processes are described by a set of equations. Subsequently, these equations are discretised in such a way that they can be solved by the use of numerical techniques (Zijlema, 2011). In section 3.3, a brief description of the model is given. For the equations of the physical processes, reference is made to literature. The numerical techniques used by the model are not described. Next, some of the settings within the model are mentioned.

3.2 GENERAL MODELLING APPROACH

The hydrodynamic and morphodynamic processes in the entrance of a tidal estuary, in this case the Western Scheldt, are highly complex. A combination of complex processes such as tide driven, wind driven and wave driven currents, waves and wave-current interaction occurs. To assess the influence of wave climate schematisation, a numerical model describing these processes is needed (i.e. a process based numerical model). For this thesis, the Delft3D numerical model (Deltares, formerly WL|Delft hydraulics) is applied, wherein all these processes are implemented. Use is made of the existing model of the whole Western Scheldt estuary, which has been developed in the studies mentioned in section 1.1. In this model, the Western Scheldt is divided in five domains, covering the whole estuary from North Sea to the rivers and canals. Since in this study the focus is on the entrance of the Western Scheldt, only two of the five domains are used: domain 1 (North Sea in front of the entrance) and domain 2 (western part of the Western Scheldt: roughly between Terneuzen and the line Westkapelle – Zeebrugge, thus including the ebb tidal delta). Figure 11 shows the calculation grid, existing of these two domains. For this study, a 2D horizontal (2DH) approach is applied. That means that there is only one layer in the vertical. Also in the study by Grasmeijer (2012), to which this thesis contributes, a 2DH approach is followed.

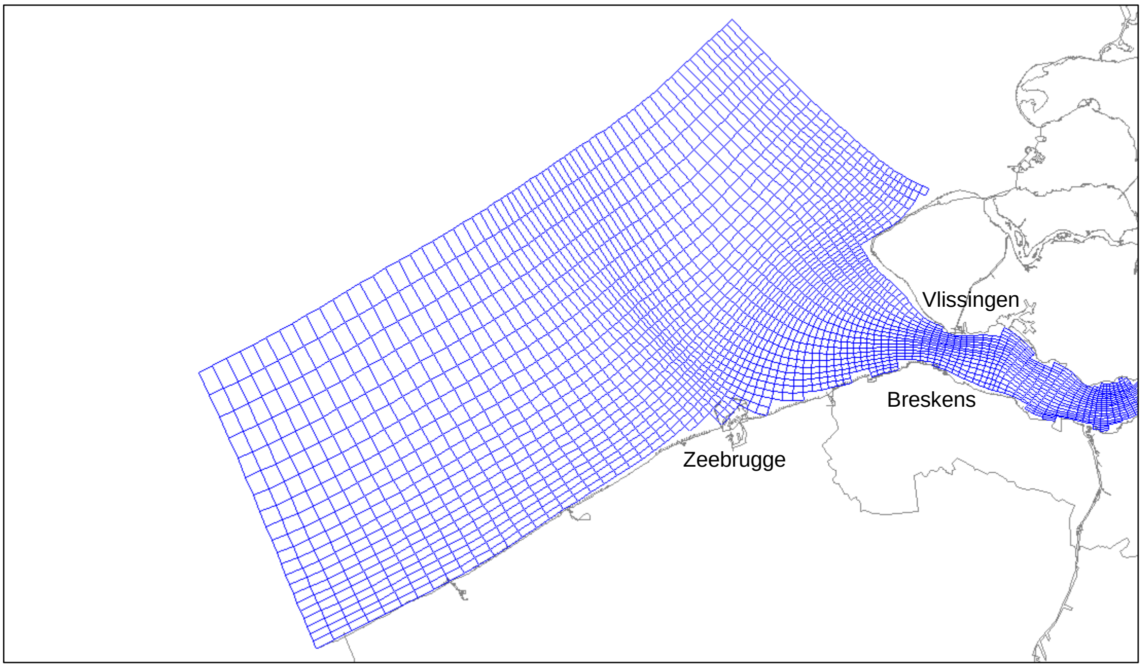

Figure 11. Calculation grid. The grid is made coarser for presentation in this figure.

3.2.1 TIME AND SPATIAL SCALE

The objective of this study (section 1.2) is to address the influence of the wave climate schematisation on the medium-term morphological development of the Western Scheldt entrance. This is an important starting point, as the appointment of time scale (medium-term, in this case one year) also determines the spatial scale on which the results of hydrodynamic and morphodynamic processes are relevant. On a medium-term morphological scale, there's no need for focus on small local scale changes. Large scale changes on the other hand (e.g. structural sedimentation and erosion on the scale of ebb and flood channels and shoals over a period of one year) are very relevant. In the applied calculation grid (Figure 11), a grid cell size in the order of 80 m by 100 m is assumed to be sufficient to simulate the hydrodynamic and morphodynamic processes on the relevant spatial scale of the ebb and flood channels and shoals (these features have sizes in the order of several thousands of meters; Figure 6).

3.2.2 MORPHOLOGICAL TIDE

The application of all relevant physical processes within the numerical model results in relative long run times of the simulation. Because of constraints on computational capacity, the amount of imposed forces (tides, wind and waves) needs to be reduced in some way in order to maintain a reasonable runtime of the simulations. Simulations based on full time series of water levels, wind and waves (i.e. non-reduced forces) for all hydrodynamic and morphodynamic processes would be too time consuming in a large area as the Western Scheldt. This especially holds when multiple years of morphological development are considered. The reduction of the imposed forces can be obtained by schematising the forces. With schematisation is meant here the selection of certain conditions (e.g. water levels, wind, waves) to represent all conditions. From this background stems the need for the schematisation of the wave climate (section 1.1).

The wave climate schematisation is constructed from selected wave classes (chapter 5). To simulate the influence of the wave classes on the morphological development, the different wave classes are individually simulated during a time series of water levels and accompanying currents. Like for the schematisation of the wave climate, also the time series of water levels needs to be schematised to maintain a reasonable runtime of the simulation. The *morphological tide* is the schematised motion of the water level and accompanying currents (i.e. the horizontal and vertical tidal motions). This morphological tide represents the influence of a full spring neap tidal cycle. The way this morphological tide is constructed in the medium-term morphological simulations is described in section 6.2.

3.2.3 MORPHOLOGICAL ACCELERATION

According to Lesser (2009), a fundamental problem with performing process-based morphological modelling is that "*morphological evolution of coastal features of interest to engineers, managers and the public usually occurs at time scales several orders of magnitude larger than the time scale of the hydrodynamic fluctuations driving the sediment transport*". What is important is that hydrodynamic processes thus occur at a much smaller time scale (seconds to hours) than large scale changes in morphology as a result of these hydrodynamic processes (months, years). Consequently, simulating the medium-term morphological development as a result of these hydrodynamic processes takes a long time. To accelerate this simulation (i.e. reduce the runtime), the effect of the hydrodynamic processes on the morphology can be multiplied with a morphologic acceleration factor. In this study, the acceleration approach as described by Lesser (2009) is used.

The morphological acceleration factor (*morfac*) by Lesser (2009) is a factor that is used to deal with the described difference in time-scales between hydrodynamic and morphological developments. The sediment fluxes to and from the bed as the result of hydrodynamic forcing, are multiplied by this *morfac* at each computational time step. Due to this, the influence of the hydrodynamic processes on the morphology are multiplied, with the result that less time steps of hydrodynamic processes need to be simulated to cover a certain period of time. This results effectively in a morphological time step equal to the morfac times the hydrodynamic time step, which is described equation 3.1.

With this approach, it is implicitly assumed that the influence of the hydrodynamic processes on the morphology is linear within the morphological time step. This however only is valid within a certain size of the time step. The reason for this is that changes in morphology influences the hydrodynamics. When the morphological time step is too large (as a result of a too large *morfac*), part of this influence on the hydrodynamics is lost. Consequently, the hydrodynamics differ from the hydrodynamics based on a smaller morphological time step (a smaller *morfac*). The difference in hydrodynamics consequently result in a difference in the simulated morphological development. The *morfac* therefore must be used with caution. The upper limit of the *morfac* can't be determined on forehand. This must be determined by comparing simulations based on different *morfac* values.

The reason for applying this morphological acceleration factor is that Lesser (2009) discusses several approaches and their drawbacks. After the discussion, the author introduces a new approach, which is considered to give the best result. The improvement arises from the simultaneous calculation of sediment transport, morphological change and hydrodynamic processes. The simultaneous calculation of all processes is also indicated as 'online' modelling. This online modelling allows the use of the morphological acceleration factor (*morfac*). Furthermore, this online *morfac* approach is used in the study to the medium-term development of the Western Scheldt estuary (Grasmeijer, 2012) to which this thesis contributes.

$$\Delta t_{morphology} = f_{MORFAC} \times \Delta t_{hydrodynamic} \qquad (3.1)$$

with $\Delta t_{morphology}$ = morphological time step

f_{MORFAC} = value of *morfac*

$\Delta t_{hydrodynamic}$ = hydrodynamic time step

In this study, the focus is on changes in the Western Scheldt on the medium-term, meaning a period of years to decades. This allows for the application of upscaling the hydrodynamics, with the caution as mentioned above. The specification of the applied values of the *morfac* in the medium-term morphological simulations is given in chapter 6.

3.3 NUMERICAL MODEL

For the modelling of the flows, waves and morphology, the numerical model Delft3D (Deltares, 2011) is used. Here, a short description of the most relevant processes for this study and some specific settings are described. For an extensive description of the model and applied equations, one is referred to Deltares (2011). Within the model different separate modules for, amongst others, flow and waves are included. For the wave module in Delft3D, use is made of the numerical wave model SWAN (Booij et al., 1999), which is shortly described in the next section. Although most of the description given in this section is generic, it shows which user defined settings are included in the formulations that are used by the model. Consequently these user defined settings are shortly described, making the choices that are made visible.

According to Deltares (2011), "*Delft3D-FLOW is a multi-dimensional (2D or 3D) hydrodynamic and transport simulation program which calculates non-steady flow and transport phenomena that result from tidal and meteorological forcing on a rectilinear or curvilinear boundary fitted grid.*"

According to Delft University of Technology (2011), "*SWAN is a third-generation wave model for obtaining realistic estimates of wave parameters in coastal areas, lakes and estuaries from given wind, bottom and current conditions. However, SWAN can be used on any scale relevant for wind-generated surface gravity waves. The model is based on the wave action balance equation with sources and sinks.*"

3.3.1 FLOW, WAVE AND TRANSPORT FORMULATIONS

Flow formulations

For flow, the model solves the Navier-Stokes equations for an incompressible fluid, under the shallow water assumptions. The Navier-Stokes equations consist of the continuity equation and the momentum equation. In the momentum equation, amongst others, Reynolds stresses are present. These stresses are modelled with the eddy viscosity concept. For a 2D simulation as applied here, only the horizontal eddy viscosity is considered. In this case, the horizontal viscosity represents 2D turbulence and a dispersion coefficient. The value of the horizontal eddy viscosity is determined manually.

Next to the Navier-Stokes equations, the transport of sediment is modelled with an advection-diffusion equation. In a 2D approach, a value for the horizontal eddy diffusivity is manually selected. For this study, a value for the horizontal eddy viscosity and horizontal eddy diffusivity of 1 m^2/s is selected. In the study by Grasmeijer (2012), these values were found adequate to model the flow in the Western Scheldt in a 2D approach (Grasmeijer, personal communication). In case of a 2D approach, the vertical profile of the horizontal velocity profile is close to a logarithmic profile.

The two way wave-current interaction as described in section 2.3 is taken into account in the Delft3D model. The calculation of waves and wave induced effects is performed with the SWAN wave model which is implemented in Delft3D via the WAVE module. For a full current-wave interaction, the currents from the FLOW module are used in the WAVE module. For the wave-current interaction, the radiation stresses due to waves from the WAVE module are used in the FLOW module.

Wave formulations

In general, wave propagation and transformation is determined by solving the wave action balance. Without the presence of a current, the wave action balance reduces to the wave energy balance. With the presence of a current however, it is possible that waves and current transfer energy. In this case, it is necessary to solve the wave action balance (Holthuijsen, 2007). Due to the propagation of the semi-diurnal tide in and out the Western Scheldt estuary, a current is also present in the entrance. When short waves interact with a current, the waves can be affected in celerity, height and direction. Therefore, currents can have a strong effect on the wave conditions, which is often forgotten (Delft University of Technology, 2012a). In this case, the prediction on waves should be based on combined wave and current model (as recommended by Van Vledder, 2007). The applied SWAN wave model is based on the wave action balance and hence takes the interaction between waves and currents into account.

Reliability wave model

In (Van Vledder, 2007) the reliability of the SWAN wave model (version 30.75) was tested for storm conditions in the Western Scheldt. The reliability was tested by use of a hindcast study. A part of the results is (of course) based on the principles used in the reliability study. The calculations were executed for two water levels (the highest and lowest water level in the Western Scheldt), no current and a constant wind field. The boundary conditions in SWAN with respect to the wind conditions were based on measured data from the station in Vlissingen, and the wave and water level data were based on measured data from the Euro platform.

Relevant conclusions from that study with respect to this study are the following (Van Vledder, 2007):

- Based on the comparison with the measured and calculated wave conditions with SWAN 30.75 it appears that the significant wave height is underestimated with approximately 10%. The underestimation of the wave periods can be up to 20%. The average underestimation of the wave height is approximately 0.1 m, the average underestimation of the wave periods is about 0.9 s. The peak period is predicted the worst by SWAN.
- The analysis of the reliability of SWAN per area shows that the best results are obtained for the entrance and the eastern part of the Western Scheldt. However, the prediction on the peak period is poor. Comparison between measured and calculated wave spectra shows that SWAN has trouble with double peaked spectra. The worst results are obtained in the middle part of the Western Scheldt.
- The reliability of SWAN is somewhat higher during high water compared to low water. This means that shallow water processes are of influence on the quantity of the results.
- The reliability of SWAN is better for situations with westerly wind directions than for north westerly wind conditions. This difference in behaviour is possibly caused by the fact that the roughness of the land surface has more influence on the wind in the Western Scheldt for north westerly winds. This causes spatial deviations in the wind field compared to the Vlissingen wind station. The behaviour can also be the consequence of the fact that the wave growth with relative short fetches in the used SWAN version is probably inaccurate.

In this thesis, the wave model is validated by comparison of calculated wave conditions with measured wave conditions. The comparison is done at locations outside the ebb tidal delta, at the ebb tidal delta and in the western part of the Western Scheldt (section 4.4).

Transport formulations

For the transport of sediment due to currents and waves, use is made of the transport formulations for non-cohesive sediment of Van Rijn (1993), as described in (Deltares, 2011a). This means that a reference concentration of sediment is calculated, after which the sediment concentration in the vertical is calculated. Formulations for bed load and suspended load are used to calculate the transport. Below the reference height, the bed load formulation is applied, above the reference height the formulation for suspended bed load is used.

The transfer of sediment between the bed and the flow is modelled by sink and source terms. These terms act on the near bottom layer above the reference height of Van Rijn (2000). To determine the value of the terms, the concentration of sediment at every level in the water column is needed. When the sediment continuity equation is averaged over time and integrated over depth (depth average approach as followed here), an equilibrium is obtained between downwards transport by velocity and upwards transport by turbulence. The solution of the amount of sediment in the vertical is based on the reference concentration. Roughly summarized, the following approach is applied:

1. The **significant wave height** and **wave peak period** are applied in the formulations to calculate, together with the water depth and roughness parameters, the wave orbital motion (path and velocity). Both the significant wave height (H_{m0}) and wave peak period (T_P) are results of the wave simulation. This orbital motion subsequently induces (wave related) bed shear stress. The *effective* bed shear stress is a function of the bed shear stress due to currents and waves and efficiency factors for both currents and waves. The effective bed shear stress is considered the part of the bed shear stress that is directly transferred to the grains as skin friction. Near the bottom, the sediment reference concentration is based on this effective bed shear stress and the critical bed shear stress.
2. Next, the concentration of sediment on any level in the water column is based on the reference concentration, i.e. sediment is entrained in the water column by imposing a reference concentration at a reference height. The concentration of sediment in the water column is furthermore dependent on the reference height, water depth, and the number of Rouse. The distribution of sediment hence is described by a parabolic curve whereby the concentration of sediment increases towards the bed.
3. Below the reference height, the sediment is assumed to respond fast to changes in bed shear stress and the formulation for bed load transport by Van Rijn et al. (2003) is applied. Above the reference height, the sediment is assumed not to respond instantaneously on hydrodynamic changes. Here, the suspend sediment transport formulation by Van Rijn (2001) is applied. Within the transport formulae, user-defined calibration factors are included. These are f_{SUSW} for the transport of suspended load and f_{BED} and f_{BEDW} for the transport of bed load by currents and waves repectively.
4. The calculated bed load transport is corrected for bed slope effects. Two bed slopes can be distinguished: the slope in the direction of the transport (the longitudinal bed slope, denoted as α_{BS}) and the slope perpendicular to that direction (the transverse bed slope, denoted as α_{BN}) (Deltares, 2011a). Use is made of the formulations by Bagnold (1966) as described in Deltares (2011b).

3.3.2 SETTINGS FLOW AND MORPHOLOGY MODEL

In the FLOW module multiple settings within the applied formulae and numerical techniques are needed. A number of them are mentioned here. Where necessary an explanation is given. Values for calibration factors are based on experience ('good practice') from members of the committee or prof. dr. ir. J.A. Roelvink [8]. These experience values are applied after personal communication.

- Wave online: the wave simulation is coupled in two ways and performed simultaneously (or 'online') with the flow simulation : FLOW-WAVE and WAVE-FLOW. This means that both simulations influence each other. After each predefined time step, a communication file is written from the FLOW module. The WAVE module continues the simulation based on the latest FLOW results and updated bottom. After the wave simulation, data is written again to the communication file. The FLOW module uses these new data and continuous with its simulation. Due to this coupling, bottom changes, currents and water levels can influence the waves and the waves can influence the currents (via radiation stress) and sediment transport. The time step between each communication is set to 30 minutes. From sensitivity analysis this appears to be a sufficient small time step to obtain usable and realistic results. Smaller time steps will increase the total run time of the simulations, larger time steps show deviations in calculated wave conditions.
- Time step: 12 s at wave simulations in chapter 4 and morphological simulations in chapter 5, 24 s at morphological simulations in chapter 6. After analysis of the influence of the time step size (section 4.4.2) it was decided to apply a 24 s time step in the medium-term morphological simulations instead of a 12 s time step to reduce the runtime of the simulations.
- Depth specified at: grid cell corners, depth at grid cells centres: mean.
- Wind: the wind conditions are imposed as area uniform values. In the simulations for wave assessment (section 0), time series of wind conditions (wind speed and direction) are imposed. In the short and longer morphological simulations (section 5.3 and section 6.3) the imposed conditions are constant in time for each defined wind and wave class.
- Bottom roughness: the bottom roughness is imposed as Manning values and are varying of the area. The variation in values is small: 0.0023 or 0.0024 $m^{-1/3}/s$.
- Sediment characteristics: median sediment diameter D_{50} = 200 μm, density = 2,650 kg/m^3.
- Reference density for hindered settling: 1,600 kg/m^3.
- Current related reference concentration factor = 0.5 (Grasmeijer, personal communication)
- Current related transport vector magnitude factor = 0.5 (Grasmeijer, personal communication)
- Wave related suspended load transport factor f_{SUSW} = 0.5 and 0.1. For the short morphological simulations in chapter 5, the value of 0.5 is used. For the simulations in chapter 6, the values are set to 0.1 for both parameters based on experience (Roelvink, personal communication).
- Wave related bed-load transport factor f_{BEDW} = 0.5 and 0.1 (equal to f_{SUSW}). For the morphological simulations in chapter 5, 0.5 is used, for the simulations in chapter 6, 0.1 is used (Roelvink, personal communication).
- longitudinal bed slope factor α_{BS} = 1.0, transverse bed slope α_{BN} = 100.0. The values for current related transport and slope factors are adopted from the study by Kuijper et al. (2004). These values were found adequate values for calibrating the model over the time period 1 January 1998 – 1 January 2002 and are also applied by Grasmeijer (2012). Different imposed wave conditions might influence the values of these calibration parameters. Since calibration can only be done afterwards and this study focusses on the influence of the way the wave climate is schematised (and not on the exact result) the values of the calibration parameters from Kuijper (2004) can be applied in this thesis as well (Grasmeijer, personal communication). When after analysis of the different schematisations one or more schematisations are recommended, these calibration parameters might be tuned again.

---

[8] Prof. dr. ir. J.A. Roelvink works at UNESCO/IHE and Deltares. Roelvink is the creator of the optimum method as applied for obtaining the wave climate schematisations.

3.3.3 SETTINGS WAVE MODEL

In the WAVE module, multiple settings to solve the wave action balance and apply numerical techniques are needed. A number of them are mentioned here. Where necessary an explanation is given. Values for numerical techniques are based on experience of dr. ir. G. Ph. van Vledder [9]. These values are applied after personal communication. For the physical parameters, use has been made of the default options in the WAVE module. These settings are used for the wave simulations (chapter 4) and the morphological simulations in chapters 5 and 6. Figure 66 and Figure 67 in Appendix 3 give an overview of all applied settings.

- Wave online: the wave simulation is coupled in two ways and performed simultaneously (or 'online') with the flow simulation (see first bullet section 0), Via the communication file, the WAVE module receives information on water levels, currents and bathymetry. The WAVE module sends information on radiation stress (influencing the currents in the FLOW module) and wave parameters (influencing the transport of sediment).
- The wave simulations are performed on the same grid as the flow and morphological simulations. The different considered wave conditions are applied as boundary conditions on the three sea sided boundaries of the model (Figure 11). The conditions are considered to be constant along the boundaries.
- Spectral shape of the wave conditions at the boundary: JONSWAP, peak enhancement factor = 3.3. The reason for this shape is that the wave conditions are predominantly locally generated and therefore not fully developed (storm wave climate, section 2.2.1). The wave height and wave period are expressed in terms of the spectrum (significant wave height (H_{m0}) and the peak period (T_P)).
- Spectral resolution = 0° – 360° (all directions). In total 36 direction bins are used, leading to direction bins of 10° each.
- Frequency space range = 0.05 Hz – 1 Hz (corresponding to wave periods of 20 s and 1 s respectively). For the frequency space, 24 bins are used, which are log-spaced, with an increment of 10%.
- The WAVE module uses the third generation SWAN model. Both wave generation and dissipation is taken into account. With regards to the *generation* of waves, wind conditions (magnitude and direction) are accounted for. For development of waves also quadruplet and triad wave-wave interactions are taken into account. For the triad wave-wave interaction default settings are used ($\alpha = 0.1$, $\beta = 2.2$). For *dissipation* of wave energy, depth induced breaking (Battjes and Janssen, $\alpha = 1.0$, $\gamma = 0.73$), white capping (Komen et al.) and bottom friction (JONSWAP, 0.067 m^2/s^3) are used. Furthermore, refraction and shifting of frequencies is activated. The forces of the waves on the current are expressed in terms of the radiation stress.
- Diffraction is not taken into account. The main reason for this is that the length scales in the Western Scheldt are relatively large, resulting in a smooth development of wave heights in the area. No large differences in wave heights occur on small length scales of a few wave lengths. Due to this, diffraction hardly occurs and has no significant influence on the wave action balance and propagation of the waves. On local places diffraction can have some influence (Van Vledder, personal communication).

[9] Dr. ir. G. Ph. Van Vledder is one of the supervisors for this MSc thesis and works at TU Delft, section Fluid mechanics and at BMT Argoss.

4 Wind and wave climate and wave modelling

4.1 INTRODUCTION

This chapter serves the first and second trace of the thesis approach (section 1.4, Figure 1). Section 4.2 gives an extensive description of the wind and wave climate of the Western Scheldt entrance and a first schematisation of the wave climate. This first schematisation forms the base for the further schematisation of the wave climate in chapter 5 and thus is part of the first trace within the thesis approach.
As part of the second trace of the thesis approach, wave simulations are performed to validate the wave model. A sensitivity analysis is performed to address the influence of modelling choices. Besides the validation, the wave simulations are used to obtain further understanding of the wave physics in the Western Scheldt entrance and to describe these in a quantitative manner. For this, a sensitivity analysis is performed to address the different influences on the wave conditions. The results from the wave simulations within the morphological simulations in chapter 5 are included in this chapter as well. These results relate to the influences *on* the wave conditions inside the estuary and are in line with the results from the sensitivity analysis as performed in this chapter. These results complement the found influences on the wave conditions from the sensitivity analysis. The influence *of* the wave conditions on sediment transport and morphological development is described in chapter 5. Based on the results of the sensitivity analysis, a simple method is introduced to address the relative influence of the imposed wind and wave boundary conditions on the local wave conditions at three areas in the estuary.

In this chapter, the subjects on wind and wave climate and wave modelling are combined. The reason for the combining of these two is that the wave modelling shows the influence of the wind and wave climate on the wave physics outside and inside the Western Scheldt entrance.

4.2 WIND AND WAVE CLIMATE

A wind and wave climate refers to the state of wind and wave conditions at a certain location over a certain period of time. Wind, and hence the generation of waves, depend on meteorological conditions. Since the meteorological conditions can vary per period of time (e.g. hours, days, season and year), also the wind and wave conditions vary at these time scales. For practical application of the wind and wave climate, it is necessary to schematise this climate in some way. For the schematisation of a wind and wave climate at a certain location, multiple years of measured wind and wave conditions must be considered to take the variation of conditions into account. Next, these wind and wave conditions are classified into directional and magnitudinal classes. A schematisation of the wind and wave climate can thus be seen as representation of the wind and wave conditions over a certain period of time.
For this study, measured data of wind speeds and wind directions, water levels, surges, wave heights, wave periods and wave directions is available. The data is obtained from three measuring stations (Euro

Platform, Scheur West and Schouwenbank) for the period 1 January 1981 – 1 January 2001. The data is available from a previous study by Van der Kaaij et al. (2004). From other stations on the ebb tidal delta and in the entrance also data on wave conditions are available. This data is freely available at www.hmcz.nl. For the wind climate at Vlissingen, data is used from the Royal Netherlands Meteorological Institute (KNMI) is used. This data is freely available at www.knmi.nl/samenw/hydra or http://kml.deltares.nl. Figure 12 presents the locations of all measurement stations of Hydro Meteo Centrum Zeeland (HMCZ). Figure 68 in Appendix 4 also shows the location of the calculation grid with respect to the measurement locations.

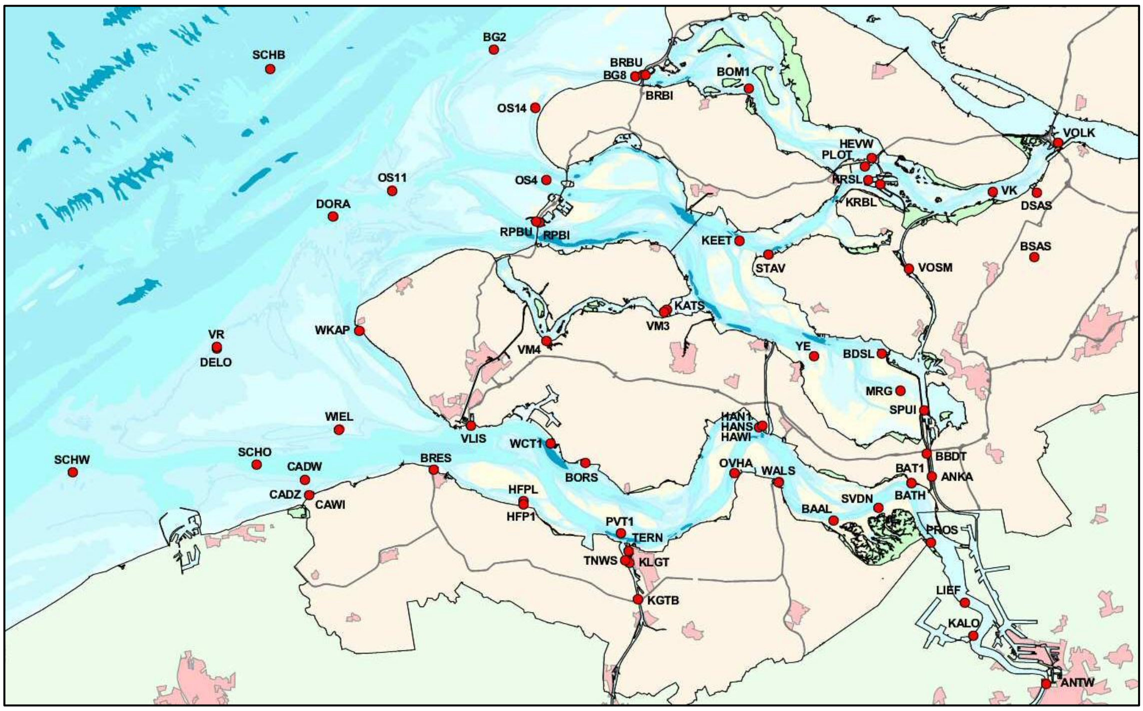

Figure 12. Overview measurement locations (Meetnet Zeeuwse getijdenwateren, www.hmcz.nl).

Data from the following measurement locations is used:

Location	Description	Coordinate[1] X	Coordinate Y	M[2]	N
SCHB	Schouwenbank (directional wave rider)	011332	419605	4 [3]	30
DORA	Domburger Rassen (wave rider)	017325	405275	18	79
DELO	Deurloo (directional wave rider)	006071	392601	103	88
SCHW	Scheur West (wave rider)	-07784	380857	216	76
WIEL	Wielingen (wave rider)	017641	383875	109	80
WCT1	Westerschelde container terminal (wave rider)	038185	383481	45	209
HFPL	Hoofdplaat (wave pole)	035614	377930	143	216
PVT1	Pas van Terneuzen (wave rider)	045053	374771	133	270
VLIS	Vlissingen[4]	030575	385290	-	-

1. Coordinates given are presented as RD coordinates (Rijksdriehoek coordinates), which are standard within The Netherlands.
2. M, N coordinates refer to the coordinates in the computational grid of the used model.
3. Schouwenbank is located just outside the computational grid, but is located *near* these coordinates (5,300 m).
4. Vlissingen is only used for wind data, the exact location is not present in the numerical model.

Table 3. Used measurement locations.

4.2.1 APPROACH IN CLIMATE REPRESENTATION

From the measurement location Schouwenbank (SCHB), located north of the ebb tidal delta, wind and wave data is used to obtain the wind and wave climate schematisation. For the time period considered, no wave direction at Schouwenbank was measured. Data on wave direction is therefore used from measurements at Euro Platform (not presented in Figure 12 as it lies just outside the figure, north of Schouwenbank, SCHB). From Vlissingen, daily mean wind data is used.

Based on the available data, a wind and wave climate schematisation has already been determined by Van der Kaaij et al. (2004) over the period 1981 – 1991. In the present study, the *approach* by Van der Kaaij et al. has been adopted. For this present study however, a wind and wave climate schematisation is obtained from measurement from a different measurement station (Schouwenbank instead of Scheur West as used by Van der Kaaij et al.) and the period over which the climate is determined is extended to 2001. The reason for this is that the station of Schouwenbank is located just outside the used model grid (Figure 68 in Appendix 4), whereas the measurement station of Scheur West is located far inside the model grid. Comparison of the wave conditions shows that at Schouwenbank, the waves are in general somewhat higher and longer than at Scheur West. The wind conditions at both stations are the same (Van der Kaaij et al., 2004). This also implies that the waves at Scheur West are locally more influenced (by e.g. bathymetry, water depth, currents) than the waves at Schouwenbank. By applying the wave climate on the boundaries of the computational grid, the transformation of the waves is taken into account by the numerical model. Furthermore, since the boundary is located relative far away from the area of interest, the relative large water depth and relative constant bathymetry, possible boundary effects are not expected to influence the results in the area of interest. The influence of the choice on the measurement stations is assessed in section 4.3.

The wind and wave climate schematisation is based on classes of wind direction and wind speed. For each wind direction and wind speed class, the average wind conditions, wave conditions and set up conditions were calculated. The reason to adopt this approach is that a large amount of wave energy from a westerly direction dissipates on the ebb tidal delta. Because of this large dissipation, the wave conditions in the entrance are to a large extent dominated by the local wind conditions (this is also confirmed by the performed sensitivity analysis of the wave model and the results from the short morphological simulations). A classification based on the wind direction and wind speed is therefore assumed to be the right approach. In section 4.4.3 this assumption is confirmed.

The wind and wave climate is imposed on the sea sided boundary of the model (Figure 11). The conditions at this boundary are derived from the Schouwenbank station. After comparison with the wind conditions at the entrance, the distribution of the wind *direction* at Vlissingen and the Schouwenbank station appear to be very similar. The *wind speed* however, is somewhat lower at Vlissingen. A possible reason for this is the presence of land at Vlissingen, which acts as a friction on the wind speed, consequently resulting in a lower wind speed. Because of the location of the measuring station at Vlissingen in the entrance, the measurements from this station are more representative for the wind conditions in the entrance. The drawback of the measurements at Vlissingen is that they are available as a daily mean value, whereas the measurements at Schouwenbank are available as a three hours mean value. Because of this and the fact that other variables (wave conditions and set-up) are measured as well at Schouwenbank, the choice was made to use the measured wind speed at Schouwenbank. To take into account the difference in wind speed between Schouwenbank and Vlissingen, a constant reduction factor f_{WIND} of 0.9 is applied.
At Schouwenbank, for the period 1981 – 2001, no data on the wave direction is available. For this, use has been made from the data on wave direction at Euro Platform. Given the very similar distribution of wind directions at both stations and the large correlation coefficient between wave and wind direction, it is

assumed that the use of the wave directions at Euro Platform for the wave climate schematisation is allowed. In section 4.4.2, the influence of the choice of measurement station for the wave direction is assessed (for a time period where also data on the wave direction is available at Schouwenbank).

Summarising, the data at Schouwenbank is used for wave height, wave period, setup, wind direction and wind speed (multiplied with a constant reduction factor f_{WIND}), the data at Euro Platform is used for wave direction. Finally, the data at Vlissingen and Schouwenbank is used to determine the wind speed reduction factor f_{WIND}.

Assumptions in schematisations leading to deviations

Within in the assumptions made in the schematisation of the wind and wave climate, some deviations from "ideal" settings or choices are induced. Here, four of them are shortly described in a qualitative manner.

- The *first* deviation stems from the distance between the sea sided boundary and the measurement station at Schouwenbank (Figure 68 in Appendix 4). Wave transformation can occur over this distance. However, since this distance is relatively short, it is assumed that the conditions at Schouwenbank are more or less equal to the conditions at the sea sided boundary of the model.
- The *second* deviation is caused by applying the reduction factor of the wind speed f_{WIND}. Due to this, the wind speed at the boundary is lower, resulting in less energy transfer from the wind to the waves, which consequently results in smaller wave conditions. However, because of the small amount of reduction (f_{WIND} is 0.9) and the fact that a large amount of wave energy dissipates on the ebb tidal delta, the influence on the wave conditions is assumed to be small. Moreover, the error made when the wind speeds at the boundary (Schouwenbank) are applied at the entrance is expected to be larger.
- A *third* error occurs with the calculation of the wave conditions per wind direction and wind speed class. Within this approach it is implicitly assumed that the occurring wave conditions are directly correlated to the prevailing wind conditions. This is only the case for sea waves and is not necessary applicable to swell waves. Swell waves are only correlated to the wind conditions in the area they were generated, and are not correlated with the prevailing wind conditions at a measuring station outside that area. Hence, swell waves are not restricted to a certain class of local wind direction and wind speed but can occur at any of these classes. Swell waves are characterised by a relatively low wave height and a large wave period. When a swell wave is classified in a low wind speed class, the wave period is large compared to the wave period of the locally generated waves. The average wave period consequently increases. When a swell wave is classified in a high wind speed class, the wave height is low compared to the wave height of the locally generated waves. The average wave height consequently decreases for this class. The consequence of this approach is again assumed to be small, since the waves in the entrance of the Western Scheldt are mainly locally generated.
- A *fourth* error is made in the processing of the measured data, since no influence of change in conditions due to external factors (e.g. climate change, long-term variations in water levels) are taken into account. The wind and wave climate are derived on the assumption that no change in distribution has taken place of the twenty years of measurements. Also, when applying the wind and wave climate to make predictions on the medium-term morphological development, it is also assumed that the climate is representative for future conditions. For the relatively short time scale considered (relative from a large scale morphology point of view) it is not expected to influence the results. For longer time scales (multiple decades or centuries) it is recommended to investigate the change in contributions of the different classes over time.

4.2.2 WIND AND WAVE CLIMATE SCHEMATISATION

Time series of wind and wave conditions are available for the period 1 January 1981 – 1 January 2001. Figure 13 presents a part of these time series for the period 1 January 1996 – 1 January 1997. The whole time series are presented in Figure 73 in Appendix 4. The schematisation of the climate, based on the full time series of wind and wave conditions, is presented in Figure 14. In section 0, the correlation of wind and wave conditions are described.

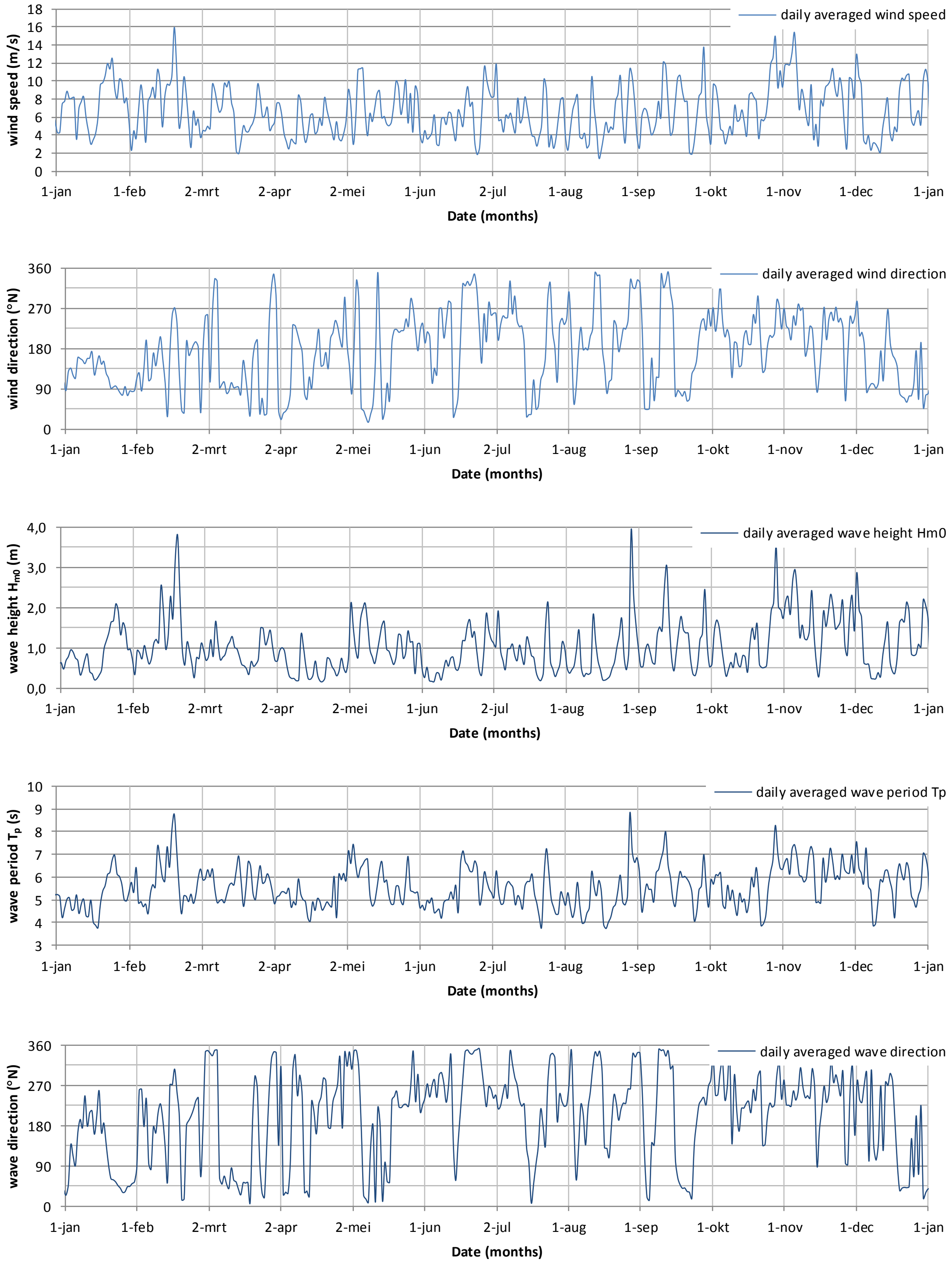

Figure 13. Time series of daily averaged wind conditions (upper two panels, light blue coloured) and daily averaged wave conditions (lower three panels, dark blue coloured) between 1 January 1996 and January 1997 at Schouwenbank.

Based on the available time series, the following figure present the schematised wind and wave climate used for this study. These climates, i.e. wind and wave conditions, are imposed on the sea sided boundary of the calculation grid.

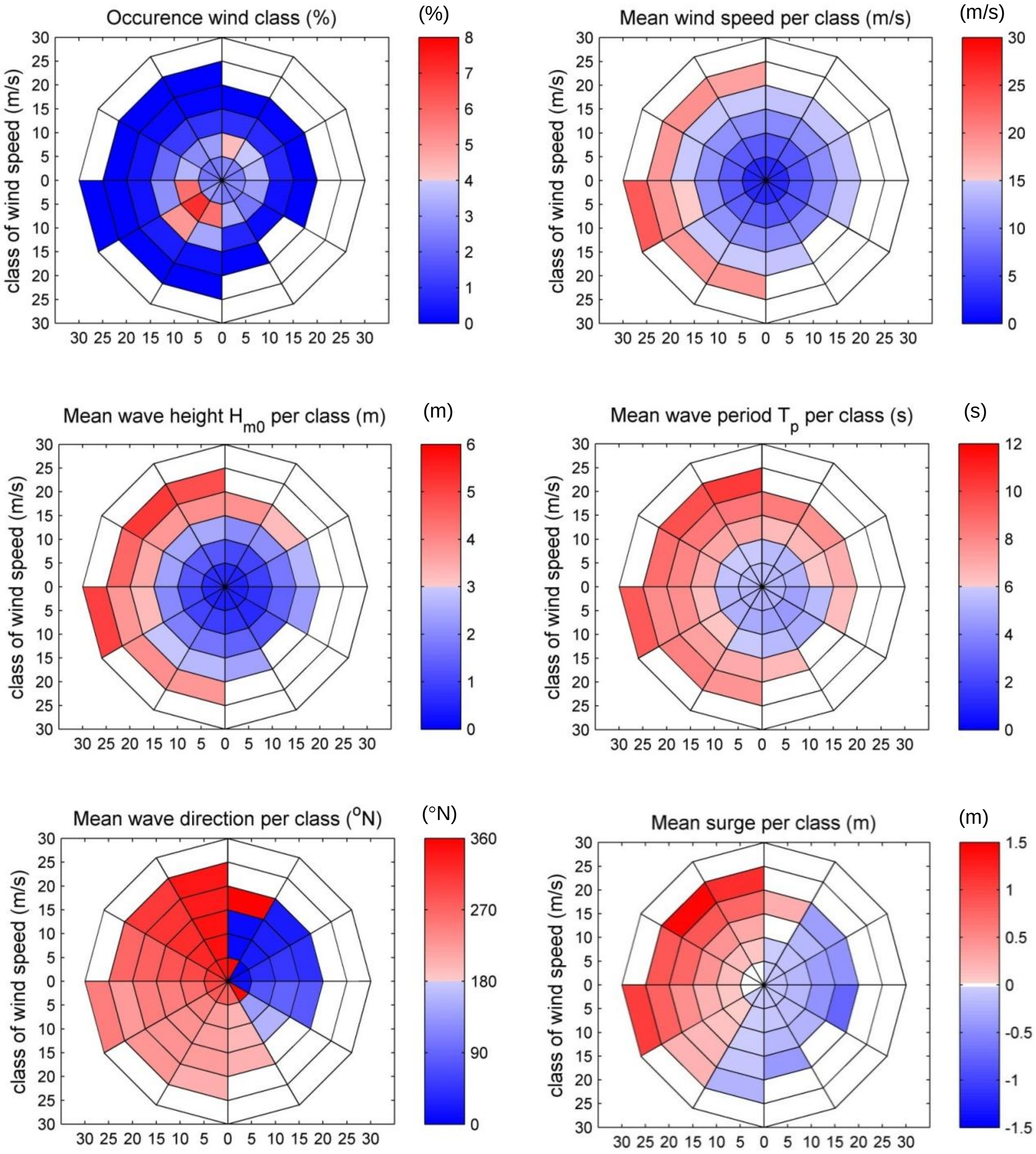

Figure 14. Overall wind, wave and surge climate at Schouwenbank. The top two figures present the wind climate. The middle and lower figures present the wave and surge climate. The climates are based on time series of measured wind, wave and surge conditions between 1 January 1981 – 1 January 2001.

Each rose exists of twelve wind direction sectors of 30° each. Each wind direction sector again exists of six wind speed classes with a range of 5 m/s each. This consequently results in 72 classes, divided over twelve direction sectors. The total range of wind direction is thus 0 °N – 360 °N, the total range of wind speed is 0 m/s – 30 m/s (classes 0-5, 5-10, 10-15, 15-20, 20-25 and 25-30 m/s). The class of wind speed can be read from the x-axis or y-axis. The wind direction can be found by relating the specific sector counter clock wise to the north, which is located at the top of the rose.

For each class, the corresponding mean measured values of wind, wave and surge conditions are calculated. These specific values are presented by a colour. The values of the colours are presented in the colour bars next to the roses. Some combinations of wind speed and wind direction didn't occur in the period 1981 – 2001; as a result, the climate schematisation exists of 54 different wind classes that did occur in that period. The top left rose presents the probability of occurrence of each class. This is obtained by counting the amount of times each class occurred in the time series of twenty years.

All classes have an individual number. A rose with the numbers of all classes is presented in Figure 69 in Appendix 4. The mean wind and wave conditions and surge for each of the 54 wind direction and wind speed classes is presented in Table 22 in Appendix 2.

Description of wind and wave climate

From the derived wind and wave climates it appears that the dominant wind direction is south-west with a typical wind speed between 5 and 10 m/s. This dominance of this wind direction is already explained in section 2.2.1. Higher wind speeds have a much smaller probability of occurrence. The westerly wind directions in general give the highest wind speeds. It appears that high wind speeds with a north-westerly wind direction lead to the highest waves and longest wave periods (explained by a longer fetch) and also result in the highest set-up (surge) of the water level. The high set-up can be explained by the fact that north-westerly wind directions are onshore directed. Easterly wind direction (offshore wind direction) lead to a set-down of the water level (negative surge). From the figure presenting the surge from different wind directions, the orientation of the coastline at the measuring station can easily be found (south-west to north-east directed). The occurring wave direction largely coincides with the prevailing wind direction, with a small deviation for wind directions between 0° N and 30° N (where the wave direction is between 330° N and 30° N) and wind directions between 150° N and 180° N (where the wave direction in between 180° N and 210° N). This might be due to refraction of the waves towards the coastline.
With the description, it is implicitly assumed that there is a strong correlation between occurring wind conditions and wave and surge conditions. The amount of correlation between different conditions and possible explanations for the correlation is presented in the next section.

Seasonality

In the presented overall wind and wave climates, no distinction is made between the winter (storm) season (October – April) and the summer (mild) season (April – September). Figure 70 and Figure 71 in Appendix 4 show the wind and wave climate for the winter and summer season over the period 1 January 1981 – 1 January 2001. From this follows that a clear distinction can be made between both seasons with respect to the occurring wind conditions. The reason for this seasonality is also explained in section 2.2.1. Storms from a westerly or north-westerly direction (20-25 m/s or higher) only occur in the storm season. Also high wind speeds between 15-20 m/s from a easterly direction only occur in the winter season. Furthermore, in the winter season, the wind direction is predominantly south-west, where in the milder summer season, next to the south-west direction there also is a large contribution from the north-west. In general, wind speeds are higher in winter, apparently leading to higher and longer waves, higher surges from the westerly directions (set-up) and larger negative surge (set-down) from the easterly directions.

4.2.3 CORRELATIONS WIND AND WAVE CONDITIONS

Measured wind, wave and surge conditions are plotted against each other to investigate the correlations. Insight in the correlation supports the analysis of the impact of different wind and wave classes on the morphological development. In Figure 73 in Appendix 4, the full time series of the wind and wave conditions over the time period January 1981 – January 2001 are presented (to keep an overview of the development of the conditions in time, the *weekly averaged* conditions are plotted. The period of time is too long to present the 3 hour or daily averaged conditions in a readable manner). To see a direct correlation between wind and wave conditions, reference is made to Figure 13 in section 4.2.2, where one year of the full time series is presented. The following tables present correlation coefficient between different conditions. The correlation coefficient (*r*) is defined by equation 4.5 in section 4.4.1. Figure 74 - Figure 76 in Appendix 4 present scatterplots of the different conditions and their correlation (correlation coefficient r^2).

Type of correlation	3 hours averaged	Daily averaged	Weekly averaged	Monthly averaged
Wind speed – wave height H_{m0}	0.83	0.88	0.91	0.92
Wind speed – wave period T_p	0.41	0.52	0.68	0.70
Wind speed – surge (wind direction sector 0° N – 90° N)	-0.49			
Wind speed – surge (wind direction sector 90° N – 180° N)	-0.58			
Wind speed – surge (wind direction sector 180° N – 270° N)	0.21			
Wind speed – surge (wind direction sector 270° N – 360° N)	0.70			

Table 4. Correlation coefficient between wind speed and wave height, wave period and surge. Location Schouwenbank.

Type of correlation	3 hours averaged	Daily averaged	Weekly averaged	Monthly averaged
Wave height – wave period T_p	0.75	0.81	0.87	0.86
Wave height – surge (wind direction sector 0° N – 90° N)	-0.44			
Wave height – surge (wind direction sector 90° N – 180° N)	-0.57			
Wave height – surge (wind direction sector 180° N – 270° N)	0.29			
Wave height – surge (wind direction sector 270° N – 360° N)	0.73			

Table 5. Correlation coefficient between wave height and wave period and surge. Location Schouwenbank.

Type of correlation	3 hours averaged	Daily averaged	Weekly averaged	Monthly averaged
Wind direction – wave direction	0.59	0.80	0.91	0.91

Table 6. Correlation coefficient between wind direction and wave direction. Location Schouwenbank.

It appears that there is a strong correlation (0.83 – 0.92) between the **wind speed** (first panel) and the **wave height (**third panel). When the wind speed and wave height are averaged over a longer period of time (3 hours average to monthly average), the correlation increases. The correlation between the **wind speed and wave period** is less clear (0.41 – 0.70). This can be explained by the fact that longer waves are not necessarily generated by the local occurring wind conditions, but are generated at a distant area and travel into the area of the interest (swell waves). The influence of swell waves also explains the relative low correlation between **wave period and wave height** (Table 5). Especially around the lower waves (H_{m0} smaller than 2.0 m), there is a large scatter of wave periods, indicating the presence of swell waves. Since swell waves have a relative low wave height, the scatter of wave periods at larger wave heights (h_{m0} larger than 2.0 m) is much smaller. This can be seen in the scatterplots in Figure 74 - Figure 76 in Appendix 4.

The correlation of the **wind speed and surge** strongly depends on the wind direction considered (table 5). The strongest correlation occurs for onshore wind directions (270° N - 360° N) and offshore wind directions (90° N - 180° N). Within these wind directions quadrants, the highest correlation occurs around 90° N (offshore directed) and around 300° N (onshore directed), both in the order of 0.75. As for the correlation between wind speed and surge, the correlation between **wave height and surge** strongly depends on the wind direction considered. The wave height and surge have the same amount of correlation per wind direction as the wind speed and surge. This is explainable, since the wave height is strongly correlated to the wind speed.

The **wind and wave direction** don't show a large correlation when the 3 hours averaged values are considered. However, it is assumed that wave direction does not change immediately with a change in wind direction, but that is lags behind. Therefore it's probably a better choice to correlate the daily averaged wind and wave direction. The daily averages show a much higher correlation than the 3 hourly averages, indicating that waves needs more than three hours to follow the change in wind direction. This improvement also stems from the fact that the wave direction around 0° N and 360° N are not corrected and therefore decrease the correlation (since the wind direction covers the full circle of 0° N to 360° N, the angle between values around 0 and 360 is small, but in the determination of the correlation the difference between 0° N and 360° N is determined as 360° N *minus* 0° N, resulting in a larger angle). When the wind and wave conditions are averaged over one day, this is implicitly solved.

4.2.4 STORM CONDITIONS

Based on theory, storms can have an large impact on the coast. To answer the research question to which extent the influence of waves during storms are taken into account (section 1.2), it is first necessary to state how storm is defined. According to the Royal Netherlands Meteorological Institute (KNMI), a wind force 9 on the Beaufort scale is called a storm (Figure 72 in Appendix 4). Wind force 9 Beaufort means a wind speed between 20.8 and 24.4 m/s and based on this criterion and the derived wind climate, seven storm classes can be distinguished, all with a westerly wind direction. These storm classes all occur in the winter season (October – April). These are classes 28, 33, 38, 39, 44, 49 and 54. The numbers of these classes can be found in Figure 69 in Appendix 4. Their average conditions can be found in Table 22 in Appendix 2.

A storm will, due to an increase in wind speed, in general, result in higher and longer local generated waves and an increase in set-up or set-down of the water level (depending on the wind direction with respect to the coastline). Furthermore, due to the increase in wave height, depth-induced wave breaking occurs further offshore compared to lower waves (under the assumption that the water level is equal for both situations and the water depth decreases when approaching the shore). With respect to the entrance of the Western Scheldt, with higher water levels due to wind set-up at westerly wind directions, waves are able to travel further into the estuary compared to the situation without a set-up of the water level.
In chapter 6, the relative influence of a storm event on one year of morphological development is assessed.

4.3 WAVE MODELLING

4.3.1 APPROACH

As mentioned in the introduction of this chapter, multiple wave simulations are performed. The objective of these simulations are threefold:

- Validation of the wave model as used in the morphological simulations in chapters 5 and 6:
- Addressing the influence of choices in the climate schematisation in section 4.2.1:
- Addressing the influence of currents, wind conditions and wave boundary conditions on the wave conditions at the entrance of the Western Scheldt.

To assess the validity of the used wave model, results on wave data from a simulation over a short period of time (fourteen days) are compared to measured wave data. At the end of this section it is concluded, based on statistics, that the wave model reproduces the actual wave conditions, outside and inside the estuary, rather well. Therefore, the results of the wave modelling are also used to obtain understanding in the influence of different contributions (wind, currents, imposed wave conditions at the boundary) on the wave conditions on the ebb tidal delta and in the estuary.

For the simulations, a time series of simulated water levels (Grasmeijer, 2012) and measured wave conditions are imposed on the sea sided boundary of the model (Figure 11). Wind conditions are imposed on the whole calculation grid. For the validation of the wave model, the simulated wave conditions are compared with measured wave conditions on seven locations: three at the sea side of the ebb tidal delta, one location at the estuary side of the ebb tidal delta and three locations inside the estuary (Figure 12 shows the locations of measurement stations):

- Domburger Rassen (DORA; sea side of ebb tidal delta)
- Deurloo (DELO; sea side of ebb tidal delta)
- Scheur West (SCHW; sea side of ebb tidal delta)
- Wielingen (WIEL; estuary side of ebb tidal delta)
- Westerschelde Container Terminal (WCT1; inside estuary)
- Hoofdplaat (HFPL; inside estuary)
- Pas van Terneuzen (PVT1; inside estuary)

After the validation of the model, a sensitivity analysis is performed. Within this sensitivity analysis, the influence of choices within the climate schematisation (such as the measuring station used for the imposed wave conditions) is assessed by applying alternative choices in the simulations (e.g. to use another measuring station for the imposed conditions). Also the influence of different contributions on the wave conditions is assessed (wind, currents, imposed wave conditions) by applying or omitting these specific contributions in the simulations and comparing the results of the simulations. The found influences are confirmed and complemented by the results of the wave simulation within the short morphological simulations from chapter 5.

The wave simulations are performed with the SWAN wave model as implemented in Delft3D. The reason for this is that the morphological simulations also use SWAN as implemented in Delft3D. All model settings for the simulation of the waves are the same as the settings used for the short and medium-term morphological simulations (section 3.2.3). Within the simulation, communication between the WAVE and FLOW module is applied on the water levels, currents and waves. Hence in the simulations, wave-current and current-wave interactions (section 3.2.3) are taken into account.

4.3.2 WATER LEVELS AND CURRENTS

The water levels and currents that are imposed on the sea sided boundaries of the calculation grid are adopted from (Grasmeijer, 2012). In that study, the boundary conditions on water levels and currents are simulated for the whole year of 2006. For the assessment of the wave modeling in this study, only use is made of the time series between 18 May 2006 and 2 June 2006. The reason for this is that the spring neap cycle over this period of fourteen days is representative for the tidal motion over the whole year (Grasmeijer, personal communication) and a period of fourteen days is assumed to be enough to assess the quality of the wave modeling for this study (Van Vledder, personal communication). The water levels and currents are imposed as a time series with a step size of 30 minutes between the individual data on water levels and currents. In (Grasmeijer, 2012) it is shown that this imposed time series reproduces the measured water level in the estuary very well.

4.3.3 WIND

For the considered period of simulation (18 May 2006 – 2 June 2006), hourly wind conditions at Vlissingen (speed and direction) are imposed as a time series. The conditions are imposed on the total area of simulation and are uniform in space. The use of the wind conditions at Vlissingen slightly differs from the used wind conditions in the morphological simulations. There, use is made of the wind conditions at Schouwenbank, corrected with a factor f_{wind} 0.9 on the wind speed to take into account the decrease of wind speed between Schouwenbank and Vlissingen (section 4.2.1). For the considered period of simulation here, no wind data from Schouwenbank is available. For this reason, wind conditions at Vlissingen are used. Comparison of the wind climates at Schouwenbank and Vlissingen shows that the wind climates are similar to a large extent. Therefor it is assumed that the use of the wind conditions at Vlissingen for the assessment of the wave model is legitimate.
Figure 77 in Appendix 4 shows the wind conditions over the considered period of simulation.

4.3.4 WAVES

The wave conditions are imposed as a time series on the sea sided boundary of the model. The wave conditions considered are the significant wave height (H_{m0}), peak wave period (T_p) and wave direction. Furthermore, spectral parameters are specified (section 3.3.3). Equal to the settings in the morphological simulations, the wave height and wave period are obtained from the measurement location at Schouwenbank, while the wave direction is obtained from the measurement location at Euro Platform. The specification of the spectral parameters is equal to that which is used in the morphological simulations (described in section 3.3.3). To impose the wave conditions as a time series in the WAVE module of Delft3D, use is made of *wavecon* files. The use of this file implies that the only wave period to be considered is the peak period (T_p). Since this period is not measured directly or derived from buoy measurements, it must be derived from the calculated spectral wave periods T_{m02} or $T_{m-1.0}$. The peak period is obtained by multiplication of T_{m02} with a factor of 1.3. This factor is more or less equal to the ratio between peak period and spectral period T_{m02} for a JONSWAP spectrum with a peak enhancement factor of 3.3 and a tail of f^{-5}. For other types and shapes of the spectrum this ratio may differ. Here, it is implicitly assumed that the real wave spectrum has the shape of such a JONSWAP spectrum. This means that possible present multiple peaks in the spectrum (due to e.g. swell waves) are not taken into account. For this part of the North Sea however, swell can be present (Bosboom and Stive, 2011); possible consequences are already mentioned in section 4.2.1.

4.3.5 VALIDATION AND SENSITIVITY ANALYSIS

For the validation and sensitivity analysis, nine different wave simulations over the same period of time were executed (fourteen days). The first wave simulation (number 10) [10] has the same settings as are used in the morphological simulations and is used as validation of the wave model. The other eight simulations all differ from that simulation to assess the influence of specific model choices (no. 11, 12, 13 and 18) or to gain insight in the contribution of the imposed wave conditions, currents and wind on the simulated wave conditions (no. 14, 15, 16 and 17). Table 7. Performed wave simulations. gives an overview of the performed wave simulations.

The results of the sensitivity analysis are described in the next section, including time series of the validation simulation (no. 10). Other figures and tables from this and other simulations are included in the Figure 78 - Figure 102 in Appendix 4.

No.	Description
10	H_{m0}, T_p from Schouwenbank, wave direction from Euro Platform. T_p based on T_{m02}.
11	As number 10, but with wave direction from Schouwenbank
12	As number 10, but with H_{m0}, T_p from Scheur West
13	As number 10, but with T_p based on $T_{m-1.0}$.
14	As number 10, but without currents and hence without wave-current interaction
15	As number 10, but without the imposed wave conditions on the model boundary
16	As number 15, but with a shift of the wind direction of 45°
17	As number 10, but without imposed wind conditions
18	As number 10, but with a step size in the FLOW module of 0.4 min (instead of 0.2 min)

Table 7. Performed wave simulations.

[10] The first simulation as presented in this thesis is simulation number 10. The nine calculation previous to that simulation were executed to test the model on a smaller time scale.

4.4 RESULTS OF THE WAVE MODELLING

4.4.1 VALIDATION OF THE WAVE MODEL

Extra post-processing on the wave period

For the comparison of the simulated and measured wave periods, extra post-processing on the simulated wave period is needed. The reason for this is that the wave periods, as measured (or derived from these measurements) by the HMCZ buoys (www.hmcz.nl) are written as specific file types *GHr2* (0 – 1,000 mHz) and *GDr2* (0 – 500 mHz). From buoy measurement of the *GHr2* type, the wave period T_{m02} is calculated from the wave spectrum between the frequency bands 0.03 Hz – 1.0 Hz. No specification is given on the frequency bands within the spectrum on which the $T_{m-1.0}$ is based. It is assumed that this is the whole range between 0 Hz and 1 Hz. Important to notice that the tail of the spectrum with frequencies higher than 1 Hz (i.e. wave periods shorter than 1 s) are *not* accounted for in the calculation of the wave conditions. In the SWAN wave model, frequencies higher than 1 Hz *are* accounted for (the parametric tail of the spectrum includes higher frequencies up to 10 Hz). The application of these higher frequencies in the simulations result in a systematic lower wave period compared to the measurements. As a result, the wave periods from measurements and simulations can't be compared directly. To account for this mismatch, the wave periods from simulation must be corrected (multiplied) with a factor 1.3 – 1.5 (Van Vledder, personal communication).

Results

Results of the wave simulation with the settings as used in the morphological simulations (no. 10) are compared to measured wave conditions [11]. Figure 15 to Figure 18 show a good resemblance between the time series of simulated wave heights and periods and the measured wave height around the ebb tidal delta and the entrance of the Western Scheldt. Further away in the estuary (Hoofdplaat and Pas van Terneuzen), the differences between the measured and calculated time series increase somewhat. The specific measurement locations are mentioned in the panels in the figures. An overview of the measurement locations are presented in Figure 12 (section 4.2). Figure 78 - Figure 84 in Appendix 4 show scatterplots of the measured and calculated wave conditions and tables with statistical parameters for the seven locations.

The resemblance between the simulated and measured wave conditions can also be found from the statistical parameters based on simulation and measurements (Figure 78 - Figure 84 in Appendix 4). Table 8 and Table 9 in this section show all considered statistical parameters for the validation simulation (no. 10). The definitions of these statistical parameters are given by equations 4.1 – 4.8. The reproduction quality is high when the correlation coefficient (r) approximates the value of 1 (-) and the scatter index (SI) approximates the value of 0 (m). In general, the correlation coefficient between the measured and simulated wave heights is high and the scatter index is low for the location outside the estuary. Inside the estuary the correlation decreases, while the value of the scatter index increases, indicating that the quality of the reproduction decreases inside the estuary.

In general, the simulated wave height correlates better to the measured wave height than the simulated wave period correlates to the measured wave period. The measured wave period is somewhat larger than the simulated (post-processed) wave period. This is in agreement with the conclusions by Van Vledder (2007) as presented in section 3.3.1. There it is stated that the underestimation of the wave periods can be

[11] Here, the simulated significant wave height H_{m0} and wave period T_p are compared with measurements. Simulated wave directions are not compared with measurements since the wave direction is not measured around the estuary entrance.

up to 20% with an average underestimation of the wave periods is about 0.9 s. From the scatterplots (Figure 78 - Figure 84 in Appendix 4), this 0.9 s can be found as well. There are multiple reasons that might explain the underestimation. First of all, there is a difference between the frequency range in the spectrum on which the wave periods are based in SWAN and the buoy measurements. In the post-processing, this is solved by multiplying the simulated wave period with a constant factor (1.3 – 1.5). In reality, this factor changes over time, as the spectrum changes over time. Furthermore, from the sensitivity analysis (section 4.4.3) it appears that the wave period is relative sensitive to currents compared to the significant wave height. Hence, larger deviations between measured and simulated wave periods and hence lower correlation coefficients can be expected at locations with large currents, such as at the channels of Honte (where the measurement station of Westerschelde Container Terminal (WCT) is located) and Pas van Terneuzen (where the measurement station of Pas van Terneuzen is located). At these locations the quality of the reproduction of the wave period is less compared to other locations and also less than the reproduction of the wave heights at these locations.

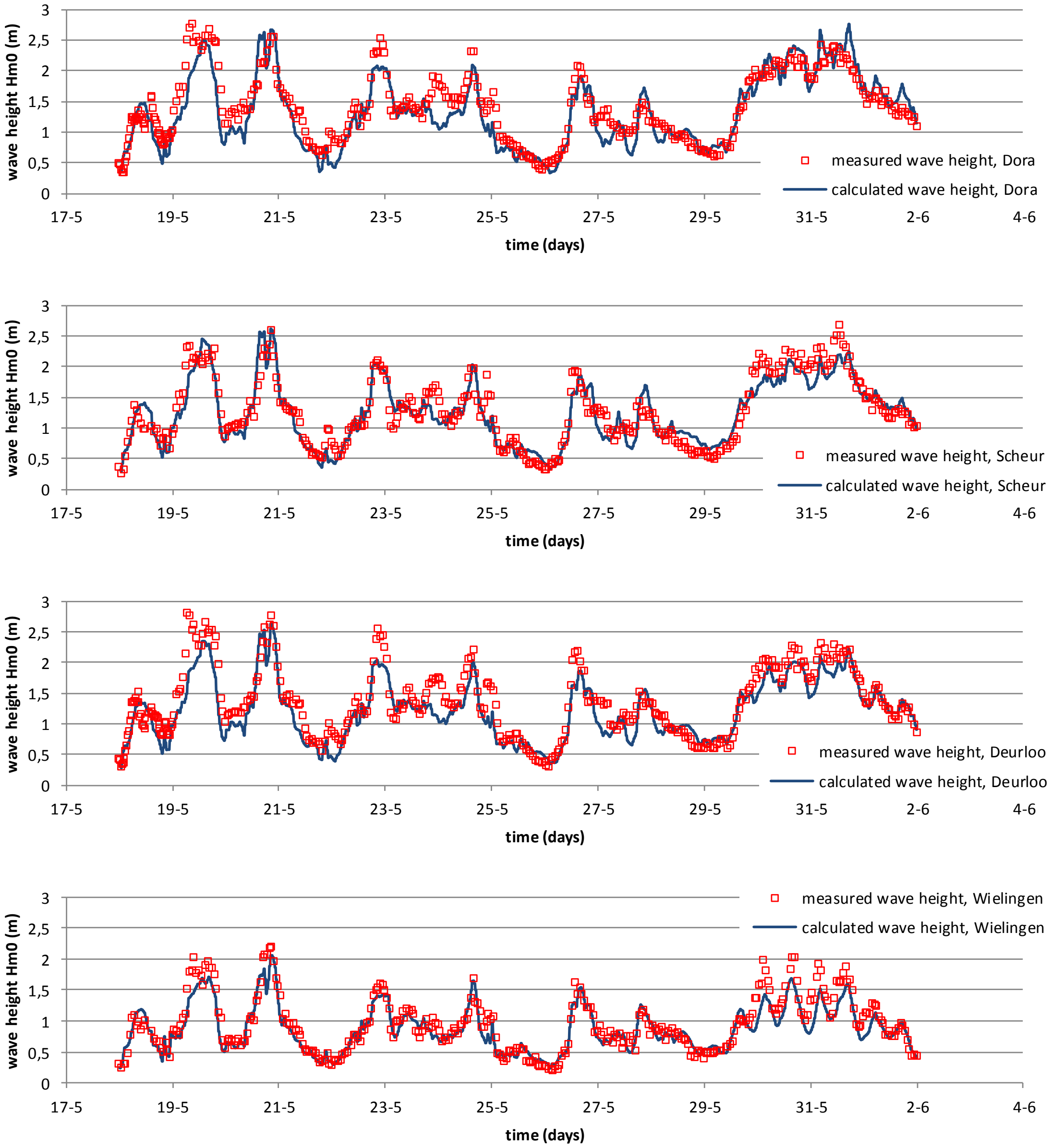

Figure 15. Comparison of simulated and measured significant wave height H_{m0} at locations outside the estuary. Locations are mentioned in the graphs.

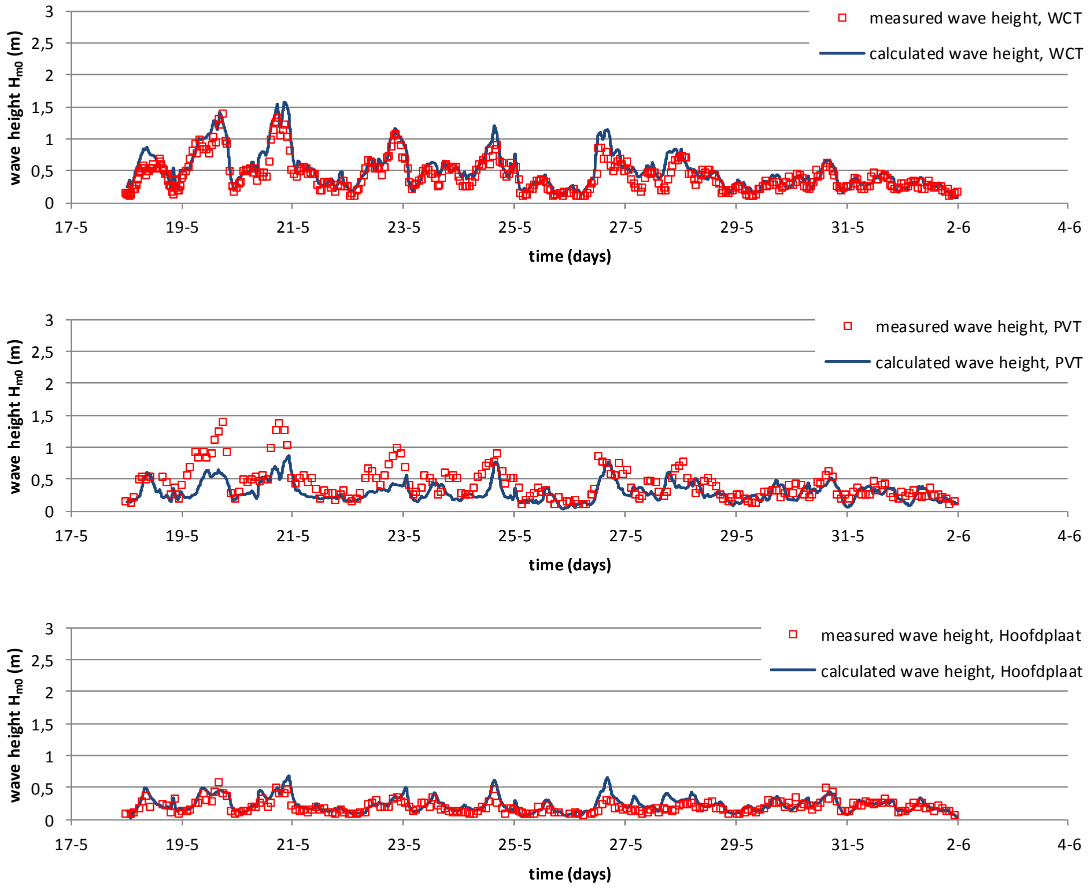

Figure 16. Comparison of simulated and measured significant wave height H_{m0} at locations inside the estuary. Locations are mentioned in the graphs.

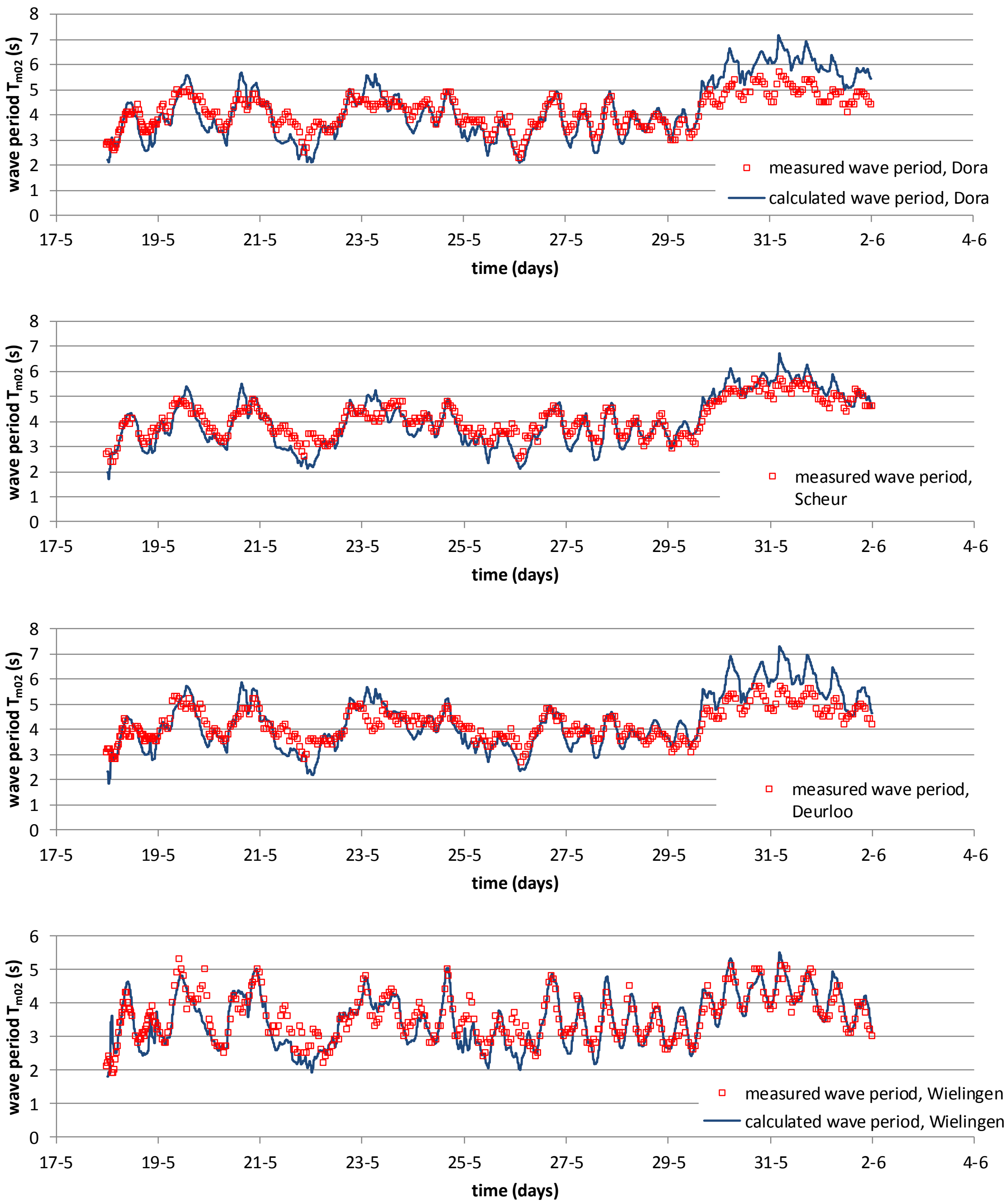

Figure 17. Comparison of simulated and measured wave period T_{m02} at locations outside the estuary. Locations are mentioned in the graphs.

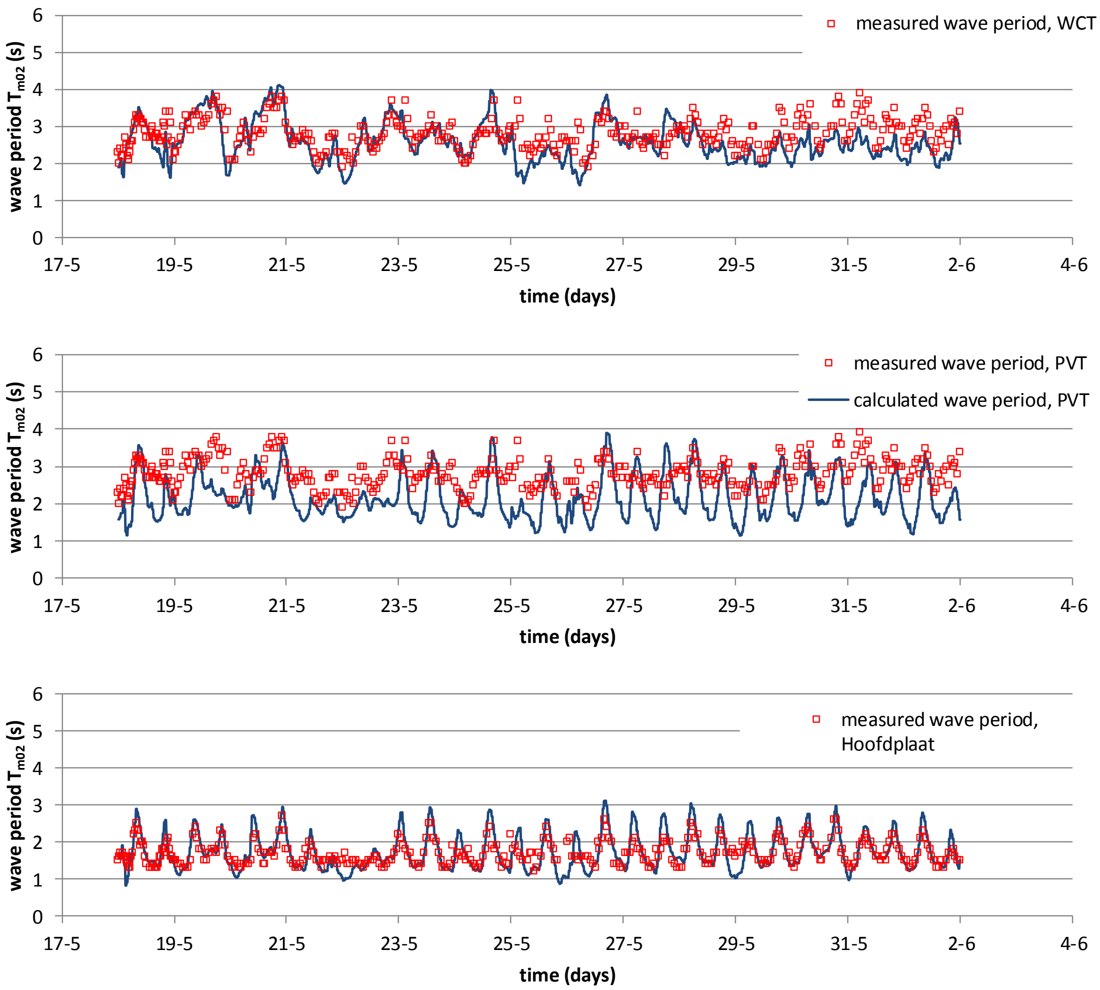

Figure 18. Comparison of simulated and measured wave period T_{m02} at locations inside the estuary. Locations are mentioned in the graphs.

Statistical parameters

The statistical performance of the wave model is expressed in statistical parameters. These are calculated from measured and simulated values for the wave parameters H_{m0} and T_p. The following statistical parameters are used, where x_i represent measured values and y_i simulated values and where n is the amount of values (obtained from Van Vledder, 2007).

The mean values of x and y become:

$$mean = \quad \bar{x} = \frac{1}{n}\sum_{i=1}^{n} x_i \qquad \bar{y} = \frac{1}{n}\sum_{i=1}^{n} y_i \tag{4.1}$$

The bias is defined as the difference between the mean measured and mean simulated value and is a measure for the difference between the measured and simulated values:

$$bias = \quad (\bar{x} - \bar{y}) = \frac{1}{n}\sum_{i=1}^{n}(x_i - y_i) \tag{4.2}$$

The root mean square difference (rms) is another value for the difference between the measured and simulated values, defined by:

$$rms = \quad \left[\frac{1}{n}\sum_{i=1}^{n}(x_i - y_i)^2\right]^{1/2} \tag{4.3}$$

The standard deviation (stdev) of the differences between measured and simulated values becomes:

$$stdev = \quad \left[\frac{1}{n-1}\sum_{i=1}^{n}[(x_i - \bar{x}) - (y_i - \bar{y})]^2\right]^{1/2} = \left[\frac{1}{n-1}\sum_{i=1}^{n}(x_i - y_i - bias)^2\right]^{1/2} \tag{4.4}$$

The linear correlation coefficient (r) between the measured and simulated values is defined by:

$$r = \quad \rho(x,y) = \frac{cov(x,y)}{\sigma(x)\,\sigma(y)} \tag{4.5}$$

Where *cov* is the covariance between the measured and simulated values, indicating in which way these values are correlated:

$$cov = \quad cov(x,y) = \frac{1}{n}\sum_{i=1}^{n}[(x_i - \bar{x})\,(y_i - \bar{y})] \tag{4.6}$$

And where σ is the standard deviation of the measured and simulated values:

$$\sigma = \sqrt{Var} = \quad \sigma(x) = \left[\frac{1}{n}\sum_{i=1}^{n}(x_i - \bar{x})^2\right]^{1/2} \qquad \sigma(y) = \left[\frac{1}{n}\sum_{i=1}^{n}(y_i - \bar{y})^2\right]^{1/2} \tag{4.7}$$

The scatter index (SI) is a measure for the root mean square difference (Rms) relative to the mean simulated value ($\bar{y}$), indicating the relative influence of the found difference:

$$\mathrm{SI} = \quad SI(y) = \frac{rms}{\bar{y}} \tag{4.8}$$

A value for the bias of zero means that the measured and simulated wave parameters are unbiased and the simulated wave parameter is an unbiased estimator for the measured wave parameter. In other words: the closer the value of the bias becomes to zero, the closer (better) the simulated value approximates the measured value. The same holds for the root mean square difference (with the difference that the rms always has a positive value) and the scatter index (the closer to zero the better). A value of the linear correlation coefficient of one indicates a perfect correlation between the measured and simulated values (which does not mean that the values are equal). Hence, for a good approximation of the measured values, the bias, rms, stdev and SI must be close to zero and the value of r must be close to one.
In the next tables, the different statistical parameters are presented for the seven measurement locations. Furthermore, the *squared* linear correlation coefficient (r^2) is presented as well, since this value is used in the scatterplots (Figure 78 - Figure 84 in Appendix 4).

Statistical parameters on wave height H_{m0}							
calculation 10							
Location	**mean (m)**	**bias (m)**	**rms (m)**	**stdev (m)**	**r (-)**	**r^2 (-)**	**SI (-)**
Dora	1.34	-0.08	0.27	0.26	0.90	0.81	0.20
Scheur west	1.25	-0.02	0.22	0.22	0.92	0.84	0.18
Deurloo	1.22	-0.14	0.27	0.23	0.91	0.83	0.22
Wielingen	0.88	-0.06	0.18	0.17	0.93	0.86	0.21
WCT	0.51	0.09	0.15	0.12	0.92	0.84	0.29
Hoofdplaat	0.24	0.05	0.09	0.07	0.78	0.61	0.38
PVT	0.30	-0.12	0.22	0.19	0.67	0.45	0.73

Table 8. Statistical parameters on simulated significant wave height H_{m0}.

Statistical parameters on wave period T_{m02}							
calculation 10							
Location	**mean (s)**	**bias (s)**	**rms (s)**	**stdev (s)**	**r (-)**	**r^2 (-)**	**SI (-)**
Dora	4.23	0.11	0.64	0.63	0.90	0.81	0.15
Scheur west	4.03	-0.05	0.44	0.44	0.92	0.85	0.11
Deurloo	4.34	0.12	0.61	0.60	0.89	0.79	0.14
Wielingen	3.51	-0.06	0.42	0.42	0.85	0.72	0.12
WCT	2.59	-0.22	0.51	0.46	0.57	0.32	0.20
Hoofdplaat	1.74	0.04	0.29	0.29	0.82	0.66	0.17
PVT	2.18	-0.64	0.84	0.53	0.49	0.24	0.38

Table 9. Statistical parameters on simulated wave period T_{m02}.

The found statistical values are in line with the statistical values as found by Van Vledder (2007). In (Van Vledder, 2007) the reliability of the SWAN wave model (version 30.75) was tested for storm conditions in the Western Scheldt (section 3.3.1). From this it can be concluded that wave simulation is performed in the right way. Based on the found statistical parameters between the measured and calculated wave conditions it can be concluded that the wave model with its specific settings performs reproduces the wave conditions rather well. Hence the wave model is applicable and therefore applied for the morphological simulations in chapter 5 and chapter 6.

4.4.2 INFLUENCE OF CHOICES IN MODELLING APPROACH

Table 7 gives an overview of the performed simulations. The influence of specific choices in the climate schematisation are investigated by simulations 11, 12, 13 and 18. Figure 78 - Figure 84 in Appendix 4 show the statistical parameters for these simulations. Figure 85 - Figure 90 in Appendix 4 show the time series of calculated wave conditions at the seven considered locations.

Influence of the wave direction Euro Platform (simulation no. 11)
In this simulation, the influence of the choice of the measurement station for the wave direction is assessed. In simulation 11, the wave direction from Schouwenbank is used instead of the wave direction of Euro Platform. Comparison of the two simulations based on graphs of time series doesn't show any difference in simulated wave conditions. Statistical parameters show that the simulation based on wave directions from Schouwenbank have a slightly higher correlation coefficient (1-3%) with the measured conditions than wave directions from Euro Platform. Furthermore, the rms deviation is slightly lower (1-5%) than wave directions from Euro Platform. Based on the higher correlation and lower rms deviation, use of wave directions from Schouwenbank is preferable. However, since no data on wave direction is available from Schouwenbank in the period 1981 – 2001 and the difference in correlation and rms deviation is small, it is allowable to use the data on wave direction from Euro Platform for the morphological simulations. Therefore, in the morphological simulations, wave directions from Euro Platform are applied.

Influence of the wave conditions Scheur west (simulation no. 12)
When wave conditions as measured at Scheur West are used as imposed boundary conditions, the correlation between measured and simulated wave conditions decreases. This can best be seen from the statistical parameters for simulation 12 (Figure 78 - Figure 84 in Appendix 4), where the *SI* with the measured conditions increases with 10% - 50% compared the simulation 10 (which is based on wave conditions at Schouwenbank). The reason for this can be explained by the location of measurement station Scheur West in the calculation grid. Scheur West lies in the middle of the grid where the wave conditions might already be affected by the local bathymetry. Applying these conditions on the boundary model therefore might result in affecting the wave conditions twice. Therefore, it is not recommended to use the measurement station Scheur West as imposed conditions for the calculation grid as applied in this study.

Influence of T_p based on $T_{m-1.0}$; (simulation no. 13)
Outside the estuary, the choice of whether the imposed wave peak period is based on T_{m02} or $T_{m-1.0}$ hardly influences the simulated wave conditions and correlation with measured conditions, with a small benefit for T_{m02} in terms of *r* and *SI*. Based on a JONSWAP shape spectrum with an peak enhancement factor of 3.3 and a tail of f^{-5}, a constant ratio between T_p and $T_{m-1.0}$ of 1.1 is applied. Inside the estuary, the correlation of the simulation based on $T_{m-1.0}$ further decreases. A possible explanation for this is that the $T_{m-1.0}$ is more sensitive to changing of the spectrum shape. From wave modelling results it is shown that an extra peak is generated in the wave spectrum, assumably caused by the local wind conditions [12]. In this case, applying the peak wave period for description of the wave spectrum (implicitly assuming one peak in the spectrum) is not ideal. Applying another spectral wave period to account for multiple peaked spectra might result in a better reproduction of the wave conditions. At this moment however, when applying wave conditions as time series, only the peak wave period can be applied in the WAVE module of Delft3D (via the *wavecon* files).

[12] From the simulations as discussed in section 4.4.3 indeed follows that the influence of the wind conditions increases when waves propagate from the North Sea towards the estuary. Inside the estuary, the wind influence becomes dominant.

Influence of a larger time step (simulation 18)

In simulation 18, the size of the time step in the FLOW module is increased from 12 s to 24 s. The reason for this is that in the relative short morphological simulations (chapter 5), the used time step is 24 s. The time step size from the short morphological simulations (section 5.3) has been doubled to decrease the simulation run time, which otherwise would be too long (related to the schedule of this thesis). The communication step between the FLOW and WAVE module is kept the same (30 min, section 0). The influence of the increase of the time step size on wave conditions, water level and depth averaged velocity is assessed by comparing simulation 18 to simulation 10. From this comparison it can be seen that there are no differences in the simulated significant wave height, wave peak period and wave direction (Figure 85 - Figure 90 in Appendix 4). Furthermore, there are no large differences in water level and depth averaged velocity. During the spin up time, differences in the water levels of the two simulations are a few cm and after the spin up time the maximum differences are a few mm. For the depth averaged velocity comparable values hold: during the spin up time, the differences are a few cm/s, after the spin up time the maximum differences are a few mm/s. Compared to the absolute values of water levels and depth averaged velocities, these differences are negligible. From these results can be concluded that the differences in simulated wave conditions, water levels and depth averaged velocities are negligible compared to the results with a time step size of 12 s. The time step as used in the morphological simulations in chapter 6 is thus 24 s. (The time step of the morphological simulations in chapter 5 remain at 12 s, because these simulations were already run before this analysis.)

4.4.3 INFLUENCE ON WAVE CONDITIONS

Table 7 gives an overview of the performed sensitivity simulations. The influence of currents, imposed wind conditions and wave boundary conditions on the local wave conditions inside the estuary are investigated by simulations 14, 15, 16 and 17. Figure 91 - Figure 102 in Appendix 4 show the time series of simulated wave conditions at the seven considered locations (section 4.3.1).

Furthermore, from the short morphological simulations for all defined wind and wave classes (54 classes, Figure 14) in section 5.3, also insight in the influences on the wave conditions inside the estuary is obtained. This insight is in line with findings from the sensitivity simulations 14, 15, 16 and 17. Moreover, insight from the 54 individual classes partly complement the found results based on the sensitivity simulations. For that reason, the description of the results from the short morphological simulation that are related to wave propagation and transformation is included in this section. The results from the short morphological simulations related to sediment transport and morphological development are presented in section 5.3. For these morphological simulations, multiple "observation points" are placed in the calculation grid. Five of them are presented in the results. These are observation points RP2, VR, G4M, G7N and G8N (Figure 24). The results on the wave propagation and transformation for the 54 individual wind and wave classes are presented in Figure 150a up an till Figure 203a in Appendix 5.

Influence ebb tidal delta

The ebb tidal delta plays a crucial role in the relative influence of the imposed wave boundary conditions at the North Sea and imposed wind conditions on the local wave conditions. A large amount the of wave energy is dissipated over the ebb tidal delta when waves approach the estuary from a westerly direction. This can also clearly be seen when the time series of wave height and wave period at the seven measurement location (Figure 15 - Figure 18) are compared: a strong decrease of wave height and wave period occurs when waves travel towards and into the estuary. When plotted in a spatial scale, as done for the 54 individual wind and classes, this influence can be seen even better. After further analysis in this section it is subsequently concluded that the influence of imposed wave boundary conditions (wave conditions at the North Sea) on the local wave conditions inside the estuary decreases when waves propagate towards and into the estuary. At the same time, the influence of the imposed wind conditions on the local wave conditions increases. A simple method to quantify both relative influences based on these results is introduced in the section 4.4.4.

The wave conditions eastwards of the shoals of Spijkerplaat are mainly locally influenced due to the presence of the ebb tidal delta in front of the Western Scheldt [13]. When waves propagate from an westerly direction, the ebb tidal delta is very determining for the wave conditions in the entrance of the estuary behind the ebb tidal delta. At the ebb tidal delta, the water depth strongly decreases. This decrease in depth results in stronger refraction of waves, dissipation of wave energy due to bottom friction, shoaling and depth induced breaking of the waves at times of relatively low water depths. When waves propagate from a westerly direction (from the North Sea) towards the entrance of the Western Scheldt, a large amount of wave energy is dissipated on the ebb tidal delta. Since the amount of dissipation of wave energy is strongly related to the water depth, more dissipation occurs at lower water levels (low water) than at higher water levels (high water).

The dissipation of energy results in a decrease of the wave height and wave period over the ebb tidal delta. This can clearly be seen in Figure 19, where the significant wave height in the considered area is presented. The significant wave height at the North is about 3.0 m, which strongly decreases over the ebb tidal delta to about 1.5 m at the line Vlissingen Breskens.

For the significant wave height (as an important indicator for morphological impact due to waves), the ratio between the significant wave heights inside and outside the estuary is to a large extent the same for all individual classes of the schematised wave climate (Figure 14). Around the line Vlissingen - Breskens, the significant wave height is around 40% – 60% of the significant wave height at the North Sea just westwards of the ebb tidal delta. Between Vlissingen en Terneuzen, the significant wave height is only about 20% – 30% of the significant wave height at the North Sea just westwards of the ebb tidal delta. Consequently, the highest wave conditions outside the estuary also result in the highest wave conditions inside the estuary (for westerly wind and wave directions). Although the influence of wind conditions dominate the local wave conditions inside the estuary this is explainable, since wave conditions strongly correlate to wind speeds.

Waves from north westerly and south westerly directions strongly refract at the shoals of the ebb tidal delta. Consequently, the waves tend to refract towards a direction perpendicular to the longitudinal axis of the Western Scheldt estuary. For waves at deep water with a wave direction already in line with the estuary (around 300° N), hardly any refraction occurs. The amount of refraction of the waves also depends on the wind direction and wind speed. When high wind speeds occur, the wave direction seems to be dominated by the wind direction and less refraction over the shoals occurs.

[13] The importance of wind conditions on the wave conditions inside the estuary justifies the approach to classify the wave conditions in wind direction and wind speed classes (section 4.2.1).

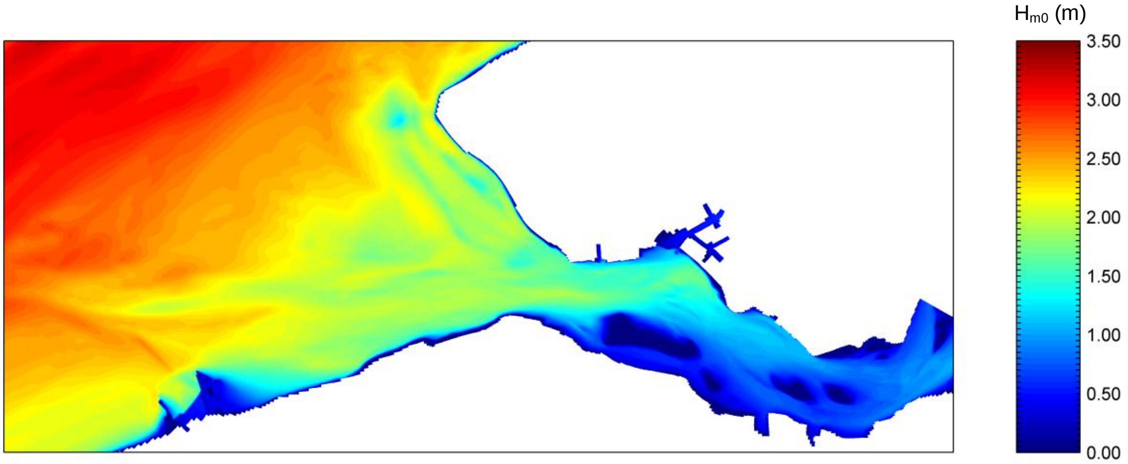

Figure 19. Influence ebb tidal delta on significant wave height of wave conditions from westerly directions. Presented is a time step from the validation simulation (simulation no. 10). Wind and waves have a westerly direction, the wind speed is 17 m/s.

Influence of tidal currents

The tidal currents have an influence on the wave conditions, both inside and outside the estuary. Inside the estuary this influence increases with the velocity of the currents. Both the wave height and wave period increase when the current is opposite to the wave direction. As a result, waves travelling to the west tend to become higher and longer when the flood current occurs (leading to high water), for waves propagating to the east this occurs during ebb currents (leading to low water). The wave height and period decrease when the wave direction is equal to the current direction. In this process, the current velocity is important; a higher velocity has more influence on the wave conditions.

The growth of the waves can be explained by the fact that waves and current have in this case an opposite direction, resulting in the bunching of energy: the waves travelling towards the current are slowed down (leading to an increase of the wave period) and start to shoal on the opposing current. This effect is strongest when wave and current direction are 180° opposite, but also occurs when the angle between the two is less (but still higher than 90°). When the direction of the current reverses (in this case from flood current to ebb current), the opposite occurs: waves travel with the current, leading to lower significant wave heights and shorter wave periods. Both can clearly be seen e.g. for wave class 16 (Figure 165a in Appendix 4), where the wave direction in the estuary is about 90° N to 120° N.

In the sensitivity simulation regarding the influence of the current (no. 14), in the estuary the currents influence the wave height with about 10% (Figure 95 and Figure 96, Appendix 4). The influence of the current on the wave conditions in time can clearly be seen when next to the wave conditions and currents, also the water level in time is presented; the variations of wave conditions coincides with the tidal motion. Without currents, the wave conditions show less fluctuation in time (tidal motion) than the conditions in the situation with currents. The influence of currents on the wave period outside the estuary is limited (Figure 98 - Figure 102, Appendix 4).

Inside the estuary, tidal currents and wind conditions influence the wave direction. When wind speeds are high, the wave direction turns towards the wind direction. When wind speeds are low (with consequently low waves) , the influence of currents on the wave direction increases. Furthermore, when wind speeds are low, the waves are in general shorter, resulting in a lower phase speed of the waves. Due to the lower phase speed, waves are more easily influenced (refracted) by currents.

Influence of imposed wave boundary conditions (waves at North Sea)
Outside the estuary, the wave conditions are to a large extent determined by the imposed wave boundary conditions and wind conditions. This can be seen when sensitivity simulation 15, where no waves are imposed on the model boundary, is compared to sensitivity simulation 10 (Figure 91 - Figure 94 in Appendix 4). For large wind speeds, the differences in wave conditions outside the estuary are small; hence the influence of imposed wave conditions decreases when the wind influence increases. When the wind speeds are low, large difference between the two simulations exist: apparently the influence of the imposed wave boundary conditions increases when the wind influence decreases. Inside the estuary, there are hardly any differences between the two simulations, only to a small extent at the WCT measurement station. The imposed wave boundary conditions thus hardly affect the wave conditions inside the estuary. From this it can be concluded that the wave conditions in the estuary are dominated by the imposed wind conditions. A method to quantify the relative influence of imposed wind and wave boundary conditions is introduced in section 4.4.4.

Influence of imposed wind conditions
As described above, wind conditions influence wave conditions outside and inside the estuary. Outside the estuary also the imposed wave boundary conditions play a role, inside the estuary, local influences are dominant over imposed wave boundary conditions. The local conditions can be divided in local bathymetry, currents and wind conditions. It appears that wind conditions are very determining in the local wave conditions. This holds for the significant wave height, peak period and direction. The influence of wind appears from comparison of simulation 17 (no imposed wind conditions) with sensitivity simulation 10 and comparison of sensitivity simulation 16 (only wind conditions, with a shift in wind direction of 45) with simulation 15. When no wind is imposed (calculation 17), the results on the wave direction differ significantly from the wave direction when wind conditions are imposed (Figure 91 - Figure 94 in Appendix 4).

A shift in wind direction results in a shift in wave direction, but also results in different significant wave heights and wave peak periods. The influence of the shift of wind direction on the significant wave height and wave peak period is larger in the estuary than outside the estuary. Outside the estuary, a change in wind direction doesn't result in significant changes of the wave conditions, but inside the estuary it does. This can be explained from the fact that a different wind direction results in a different fetch. Due to the meandering of the estuary and the presence of shoals, fetch and consequently wave conditions are dependent on the wind direction.

4.4.4 METHOD OF RELATIVE INFLUENCE

From the results of the previous section it can be concluded that the relative influence of the imposed waves or the imposed winds on the local wave conditions inside the estuary does not depend on the absolute value of both influences, but on the ratio between these two. Here, a simple method is introduced to quantify the relative influence of the imposed wind and wave boundary conditions on the local wave conditions inside the estuary in a spatial way.

To investigate the relative influence of imposed wave conditions and imposed wind conditions, a dimensionless coefficient $\beta_{influence}$ is obtained. This dimensionless coefficient is given by equation 4.9 and depends on the imposed wave boundary condition (multiplied by an efficiency factor α_H) and the wave height as a result of wave growth due to imposed wind conditions. The exact description is given after the equations. An increase in the value of the coefficient $\beta_{influence}$ means an increase of the influence of the imposed wave boundary conditions. A decrease of the coefficient $\beta_{influence}$ means an increase of the influence of the imposed wind conditions.

The dimensionless coefficient $\beta_{influence}$ can be presented as a time series (Figure 20), derived from the time series of imposed wind and wave boundary conditions. For each value of the coefficient in the time series, the relative influence of the imposed wave boundary conditions and imposed wind conditions on the local wave conditions inside the estuary can be determined. The influence of the imposed boundary conditions is obtained by comparing spatial results of the significant wave height from simulation 10 (imposed wind *and* wave boundary conditions) with spatial results of the significant wave height from simulation 15 (only imposed wind conditions) at certain values of $\beta_{influence}$ and express the difference in significant wave height in a percentage of the total significant wave height (as calculated by simulation 10). To address the influence of the imposed winds on the significant wave heights the same is done, now comparing simulation 10 with simulation 17 (only imposed wave boundary conditions).

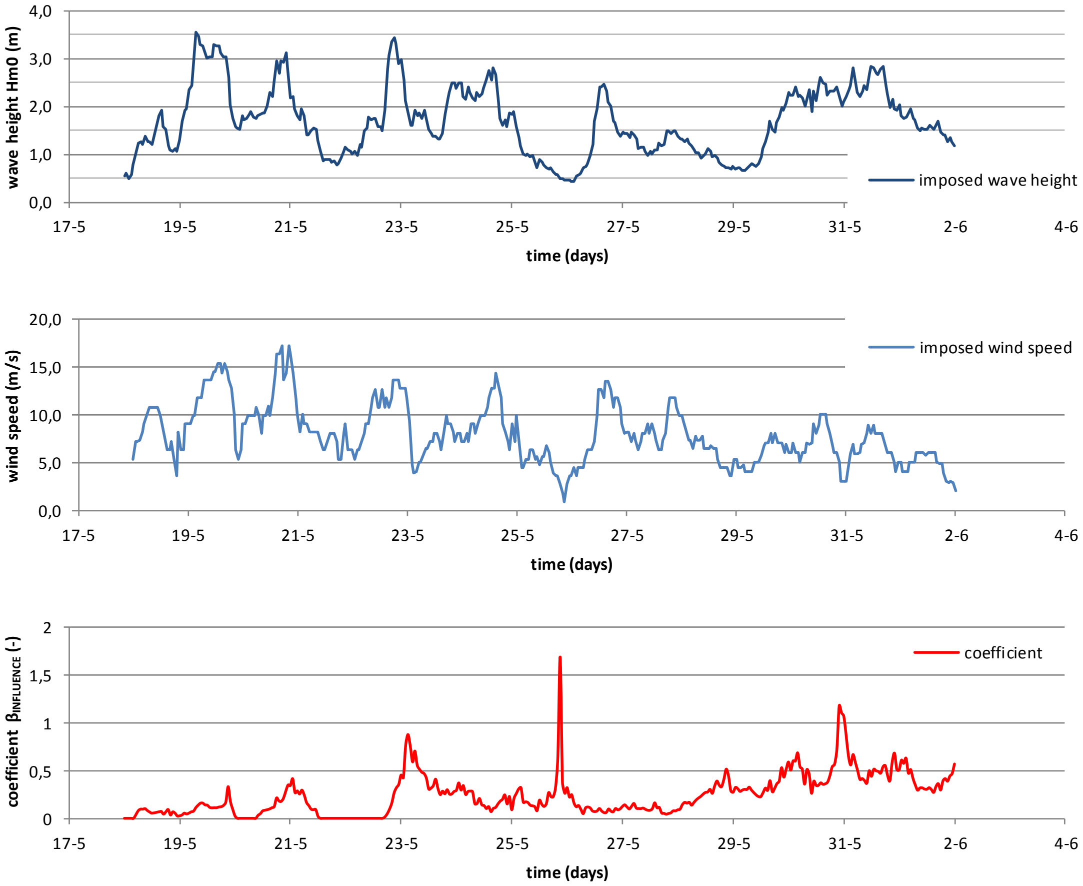

Figure 20. Time series of the coefficient $\beta_{influence}$ (lower panel), derived from time series of imposed wave height (upper panel) and imposed wind speed (middle panel).

From Figure 20, the correlation between $\beta_{influence}$ and the wind and wave conditions can clear be seen. Peaks for $\beta_{influence}$ occur at times where the imposed wave height is relative large compared to the imposed wind speed (which is converted in a wave height by equation 4.11). For several values of $\beta_{influence}$ from the time series in Figure 20, the relative influence (%) of imposed wave boundary conditions and imposed wind conditions are derived from spatial results (wave height plots, Figure 103 - Figure 147 in Appendix 4) From the spatial results, one representative value (%) was selected per area for each of the distinguished values of $\beta_{influence}$. When these results are plotted in a graph (Figure 22), a clear trend in the influence as a function of $\beta_{influence}$ per distinguished area appears.

$$\beta_{influence} = \frac{H_{m0\ imposed} \times \alpha_H}{H_{imposed\ wind}} \tag{4.9}$$

Where:

$$\alpha_H = \frac{\cos(\theta_{wave} - 300°\mathrm{N}) + |\cos(\theta_{wave} - 300°\mathrm{N})|}{2} \tag{4.10}$$

$$H_{imposed\ wind} = \frac{\tilde{H} \times U_{10}^2}{g} \tag{4.11}$$

$$\tilde{H} = a_1 \times \tilde{F}^{b_1} \tag{4.12}$$

$$\tilde{F} = \frac{g \times F}{U_{10}^2} \tag{4.13}$$

$$F = 2{,}000\ \mathrm{m} + \alpha_F \times 6{,}000\ \mathrm{m} \tag{4.14}$$

$$\alpha_F = |\cos(\theta_{wind} - 300°\mathrm{N})| \tag{4.15}$$

with $H_{m0\ imposed}$ = imposed significant wave height; wave boundary condition (m).

α_H = efficiency factor (-) for imposed waves (range 0 -1), highest efficiency when wave direction θ_{wave} is equal to 300°N.

θ_{wave} = wave direction (°N)

$H_{imposed\ wind}$ = wave height in estuary (m), based on wind conditions and fetch, based on wave growth formulation of Kahma and Calkoen [14] (eqs. 4.11 – 4.13)

$\tilde{H}$ = dimensionless wave height (-)

U_{10} = wind speed at 10 m above ground (m/s)

g = gravitational acceleration (m/s²)

$\tilde{F}$ = dimensionless fetch (-)

F = fetch (m), with a minimum of 2,000 m (fetch perpendicular to the channels) and a maximum of 8,000 m (fetch parallel to the channels)

α_F = efficiency factor (-) for occurring fetch (range 0 -1), highest efficiency when wind direction θ_{wind} is equal to 300°N or 120°N (parallel to the channels).

θ_{wind} = wind direction (°N)

---

[14] The fetches inside the estuary are limited, hence the wave growth formulations of Kahma and Calkoen (deep water, short fetches) can be applied (Holthuijsen, 2007) . A check with the formulations of Young and Verhagen for arbitrary water depths gives the same calculated wave height (for a water depth of 10 m). The formulation of Kahma and Calkoen is used here since no water depth is included; this is handy since the water depth in the estuary varies strongly with space and time.

The imposed wave conditions are multiplied with an efficiency factor to take the direction of the waves into account. From simulations in this section it appears that imposed waves have the most influence on the wave conditions inside the estuary when they approach the estuary entrance perpendicular (300 °N). When the direction of the waves deviate from this direction, the influence decreases (included by the cosines function in eq. 4.10). When the wave direction is east between 30° N and 210° N, imposed wave boundary conditions hardly have influence on the wave conditions inside the estuary. For these directions the influence of imposed wave boundary conditions is therefore automatically set to zero.

The calculated wave heights according to the formulations of Kahma and Calkoen (Holthuijsen, 2007) are applied here to give the *order of wave height* in the whole considered area. The intention of these calculations is in this case *not* to calculate the exact wave height at specific locations. The local generated wave heights depend on the fetch in the estuary. Due to the meandering of the estuary and the presence of shoals, the length of the fetch and hence the wave height depends on the wind direction. Here, the minimum fetch is set to 2,000 m, which is a typical fetch when the wind direction is perpendicular to the channel axes. When the wind direction is parallel to the channel axes (around 300 °N), the fetch increases up to a maximum of 8,000 m. The dependency of the fetch on the wind direction is included in eq. 4.14.

The estuary can roughly be divided in three sections with different relative influences of the imposed wave boundary conditions and the imposed wind conditions. Figure 21 shows these areas. In Figure 148 (Appendix 4) the influences (in percentages) of imposed wave boundary conditions and imposed wind conditions as found from the simulations are presented.

Figure 21. Distinguished areas within the estuary with different influences of imposed wave boundary conditions and winds. Source photo: Google Earth Pro.

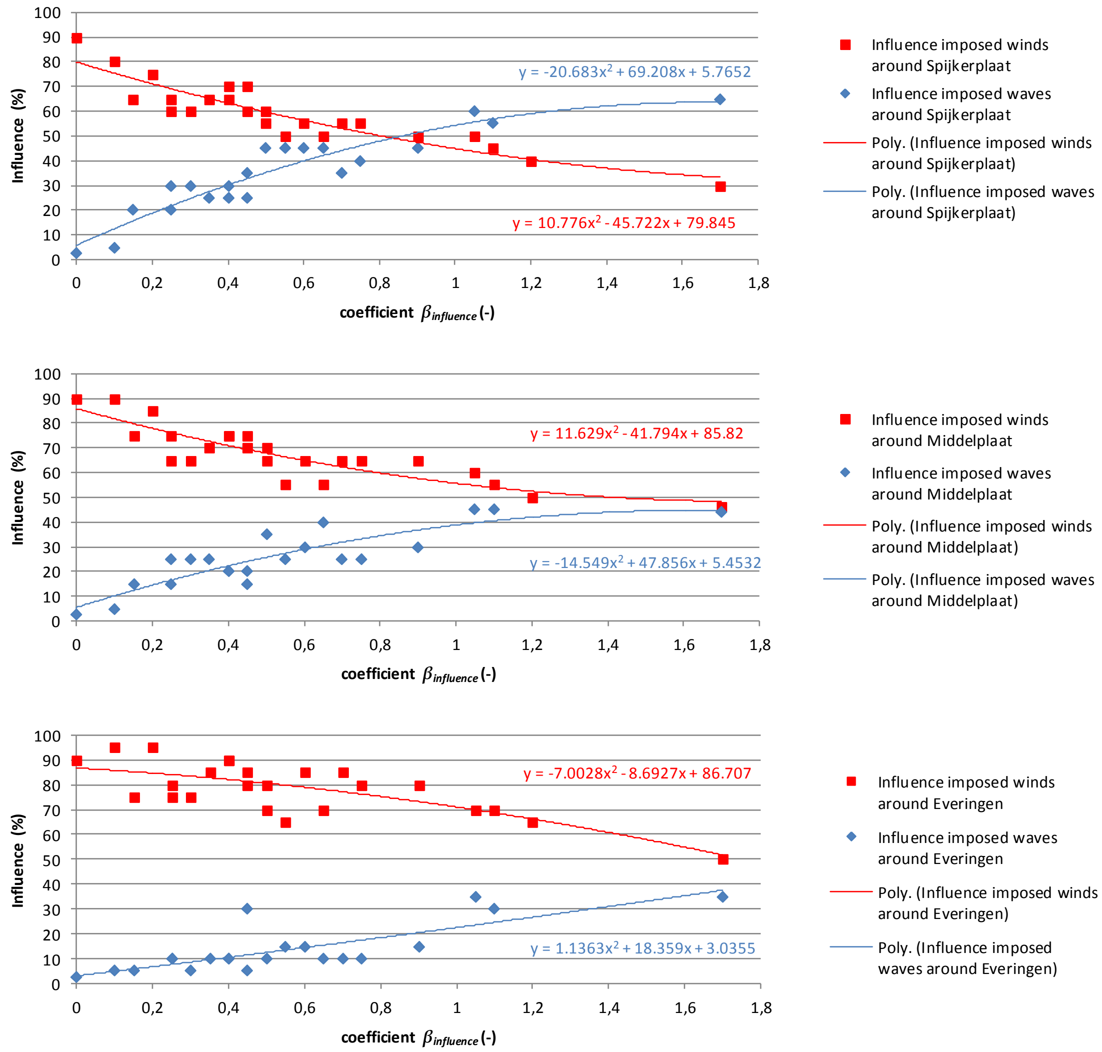

Figure 22. Influence (%) of imposed wind and wave boundary conditions per area as a function of the coefficient $\beta_{influence}$. The top panel presents the influence around the shoals of Spijkerplaat, the middle panel presents the influence around the shoals of Middelplaat and the lower panel presents the influence around the shoals south of Everingen.

Figure 22 shows that there is a clear relation between the influence of the imposed wave boundary conditions and imposed wind conditions and the coefficient $\beta_{influence}$ as defined by eq. 4.9. The scatter around the polynomial trend line is relatively large (order 10%) as a result of representing the influence in the areas by one value. Despite this, a clear distinction is found in the order of influence of imposed wind and wave boundary conditions and the development of this influence per area of the western part of the Western Scheldt.

From the figures and the found relationship follows that for most values of $\beta_{influence}$ the influence of the imposed wind condition on the wave conditions in the estuary is dominant over the influence of the imposed wave boundary conditions. This was already found from time series analysis, but is now also confirmed from a spatial point of view. The influence of the wind conditions over imposed wave boundary conditions increases when the considered area lies further into the estuary. Around the shoals of Spijkerplaat (near the entrance), the influence of the wind conditions is dominant for most cases with a influence between 50-80%. Only for values of $\beta_{influence}$ around 0.8 or higher (relative large imposed wave boundary conditions, relative low imposed wind speeds) the imposed wave boundary conditions dominate over the wind influence. Around the shoals of Middelplaat the influence of the imposed wind conditions further increases to 60-90%. Around the shoals of Everingen this influences increases up to 70-100%. With an increase of the influence of the wind conditions on the local wave conditions, the influence of the imposed wave boundary conditions automatically decreases: this can also be seen at Figure 22.

The found relationship is important, since it can now be shown in a spatial way that the wave conditions are to a large extent dominated by the imposed wind conditions and thus locally generated. The local wave conditions are therefore more dependent on the local wind conditions and fetch than on the conditions outside the estuary.

The found relationship is also important to investigate the influence of imposed wave boundary conditions and wind conditions in new sets of wind and wave conditions. With the found relationship, it is now possible to address the relative influence of imposed wave boundary conditions and imposed wind conditions on the local wave conditions based on the coefficient $\beta_{influence}$, rather than comparing simulations with and without imposed wind and wave conditions. This relationship therefore comes in hand to address the relative influence of imposed wind conditions and wave boundary conditions within the wind and wave classes as determined in section 4.2.2.

Application method to classes of schematised wind and wave climate

When the method is applied (application of the polynomials as presented in Figure 22) to the classes of the schematised wind and wave climate (Figure 14, section 4.2.2), the Figure 23 is obtained. From this figure it can be seen that the wave conditions inside the estuary for these specific classes are always dominated by the imposed wind conditions. At the shoals of Spijkerplaat, the relative influence of the wind conditions on the local wave conditions is 60% - 80%, depending on the specific conditions of the classes. Further into the estuary the relative influence of the wind conditions increases to 70% - 80% around the shoals of Middelplaat and to 80% - 90% at the shoals south of Everingen.

Since the high amount of correlation between the wind speed and wave height (section 0), no combination of high wave boundary conditions and low wind speed occur. Only in that situation the influence of imposed wave boundary conditions can dominate the wave conditions inside the estuary (Figure 22). It also appears that wave boundary conditions during a storm don’t dominate the wave conditions inside the estuary. Also in this case, the wind speed (which is relatively high during a storm) dominates the local wave conditions.

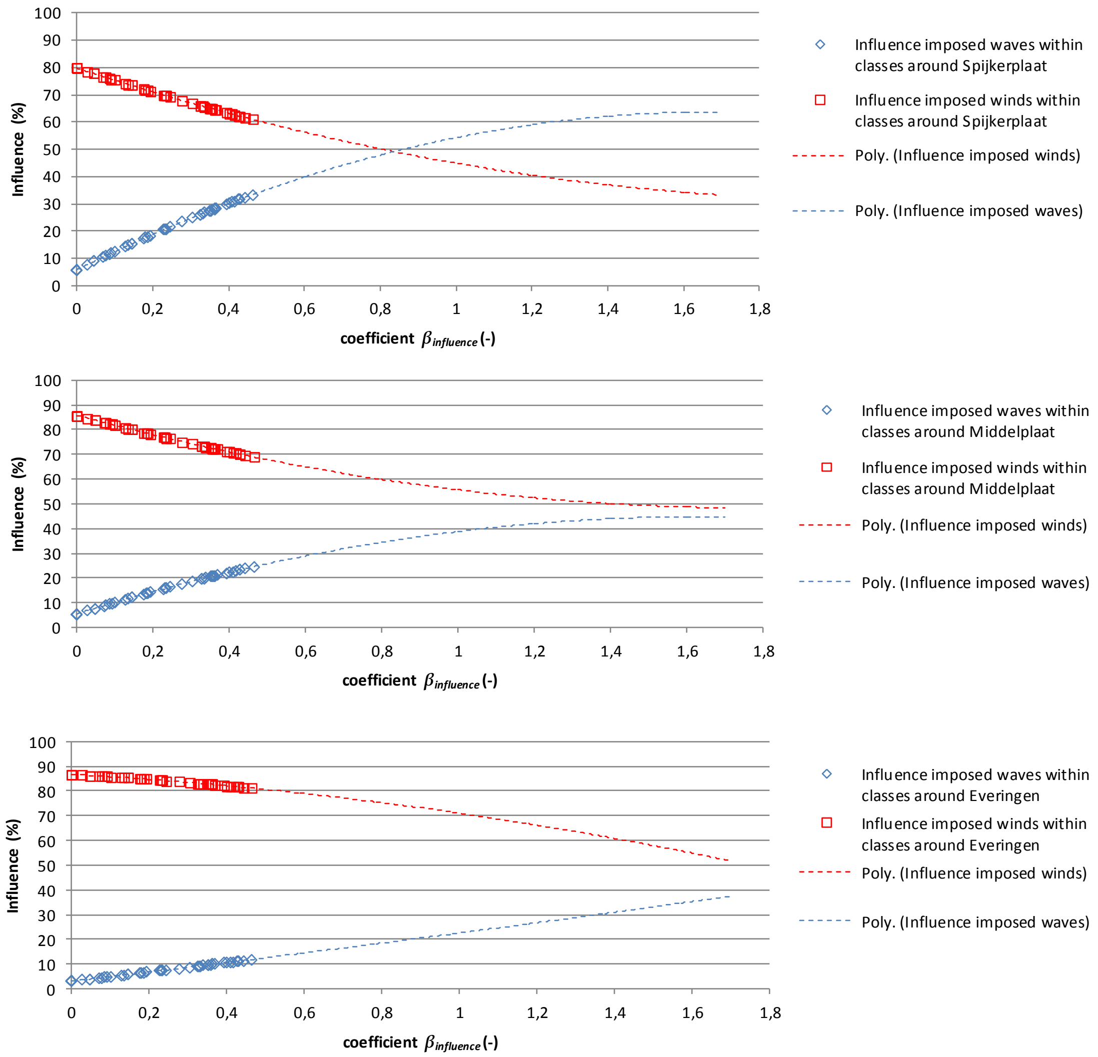

Figure 23. Influence (%) of imposed wave boundary conditions and wind conditions on local wave conditions. Upper panel: influence around shoals of Spijkerplaat. Middle panel: influence around shoals of Middelplaat. Lower panel: influence around shoals south of Everingen. The red lines and symbols indicate the influence of winds, the blue lines and symbols indicate the influence of imposed wave boundary conditions.

4.5 CONCLUSIONS

The objective of this chapter is to obtain the first schematisation of the wave climate for further use in the climate schematisation methods in chapter 5. The other objective is to validate the applied wave model, address the influence of choices in the schematisation of the wave climate and address physical influences on the wave conditions inside the estuary. This chapter thus serves traces 1 and 2 in the thesis approach (section 1.4).

Wind and wave climate

The time series of the wind and wave climate from 1 January 1981 – 1 January 2001 can be schematised in 54 different classes of wind direction and wind speed. The dominant wind direction is south-west and has a typical wind speed between 5 and 10 m/s. The climate is subject to seasonality; in the winter season, the wind direction is predominantly south-west, where in the milder summer season, next to the south-west direction there also is a large contribution from the north-west. Furthermore, storm classes only occur in the winter season.

Model validation
An important conclusion is that the wave model (with the used settings) as used for the morphological simulations is applicable for the simulation of the wave conditions in the entrance of the Western Scheldt. The measured wave conditions over a time period of fourteen days at seven locations inside and outside the estuary are reproduced rather well. The wave model is therefore applied for the simulation of wave conditions within the morphological simulation in chapters 5 and 6.

Influence choices within climate schematisation on simulated wave conditions
The simulated wave conditions show the best resemblance with measurements when all wave conditions are derived from the measurement station at Schouwenbank. Wave conditions from Scheur West clearly shows less resemblance with the measured conditions. When data on the wave direction from Schouwenbank is used, a slightly better resemblance is found compared to the simulation were data on the wave direction from Euro Platform is used. Inside the estuary, this difference in wave direction decreases, as the wave conditions inside the estuary are mainly locally influenced. Since the benefit of the used wave directions from Schouwenbank is small (in terms of statistical parameters), it is concluded that for this study the use of wave directions from Euro Platform is allowed. Hence, the data on the wave direction from this measurement station is used in the climate schematisation.

The use of the spectral period T_{m02} or $T_{m-1.0}$ for T_p doesn't seem to influence the simulated wave conditions much. However, the spectral period T_{m02} is generally more sensitive for the larger frequencies in the tail of the spectrum (above 1 Hz). This can be important for wave spectra with relatively small waves. The spectral wave period $T_{m-1.0}$ is considered to be a more robust spectral period, as it is mostly based on the lower frequencies in the wave spectrum (Van Vledder, personal communication). For this study, where the focus is on the relative influence of different wave conditions on the morphological development, the use of T_{m02} for T_p is allowed. This is also concluded from the good resemblance between simulations and measurements. Furthermore, in the performed wave modelling, the results where T_p is based on T_{m02} show better results far in the estuary (Pas van Terneuzen) than the results where T_p is based on $T_{m-1.0}$.

The general use of T_p in the time series in the WAVE module (via the *wavecon* files) makes it impossible to impose multiple peaked wave spectra. The shape of the spectrum (JONSWAP spectrum with one peak) is an implicit assumption in the simulations. The influence of the shape of the spectrum on the simulated wave conditions is not considered in this study. It can however be expected that the simulated wave conditions show a better resemblance with the measured wave conditions when also the shape of the spectrum with respect to the amount of peaks is considered (e.g. to take swell waves into account as well). This is expected to be mainly of influence at the ebb tidal delta . Inside the estuary this will have less influence, as it is already shown that the wave conditions inside the estuary are mainly determined by local imposed wind conditions.
In general, the use of SWAN via the WAVE module in Delft3D gives less flexibility with respect to the settings compared to the SWAN model itself. Certain options which are available in SWAN, and which might be more appropriate for the situation considered, are not available via the WAVE module. Fine tuning of the settings can result in a better simulation in terms of reproduction of the measured conditions. This is outside the scope of this thesis and therefore not considered.

Influences on wave conditions inside estuary
The ebb tidal delta has a large influence on the wave conditions inside the estuary. The ebb tidal delta blocks most of the wave action that is travelling from the North Sea towards the estuary: a large amount of

wave energy is dissipated over the ebb tidal delta. This results in a shifting of the influencing conditions on the wave conditions. Outside the estuary the wave conditions at the North Sea and the ebb tidal delta are mainly determined by the imposed wave boundary conditions and local wind conditions. The influence of the wave imposed conditions slowly reduces when waves travel into the estuary where the relative influence of local conditions (winds, currents, depths) increases. It is concluded that the influence of the wind conditions on the wave conditions inside the estuary are dominant over the influence of the wave boundary conditions (the wave conditions at the North Sea).

The dominant influence of wind conditions on the wave conditions inside the estuary is found from time series analysis and spatial data at fixed time steps. Based on these data, a method is introduced to address the relative influence of wind conditions and wave boundary conditions on the wave conditions inside the estuary. Via this method it was found that three mean areas can be distinguished with different relative influences of imposed wind and wave boundary conditions. Around the shoals of Spijkerplaat (near the transition to the North Sea), the influence of imposed winds on the local wave conditions is between 60% to 80%. Further into the estuary, around the shoals of Middelplaat, the wind influence increases to 70% 90%. Around Terneuzen, at the shoals south of the Everingen flood channel, the influence of the wind conditions is about 80% - 100%.

When the introduced method is applied to the classes of the schematised wind and wave climate, it is concluded that for all these classes, the wind influence on the wave conditions inside the estuary is dominant (with about the values as described above). It also appears that wave boundary conditions during a storm don’t dominate the wave conditions inside the estuary. Also in this case, the wind speed (which is relatively high during a storm) dominates the local wave conditions.

The dominance of local wave conditions inside the estuary justifies the approach as followed in the schematisation of the wave climate, where the classification of the wave conditions is based on wind direction and wind speed. If the classification would be based on wave direction and wave height at Schouwenbank, the different classes would be equalized in the estuary to a large extent by the influence of the ebb tidal delta. Furthermore, not necessarily all wind directions and wind speed might in that case be included in the schematisation: hence certain wave conditions based on these wind conditions are lost in that case. It can thus be concluded that the wave schematisation based on wind direction and wind speed is the right approach.

The importance of the wind influence on the wave conditions inside the estuary indicates that imposing the correct wind conditions is very important for obtaining the correct wave conditions inside the estuary. This holds both for the wind speed and the wind direction. The wind direction plays an important role, since the direction determines the fetch in meandering estuary. Since for this study the wind conditions at Vlissingen are used for assessment of the wave model and wind conditions at Schouwenbank for the morphological simulations, it can be expected that simulated wave conditions deviate more from the measured conditions when the location considered lies further into the estuary. It is therefore recommended to investigate the spatial variations of the wind conditions over the estuary. According to Van Vledder (personal communication) this need for spatial information on wind conditions over the Western Scheldt is acknowledged in other studies as well, but up till now no method is available to take the spatial variations of the wind conditions into account. The reason for this is the shortage of wind measurement stations along the estuary. Often the wind conditions at Vlissingen are assumed to be representative for the whole of the estuary, while this is very likely to be one of the causes of deviations between measured and simulated wave conditions at locations in the estuary at a distance from Vlissingen. Differences in roughness of the land might be an explanation for this.

5 Schematisation of the wind and wave climate

5.1 INTRODUCTION

The objective of this chapter is to obtain multiple schematisations of the wave climate. These schematisations are reviewed based on insight in physics of the waves in the entrance and are consequently applied in the medium-term morphological simulations. This chapter hence serves the first and second trace of the thesis approach (section 1.4). First, the results of the short morphological simulations of all defined wave classes (section 4.2.2) are described. These results are the input for the methods of climate schematisation and are used to obtain understanding of the wave physics in the area. Next, the two applied methods of schematisation are described, together with the obtained wave climate schematisations.

The need for the schematisation of the wave climate stems from the need to limit the simulation run time for morphological simulations (section 1.1). In order to limit the calculation time to an "acceptable" duration, the input of the forcing by waves is reduced by means of a wave climate schematisation. Here, the main idea behind the schematisation is to reproduce the effect of the total (non-reduced) wave conditions on a medium-term time period by a schematised wind and wave climate, within a certain range of accuracy (to be defined later). This schematised wind and wave climate results in a reduced simulation time and is therefore (in theory) preferable. The results of morphological simulations based on the different wave climate schematisations need to be assessed in terms of this accuracy. Based on the advantages and disadvantages (respectively a shorter duration time and a possible less accurate result) a statement can be made whether or not a certain schematisation is preferable. Accuracy and simulation runtime are described in chapter 6.

5.2 APPROACH

There is no standard approach to schematise the wave climate. The way the wave climate is schematised depends on the objective of the schematisation and the available data on wave and wind conditions. Here, the wind and wave climate as described in section 4.2.2 is used as a base for further schematisation of the climate. The morphological impact for all the 54 classes of that climate schematisation is determined. This is done over a relative short period of time, i.e. one tidal cycle of 12.5 hours. The short morphological simulations give insight in the influence of the different wind and wave classes on the initial sediment transport and resulting bottom changes (if any). For this insight, per class the wave conditions are calculated, together with the sedimentation and erosion pattern, spatial variation of the wave orbital velocity, depth averaged velocity, bottom shear stress and sediment transport and resulting bottom changes. Difference plots are made from which the influence of waves on these processes clearly can be found. All these processes are presented just before high water and low water. Two classes are described in this chapter in detail. Conclusions stated in this chapters related to the influence of waves on the transport of sediment and morphology are based on analysis of all 54 classes. The results of the short morphological simulations are presented in Figure 149 - Figure 203 in Appendix 5.

Next, the full wind and wave climate schematisation (existing of 54 classes, Figure 14) are further schematised to a wind and wave climate with less classes. To assess the influence of the schematisation of the wave climate on the morphological development, different schematisations are derived. The way the schematisations differ regards to the amount of remaining classes within a schematisation (15, 10, 5 or 1 class remaining), the quantity on which the schematisation is based (sediment transport or bottom change), the considered area (ebb tidal delta, estuary or whole area), including seasonality and storm event within the schematisation and the method of schematisation (optimum method or method of correlation). This finally results in 29 different schematisations of the wind and wave climate.

The obtained understanding in the physics of waves in the entrance and their influence on the morphological development is used to review the obtained schematisations in a general way (section 5.6). This review relate to the included classes, weight of classes and variation between the classes.

The results of the simulations of the individual wind and wave classes are divided in terms of the influence of waves on sediment transport and morphological development (section 0) and wave transformation and propagation (section 4.4.3). The results from the wave simulation (the transformation and propagation) is described in the previous chapter since this complements the results on wave modelling in that chapter (and in this case all results on wave modelling can be found in one chapter instead of two).

The main similarities and differences between the individual classes in are described (section 5.3.4), after which recommendations are made with respect to the schematisation of the wave climate (section 5.3.5). By the judgement of the obtained wave climate schematisations, it is verified whether and how these recommendations are implemented in the schematisations.

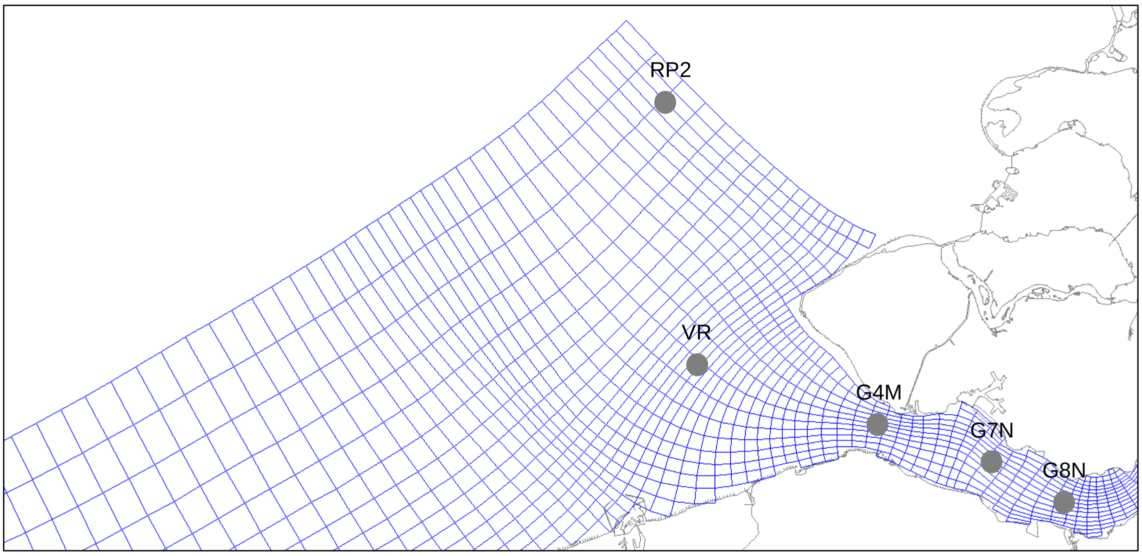

Figure 24. Location of "observation points" in the calculation grid. Applied for the morphological simulations.

Observation points

To investigate the propagation and transformation of waves over time and distance, multiple "observation points" are placed in the calculation grid. Five of them are presented in the results. These are observation points RP2, VR, G4M, G7N and G8N (Figure 24). Observation points RP2 and VR lie outside the estuary; RP2 lies near the northern border, VR lies at the western edge of the ebb tidal delta . The other three points lie east of the ebb tidal delta (at the real entrance an further into the estuary. By doing so, the wave propagation and transformation from outside to inside the estuary can be monitored. Observation point G4M is located right at the entrance between Vlissingen and Breskens, observation point G7N is located eastwards of Spijkerplaat. Since the shoals of Spijkerplaat lie near the entrance of the estuary, this location is considered to be a border between two area's: at Spijkerplaat and further eastwards the wave conditions are dominated by the local (wind) conditions (as is described in sections 4.4.3 and 0), westwards of Spijkerplaat the wave conditions are determined by the local conditions and wave conditions at the North Sea (for westerly directions).

The wave and morphological simulations are performed with Delft3D. Within Delft3D, the wave simulation are performed with the SWAN wave model as implemented the WAVE module. In chapter 3 a brief description of these models and their settings is given.

5.3 SIMULATION OF WIND AND WAVE CLASSES

5.3.1 DESCRIPTION OF RESULTS OF MOST OCCURRING CLASS

In the *next* section (section 5.3.2), the results of the 54 morphological simulations are described in terms of sediment transport end morphological development. There, the general results of all classes are described, together with the main conclusions. A reference to the figures of these simulations is made. In *this* section, one of these classes is selected to explain more on the figures as a result of the simulations. This explanation helps to interpret the figure of the results of other classes as included in Appendix 5. It also gives a better understanding on which type of results the conclusions in the next sections are based. The class as described here is class 30. This class has highest probability of occurrence (Figure 14, section 4.2.2).

To gain insight in the influence of the different wind and wave classes, the underlying steps between waves conditions and sediment transport (orbital velocity, bed shear stress and depth averaged velocity) are presented in at two different time steps. Since all depend on the water level, these processes are presented 30 minute before **low water** and 30 minutes before **high water**. Here, only the situation before low water is described (Figure 25). Next, to distinguish the influence of waves from the influence of currents another figure is made: Figure 26. This figure is obtained by *subtracting* the result of the simulation only due to currents (no wind and waves [15]) from the result of the simulation due to currents, wind and waves (Figure 25). This is also done for the situation just before low and high water. In section 5.3.2, the difference between these two time steps in terms of influence of waves is described.

The results of the simulation of each class are presented in five figures: #a, #b, #c, #d and #e. Figure #a shows the results in terms of wave propagation and is already described in section 4.4.3. Figures #b and #c present the results due to the combined influence of currents and waves. Figures #d and #e present the results only due to waves.

[15] The results of the simulations without wind and waves are also included in Appendix 5: Figure 149a - Figure 149e.

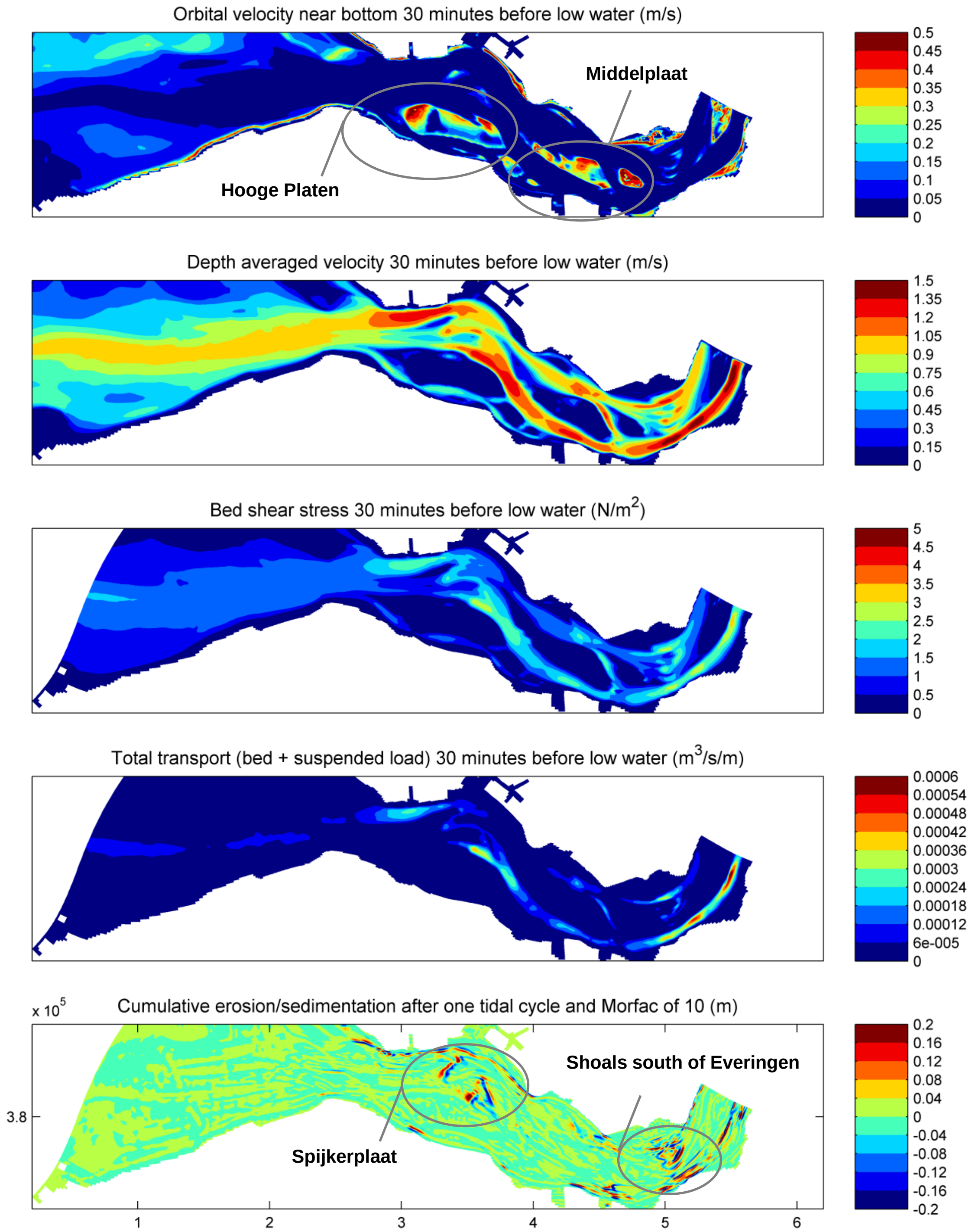

Figure 25. Influence of current, wind and waves on the sediment transport and morphology, just before low water. Wind and wave class 30.

In the first panel, the wave orbital velocity is presented. This velocity is the highest around the edges of the shoals during low water. The depth averaged velocity is the highest in the ebb channels (the second panel). At the locations of high velocity, also the bed shear stress (third panel) and transport of sediment (fourth panel) is high. At the locations where both current velocities and wave orbital velocities are present, most changes in morphology occur (shoals of Spijkerplaat, shoals south of Everingen). Although the wave orbital velocity is higher at other places (the edges of the shoals of Hooge Platen and Middelplaat), no large changes in morphology occur: sediment is stirred up by waves, but no significant current is present at these locations to transport it.

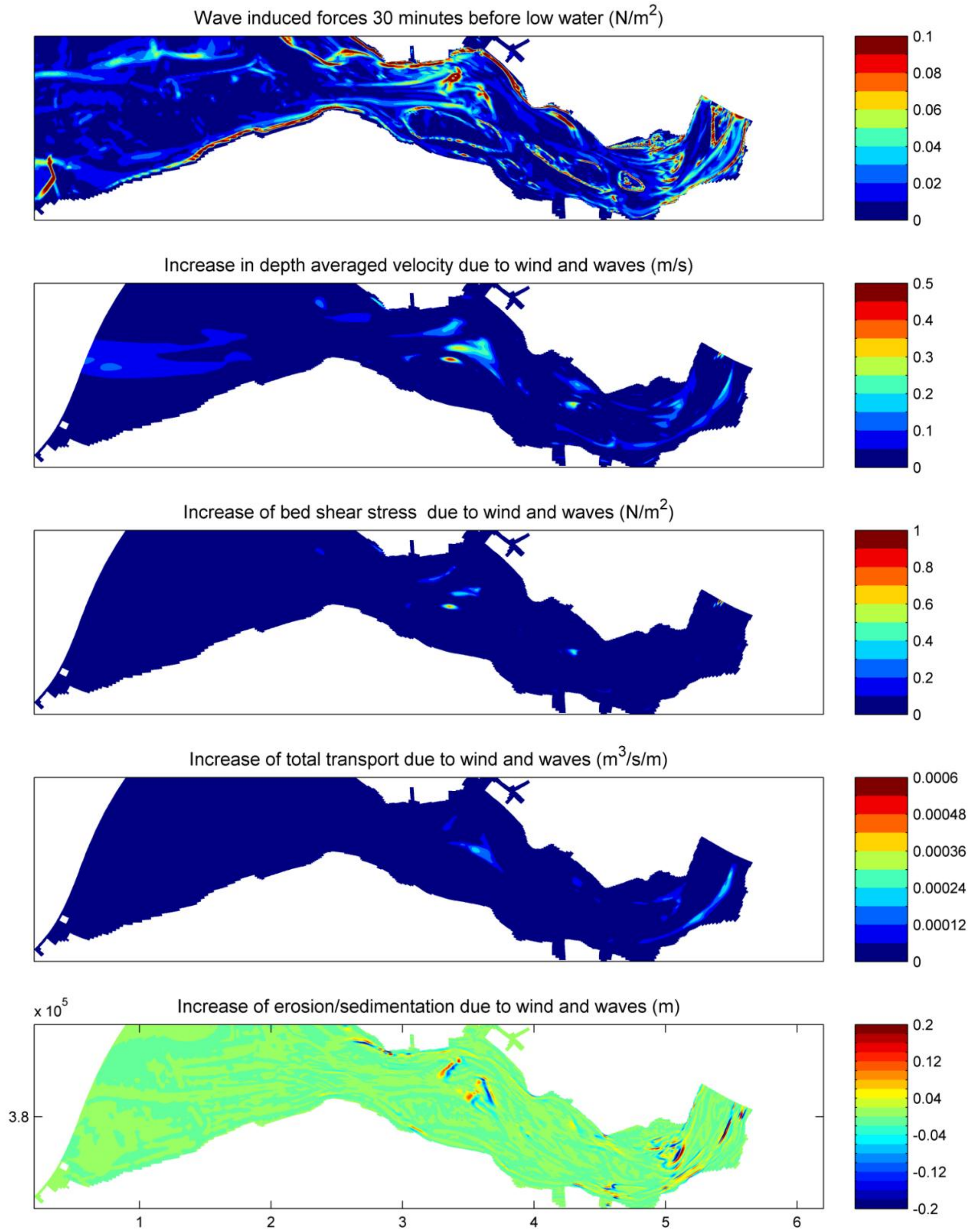

Figure 26. Influence of only wind and waves on the sediment transport and morphology, just before low water. Wind and wave class 30.

When only the influence of wind and waves is analysed, a few interesting things can be noticed. First of all, wave induced forces (first panel) are highest low-lying shoals of Spijkerplaat and south of Everingen. This indicates breaking of waves. Second, as a result, the depth averaged velocity increases at these locations (second panel). This consequently results in a higher bed shear stress, more transport of sediment and changes in the pattern of sedimentation and erosion at these locations. It can thus be concluded that the influence of waves have most influence on the low-lying shelves of Spijkerplaat and the shoals south of Everingen. Furthermore, this influence is twofold: the waves stir up sediment to be transported with the tidal currents, but waves also locally increase the depth averaged velocity.

5.3.2 RESULTS ON SEDIMENT TRANSPORT AND MORPHOLOGICAL DEVELOPMENT

The influence of one wind and wave class is presented in the previous section. The other 53 wind and wave classes are simulated and analysed in the same way. The results of these simulations are presented in Figure 149 - Figure 203 in Appendix 5. This section describes the result from all these simulation in a general way.

As can be expected, there is a large consistency between the hydrodynamic forces and the transport of sediment and morphological development. Hence, the transport of sediment and possible morphological changes are directly related to occurring wind and wave conditions. It is not unambiguous to point the influence of individual processes or characteristics of the system since they are influence by one another as well. However, the main influences are described below.

Influence tidal current

To assess the influence of the waves and wind on the predicted morphological development, a reference simulation is made. In this reference simulation, no waves and no winds are imposed on the calculation grid. The result shows the influence of the tidal currents on the sediment transport and the resulting morphological development (Figure 149, Appendix 5) . When this result is subtracted from the simulation with wind and waves, the influence of the waves on sediment transport becomes visible. From Figure 149 - Figure 203 (Appendix 5) it can be concluded that the highest depth averaged velocity result in the highest bed shear stress and consequently to the highest rates of sediment transport. The highest values of these quantities occur at the channels of Honte, Everingen and the entrance (line Vlissingen – Breskens) and at the shoals of Spijkerplaat and Everingen. In the bends of the channels, the velocity increases.

When transport due to the combination of currents and waves is analysed, it appears that transport of sediment due to the influence of waves occur mostly at the same locations, but with an increase of the transport rate at the shoals of Spijkerplaat and Everingen. This is due to the effect of stirring sediment by the waves (stirring makes the sediment available for transport), which is consequently transported with the current. Moreover, wave transformation at these shoals also results in an increase of the depth averaged velocity. As expected, the influence of the waves is concentrated at the shallow parts of the ebb tidal delta and the estuary. These are the low lying shoals and the edges of the estuary. At the deeper parts, the influence of waves on the transport of sediment is very limited. Due to this, the main influence of waves is similar for all considered conditions.

Orbital velocities near bottom

Since orbital velocities are a function of the wave height, wave period (via wave length and celerity) and water depth, the orbital velocities change per wave class and over time (since the water depth and wave conditions are a function of time). By definition, the highest orbital velocities occur where the water depth is low compared to the wave length. From Figure 149 - Figure 203 (Appendix 5) it can be seen that the highest orbital velocities indeed occur at the locations with the lowest water depths, i.e. the ebb tidal delta and the shoals (Spijkerplaat, Hooge Platen, Middelplaat). The absolute values differ per wind and wave class.

At the channels inside the estuary and around the ebb tidal delta , the orbital velocities are relatively low. This can be explained by the fact that the water depth is relatively large in these channels compared to the wave length. Furthermore, due to the presence of the channels, the currents are focussed in the channels. Outside the channels, the depth averaged velocity is relatively low. For the transport of sediment due to the presence of waves, a combination of both orbital velocity and (tidal) currents is needed (since waves stir up sediment and currents transport the stirred up sediment). Without this combination, the influence of waves on the transport is absent.

Currents occur in the channels around the shoals. When higher water levels occur, waves occur higher at the shoals. Hence, high wind and wave classes result to more wave higher at the shoals. At higher water levels, also the current has a larger velocity around those places. As a result, more sediment is transported. This can be found when figures with low conditions are compared with figures which present severe conditions. Higher waves; higher orbital velocity and, since high waves occur at higher water levels, also occur at higher places. It can clearly be seen that most of the transport of sediment occurs where the depth averaged current velocities are the strongest.

Next to the wave height, the occurrence and magnitude of the orbital velocity on the shoals is very dependent on the wave direction. The shoals are attacked most heavily at the side where the waves approach.

As a consequence of the increased transport of sediment due to waves, the cumulative erosion and sedimentation patterns changes (the bottom change). From Figure 149 - Figure 203 (Appendix 5) it can be concluded that most differences [16] are concentrated at the edges of the shoals of Spijkerplaat and Everingen. Waves especially have effect at the low lying shoals (as Spijkerplaat and Everingen) where also currents occur. At the higher shoals, such as Hooge Platen and Middelplaat, higher orbital velocities occur. Due to the absent of currents at these locations however, no transport of sediment occurs.

Shoals of Hooge Platen, Spijkerplaat and Everingen

The main currents in the entrance are conducted (contraction of the streamlines) by the relative narrow passage between Vlissingen and Breskens. Due to this, the currents mainly follow the south coast of Walcheren. Due to this, the shoals of Hooge Platen have a sheltered position relative to the current. As a result, the morphology of the shoals of Hooge Platen remains unchanged to a great extent. Waves at Hoogte Platen result in the stirring of sediment, but due to the absent of current velocities this sediment is not transported. At the shoals of Spijkerplaat, the opposite occurs. The shoals of Spijkerplaat lie in middle of the currents in the entrance. The level of the shoals (around 1 m below low water), makes that these shoals are susceptible for both currents and wave impacts. Here, the orbital velocities are low compared to Hooge Platen, but the presence of currents makes that the stirred up sediment is transported.

Influence water level

Higher water levels allow wave to propagate further into the estuary and further on shoals. Higher water levels also allow currents at higher levels, which is important for the transport of sediment at the shoals, where wave stir up sediment. Such conditions occur e.g. in storm classes 39 and 49 (Figure 188 and Figure 198, Appendix 5). These conditions result in changes in morphology at higher shoals (Hooge Platen and Middelplaat), where other conditions do not. Higher water levels as a result of storm surges also are accompanied by higher waves. These higher waves result in an increase of the orbital velocities and hence stir up more sediment.

---

[16] It must be noticed that the used value of the calibration factor for transport due to waves in Delft3D (SUSW and BEDW) is too high (0.5). Based on personal communication with prof. dr. ir. J.A. Roelvink (UNESCO/IHE), these values are adjusted to 0.1 in the morphological simulations in chapter 6. Here, the use of the value of 0.5 is not a problem for constructing the wave schematisations, but gives a somewhat exaggerated impression on the influence of waves. For the purpose of illustration however this is quite usefull, since the locations where the waves have the largest influence are clearly marked.

A clear distinction can be made between the situation around low water and high water. At low water, the water level is below shoal level. As a consequence, waves don't occur on top of the shoals but only at the edges of the shoals. This can clearly be seen in the top panel of Figure 149 - Figure 203 (Appendix 5). The orbital velocities only occur at the edges of the shoals. At high water, most of the shoals are below water, allowing waves to travel over the shoals. This can be seen on the top panels of the conditions during high water, where orbital velocities occur on top of the shoals.

Furthermore, a distinction can be made in the ebb and flood channels. Just before high water (flood current), the highest flow velocities occur in the entrance, Schaar van Spijkerplaat [17], and Everingen. These locations are also considered as flood channels (section 2.2.3). Just before low water (ebb current) higher flow velocities occur at Pas van Terneuzen, which is classified as an ebb channel.
It appears that more sediment is transported just before high water than just before low water. Just before high water, the most sediment is transport at the locations with the highest velocities, i.e. the bends of the flood channels: the entrance between Vlissingen and Breskens, around (Schaar van) Spijkerplaat and the shoals of Everingen. Just before low water, the most sediment is transported at locations with the highest velocities; i.e. the bends of the ebb channels: the south side of (Schaar van) Spijkerplaat.

At low water, the transport of sediment is closer to the edges of the shoals (especially at Schaar van Spijkerplaat and Middelplaat at Zuid Everingen). This can be explained by the fact that more sediment at the edges is stirred up by the waves, which consequently can be transported by the ebb current. At high water, the waves travel up on the shoals and the orbital velocity at the edges is somewhat less.

Due to the imposed wind and wave conditions, the depth averaged velocity increases at certain places. This increase can be caused by the wind, waves or a combination of both. The increase of the depth averaged velocity mainly occurs around the shallow parts in the estuary. This can't be only due to the wind conditions, since these conditions are constant throughout the whole area. Furthermore, at these shallow parts also the wave induced forces are the highest in the estuary. From this it can be concluded that at locations where currents are present and wave breaking occurs, the wave induced forces generate a wave driven current and therefore result in an increase of the depth averaged velocity. The increase of the depth averaged velocity directly results in increase of the local bed shear stress and hence result in an increase of the transport of sediment at the locations where currents are present. Finally, the bottom changes increases when there is a gradient in the increased transport of sediment.

The orbital velocities also results in an increase of the bed shear stress. Due to this, more sediment is entrained (stirred up) and available for transport via some current. At some places, these orbital velocities occur at locations where also currents occur (Spijkerplaat, shoals of Everingen). At other places, no significant current is available (shoals of Hooge Platen).

5.3.3 MORPHOLOGICAL IMPACT PER CLASS

In the previous section, the influence of waves on the sediment transport and morphology is described in a qualitative way. To get a grip on the quantitative influence of the different classes in the whole are, a simple presentation is applied. Therefore, the morphological impact per class is calculated. When the morphological impact per class is expressed in terms of total vertical displacement of the bottom (sedimentation and absolute values of erosion added together), practical insight is gained in which classes have the largest morphological impact. Figure 27 - Figure 29 present this morphological impact per class in

[17] A 'schaar' (Dutch) or flood branch is a typical feature of a flood current.

the three distinctive areas of the ebb tidal delta, the estuary and the whole area (ebb tidal delta and estuary).

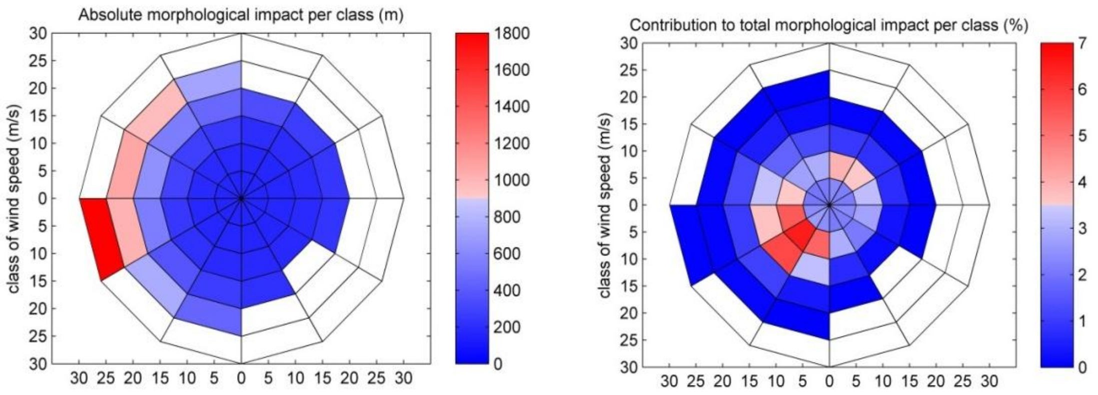

Figure 27. Morphological impact on the ebb tidal delta per class; absolute impact (left) and relative impact (right).

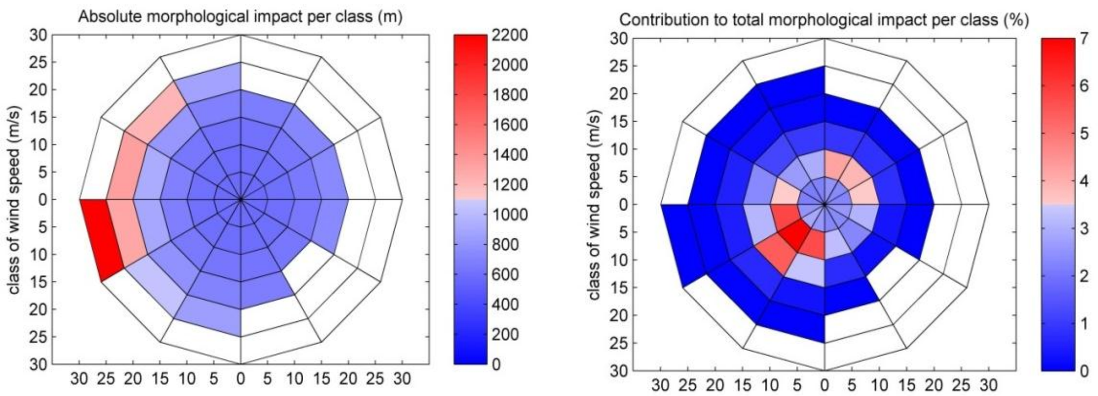

Figure 28. Morphological impact on the estuary per class; absolute impact (left) and relative impact (right).

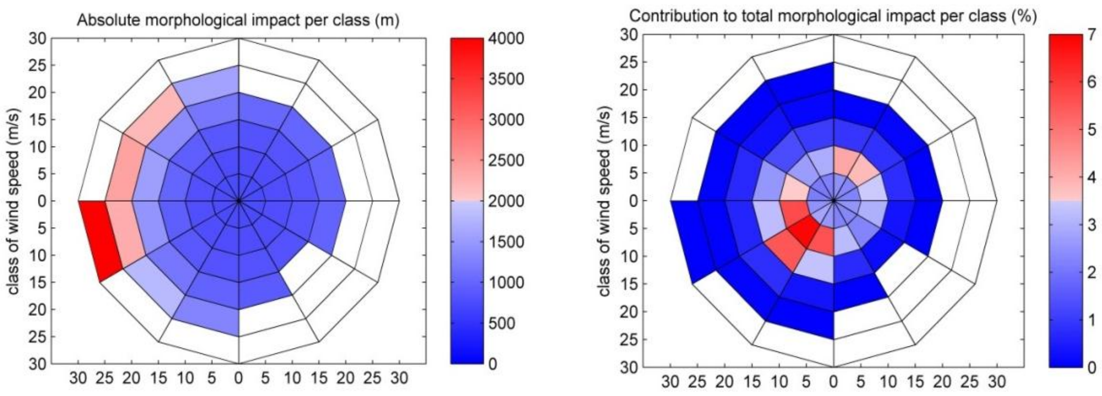

Figure 29. Morphological impact on the whole area per class; absolute impact (left) and relative impact (right).

As expected, the highest wind speeds and highest waves result in the largest morphological impact. The morphological impact from the lower wind and wave classes are considerably lower. It further appears that the morphological impact of the lower and moderate classes are much alike. This can be explained by the fact that the waves are dominated by the local wind conditions, and hence are much alike due to small fetches and moderate wind speeds. Furthermore, the wave influence focusses on the shoals of Spijkerplaat and the shoals south of Everingen, where the wave direction is subordinate to the main influence of wave at these locations (stirring up sediment, section 4.4.3) .

When the absolute morphological impact of each class (left panels in Figure 29-Figure 28) is multiplied with the probability of occurrence of each class, the figure changes completely: on a longer time scale of 20 years (on which the probability of occurrence is based) it appears that the smaller to moderate classes contributes most to the total morphological impact, especially the south-western directions. Due to the low probability of occurrence, the storm classes appear to only contribute to a small extent to the long term morphological development. When the obtained figure of the relative contribution of each class is compared to the wind climate (Figure 14, section 4.2.2, top left rose) a great resemblance is found. This can be explained by the fact that the absolute morphological impact is to a large extent the same for moderate classes, hence the relative contribution of each class is determined by the probability of occurrence. In the figures, the total elevation of sediment (sedimentation and erosion) in the area is added per class. Next, these values can easily be compared and the figure shows which class has the most morphological impact. Within this presentation, the location where the morphological impact occurs is not considered. This is allowed, since the sedimentation and erosion patterns are much alike for all classes in the estuary (Figure 149 - Figure 203, Appendix 5).

5.3.4 CONCLUSIONS

It appears that the influence of waves on the transport of sediment and morphological development is twofold. First of all, due to the orbital velocity of the waves, more sediment is stirred up compared to the situation without waves. At places where there is current present, this consequently results in an increase of the transport of sediment. Second, the wave induced forces result in an increase of the depth averaged velocities at the shallow parts in the estuary. Since both the orbital velocity and wave induced forces increase with a decrease of the water depth, the influences of the waves strongly focusses on the edges of the shoals in the estuary. The shoals where tidal currents, wave orbital motion and wave induced currents (wave breaking) occur (shoals of Spijkerplaat and shoals south of Everingen) are subject to the strongest increase of the transport of sediment and also show the largest increase in sedimentation and erosion.

Since the wave conditions inside the estuary are dominated by local conditions, the wave conditions can’t grow unlimited and don’t differ much from each other (opposite to wave conditions outside the estuary). Hence, the morphological impact of these classes is also much alike (as can be seen from figures Figure 27 - Figure 29). For all wind and wave classes (including the situation without wind and waves) applies that the highest rates of sediment transport and morphological change occur at the shoals of Spijkerplaat (east and west borders) and at the shoals south Everingen. This is due to the fact that around these shoals, currents are present to actually transport stirred up sediment. The result on the morphological development is to a great extent the same for all classes. This is due to the effect of currents and waves on a large spatial scale: waves are mostly effective at parts where already a current exist. At these places, waves result in the stirring of sediment and also increase the depth averaged flow velocity. At the locations where this happens (shoals of Spijkerplaat and shoals of Everingen), the water depth is about 1 to 3 m. As a result, the wave direction is not much of influence, as long as the sediment is stirred up. At other locations where no high flow velocities occur, the wave impact is less effective (at a large spatial scale considered here). It can thus be concluded than for the transport of sediment, currents, a limited depth and stirring by waves is needed.

Small differences between conditions occur in this case mainly due to different water levels and wave directions, due to which the waves stir up sediment at different locations on the shoals. The amount and magnitude of orbital velocity at specific locations on the shoals is very sensitive to the water level and wave direction. The edges of the shoals facing the same direction as the propagation direction of the waves receive the largest impact. For waves from a northern direction, it applies that the orbital velocities are high at the northern borders of the shoals and the coastline of Zeeuwsch Vlaanderen. Waves from a southern direction have impact and thus large orbital velocities on the southern borders of the shoals and on the coastline of Walcheren en Zuid Beveland. Since no high flow velocities occur at these places, the impact on changes in morphology is relatively low.

The influence of waves on sediment transport and morphological development mainly focusses on the shoals of Spijkerplaat and the shoals south of Everingen. At these locations, the wave direction is of less influence than the general influence of stirring of sediment by waves. Furthermore, the tidal currents transport the stirred up sediment. At location where the wind and consequently wave direction is of influence (edges of the higher shoals, e.g. Hooge Platen), no strong currents are present to transport sediment. Hence, no large morphological development occurs at these locations. The only difference that can be found is that the morphological impact is somewhat higher when waves come from a westerly direction than when waves come from a easterly direction. Due to this, the roses of the relative morphological impact per class (Figure 27 - Figure 29) are to a large extent similar to the rose of the probability of occurrence of each class (Figure 14, section 4.2.2, top left rose).

It appears that the largest contribution to the total morphological impact comes from the moderate wind and wave classes from a westerly to south-westerly directions. This is caused by the high probability of occurrence of these classes. The absolute morphological impact of the storm conditions is the largest, as was already expected (section 4.2.4). On a longer time scale however the influence of the storm conditions are negligible. The only possible influence of a storm on a longer time scale is that during such a condition the system changes (e.g. a breach in a shoal). It is therefore recommended to investigate the influence of a storm condition on a longer time scale as well.

5.3.5 RECOMMENDATIONS ON SCHEMATISATIONS

Based on the simulations of all classes and analysis of the results, three recommendations are made with respect to the wave climate schematisations in section 5.6. After the wave climate schematisations are obtained in that section, the schematisations are reviewed with respect to these recommendations.

1. To take the influences of waves on the large scale and smaller local scale into account in a proper way, multiple wind and wave directions must be represented in the schematised wave climate. The reason for this is that in this case also the relative small local differences in bottom change are taken into account.
2. The westerly wind and wave directions occur more often than easterly wind and wave directions and have a relative large contribution to the morphological impact. It is therefore recommended to include westerly classes with a high probability of occurrence.
3. Storm classes have the largest impact on the sediment transport and morphology, but occur only at small amount of time (the probability of occurrence is low). Hence, due to this low probability of occurrence, the influence on the mean medium-term morphological development is assumed to be small. Because of the possibility that a storm condition creates a new (local) morphology (e.g. by breaching a shoal) and results in irreversible changes in the system (e.g. change of the path of a channel or the dividing of a shoal) it is recommended to investigate the influence of a storm condition within a wave climate on a longer time scale as well.

5.4 METHODS OF WAVE CLASS SELECTION

The main objective of a schematisation of the wave climate is to reduce the run time of a morphological simulation. Classes are selected which together form the wave climate schematisation. In general, there are several approaches of selecting multiple wave classes for a wave climate schematisation. Two of them are frequently used (Delft University of Technology, 2012a).

- The first approach is to determine the classes manually, based on the wave height, direction and morphological impact associated with the wave height. The morphological impact is considered to be proportional to the wave height to the power of 2.5 ($H^{2.5}$). This stems from the CERC formula for sediment transport in alongshore direction at a uniform coastline. The situation in this study however can't be compared with a uniform coastline.
- For more complicated coastal areas, such as the entrance of the Western Scheldt, it is advised to use a second approach. Within this approach, a *target data set* is constructed with a numerical morphological model, which takes into account all hydrodynamic and morphodynamic processes and the interaction between these processes. This target data set is based on the quantity that needs to be reproduced by the selected classes. This quantity can be the bottom changes (the sedimentation and erosion patterns) or sediment transports in the considered area. Here, the second approach is used, by means of the optimum wave class selection (the so called Opti method). The Opti method is used to obtain schematisations based on multiple classes and schematisations based on one class. The results of the schematisation are reviewed, based on the recommendations from section 5.3.5.

Next to the approaches to select multiple wave classes within a wave climate schematisation exists the *method of correlation*. This method can be applied to select one single wave class for the schematisation. This method is applied in this thesis as well. This is done to interpret the one remaining condition from the Opti method.

5.4.1 OBJECTIVE

Before input is reduced, for a *sensible* reduction of the input, it is always necessary to first state the objective one is aiming for with the reduction. Without a stated objective, the schematisation does not make sense. The main objective of a schematisation of the wave climate is to reduce the run time of a morphological simulation. The requirement with this objective is that this schematisation reproduces the result of the complete climate schematisation within a certain range of accuracy. This schematisation exists of a reduced amount of classes. This schematisation is subsequently used to simulate the *medium-term* morphological development of the entrance of the Western Scheldt estuary. As mentioned in section 3.2.1, this is an important starting point, as the appointment of time scale (medium-term, in this case one year) determines the spatial scale on which the results of the reduced and non-reduced amount of classes need to be compared. On a medium-term morphological scale, there's no need for focus on small scale changes. Large scale changes on the other hand (e.g. sedimentation and erosion on the scale of ebb and flood channels and shoals over a period of one year) are very relevant. Changes on this time and spatial scale are to be reproduced by the reduced amount of classes within a certain range of accuracy. Summarised:

> The objective of the schematised wave climate is to reproduce the cumulative sedimentation and erosion patterns of the complete schematised wave climate on the spatial scale of ebb and flood channels and shoals in the entrance of the Western Scheldt and on a time scale of one year within a certain range of accuracy. The range of accuracy is 1% on the correlation coefficient and 10% on the root mean square difference.

Range of accuracy
The results of the simulations based on the different obtained schematisations are compared to benchmark simulations; this is done in terms of correlation and root mean square difference (section 6.4). The results of two simulations are equal when the correlation is equal to 1 and the root mean square difference is equal to 0 m. A combination of these two is necessary; when only one of the requirements is fulfilled, the results of the two simulations can still differ: e.g. a low value for the root mean square difference indicates the same sedimentation and erosion pattern, but when the correlation at the time is low as well, this means that the two results might be shifted with respect to each other.
The values of the range of accuracy are not fully objective. The final choice for a specific wave climate schematisation is a trade-off between available time (and costs) and the acceptable range of accuracy given the objective.

5.4.2 TARGET

To accomplish the objective, the wave climate schematisation can be based on the sedimentation and erosion patterns or sediment transport of the full set of wind and wave classes. The results of the full set of wind and wave classes is the *target data set.* This is the target that is aimed for when the wave climate is schematised. The way the target is constructed is described in the next section. Since this study focusses on the influence of the way the wave climate is schematised, two target data sets are constructed: one target data set based on the sedimentation and erosion patterns and one target data set based on the transport of sediment.

5.4.3 OPTIMUM METHOD

In this study, the wave class selection for the wave climate schematisation with multiple classes is based on the optimum approach. This choice is made since the hydrodynamic and morphodynamic processes in the entrance of the Western Scheldt are complex and multiple coastline orientations are present. Because of this complexity, a target data set is obtained by use of a morphological model (in this case Delft3D) which takes these processes and interactions into account. This comprehensive target forms the starting point for the optimum method.

Background of the optimum method
In order to reduce the run time of medium to long-term morphological simulations, the number of wave conditions in a wave climate should be reduced. However, the results of the simulation should not be affected significantly. To this purpose, the Opti method is developed (Roelvink, 2006 and adjusted by Mol in 2006, Lesser in 2007 and Morelissen in 2007 (Mol, 2007)). In general, a set of classes in a climate schematisation is reduced to a smaller set of classes within the schematisation, which should reproduce the result of the full set of conditions within a certain range of accuracy. More or less unnecessary classes are left out. However, the more the set is reduced, the less accurate the reduced set reproduces the result of the full set of classes. The result of the full set of conditions can be e.g. the weighted sediment transport or sedimentation and erosion patterns (i.e. bottom change). The accuracy of the reduced set with respect to the full set is described in terms of statistical parameters, whereby the correlation coefficient (eq. 4.5) and the root mean square difference (5.4) are the most important ones.

Figure 30 shows the development of the correlation coefficient and the root mean square difference when the amount of classes decreases.

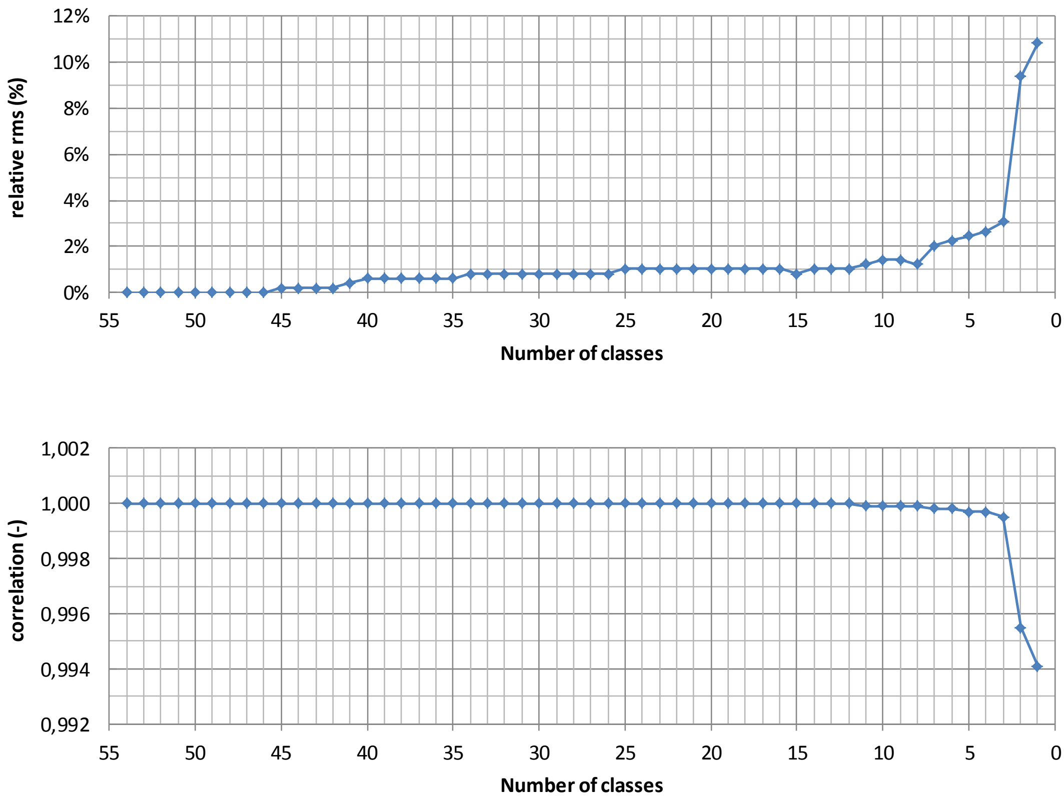

Figure 30. Deviation (relative rms) and correlation coefficient as a function of the amount of classes. Based on 20,000 iterations.

Procedure of the optimum method

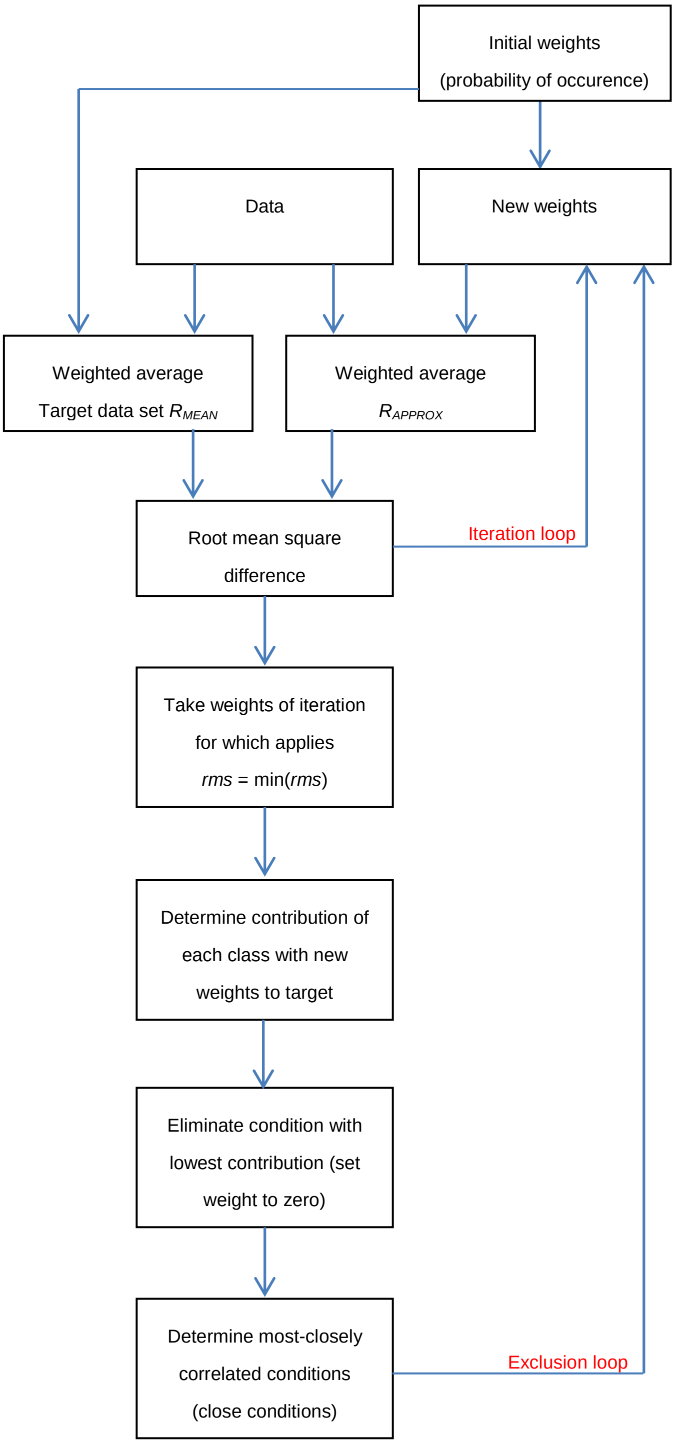

Figure 31. Overview of the procedure within in the optimum method (derived from Roelvink and Reniers, 2011).

The target data set consists of the results of a series of short morphological simulations (in this case 54 simulations). These simulations are performed for all appointed wind and wave classes during a certain (short) period of the tidal motion (section 5.3) and form the base form the further schematisation. For all classes the initial weight factor ($W_0\ (c_i)$, equal to the probability of occurrence of that class) is included.

Based on these separate simulations, the Opti program calculates an overall weighted averaged result due to all wind and wave classes. This weighted averaged result (R_{MEAN}) is the summation of the results per wind and wave class, multiplied with the specific weight factor of that class. The result per class consists of the result in each grid point of the calculation grid. In fact, R_{MEAN} can be displayed as the calculation grid (or matrix with size X times Y) with weighted average values in each individual grid cell of the calculation grid. The weighted averaged result (R_{MEAN}) is called the target data set, as it acts as a target which has to be achieved (approximately).

$$R_{MEAN} = \sum_{i=1}^{n} (result\ (c_i) \times W_0\ (c_i)) \tag{5.1}$$

with	R_{MEAN}	= weighted averaged result, or target data set
	n	= number of all classes
	$result\ (c_i)$	= sediment transport or sedimentation and erosion per class
	$W_0\ (c_i)$	= initial weight factor per class

Based on the relative contribution of all classes to the total result (the target data set, R_{MEAN}), the Opti program determines which class contributed the least to the total result. Consequently, this condition is dropped (the weight factor of that class is set to zero). From this point, the exclusion step starts, which is an iteration loop. The remaining (*m* or *n-1*) classes are all assigned a new individual weight factor (*W*). With this set of new weight factors, the new average result (R_{APPROX}) is compared to the target data set (R_{MEAN}). This new averaged result is named R_{APPROX}, since the objective of this result is to *approximate* the target data set R_{MEAN}.

$$R_{APPROX} = \sum_{i=1}^{m} (result\ (c_i) \times W\ (c_i)) \tag{5.2}$$

with	R_{APPROX}	= weighted average result of remaining classes
	m	= number of remaining classes
	$W\ (c_i)$	= new assigned weight per remaining class

The new weight factor is the product of the original weight, times a value from the range 0 – 2. The data between the range 0 – 2 has a uniform distribution; as a result the expected value to be drawn from the range is around 1 (E[X] = 1), when enough draws are done. Consequently, when enough draws are done, the new weight of a certain class is multiplied with a value close to one and hence very similar to the original weight, which is based on the probability of occurrence (Roelvink, personal communication). This assigning of new weights (draws) is performed about several hundreds of times (user defined) for the situation with a constant amount of remaining classes (*m*), resulting in an equal amount of R_{APPROX} results. This is the secondary iteration loop within the exclusion step. One of these several hundreds of results reproduces the target data set the best. From the combination of classes and weights which reproduces the target set the best, again the class with the smallest contribution is dropped (the weight factor of that class is set to zero). After this, the following exclusion step is started: the remaining conditions (*m-1*) are again assigned a new weight (again this is performed about several hundreds of times in the secondary iteration loop), several hundreds of R_{APPROX} are compared to R_{MEAN}, the combination of classes and weight factors that approximates R_{MEAN} the best is kept, from which the class with the smallest contribution is dropped again. This whole procedure of exclusion steps and secondary iteration loops continues until finally one class with a certain weight factor remains. The weight of the remaining classes consequently increase when other classes are dropped. The weight of the classes is redistributed over the remaining classes.

Comparison of results within the optimum method

The comparison of R_{APPROX} (equation 5.2) with R_{MEAN} (equation 5.1) is based on several statistical parameters. These are calculated from the simulated values for R_{APPROX} and R_{MEAN}. The bias, root mean square difference (*rms*), and linear correlation coefficient (*r*) are used. From the Opti script (Roelvink, 2006) is obtained to which quantity these parameters relate. The bias and root mean square difference relate to differences in *local deviations from the mean value* (where for the assessment of the wave modelling the bias and root mean square difference relate to difference in *mean value*). The linear correlation coefficient (indicating the amount of correlation between the two data sets) is already defined by equation 4.5.

The bias is defined as the average difference in local deviations from the mean value between R_{MEAN} ($\bar{x}$) and R_{APPROX} ($\bar{y}$) and is a measure for the difference:

$$\text{bias} = \frac{1}{n}\sum_{i=1}^{n}[(x_i - \bar{x}) - (y_i - \bar{y})] \qquad (5.3)$$

The root mean square difference (rms) is also a value for the difference between the measured and simulated values, defined by:

$$\text{rms}^{18} = \left[\frac{1}{n}\sum_{i=1}^{n}[(x_i - \bar{x}) - (y_i - \bar{y})]^2\right]^{1/2} \qquad (5.4)$$

First of all, for both results, the standard deviation is calculated (abbreviated to *stdm* for R_{MEAN} and *stdc* for R_{APPROX}). The standard deviation is a measure for the average deviation with respect to the average value in the considered area (e.g. the average value of sediment transport or sedimentation and erosion). Next, for the relation between R_{MEAN} and R_{APPROX} the bias, the root mean square difference (*rms*), the covariance (*cov*) and the correlation coefficient (*corr*) are calculated. For the bias, at each individual grid point the difference between the deviation from the average value in R_{APPROX} and R_{MEAN} is determined. The bias itself is the average difference in local deviations from the mean. For the perfect approximation of R_{MEAN} by R_{APPROX}, the individual values at the grid points and the average value are the same for R_{MEAN} and R_{APPROX}, which results in a bias of zero. The larger the bias, the larger the difference between R_{MEAN} and R_{APPROX}. The root mean square difference (rms) is comparable to the bias, but now the differences are squared before they are added. After the summation, the square root is taken. The advantage of the root mean square difference is that all differences are expressed in positive values. Again, the root mean square difference is an average difference over all grid points where differences occur. When added together, a good insight in the overall difference between R_{MEAN} and R_{APPROX} is obtained. When the difference is small, the differences between R_{APPROX} and R_{MEAN} are small as well and the results are similar to a large extent. Within the iteration loop as described in the previous section, the set of weights which result in the smallest root mean square difference (and thus approximates R_{MEAN} the best) is taken as the new set of weights. Finally, the covariance and the correlation coefficient are calculated. Both parameters express the

[18] Here, the root mean square difference is equal to the standard deviation (*stdev*) of the differences between two data sets as defined by equation 4.4. This is due to the quantity (the local difference with the mean value) to which the root mean square difference relates to.

relation between R_{MEAN} and R_{APPROX}, where the correlation coefficient is a standardized version of the covariance. A positive covariance is obtained when the trend in R_{MEAN} and R_{APPROX} is the same, i.e. when the value at a local grid point is larger than the average value in R_{MEAN}, this is also the case in R_{APPROX}. The extent to which both sediment transports are correlated is determined by the correlation coefficient: the correlation is highest for a value of the correlation coefficient of 1.

Summarised, for a 'good' approximation of R_{MEAN} by R_{APPROX}, the root mean square difference must be small (approximate 0.0 m), the covariance must be positive (>1) and the correlation coefficient must approximate the value of 1.

Development of difference between simulations
To quantify the root means square difference (*rms*) relative to the weighted average result (R_{MEAN}), the relative root mean square difference is defined by the ratio between the rms and the standard deviation of R_{MEAN} (stdm or $\sigma(x)$, equation 4.7):

$$\text{Relative rms} = \frac{Rms\ (x,y)}{\sigma(x)} \times 100\% = \frac{\left[\frac{1}{n}\sum_{i=1}^{n}[(x_i-\bar{x})-(y_i-\bar{y})]^2\right]^{1/2}}{\left[\frac{1}{n}\sum_{i=1}^{n}(x_i-\bar{x})^2\right]^{1/2}} \times 100\% \tag{5.5}$$

Here, the *difference in deviations from the mean* are compared to the original *deviations from the mean* [19]. Consequently, an increase of the absolute difference results in an increase of the relative difference. From this relative difference, insight in the seriousness of the difference is gained.

Interpretation of the root mean square difference
The relative and absolute root mean square differences are difficult parameters to interpret. First of all, the absolute root mean square difference is a measure for the difference between the *local deviations from the mean bottom change* of two simulations. When two simulations are very similar, the bottom change in the considered area is similar. As a consequence, the mean bottom change is similar and also the *local deviations from the mean bottom change* are very similar. Hence, the difference in local deviations from the mean bottom change are small in this case. To express this difference in one parameter, all differences are added and squared. After this, the mean value is calculated after which the root is taken (hence the name *root, mean, square*). When the results of two simulations are very similar, the local differences are small and hence the root mean square difference is small. To interpret the *relative* value of the root mean square difference, it can be divided by the *standard deviation* of the reference (i.e. benchmark) simulation. This standard deviation is a measure for the average local deviation from the mean bottom change.

Influence amount of iterations
The amount of iterations made in the exclusion step in the Opti method is of influence on the selected classes. Ideally, a high number of iterations (draws) is made to increase the probability of finding a 'perfect' set of new weights, and hence decreasing the error between R_{MEAN} and R_{APPROX}. This certainly holds for the situation where a higher amount of classes is used in the schematisation (five classes or higher). Below a number of five classes, a higher amount of iterations doesn't necessarily results in the lowest error; especially when only one or two classes are considered. The reason for this is that in the

[19] This is comparable to the scatter index in section 4.5.1, where the *difference in mean value* between measurement and simulation are compared to the *mean value* of the measurement. There it is called the scatter index, here it is called the relative root mean square difference. Different quantities are considered, but both are a measure for the difference relative to a reference situation.

previous steps, some classes are dropped out that might give a better result than the 1 or 2 classes that still remain. Once a class is dropped, it can't be taken into account anymore. When a different amount of iterations is applied within the Opti method, different classes may remain in the end. It is therefore possible that the single class that remains when e.g. 500 iterations are used shows a smaller deviation compared to the target data set than the single class that remains when e.g. 10,000 iterations are used.

For this study a number of 20,000 iterations per exclusion step has been used (Figure 30). For the schematisations based on 5, 10 or 15 classes this amount of iterations results in the lowest deviation (rms) with respect to the target data set. It was found that a higher amount of iterations doesn't result in smaller errors. For the schematisation based on 1 class, this amount of iterations does not result in the lowest error. When a different amount of iterations is used (e.g. 1,000) a smaller error was found since a different class remains. For this study, the choice is made to obtain the lowest errors for the schematisations based on 5, 10 and 15 classes, and hence the amount of 20,000 iterations is applied. For consistency, this amount is also applied to determine the class for the schematisation based on 1 class.

Output of the optimum method

After each exclusion of a wind and wave class, the Opti program writes the results to two output files (*opti.txt* and *corr0.tek*). In *opti.txt* the new statistical parameters and the new weight factors for each class are written. In *corr0.tek* for each grid point the new averaged morphological change (the best R_{APPROX} per amount *(m)* of classes) and the original morphological change (R_{MEAN}) are written. When the program is finished, the user can select the number of classes to use on the basis of the required accuracy, which can be read from the statistical output (*opti.txt*).

5.4.4 METHOD OF CORRELATION

The method of correlation is applied to select one single class for the climate schematisation. This method is applied in this thesis to interpret the selected single class when the Opti method is used. It is expected that the remaining class from the method of correlation gives a better representation of the complete wave climate schematisation than the remaining class from the Opti method. The reason for this lies in the difference in approach to select this one class. In the method of correlation, first the weighted average result of all classes and their individual initial weights is calculated (R_{MEAN}, eq. 5.1). Next, the results of all individual classes are related to this weighted average result. The class with the highest correlation with the weighted average is selected as the one single class to represent the complete wave climate schematisation. This differs from the Opti method, where the one single class in the end of the procedure is selected from the remaining classes. At each step in the Opti method, certain classes are excluded, hence not all classes are individually correlated to the weighted average. Due to this is expected that to select one single class, the method of correlation is more appropriate than the Opti method. The method of correlation can't be used to select multiple wave classes. Results of the influence of the applied method for climate schematisations existing of one class are presented in section 6.4.2.

5.4.5 DISCUSSION

The Opti method can be considered a default method for input reduction for comprehensive targets (Delft University of Technology, 2012a). The reason for this is that the method is automated (it is run as a Matlab program), and it is relative objective in its assessment of the different schematised wave climates with respect to the complete wave climate schematisation. Besides the choice on the type of target, area of interest and amount of iteration within the procedure, the result is not influenced by the user of the method. A drawback of the method from a practical point of view is that it is relative (computational) expensive since all wave conditions have to be simulated to construct the target data set.

When the obtained wave climate schematisations are applied in order to simulate the medium-term morphological development, it is important to realize the difference in time scales between the medium-term time scale and the time scales of the short simulations on which the schematisations are based. The time period of these short simulations is too short to let bottom changes influence the hydrodynamics; i.e. the wave climate schematisations are based on initial changes. The schematised wave climate is however constructed to predict morphological changes on a (much) longer time scale, in this case one year. When the schematised wave climate is used for this purpose, implicitly some assumptions are made:

- First of all, the order in which the classes occur doesn't influence the result of the morphological development (since the benchmark is the weighted average result).
- Second, as a result of this, all processes and influences by the different classes are assumed to be reversible, i.e. there is not one class that influences the morphology in such in way that it can't be reversed by other classes.
- Finally in the short simulations, enough sediment is available to entrain and transport; on a longer time scale this might not be the case.

As a result of these assumption, the question arises what predictive value the wave climate schematisations, based on initial changes, have. To address this predictive value, also a benchmark on a longer time scale is needed. Performing a benchmark simulation over a longer time period (in this case one year) is however not recommendable, since this construction would take a large amount of time (since in that case all defined class should be run over one year) [20]. Within the schedule of this thesis study, this would take too much time. An alternative might be to use a measured bottom change as a benchmark. This however has the drawback that the result of the morphological simulation over a period of one year might differ from the measured situation for other reasons than wave climate schematisation (such as the user defined parameters for wave and current related transport, slope factors, morphological tides, sediment characteristics…). The model as used is calibrated for the time period 1 January 1998 – 1 January 2002. As a result, comparing the simulation of a certain wave climate schematisation with a measured change is not a good method to address the predictability of a wave climate schematisation with respect to the complete wave climate schematisation. The approach followed in this study is therefore to use the wave schematisation existing of 15 classes as the benchmark simulation. The reason for this is that on a short time scale, the error made with the target data set (based on the full wave climate schematisation) is small (Figure 30, 5.4.3). Since in the 15 classes all directions are represented and also different wind speed classes are represented it is consequently assumed that also on a time scale of one year the error made with respect to the full wave climate is small.

---

[20] Ideally, the benchmark simulation is a brute force simulation during the period of interest, based on the full time series of water levels, currents, wind and waves (Lesser, 2009).

5.5 WAVE CLASS SELECTION

The objective of this section is to select wave classes and with this classes obtain multiple different wave climate schematisations. The classes are selected from the complete wave climate schematisation (Figure 14, section 4.2.2). The wave classes are selected by use of the Opti method and by use of the method of correlation. Both methods are described in the previous section. The Opti method is applied to obtain wave climate schematisations existing multiple wave classes *and* schematisations existing of only one wave class. The method of correlation is applied to obtain wave climate schematisations existing of only one wave class.

Before a wave climate schematisation can be constructed from selected wave class, multiple decisions have to be made. These decisions influence which classes are selected and hence influence the wave climate schematisation. It is expected that different wave climate schematisation result in different simulated morphological developments. Decisions for the selection of the wave classes have to made on:

- the method of wave class selection: Opti method or method of correlation:
- type of target (R_{MEAN}, section 5.4.2): bottom changes or sediment transport:
- location of target: estuary, ebb tidal delta or both locations:
- amount of classes: one wave class or more wave classes (and how many):
- including seasonality and storm events.

As described in section 1.2, this thesis investigates the influence of the wave climate schematisation on the simulated morphological development. Therefore, multiple different wave climate schematisations are constructed, based on all above mentioned choices. This finally results in 29 different wave climate schematisations. In the following, the type and location of the target, the amount of classes and including seasonality and storm events are described. The resulting wave climate schematisations are presented in section 5.6, where all the different schematisation are coded. The influence of these wave climate schematisations on the simulated morphological development are quantified in chapter 6, where simulations based on these schematisations are described and discussed.

5.5.1 TYPE OF TARGET

For the wave climate schematisation, distinction is made between two different types of target. The first target is the sedimentation and erosion in the considered area (i.e. the bottom change), the second target is the transport of sediment in the considered area. This distinction is made since from the analysis of the 54 classes appears that transport of sediment not always results in a bottom change. This is explainable, since changes in morphology only occur when a transport *gradient* is present. Since transport and bottom changes occur not necessarily at the same places, it is expected that schematisations based on transport or bottom change differ.

5.5.2 LOCATION OF TARGET

For the selection of the classes, the target (bottom change or transport of sediment) is based on three distinctive areas. These are the western part of the estuary between Vlissingen and Terneuzen, the ebb tidal delta and the two areas combined. Figure 32 shows these areas. The reason for this distinction is that inside the estuary, the wave conditions and thus the wave related morphological development are mainly influenced by local wind and current conditions (estuary wind climate, as discussed in section 4.4.3). Outside the estuary the wave conditions, and consequently the wave related morphological development, are influenced by imposed wave conditions and local wind conditions (North Sea wind and wave climate). From this can be expected that the selected classes (and hence the wave climate schematisation) based on the areas differ; for the ebb tidal delta it is expected that larger classes (higher wind speeds, higher waves) are included in the schematisation (since only the higher classes influence the morphology on the ebb tidal delta). For the estuary, it is expected that lower classes (lower wind speeds, lower waves) are included in the schematisation (since these are the main occurring classes in the estuary).

Figure 32. Locations of targets: area of the ebb tidal delta (between line Vlissingen – Breskens and line Westkapelle - Zeebrugge) and the area of the estuary (east of the line Vlissingen – Breskens).

5.5.3 AMOUNT OF CLASSES

In general, the amount of wave conditions can reduced till about 30% of the original amount remains without significantly affecting the result (good practise, Delft University of Technology, 2012a). With regard to the amount of appointed classes in this study (54), the hypotheses is that a reduction to 15 remaining classes (about 30% of 54) will not significantly affect the result.

For the wave climate schematisations, four different amount of classes are considered. The schematisations are based on 15 classes, 10 classes, 5 classes and 1 class. It can be expected that from 15 classes on that the results starts to deviate from the full amount of classes. Therefore, 10, 5 and 1 class schematisations are considered as well. To compare the results of the schematisations, a benchmark simulation is needed. As discussed in section 5.4.5, the wave climate schematisations based on 15 classes will serve as benchmark simulations. The Opti method is used to determine four different amount of classes within the wave climate schematisations:

- 15 wave classes
- 10 wave classes
- 5 wave classes
- 1 wave class

5.5.4 SEASONALITY AND STORM EVENT

The type of target and location of the target determine which classes are selected in the wave climate schematisation. Within the selected classes, distinction can be made between classes typical for a winter (storm) season and classes for a summer (mild) season (the seasonality is described in section 4.2.2). By doing so and consequently placing the typical classes within the winter or summer season, seasonality is taken into account. When the wave schematisations are investigated in further detail, it shows however that all selected wind and wave classes in the obtained climate schematisations occur in winter ánd summer season. This is not surprising, since the winter season can be distinguished from the summer season by the occurrence of high wind and wave classes. These high wind and wave classes are not selected in the final schematisations (due to the low probability of occurrence). Since all selected classes in the wave schematisation can occur in both winter and summer season, they can't be classified as only a winter or summer class. However, from analysis of the wind and wave climate for both seasons, it becomes clear that the probability of occurrence of individual classes can differ for both seasons.

To investigate the influence of seasonality, a schematisation existing of five wind and wave classes is used as a reference (code M03, Table 13). First, these five classes are assumed to occur in the winter season. Next, the same five classes are assumed to occur in the summer season. The difference between the two seasons is made by appointing different weight to the conditions in winter and summer season. Table 10 clarifies this. By the approach, a total of ten wind and wave classes are applied (two times the same selected five conditions), each with a different weight in accordance with the winter of summer season.

Class	Wind direction class (°N)	Wind speed class (m/s)	Probability of occurrence per year (%)	Probability of occurrence per winter season (%)	Probability of occurrence per summer season (%)
6	30 – 60	5 – 10	3.92	2.40	5.44
17	120 – 150	0 – 5	2.48	2.73	2.24
24	180 – 210	0 – 5	2.75	2.87	2.64
36	240 – 270	10 – 15	2.79	3.41	2.18
45	300 – 330	0 – 5	2.25	1.31	3.18

Table 10. Probability of occurrence of the wind conditions of the five selected classes per year, per winter season and per summer season. The selected classes are based on a five classes schematisation with the Opti method and based on bottom changes (sedimentation-erosion patterns). Probability of occurrence is based on the time series 1981 – 2001.

As part of the selection procedure within the Opti method, the original probabilities of occurrence per year (as presented in Table 10) are modified to a new probability of occurrence (or 'weight' as used term in the Opti method). The sum of the probabilities of occurrence of the five selected classes is 100%. Based on the new weights, the morphological acceleration factor (*morfac*) is determined as described in section 6.2.1 (eq. 6.1). Here, the *morfac* of the five individual classes to cover one year, one winter season and one summer season are presented.

Class	Wind direction bin (°N)	Wind speed bin (m/s)	Morfac per year (-)	Morfac per winter season (-)	Morfac per summer season (-)
6	30 – 60	5 – 10	85.59	26.17	59.32
17	120 – 150	0 – 5	52.74	29.08	23.83
24	180 – 210	0 – 5	98.19	51.16	46.95
36	240 – 270	10 – 15	70.33	43.10	27.33
45	300 – 330	0 – 5	45.23	13.32	31.89

Table 11. Selected classes, based on five classes schematisation and based on bottom changes (sedimentation-erosion patterns).

The sum of *morfac* values per class in winter and summer season is equal to the morfac value of that class over one year. The distribution of the morfac values is based on the probability of occurrence of a certain class per winter and summer season. As example: class 6 has a probability of occurrence of 2.40% in winter (Table 10) and a probability of occurrence in summer of 5.44%. The morfac per year for that class is 85.59 (based on Opti method, Table 11). Hence, the *morfac* for class 6 for the winter season is 2.40/(2.40 + 5.44) x 85.59 (equal to 26.17) and the *morfac* for class 6 in the summer season is 5.44/(2.40 + 5.44) x 85.59 (equal to 59.32). In this way, the applied *morfac* takes into account the probability of occurrence of a certain selected in winter and summer season. The morphological simulation (code M25) consists of five classes in the winter season with the morfac values for the winter season and again these five classes in the summer season with the morfac values for the summer season.
To answer the question what for this situation the influence of the seasonality is on the predicted morphological development, results of the described simulation (code M25) must be compared to the simulation with the same five conditions without seasonal influence (code M03).

Sensitivity to storm event
So far, the influence of the different wind and wave classes on the *mean* morphological development on a medium-term time scale have been addressed. With the approach followed, an idea is gained on the mean continuous development, without taking into account the influence of storms or sequence of different conditions. Consequently, with that approach, possible switching points in the natural system (if there are any) are overlooked. Possible switching points are e.g. the formation of a new channel due to breaching of a tidal flat or the change of pattern of an existing channel.

To address the sensitivity of the system to events that possibly result to switching points in the system, such an event (a severe storm condition) is imposed. It is thus investigated whether a severe storm event can results in a switching point in the system (a permanent change in the system which can't be reversed). Since storm events only occur in the winter season (section 4.2.2), they are a typical characteristic of seasonality. For this reason, a storm condition is imposed on the wave schematisation based on seasonality, described earlier in this section. The imposed storm condition is that of class 39. The averaged values of wind and wave conditions of this storm class are presented in Table 12.

Class	Wind direction (°N)	Wind speed (m/s)	Wave height H_{m0} (m)	Wave period T_p (s)	Wave direction (°N)	Surge (m)	Probability of occurrence (%)
39	260.0	22.39	5.05	9.36	249.0	1.06	0.3

Table 12. Characteristics of storm conditions, class 39. Characteristics are averaged values over the measured storm seasons 1981 – 2001.

The storm event is imposed as an extra class within the wave climate schematisation. Due to the low probability of occurrence, the total percentage of occurring wind and wave classes remains approximately 100. The storm conditions are assumed to last for 26 hours (equal to 0.3% of the total duration of the year). A severe storm might last longer (up to 36 hours or more), but in a real storm, the conditions aren't constant throughout the storm. Here a storm is presented with a duration of 26 hours and conditions constant throughout the duration. According to the followed approach, this results in a morfac of 1.05.

When the morphological development is compared to the simulation with seasonality excluding the storm event (code M25), insight is gained in the time scale of the effect on the storm condition and hence the sensitivity of the predicted morphological development to such a storm event. Results of the simulations based on the wave climate schematisation are described and discussed in chapter 6.

5.6 WAVE CLIMATE SCHEMATISATIONS

In the previous section the choices on the method of selection, the type and location of the target are described, the different amount of classes and the implementation of seasonality and storm events are described. Altogether, this results in 29 different wave climate schematisations: 26 schematisation based on selected classes with the Opti method (2 types of target x 3 locations of target x 4 different amount of classes + 2 classes for seasonality and storm events) and three schematisations based on the method of correlation. Table 13 presents the codes of the wave climate schematisations.

Type of target	Location of target	15 classes (benchmarks)	10 classes	5 classes	1 class (opti)	1 class (correlation)
Bottom change	Whole area	M01	M02	M03	M04	M27
Bottom change	Ebb tidal delta	M05	M06	M07	M08	M28
Bottom change	Estuary	M09	M10	M11	M12	M27 [21]
Transport	Whole area	M13	M14	M15	M16	M27
Transport	Ebb tidal delta	M17	M18	M19	M20	M27
Transport	Estuary	M21	M22	M23	M24	M29
Seasonality				M25		
Storm				M26		

Table 13. Code of wave climate schematisations. Simulation M01 forms the benchmark for M02, M03 and M04, simulation M05 forms the benchmark for M06, M07 and M08, et cetera. The M in the code name refers to the fact that the simulations based on the schematisations refer to Morphological development.

The simulations with included seasonality and storms are based on M03. The reason for this is that M03 has a five class schematisation, which has a shorter simulation run time than a 10 or 15 class schematisation. The choice on the type (bottom change) and location of target (whole area) is arbitrary for addressing the influence of seasonality and a storm event. The simulation with the included seasonality is coded M25, the simulation with the included storm is coded M26. To assess the influence of seasonality, M25 must be compared to M03, since the same classes are included. To assess the influence of a storm, M26 must be compared to M25.

[21] Schematisation M27 is based on wind and wave class 140. From comparison of correlation between individual classes and the weighted average, this class shows the highest correlation for four of the six combinations of type and location of target. The schematisation is therefore mentioned four times.

5.6.1 SELECTED CLASSES AND WEIGHT

The following figures present the different obtained wave climate schematisation with their selected classes and their individual weights. These wave climate schematisations represent the complete wave climate schematisation as presented in Figure 14 (top left rose).

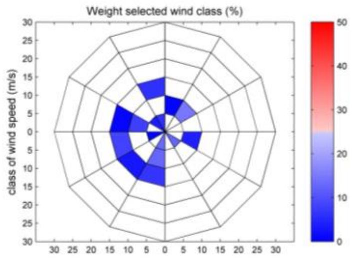

M01; Sed-ero, **whole area**, 15 classes

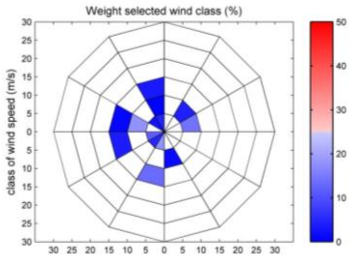

M05; Sed-ero, **outer delta**, 15 classes

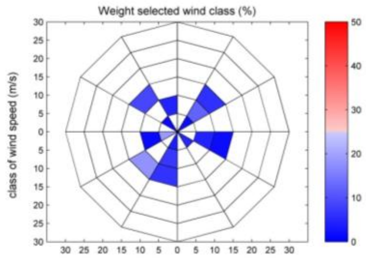

M09; Sed-ero, **estuary**, 15 classes

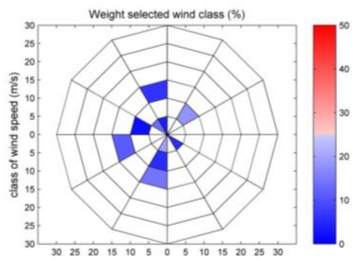

M02; Sed-ero, **whole area**, 10 classes

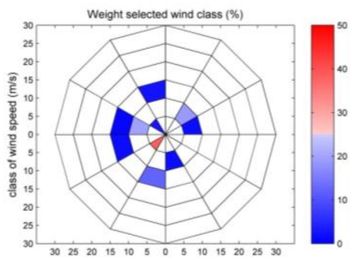

M06; Sed-ero, **outer delta**, 10 classes

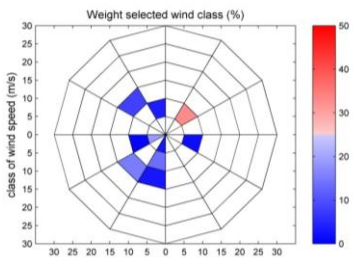

M10; Sed-ero, **estuary**, 10 classes

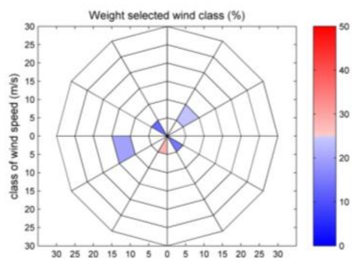

M03; Sed-ero, **whole area**, 5 classes

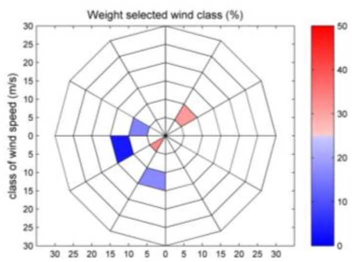

M07; Sed-ero, **outer delta**, 5 classes

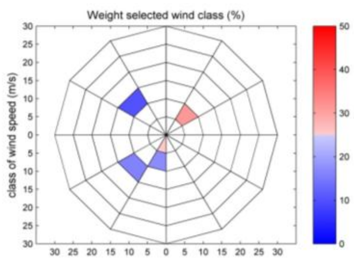

M11; Sed-ero, **estuary**, 5 classes

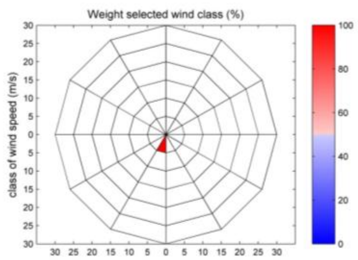

M04; Sed-ero, **whole area**, 1 class

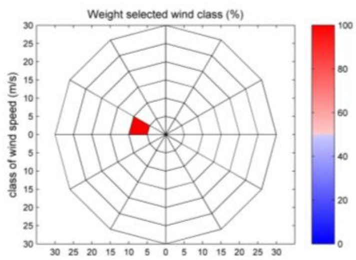

M08; Sed-ero, **outer delta**, 1 class

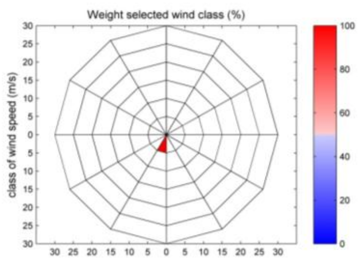

M12; Sed-ero, **estuary**, 1 class

Figure 33. Schematised climates, based on sedimentation and erosion

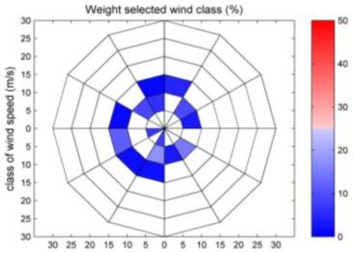

M13; Transport, **whole area**, 15 classes

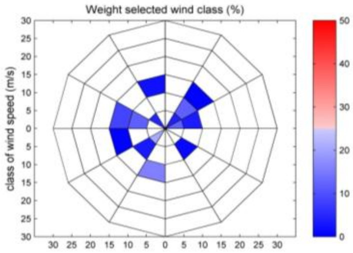

M17; Transport, **outer delta**, 15 classes

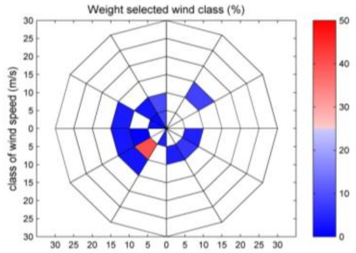

M21; Transport, **estuary**, 15 classes

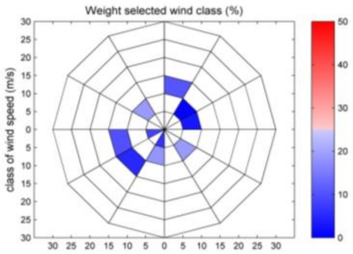

M16; Transport, **whole area**, 10 classes

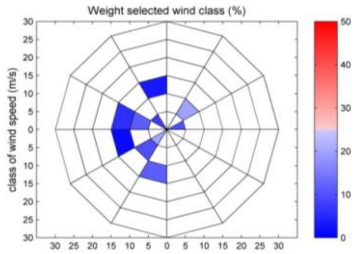

M18; Transport, **outer delta**, 10 classes

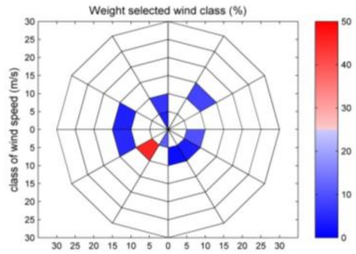

M22; Transport, **estuary**, 10 classes

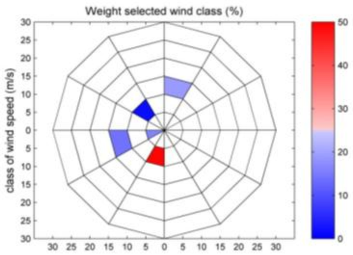

M15; Transport, **whole area**, 5 classes

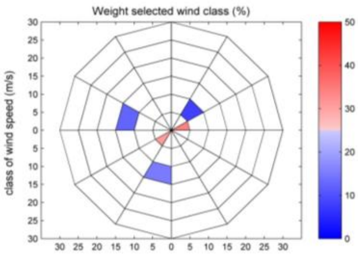

M19; Transport, **outer delta**, 5 classes

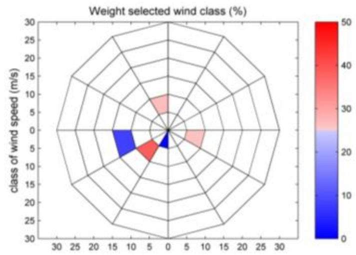

M23; Transport, **estuary**, 5 classes

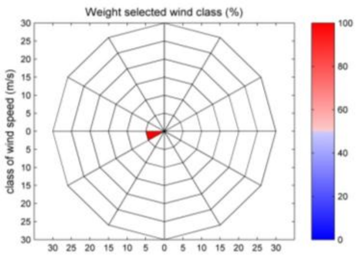

M15; Transport, **whole area**, 1 class

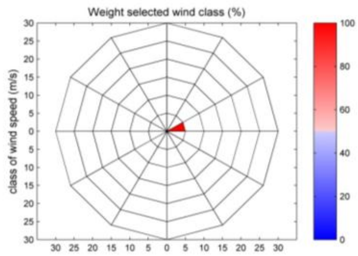

M20; Transport, **outer delta**, 1 class

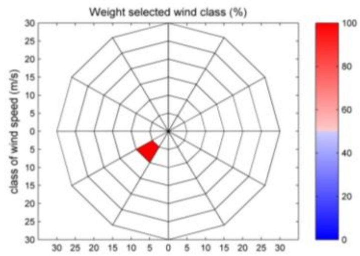

M24; Transport, **estuary**, 1 class

Figure 34. Schematised climates, based on sediment transport.

5.6.2 CONCLUSIONS ON SCHEMATISATIONS

The objective of this chapter is to obtain multiple wave climate schematisations and to review these schematisations based on insight in the physics of the waves and their influence on morphological development. Finally, 29 different schematisations are obtained. When the schematised climates are analysed, several conclusions can be made:

1. In all schematisations with five or more classes, both westerly and easterly directions are presented. The south-westerly directions have in all schematisations of five or more classes the highest contribution to the schematisations. This is in agreement with Figure 27Figure 29, where the south-westerly directions are shown to have the highest contribution to the morphological impact (right column of the figure);
2. When the amount of classes reduces, the weight of classes close by the dropped-of class increases; this is explainable, since the class close-by is likely to have more or less the same morphological impact;
3. Between the different areas considered, there is a large similarity between the selected classes. When the schematisation is based on the estuary, easterly directions have a slightly higher contribution in the schematisations compared to the schematisations based on the ebb tidal delta. The schematisations based on the whole area combines wave classes that are selected for the ebb tidal delta and the estuary and are therefore also very similar.
4. The classes taken into account have a maximum wind speed of 15 m/s. Higher wind speed classes are dropped. This is in line with the relative morphological impact of those classes, which is relatively small (as can be seen from Figure 27 - Figure 29).
5. In the wave climate schematisations of five classes or more, multiple wind speed classes are represented. The morphological impact depends amongst others on the surge, which is taken into account in this way.
6. Between the schematisations based on sedimentation and erosion and based on sediment transport, no significant differences in selected classes occur.
7. When the amount of classes is considered, the schematisations show large similarities for 15, 10 and 5 classes. The same classes, or classes close-by, are selected. Also the weight of the selected classes show great similarity. This does not hold for the schematisations based on one class: here the selected class can differ significantly between the different schematisations. In all but one schematisations of one class, the remaining class has a westerly direction. Exception is the selected class in schematisation M20, which has a easterly direction.

Reference to recommendations

In section 5.3.5 three recommendations on the wave climate schematisations were made based on the analysis of the short morphological simulations of all classes. Summarized it was recommended to:

1. Include multiple wind and wave directions in the schematised wave climate to take the influences of waves on the large scale and smaller local scales into account in a proper way;
2. Include westerly classes with a high probability of occurrence since they have a large contribution to the morphological impact;
3. Investigate the influence of a storm condition within a wave climate on a longer time scale than the storm duration.

The last recommendation is followed by manual including a storm class in the schematisation. The first two recommendations are well included in the schematised climates. From this and the other remarks made on the schematisations can be concluded that the schematisations seem reliable. Consequently, the wave climate schematisations are judged to be applicable for the simulation of the medium-term morphological development.

6 Modelling of the morphological development

6.1 INTRODUCTION

This chapter serves the third and last trace of the thesis approach (section 1.4). This chapter thus builds on the results of the previous chapters. Based on the results and conclusions of this chapter, the research questions of this thesis can be answered. This chapter describes the morphological simulations based on the 29 different obtained wave climate schematisations from chapter 5. From the results of these different morphological simulations, conclusions are stated on the influence of the way the wave climate is schematised. As stated in the objective (section 1.2), the results of the different simulations are compared at the spatial scale of the ebb and flood currents and the shoals and a time scale of one year.

First, the important details of approach in modelling the morphological development are described (section 6.2). After that, the results of six benchmark simulations are described. These are the simulations which are based on the wave climate schematisations that consist of fifteen wave classes (as discussed in section 5.4.5). Third, the results of the simulations based on the other wave climate schematisations (based on 10, 5 and 1 class) are described. These are compared to the benchmark simulations and with each other. The comparison is described in terms of statistical and physical parameters. The physical parameters applied are sedimentation and erosion patterns, volume changes in ebb and current channels and hypsometric curves. The found differences in statistical and physical parameters between the wave climate schematisations are related to the way the wave climates are schematised. Subsequently, from these results, conclusions on the way the wave climate is schematised can be stated.
After defining the influence, a discussion on the pros (accuracy) and cons (simulation run time) of the wave climate schematisations is included.

6.2 MODELLING APPROACH

For each obtained wave climate schematisation, a morphological simulation is made for a period of one year. 29 schematisations are obtained in chapter 5, consequently resulting in 29 different morphological simulations. Each of these simulations is based on a number of wind and wave classes. The wind and wave conditions within one climate schematisation are assumed to last for a period of one year. Each individual wind and wave conditions is imposed on a morphological tide (section 6.2.2), which has a duration equal to two tidal cycles (25 hours). Because of the difference in time scale between the considered period of morphological development (one year) and the used morphological tide (25 hours), the imposed conditions must be multiplied with a morphological acceleration factor (f_{MORFAC}, section 3.2.3) to account for one year.

6.2.1 MORPHOLOGICAL ACCELERATION FACTOR

Each class within a schematised climate has its own morphological acceleration factor. This factor can be calculated by equation 6.1. The value of f_{MORFAC} depends on the weight of the class (based on its original probability of occurrence and further developed in the Opti method), the duration of the used morphological tide and the duration of the considered period of time.

$$f_{MORFAC} = \frac{p_c \times year\ duration}{T_{morphological\ tide}} \tag{6.1}$$

with f_{MORFAC} = morphological acceleration factor (-)

p_c = weight of the wind and wave class (-)

$year\ duration$ = duration of one year (hours)

$T_{morphological\ tide}$ = duration of one morphological tide (hours)

As described in chapter 1, this study contributes to a larger study on the modelling of the morphological development of the Western Scheldt estuary. Ideally, the morphological tide to be used in the morphological simulations would be equal to the morphological tide as used in that study. Unfortunately, that morphological tide is equal to a full neap spring tidal cycle (Grasmeijer, 2012). As a result, the run time of all simulations would take too much time, since every wave class is run during one morphological tide. Therefore, a shorter morphological tide of 25 hours (two tidal cycles) is used (section 6.2.2). A drawback of this shorter morphological tide is that the morphological acceleration factor is strongly increased (with a factor of about 15 compared to the situation where a neap spring tidal cycle is used). The applied morfac values vary from around 25 (15 classes) to around 350 (1 class). Multiplying these values further might result in too high morfacs, i.e. the simulated morphological development is exaggerated compared to real life development. The influence of the *morfac* value is addressed in section 0.

For the modelling of the morphological development during one year, all wind and wave classes are run in sequence. With this approach, the resulting changed bathymetry due to a particular condition is the input bathymetry for the next condition. The order of the classes within a simulation is randomly assigned. This prevents that the selected classes from the same specific direction (e.g. westerly) are run first, followed by classes from with the same different direction (e.g. easterly), resulting in a unilateral morphological development. Also in real life, wind and wave directions occur random (within the described wind and wave climate, section 4.2.2). The classes within the schematisations all have different *morfacs*. According to Lesser (2009), when these classes with different *morfacs* are run in sequence, special care needs to be taken when changing *morfac* values between classes. The reason for this is that it is important that approximately the same suspended wave concentrations exist at the start and end of every morfac value. If not, significant discontinuities in sediment mass will occur. The approach used in this study is adopted from Lesser (2009) and discussed and approved by Roelvink (personal communication). The approach is to:

1. Set morfac to zero at the end of a morphological tide (this stops the morphological model),
2. Alter the required hydrodynamic model boundary conditions (wind, waves) over a period of 60 minutes to avoid shocking the models (spin up 1),
3. Allow the hydrodynamic and wave models to stabilise to the new boundary conditions over the following 690 minutes (spin up 2: together with the 60 minutes in spin up 1 this forms a total spin up time of 12.5 hours),

4. Set f_{MORFAC} to the appropriate value for the new wave class (this restarts the morphological model),
5. Compute hydrodynamics, sediment transport and accelerated morphological change through exactly one morphological tide,
6. Set f_{MORFAC} to zero to halt the morphological model
7. Repeat the above steps until all classes within a schematisation have been completed.

Figure 35. Schematisation of the way the variable morfac is applied. presents this approach in a schematised manner.

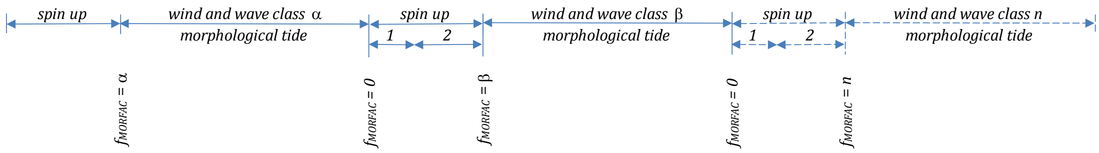

Figure 35. Schematisation of the way the variable morfac is applied.

with	$f_{MORFAC} = \alpha, \beta, \ldots n$	= Morphological acceleration factor (-) for wind and wave class $\alpha, \beta, \ldots n$.
	morphological tide	= two tidal cycles (25 hours)
	Spin up 1	= period (60 min) for altering of wind and wave conditions (to avoid shocking the models).
	Spin up 2	= period (690 min) to stabilise the hydrodynamic and wave model to the new conditions.

In the simulations, the morphological development during one year is considered. The simulations however are run over a period twice as long, i.e. two years. Actually, the simulation for one year (with all selected classes and applied morfacs) is repeated. The first year is used as a spin up year, where the hydrodynamics, morphodynamics and morphology are adjusted to each other. The morphological development in the second year is assumed to represent the morphological development over one year (Grasmeijer, personal communication). To obtain the new bed level, this morphological development is added to the initial bed level.

6.2.2 MORPHOLOGICAL TIDE

The morphological tide of 25 hours (two tidal cycles) is derived from the full neap spring tidal cycle as is used by Grasmeijer (2012). The morphological tide is derived from the full neap spring tidal cycle by means of correlation. The morphological development of every 25 hours in the neap spring tidal cycle is compared to the morphological development of the full neap spring tidal cycle. The 25 hours with the highest correlation with the full neap spring tidal cycle is selected as the morphological tide for this study. In principle, the simulation run time can be further decreased by using an even shorter morphological tide (e.g. one tidal cycle of 12.5 hours, as is used in the short simulations). However, the *morfac* values to be used are in that case doubled and are considered to be too high (especially for the schematisations where 1 class is used and the morfac would increase to about 750).

6.2.3 BENCHMARK SIMULATIONS

The different simulations are compared with each other and with a benchmark simulation. Within this comparison, the focus is on the large scale developments at the ebb and flood channels (the macro cells, as described in section 2.2.3). Ideally the benchmark simulation would be a brute-force simulation wherein all occurring wind, wave, current and water level conditions during one year are imposed as time series and the resulting sediment transport and morphological development is simulated (Lesser, 2009). This would however take too much time within the schedule of this thesis. Here, a practical approach is used. Within this approach, simulations based on a 15 class wave climate schematisation are used as benchmark simulations (as discussed in section 5.4.5). The results of all other schematisations are compared to these benchmark simulations. There are two reasons for the choice of a 15 class wave climate schematisation as a benchmark. First of all, in the numerical approach to come to an schematisation with the Opti method, it was found that on a small morphological time scale no large deviations from the weighted average development are found up until 15 of the 54 classes remain (*relative rms* of 1%, Figure 30, section 5.4.3). Here it is assumed that the same holds for longer time scales. Within these 15 classes still all relevant classes (directions and wind speeds) are present with an increased weight to also represent more or less equivalent classes. Second, in practical studies, it is expected that no more than 15 classes will be applied in a morphological simulations because of the runtime accompanied with 15 classes, especially when a relative long morphological tide is applied.

In the benchmark simulations, no storm conditions are applied. Although the morphological impact of such a condition is large on a short time scale, for medium-term morphological development it is not taken into account. The reason for this is its low probability of occurrence and hence relatively small contribution to the total morphological development. An impact of such a storm on the medium-term morphological development is assessed in the extra derived wave climate schematisation (M26, section 5.6.1). This simulation is also compared to the benchmark simulations.

For each type of target (sedimentation and erosion pattern or sediment transport) and each area of target (whole domain, ebb tidal delta or estuary) a benchmark simulation is made. In total there are six different benchmark simulations which are also compared with each other. In the Opti method of wave input reduction (section 5.4), the result of the remaining classes is compared based on statistical parameters as the root mean square difference and the correlation coefficient. In this chapter, the results of the schematised climates are compared based on physical results as sedimentation and erosion patterns, cross section profiles and hypsometric curves and on statistical parameters as well. The applied statistical parameters are the relative *rms* and the correlation coefficient.

6.2.4 INFLUENCE OF WIND AND WAVES

To address the relative influence of waves on the simulated morphological development compared to the influence of the currents, four simulations without the influence of wind and waves are performed. These four simulations are based on 1, 5, 10 and 15 morphological tides. These simulations are coded as M00 1C, M00 5C, M00 10C and M00 15C respectively. M00 in the code appoints that no wave classes are include, the #C appoints that the simulations is based on # amount of morphological tides. In this way, the same order of morphological acceleration factor is applied as for the simulations based on different amounts of classes. For example; when the influence of waves of a 10 class schematisation have to be addressed, the results of the simulation without wind and waves based on 10 morphological tides must be subtracted, since the value of the morfac is for both simulations in the same order. Hence, when the influence of waves is addressed, no additional error caused by differences in the morphological acceleration factor is included. The values of the morfacs however differ a little. The reason for this is that in the simulation with waves, the imposed classes have different weights and consequently different morfacs. In the simulations without waves, the multiple morphological tides are all assigned the same (average) morfac value. More important is that the order of the morfac value is equal.

6.3 RESULTS OF BENCHMARK SIMULATIONS

As described in the previous section, the six climate schematisations based on 15 selected classes form the benchmark simulations for the schematisations based on 10 classes, 5 classes and 1 class. These six benchmarks simulations are performed for two types of target and three locations of target (per type of target). As will be shown, the results of the six benchmark simulations are very similar in terms of erosion and sedimentation patterns, volume changes in macro cells and hypsometric curves. For this reason, the results of one benchmark simulation is described in detail. The other five benchmark simulations are compared to that simulation. The one benchmark simulation that is described in detail in this section is simulation M01. The result of the benchmark simulation is described in terms of sedimentation and erosion patterns, cross section profiles, volume changes and hypsometric curves. Furthermore, the differences in influence of currents and waves on the morphological development is described.

Table 13 gives an overview of the choices on which the climate schematisations are based. Figure 33 and Figure 34 present the selected classes.

6.3.1 EROSION AND SEDIMENTATION PATTERNS

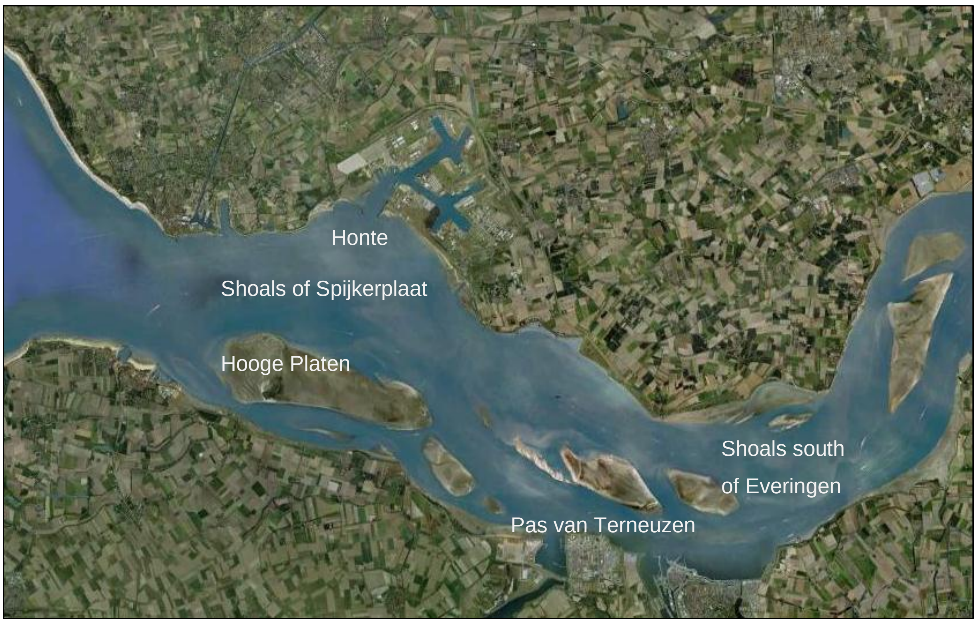

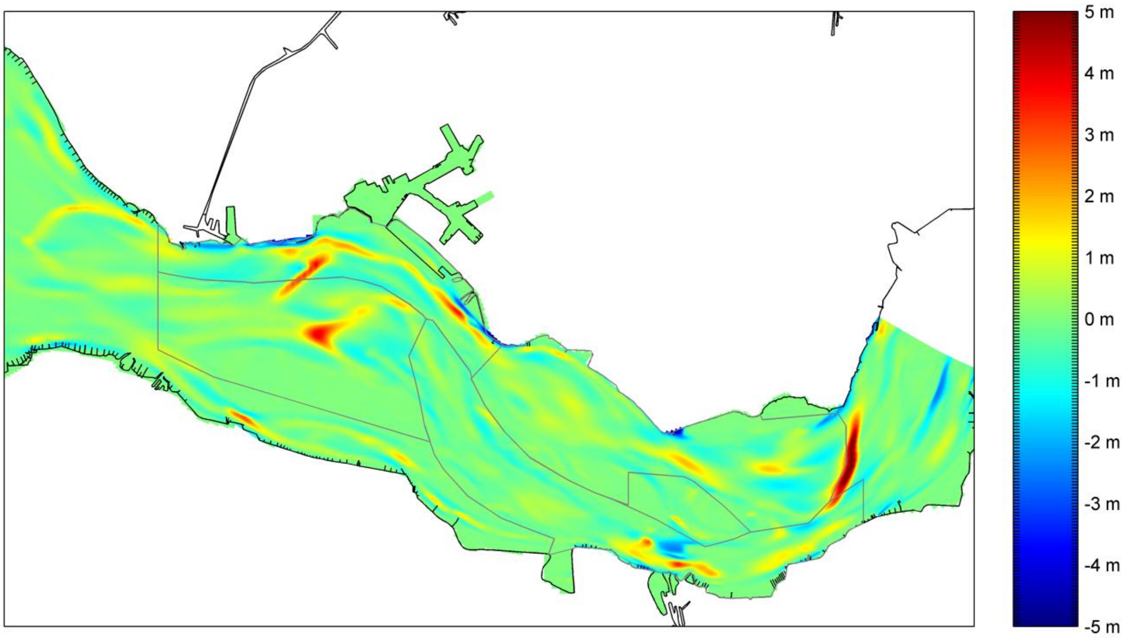

Figure 36. Sedimentation (red) and erosion (blue) pattern as a result of benchmark simulation M01. The gray lines indicate the boundaries of the ebb and flood current channels.

Figure 36 shows the erosion and sedimentation pattern of the benchmark simulation based on schematisation M01. From this figure it can be seen that most changes in bathymetry occur at the boundaries of the channels, i.e. at the edges of the shoals. The highest amount of erosion (4 m – 5 m) occurs at the channels where the highest flow velocities occur, especially at the bend of the ebb channel at Terneuzen and the Honte ebb channel. The highest amount of sedimentation (4 m – 5 m) occurs at the shoals of Spijkerplaat and the shoals south of Everingen.

When the results of the simulation are compared to the simulation without imposed waves and winds, similarities and differences are found. Figure 37 shows the erosion and sedimentation pattern only due to currents (no wind and waves); Figure 38 consequently shows the influence of imposed wind and waves, obtained by subtracting Figure 37 from Figure 36.

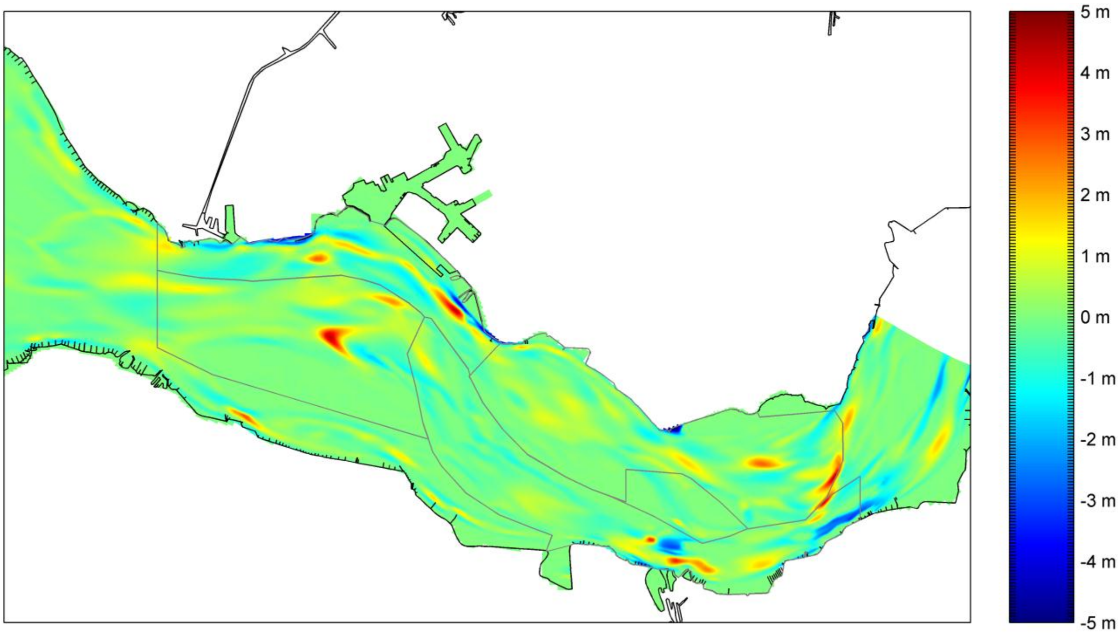

Figure 37. Sedimentation (red) and erosion (blue) pattern as a result of a simulation *without* wind and waves (M00 15C). The gray lines indicate the boundaries of the ebb and flood current channels.

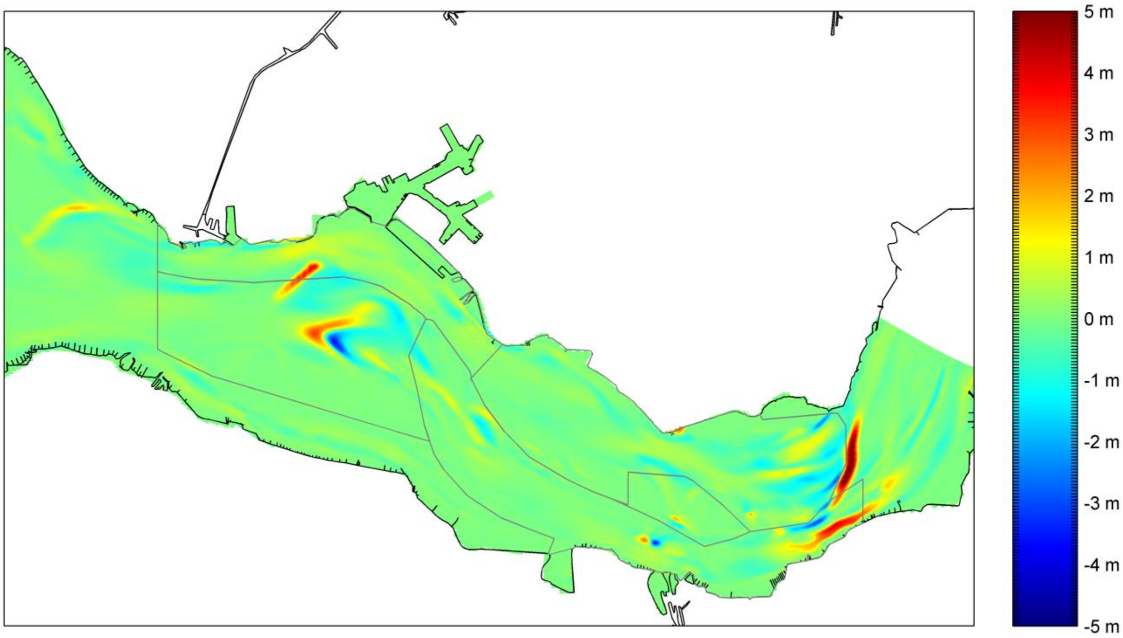

Figure 38. Influence of imposed wind and waves on the sedimentation and erosion pattern. Figure is obtained by subtracting the result *without* wind and waves from the result *with* wind and waves (M01 – M00 15C). The colours now show the *difference* in sedimentation and erosion. Red shows that in the simulation with wind and waves more sedimentation occurs than in the simulation without wind and waves, blue shows that less sedimentation occurs. The gray lines indicate the boundaries of the ebb and flood current channels.

The sedimentation and erosion patterns of the simulation with wind and waves (M01) are to a great extent *similar* to the pattern of the simulations without wind and waves. Where waves are of influence these patterns are enforced, i.e. at locations where already sedimentation occurs, this sedimentation increases, and at locations where already erosion occurs, this erosion increases. The main differences occur at the low lying shoals of Spijkerplaat and the low lying shoals south of Everingen, where strong sedimentation occurs as a results of wind and wave influence. This is explainable, since the wave influence on sediment transport and morphological development is largest at these locations (section 0). Furthermore, at these locations, the patterns of sedimentation and erosion *shift* due to the influence of waves. This can be seen at Spijkerplaat in Figure 36, where directly eastwards of the large amount of sedimentation, a deficit of sediment occurs compared to the situation without wind and waves. It can be seen that the pattern shifts towards the west and is larger in magnitude as well. At the shoals south of Everingen, the pattern shifts to the east. Also here, an increase in sedimentation occurs compared to the simulation without waves.

Around the edges of the shoals both sedimentation (light green) and erosion (light blue) occurs. From the sedimentation and erosion pattern it is difficult to see whether sediment is transported onshore (towards the shoal edge) or off shore (towards the channel). Therefore, cross sections are defined over the shoals and the change in hypsometric curve of the area is determined. Figure 39 shows the location of these cross sections. The cross sections are located at the locations where waves have the most influence and at Hooge Platen (cross section 5).

Figure 39. Locations of cross section profiles.

Figure 40 shows the changes in cross section profiles. Presented are the original profile (black line), the new profile due to currents, wind and waves (schematisation M01, red line) and a profile due to currents only (schematisation M00 15C, blue dashed line). The presented erosion and sedimentation are cumulative after one year of morphological development.

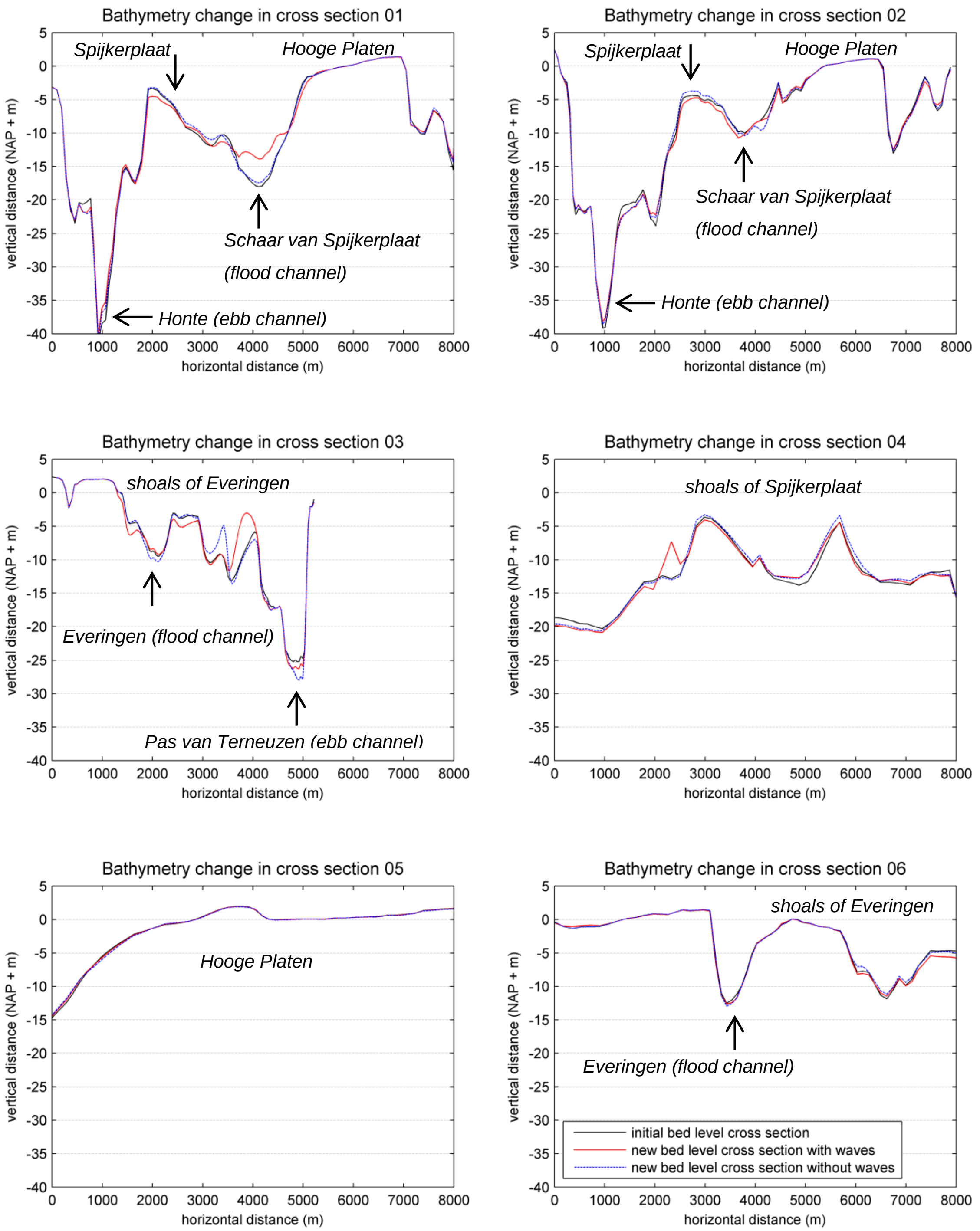

Figure 40. Cross section profiles over the shoals of Spijkerplaat and Hooge Platen (cross sections 1, 2, 3 and 5) and over the shoals south of Everingen (cross sections 3 and 6). Shoals and channels can clearly be distinguished.

The influence of waves on the sedimentation and erosion pattern can be found by comparing the new bed level due to currents and waves with the bed level due to only currents. The influence of waves on the sedimentation (sed. waves) and erosion (ero. waves) is indicated in Figure 41. When the new bed level due to only currents is compared to the initital bed level, also the influence of the currents on the sedimentation and erosion is found. The influence of currents on the sedimentation (sed. current) and erosion (ero. current) is indicated in Figure 42.

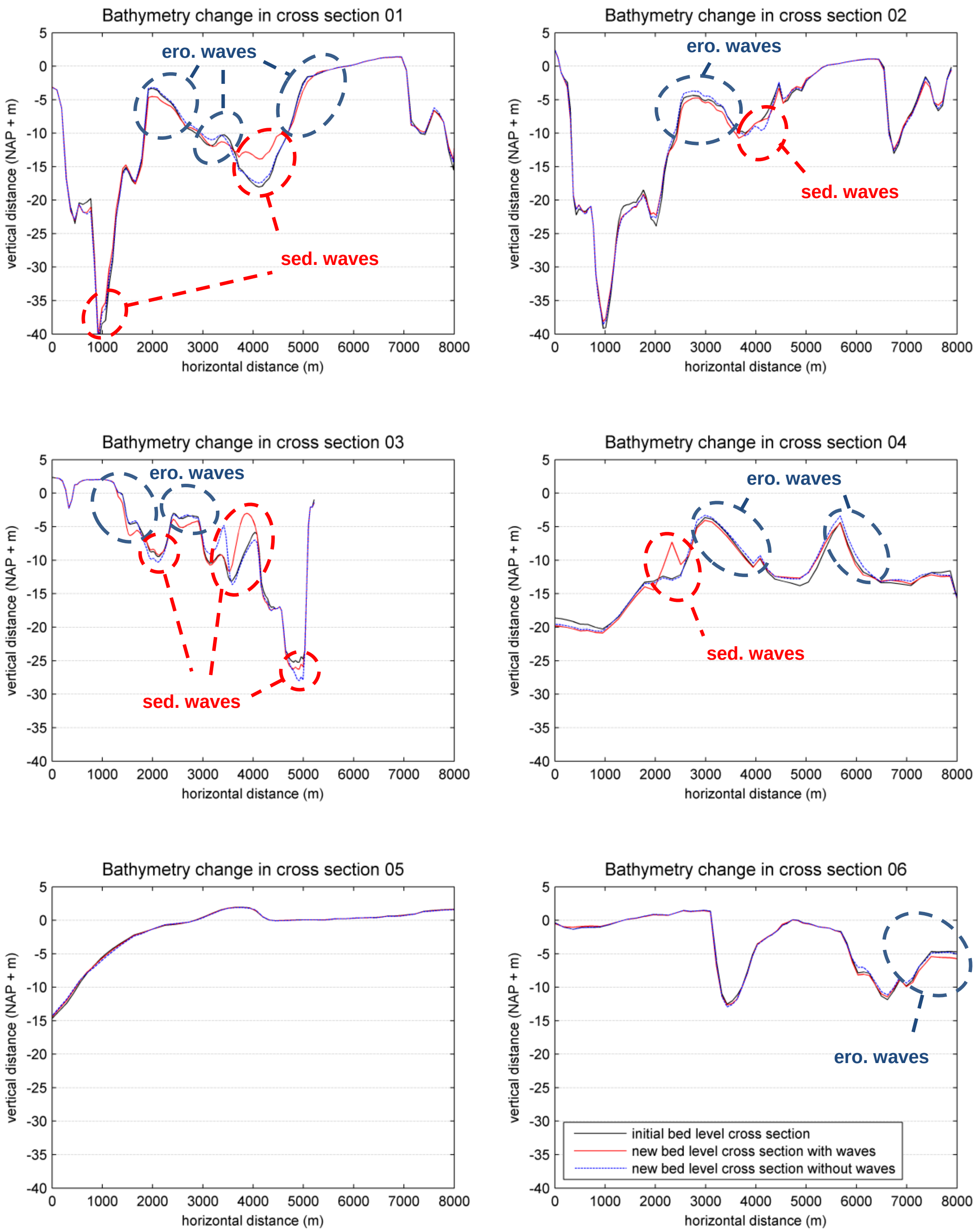

Figure 41. Erosion and sedimentation due to the influence of waves.

Although the sedimentation and erosion is a result of processes in longitudinal and cross shore direction, some consistent features can be recognised from the cross section profiles [22]. From cross sections 1 – 4 in Figure 41 it can clearly be seen that the waves erode the slopes and edges of the shoals. Sedimentation occurs in the flood channels in between the shoals: at the shoals of Spijkerplaat and the shoals south of Everingen. The erosion due to waves focusses on the area between NAP 0 and NAP – 10 m.

[22] Because of the contribution in longitudinal direction as well, not necessarily both erosion and sedimentation (or vice versa) are visible in a cross section profile.

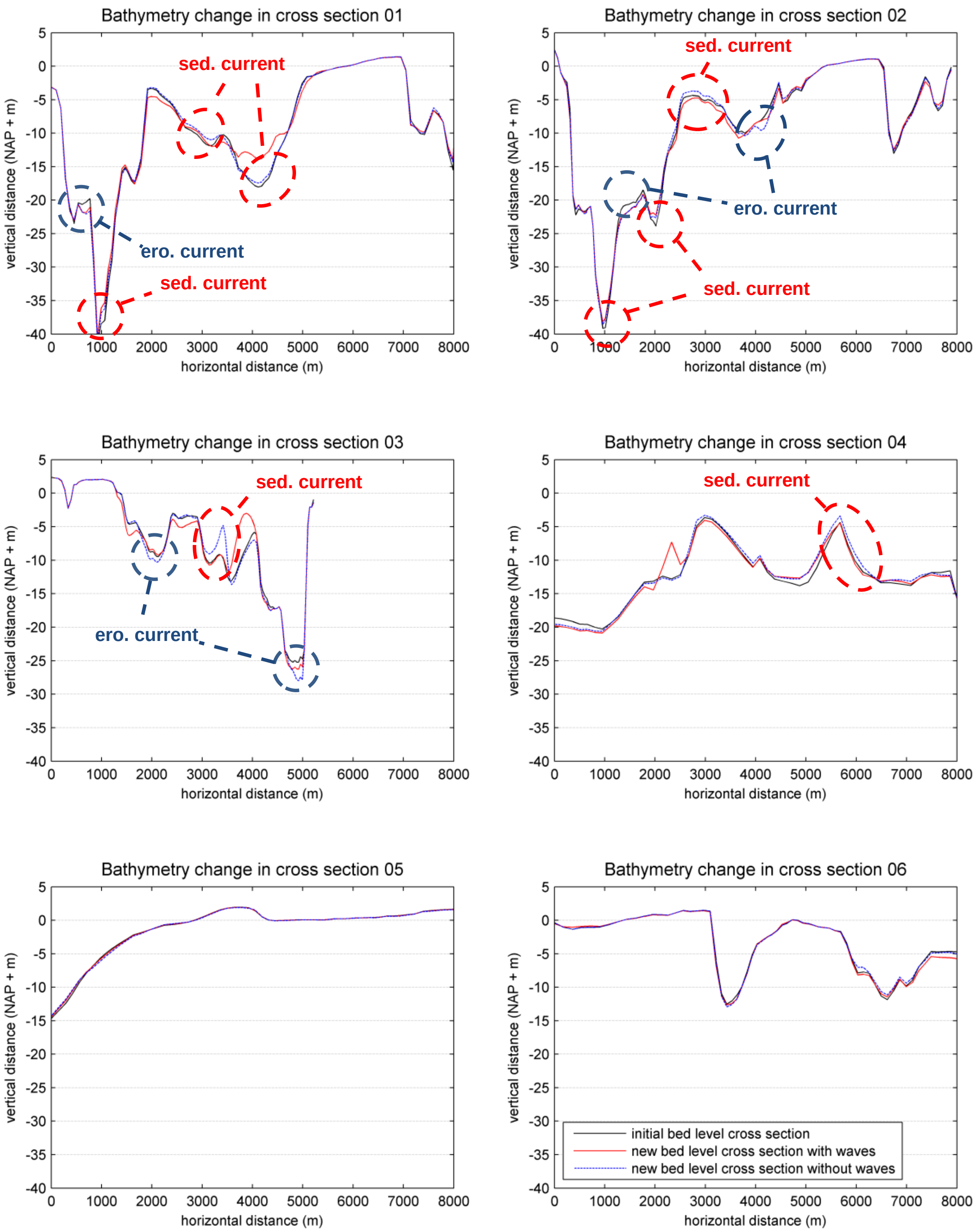

Figure 42. Erosion and sedimentation due to influence of currents.

From cross sections 1 – 4 Figure 42 it clearly can be seen that the erosion and sedimentation due to currents mainly occur at the channels. Currents also have influence on the shoals of Spijkerplaat and Everingen because of the relative low bed levels of these shoals. The influence of currents is not consistent throughout the area: sedimentation occurs in the Honte ebb channel, while erosion occurs in the ebb channel at Terneuzen. From cross sections 3 and 4, the shift in sedimentation under the influence of waves can clearly be seen.

Summarized; the waves erode the slopes and edges between NAP 0 m and NAP – 10 m and deposit sediment at the adjacent flood channels. The currents mainly focusses on the flood and ebb channels, resulting in sedimentation at Honte ebb channel and erosion at Terneuzen ebb channel. The waves result in a shift of the sedimentation at Spijkerplaat and Everingen. The location of the influences of waves around the waterline and influence of currents in the channels is in line with the description in section 2.3.

6.3.2 VOLUME CHANGES IN CURRENT CHANNELS OF THE MACRO CELLS

In this section, the volume changes in the ebb and flood channels in the macro cells are considered. Again, the result of benchmark simulation M01 is described. The volume change (m^3/year) is measured as the vertical change (m/year) per grid cell times the area (m^2) of that grid cell. For the volume change per year channel in the macro cells, the changes per grid cell within the channel boundaries are added to obtain the total change in volume per channel area. The boundaries of the channels are shown in Figure 43 and coincide with Figure 9. The changes in volume are the cumulative changes over the period of the simulation, i.e. one year.
The two macro cells in the Western Scheldt entrance each consist of a flood current channel and an ebb current channel. These are the Honte ebb channel and Schaar van Spijkerplaat flood channel of macro cell 1 and the Terneuzen ebb channel and Everingen flood channel of macro cell 2 (Table 2). The morphological development focusses on these channels and adjacent shoals. In Figure 44, the change in volume of sediment of the different channels is presented. Next to the benchmark simulation M01, also the simulation without the influence of wind and waves is presented (M00 15C). From comparison of these two results, the influence of wind and waves on the volume changes can be found.

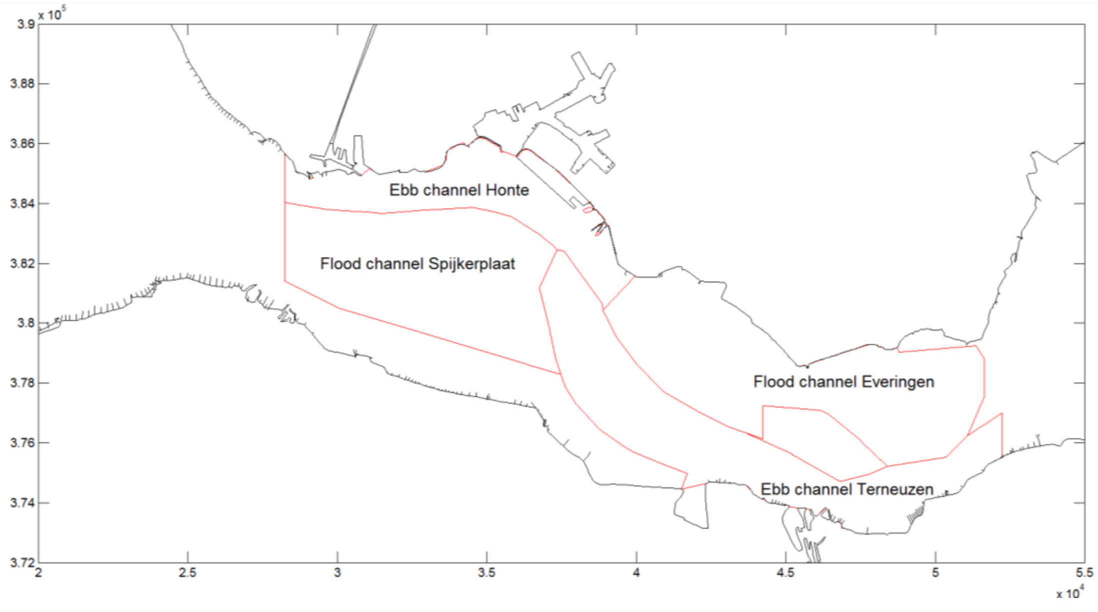

Figure 43. Areas of ebb and flood channels.

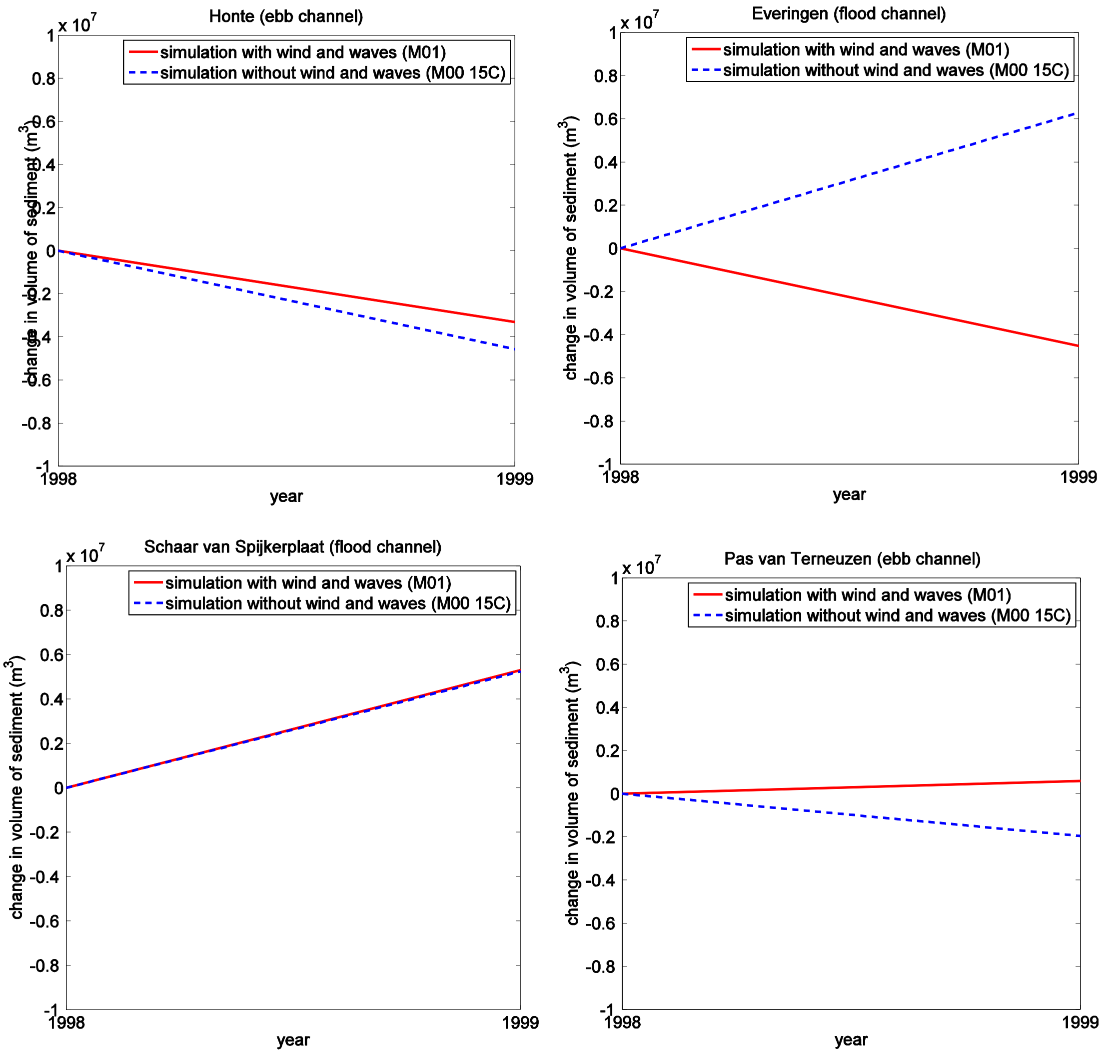

Figure 44. Changes in volume of sediment in the ebb and flood channels.

At the Honte ebb channel (left upper panel), both for the simulation with and without wave influence, the change in volume of sediment is negative (i.e. a decrease in the volume of sediment takes place), however with waves, this change is about 25% less (4.5 million m^3 and 3.5 million m^3 respectively). When the pattern of sedimentation and erosion is considered (Figure 38), it appears that there is an increase of sediment at the edge of the Spijkerplaat, just located inside the area of the Honte ebb channel. This increase of sedimentation due to waves apparently causes the difference in the change of volume.

At the flood channel Vloedschaar van Spijkerplaat (left lower panel), there is practically no difference between the simulations with or without the wave influence. As is described earlier, the sedimentation and erosion pattern around Spijkerplaat differ between the situation without waves and the situation with waves (Figure 38). Since there is no significant difference in changes of volume, the main difference appears to be the shift of the location of sedimentation due to waves, which occurs in the middle of the considered area.

At the ebb channel of Pas van Terneuzen (right lower panel), including wind and waves in the simulation results in a positive change in volume (i.e. an increase of volume of sediment in that area with 0.5 millon m^3), where the simulation without waves results in a negative changes of 2.0 million m^3. The difference is consequently about 2.5 million m^3. When again the sedimentation and erosion patterns from Figure 36

Figure 38 are considered, it appears that the main difference occurs in the bend of the channel at Terneuzen. The current erodes the channel, resulting in a decrease of the volume in the area. At the same location, waves deposit sediment at the channel, resulting in sedimentation and hence an increase of volume in the area instead of an decrease. This can also be seen from cross section 3 (Figure 41 andFigure 42).

At the flood channel of Everingen (right upper panel), the results are most influenced by including waves in the simulations. Including waves in the simulation results in a negative change in volume of 5 million m³, where the simulation without waves results in a *positive* change in volume of 5 million m³. However, when also the sedimentation and erosion patterns of both simulations are considered (Figure 36 and Figure 37), it appears that the waves result in a shift of the location of sedimentation (as described earlier). Without waves, the sedimentation at the shoals of Everingen occurs just within the east boundary of the flood channel, resulting in an increase of the volume of sediment within the area. With waves, the sedimentation occurs just eastwards of the boundary, resulting in an decrease of the volume of sediment within the area. Furthermore, the area is connected to the area of the ebb channel of Pas van Terneuzen; due to the shift of sedimentation also more sedimentation occurs at that area (partly explaining the increase of volume there). The influence of waves thus mainly results in a shift of the location of sedimentation. Due to the location of sedimentation and the area boundary the influence of waves seems enormous, but this must be nuanced.

6.3.3 HYPSOMETRIC CURVES

A hypsometric curve is a cumulative distribution function of bottom levels in a specific area. In other words; a hypsometric curve shows the total amount of area below a specific bottom level are. The vertical axis presents the bottom level (in this case in meters above Normaal Amsterdams Peil (NAP + m), the Dutch reference datum), the horizontal axis presents the cumulative area (in this case in hectares). Figure 45 shows the hypsometric curve of the original situation before the simulation, the new curve due to currents (without wind and waves) and the curve including the influence of waves.

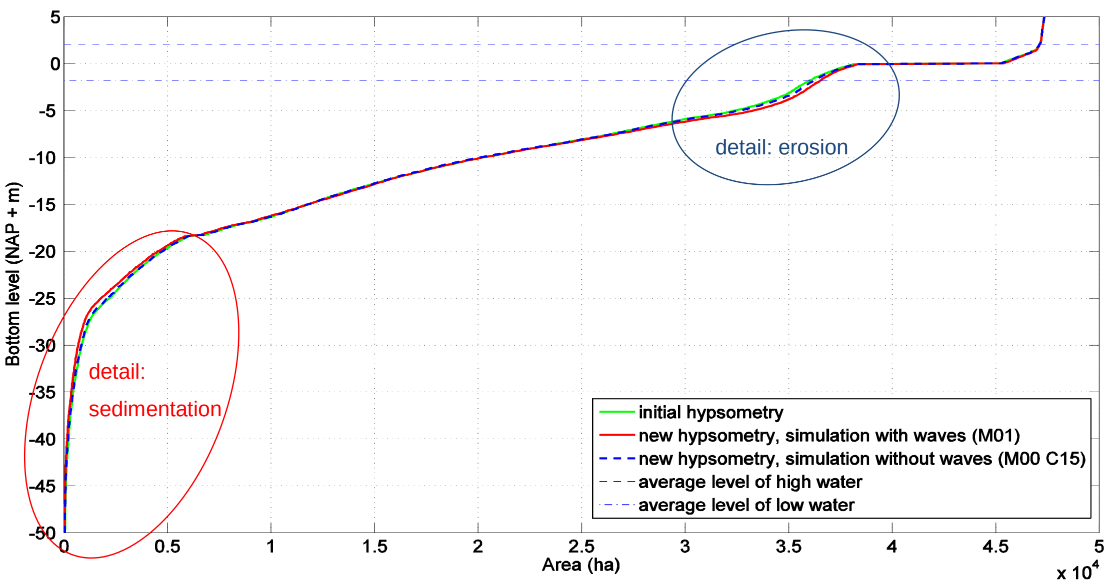

Figure 45. Curves of hypsometry of the initial situation, benchmark simulation with waves (M01) and simulation without waves (M00 15C). Circles indicating sedimentation between NAP -20 m and NAP -50 m and erosion between NAP 0 and NAP -6 m.

For the simulation with waves included (M01), a shifts of the hypsometric curve occur. Around the average low water level, the curve shifts to the right. This implies an increase of the area with a bottom level just below the average low water level. The right panel of Figure 46 shows this in more detail. The increase of the area between NAP 0 m and NAP -6 m indicates erosion of the edges of the shoals. It can be seen that without waves, already small erosion occurs: the area between NAP 0 m and NAP -6 m increases with about 100 ha – 250 ha. With waves, much more erosion occurs: the area between NAP 0 and NAP -6 m increases with about 500 – 1,000 ha. The erosion due to waves around this level is in agreement with the changes in the cross section in Figure 41, where also most erosion due to waves occurs at the slopes and edges of the shoals between NAP 0 and NAP -5 m. As described in section 0, the influence of waves on the transport of sediment at the edges of the shoals is in general higher around low water than around high water. This explains the location of the shift of the curve around average low water.

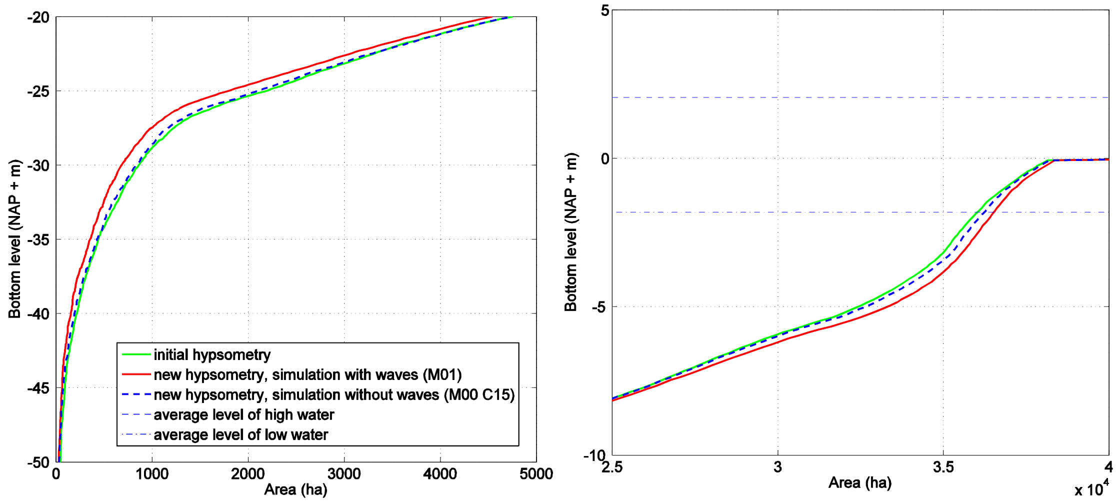

Figure 46. Details of hypsometric curves: sedimentation between NAP -20 m and NAP -50 m (left panel) and erosion between NAP 0 m and NAP -6 m (right panel).

A second shift in the hypsometric curves occurs at the deeper parts of the estuary between NAP -20 m and NAP -50 m (the channels). This shift to the left indicates that here, a decrease of area occurs. This decrease indicates sedimentation at the channels (filling up with sediment). Without waves, only a small amount of sedimentation occurs at a higher level (decrease of area between NAP -20 m and NAP -50 m with about 50 ha). With waves, the amount of sedimentation increases significantly (decrease of area between NAP -20 m and NAP -50 m with about 200 ha). This is also in agreement with the cross sections in Figure 41. Erosion and sedimentation due to the influence of waves., where it was found that waves result in sedimentation at the channels. It must be noticed however, that the hypsometric curves presents the mean increase and decrease of area at the whole considered area. It is obvious that locally, deviations from this curve can occur.

6.3.4 COMPARISON OF BENCHMARK SIMULATIONS

In the previous sections, the morphological development of one benchmark simulation (M01) has been described. In the introduction of section 6.3 it is mentioned that the six distinguished benchmark simulations are very similar. This is shown in the following.

Sedimentation and erosion patterns
First of all, the sedimentation and erosion patterns of the other five benchmark simulations (M05, M09, M13, M17 and M21) are presented in Figure 47. From this figure appears that the different benchmark simulations all have the same erosion and sedimentation pattern. Figure 48 shows the local differences. The largest differences occur at the locations where the influences of the waves is most prominent: the shoals of Spijkerplaat and the shoals south of Everingen. The local differences are small in an absolute and relative sense. The local differences are in the order of 0 m – 0.1 m for benchmark simulations M05, M09 and M13, which is 0% - 2% of the local bottom change due to erosion or sedimentation (which is in the order of 4 m - 5 m). For benchmark simulations M17 and M21, the local difference is somewhat higher. For these simulation, the *maximum* local difference are in the order of 0.25 m – 0.4 m, which is 5% - 8% of the local bottom change due to erosion or sedimentation. For the remaining part of the area, the differences are also in the order of 0% - 2%.

Volume changes in the ebb and flood current channels
Figure 49 presents the volume changes as a result of the benchmark simulations. At the channels of Honte, Vloedschaar van Spijkerplaat and Pas van Terneuzen, no differences occur in the changes of volume. At the flood channel of Everingen, small deviations (order 5% - 10%) between the different benchmark simulations occur. The found similarities are in line with the differences between the sedimentation and erosion patterns. What is remarkable, is that at the flood channel of Terneuzen, the schematisations based on transport (M13, M17 and M21) show a larger change in volume than the schematisations based on bottom change (M01, M05 and M09). The influence of the type of target (bottom change or sediment transport) is described in section 6.4.4.

Hypsometric curves
The six benchmark simulations all result in the same hypsometric curve. This can be seen from Figure 50. The small differences found in the sedimentation and erosion patterns and the changes in volume in the ebb and flood channel are not visible at the scale of the hypsometric curves. It can be concluded that the local deviations are small compared to the total morphological development in the entrance of the Western Scheldt. The general influence of waves can however clearly be seen; this indicates that at the spatial scale of the whole area, the influence of the choice for a certain type or location of the target is an order lower than the general influence of waves.

Statistical parameters
The differences between the benchmark simulation can be expressed in statistical parameters. Here, use is made of the linear correlation coefficient *r* and the absolute and relative root mean square differences (*rms* and relative *rms*). These parameters are the most important ones, as they are measures for the similarity between two simulations. Next to these parameters, also the standard deviation (*sd*) and covariance (*cov*) are presented to found the correlation coefficient and the root mean square differences. All statistical parameters are described and defined in sections 4.3.5 and 5.4.3. Table 14 presents the values of the different statistical parameters. Furthermore, the statistical parameters are presented in Figure 48 as well. By doing so, the statistical parameters can be interpreted in terms of differences in bottom changes.

Interpretation of the relative rms
Due to the squaring of differences by calculating the root mean square difference (equations 5.4 and 5.5, section 5.4.3), large local differences can strongly influence the root mean square difference of the whole considered area. Consequently, the outcome of this parameters must be interpreted together with a spatial view of the considered area, e.g. the difference in the sedimentation and erosion patterns of the two simulations. Even with large value of the root mean square difference, it is very well possible that the simulations are similar to a large extent with large differences at certain locations. This also appears to be

the case in the simulations considered in this chapter: differences occur at location where waves have the most influence, i.e. the shoals of Spijkerplaat and the shoals south of Everingen. Here, large differences can occur while in the remaining part of the area hardly any differences occur. Due to the squaring of these local, relative large, differences, the root mean square differences can strongly increase.
It can be concluded the (relative) root mean square difference is a good measure, but must be interpreted with spatial information. When the value is relatively high, the cause must be appointed in the spatial area.

Benchmark Simulation	*r* (-) eq. 4.5	*rms* (m) eq. 5.4	relative *rms* (%) eq. 5.5	*sd* (m) eq. 4.7	*cov* (m) eq. 4.6
M01	1.000	0.000	0.0	0.776	0.602
M05	0.999	0.030	3.9	0.771	0.598
M09	0.999	0.036	4.7	0.774	0.600
M13	0.999	0.036	4.6	0.773	0.599
M17	0.998	0.043	5.6	0.770	0.597
M21	0.998	0.055	7.1	0.770	0.596

Table 14. Statistical parameters of the six benchmark simulations. *r, rms* and *relative rms* are related to M01.

From Table 14 it can be concluded that the amount of correlation (*r*) between M01 and the other benchmark simulations is high. The relative root mean square differences vary around 5%. This is in accordance with the found maximum differences in the sedimentation and erosion patterns, as described earlier in this section. Local relative large difference mostly determine the *rms* and relative *rms* (as described above). From the differences in sedimentation and erosion patterns can be seen that this is the case here as well: the difference are relatively large at the shoals of Spijkerplaat and the shoals south of Everingen, at the remaining vast area the differences are relatively small. Hence, the sedimentation and erosion patterns indicate that the *rms* and *relative rms* mostly focus on the area where waves are of most influence. Furthermore, it appears that the *relative rms* is a good indication of the relative difference (difference in bottom change compared to the reference bottom change)

The correlation with benchmark simulations M05 and M09 is slightly higher than the correlation with M17 and M21. The *relative rms* is lower for M05 and M09. This can be explained by the fact that in the schematisation of the wave climate, M01, M05 and M09 are based on the same type of target (bottom change). The other benchmark simulation are based on another type of target (sediment transport). Hence, a small difference as a result of the type can be seen.

Conclusions

From the physical and statistical parameters it can be concluded that the six benchmarks simulations all result in the same morphological development of the area, with small local differences in bottom change in the order of 5% of the total bottom change. These local differences occur at the locations where the waves have the most influence on the morphological development (shoals of Spijkerplaat and the shoals south of Everingen). Although the benchmark simulations are based on different types of target and location of the target (Table 13, section 5.6), the differences in sedimentation and erosion patterns, volume changes and hypsometric curves hardly differ (locally in the order of 5% of the total bottom change). The reason for this is that the 15 selected classes (Figure 33 and Figure 34, section 5.6) in all benchmark schematisations represent all relevant wind and wave directions. Moreover, as concluded in chapter 4, the wave conditions inside the estuary are strongly determined by the local wind conditions. The morphological impact of these classes is similar to a great extent (Figure 27, section 5.3.3).

Although the differences between the benchmark simulations are small, in the following section the other simulations are all compared with their own specific benchmark simulation (determined by the type and location of the target; Table 13). The reason for this is that an acumulation of small differences can result in larger differences and hence in wrong insights with respect to the influence of type and location of the target and the amount of selected classes.

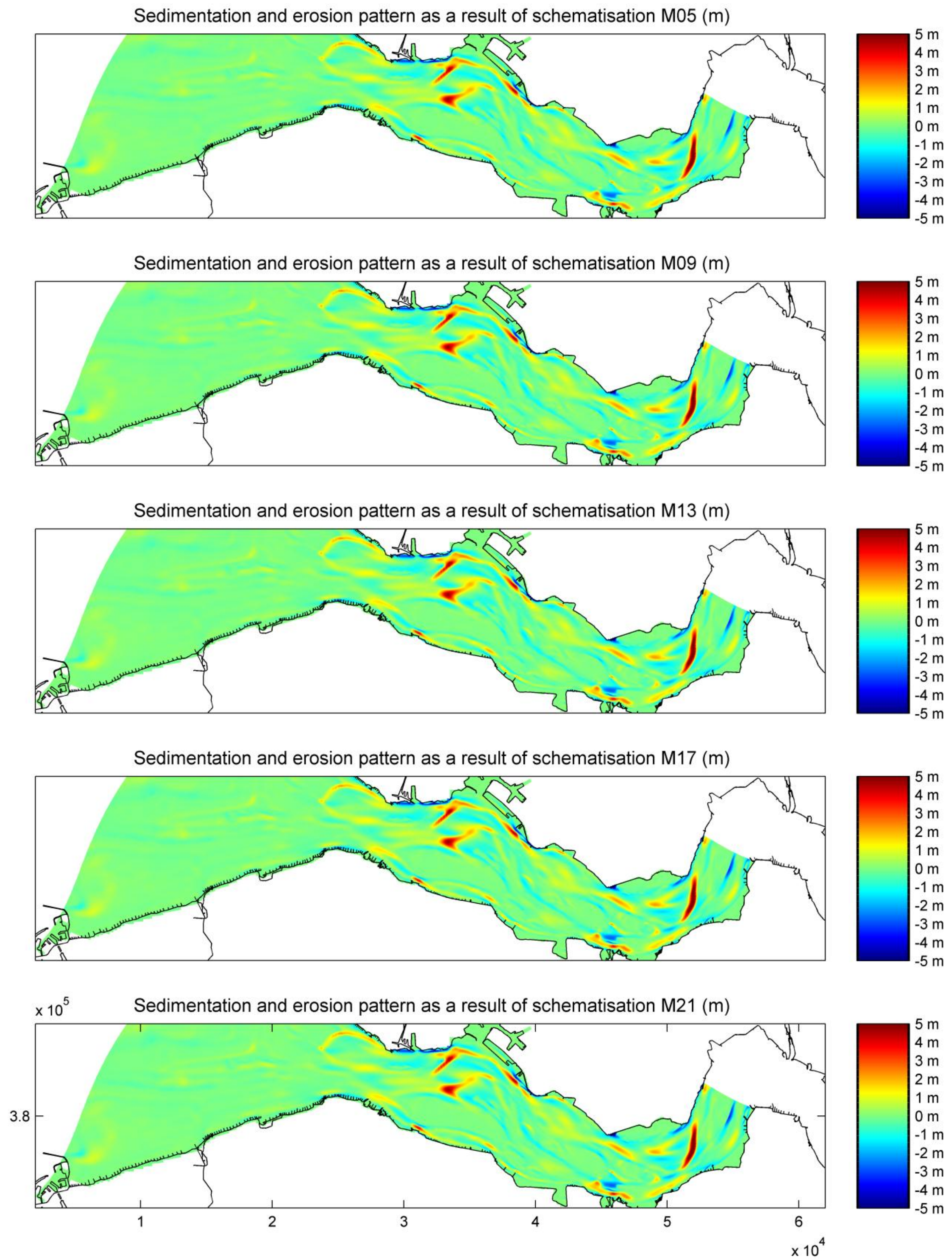

Figure 47. Sedimentation (red) and erosion (blue) patterns as a result of benchmark simulations M05, M09, M13, M17 and M21.

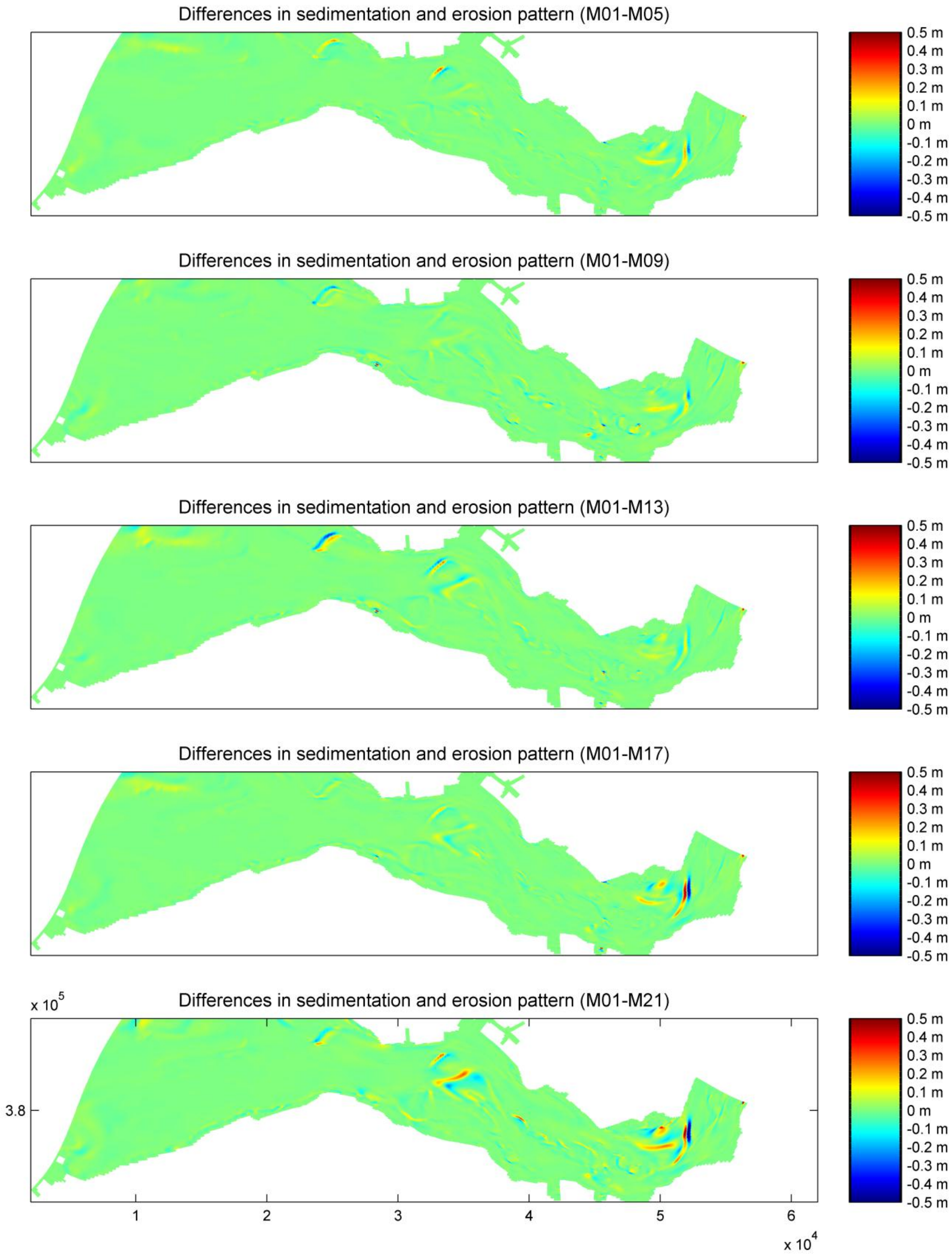

Figure 48. Differences in sedimentation and erosion patterns between benchmark simulation M01 and the other five benchmark simulations (M05, M09, M13, M17 and M21).

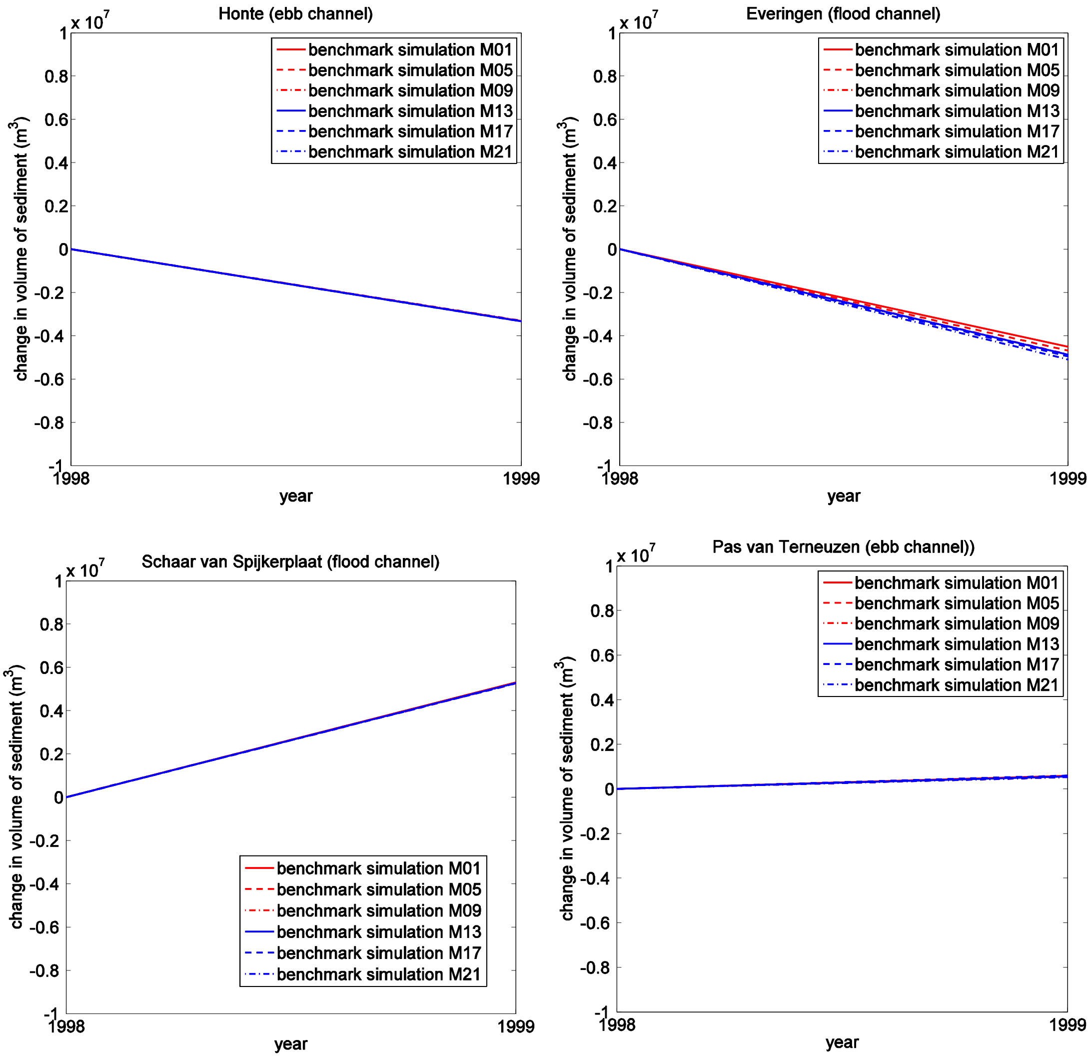

Figure 49. Change in volume of sediment in the ebb and flood channels for the six benchmark simulations.

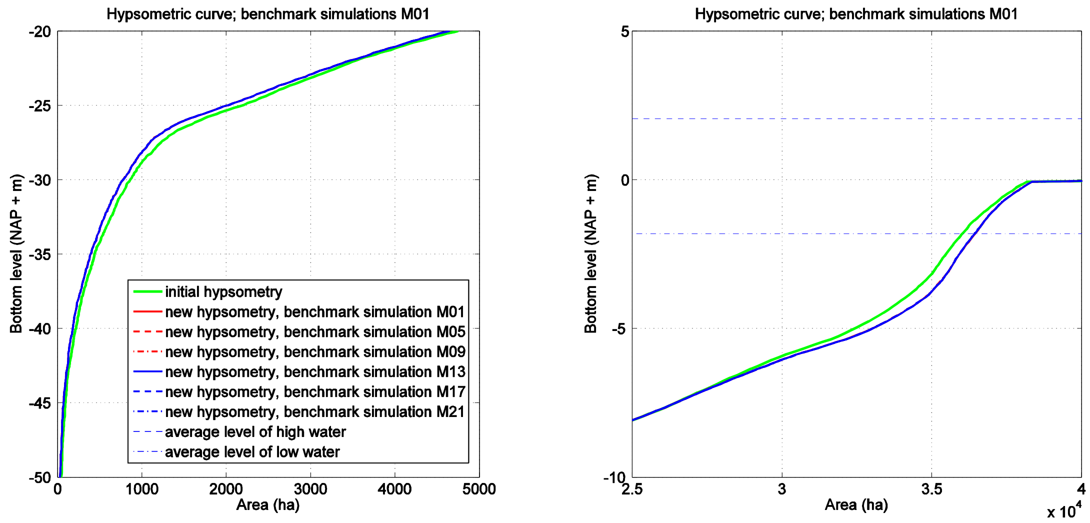

Figure 50. Details of hypsometric curves for the six benchmark simulations: sedimentation between NAP -20 m and NAP -50 m (left panel) and erosion between NAP 0 m and NAP -6 m (right panel).

6.4 INFLUENCE OF WAVE CLIMATE SCHEMATISATION

To address the influence of the wave climate schematisations, the 29 schematisations are divided into groups to address different influences. Within these groups, the schematisations are compared with one reference simulation (marked red) and with each other. Table 15Table 17 Table 18 show these different groups.

Type of target	Location of target	15 classes (benchmarks)	10 classes	5 classes	1 class (opti)	1 class (correlation)
Bottom change	Whole area	M01 →	M02	M03	M04	M27
Bottom change	Ebb tidal delta	M05 →	M06	M07	M08	M28
Bottom change	Estuary	M09 →	M10	M11	M12	M27
Transport	Whole area	M13 →	M14	M15	M16	M27
Transport	Ebb tidal delta	M17 →	M18	M19	M20	M27
Transport	Estuary	M21 →	M22	M23	M24	M29

Table 15. Comparison of schematisations to address influence of amount of selected classes. The red coloured simulations (15 classes) form the benchmarks for the simulations in the same red coloured box.

To address the influence of the **amount of classes**, climate schematisations based on 10 classes, 5 classes and 1 class are compared to the benchmark simulations of 15 classes (Table 15). This is done for all six combinations of type and location of target. From these comparisons, also the influence of the method of schematisations is addressed (Opti method or method of correlation; last column).

Type of target	Location of target	15 classes (benchmarks)	10 classes	5 classes	1 class (opti)
Bottom change	Whole area	M01 ↓	M02 ↓	M03 ↓	M04 ↓
Bottom change	Ebb tidal delta	M05	M06	M07	M08
Bottom change	Estuary	M09	M10	M11	M12
Transport	Whole area	M13 ↓	M14 ↓	M15 ↓	M16 ↓
Transport	Ebb tidal delta	M17	M18	M19	M20
Transport	Estuary	M21	M22	M23	M24

Table 16. Comparison of schematisations to address influence of the location of target. The red coloured simulations form the references for the simulations in the same red coloured box.

To address the influence of the **location of target**, climate schematisations based on the ebb tidal delta and estuary are compared to schematisations based on the whole area. This is done for both types of target and all amount of classes (Table 16).

Type of target	Location of target	15 classes (benchmarks)	10 classes	5 classes	1 class (opti)
Bottom change	Whole area	M01 ↓	M02 ↓	M03 ↓	M04 ↓
Transport	Whole area	M13	M14	M15	M16
Bottom change	Ebb tidal delta	M05 ↓	M06 ↓	M07 ↓	M08 ↓
Transport	Ebb tidal delta	M17	M18	M19	M20
Bottom change	Estuary	M09 ↓	M10 ↓	M11 ↓	M12 ↓
Transport	Estuary	M21	M22	M23	M24

Table 17. Comparison of schematisations to address influence of the type of target. The red coloured simulations form the references for the simulations in the same red coloured box.

To address the influence of the **type of target**, climate schematisations based on bottom change are compared to schematisations based on transport of sediment. This is done for all three locations and all amount of classes (Table 17).

Type of target	Location of target	Characteristics	5 classes
Bottom change	Whole area	No seasonality, no storm	M03 ↓
		Seasonality, no storm	M25
		Seasonality, no storm	M25 ↓
		Seasonality, with storm	M26

Table 18. Comparison of schematisations to address influence of seasonality and a storm event. The red coloured simulations form the references for the simulations in the same red coloured box.

To address the influence of **seasonality**, the schematisation with seasonality (M25) is compared to the schematisation with the same selected classes without seasonality (M03). A description of the seasonality is given in section 5.5.4. Finally, to address the influence of as **storm event**, the schematisation with seasonality and with a storm (M26), is compared to the schematisation with seasonality and no storm (Table 18).

Comparing all these schematisations results in a large amount of data and figures. To maintain an overview of the most important results, in the following sections first the statistical parameters are presented in graphs. Of each type of influence (Table 15 - Table 18), one group is described in detail. From analysis of all groups it appears that the results as described for one group are similar for the groups within that type of influence. Figures of the described groups are presented to illustrate the meaning of and conclusions from the statistical parameters. The figures of the results of the other groups are included in Appendix 6 (
Figure 204 - Figure 224). Based on the statistical parameters and physical parameters, conclusions on the influence of wave climate schematisations can be stated.

Just like the benchmark simulations in section 6.3, the physical results of a number of schematisations are described in terms of erosion and sedimentation patterns, volume changes in ebb and flood channels, hypsometric curves. To investigate the similarity or difference between different schematisations, the results of the simulation on all of these components and the statistical parameters need to be combined. Individual components show to little information to state fully supported conclusions.

6.4.1 INFLUENCE OF AMOUNT OF CLASSES

Figure 51 presents the correlation coefficient and *relative rms* between the schematisations and their benchmark simulation, as a function of the amount of selected classes.

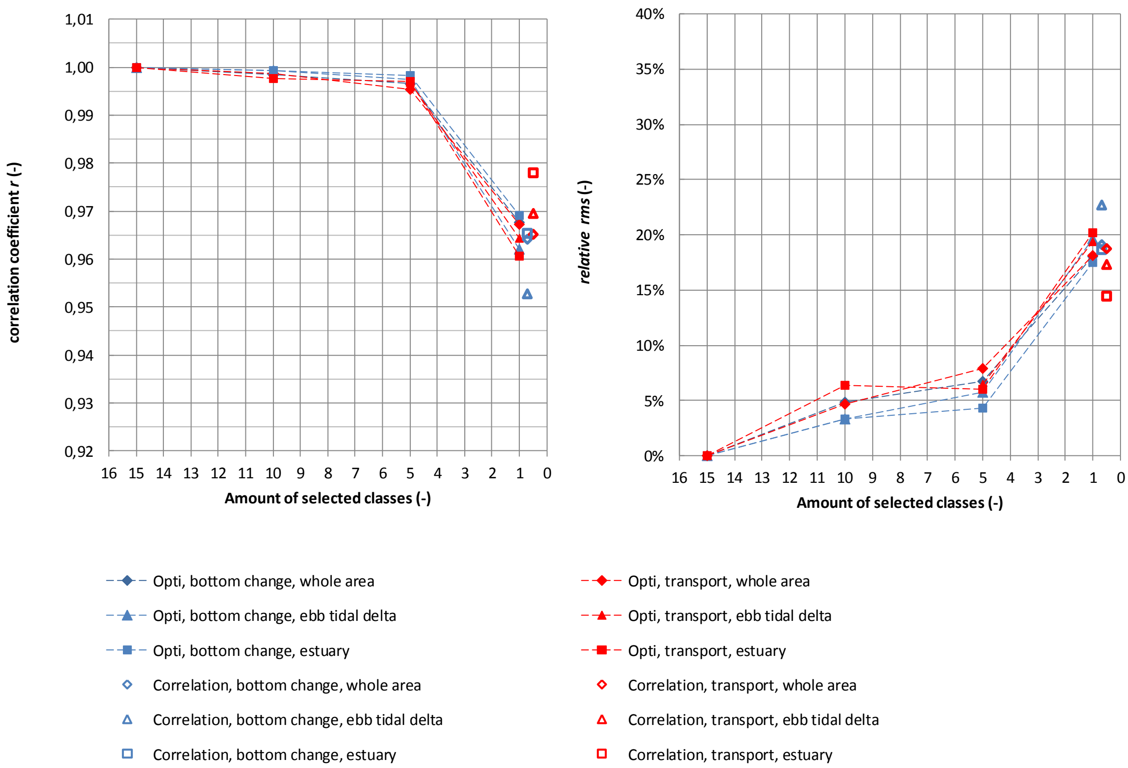

Figure 51. Correlation coefficient *r* and relative *rms* as a function of the number of selected classes for all wave climate schematisations. All values are related to the benchmark simulations of 15 classes.

From Figure 51 it can clearly be seen that the correlation coefficient and relative rms are a function of the amount of classes. The correlation with the benchmark simulations (15 classes) decreases when the number of selected classes decreases. At the same time, the relative *rms* increases. This means that the simulated morphological development increasingly differs from the benchmark simulations of 15 classes when less classes are selected in the wave climate schematisation.

The *trend* in development of the correlation coefficient and relative *rms* with an decreasing amount of classes is the same for all types and locations of the target. Also the order or correlation and *rms* is similar for all types and locations of the target. The trend is that the correlation with the benchmark simulations remains high (between 0.995 and 1) when the amount of classes decreases to ten or five classes. At the same time, the relative *rms* remain low (between 3% and 8%). When only one class is selected, the correlation decreases significantly (between 0.96 and 0.97 for the schematisation based on the Opti method and between 0.95 and 0.98 for the schematisations based on the method of correlation). The relative *rms* increases significantly when only one class is selected; around between 18% and 20% for the schematisations based on the Opti method and between 15% and 23% for the schematisations based on the method of correlation.

To visualize the meaning of the values of the correlation coefficient and relative *rms*, the sedimentation and erosion patterns, volume changes and hypsometric curves are presented. Since all types and locations of the target show the same trend, only one (arbitrarily) group of schematisation is presented here. Table

19 shows which group from Table 15 is described here in detail. The other groups related to the influence of the amount of classes show similar results; the conclusions stated here also hold for these groups.

Type of target	Location of target	15 classes (benchmarks)	10 classes	5 classes	1 class (opti)	1 class (correlation)
Bottom change	Whole area	M01 →	M02	M03	M04	M27

Table 19. Selected group to be described in detail.

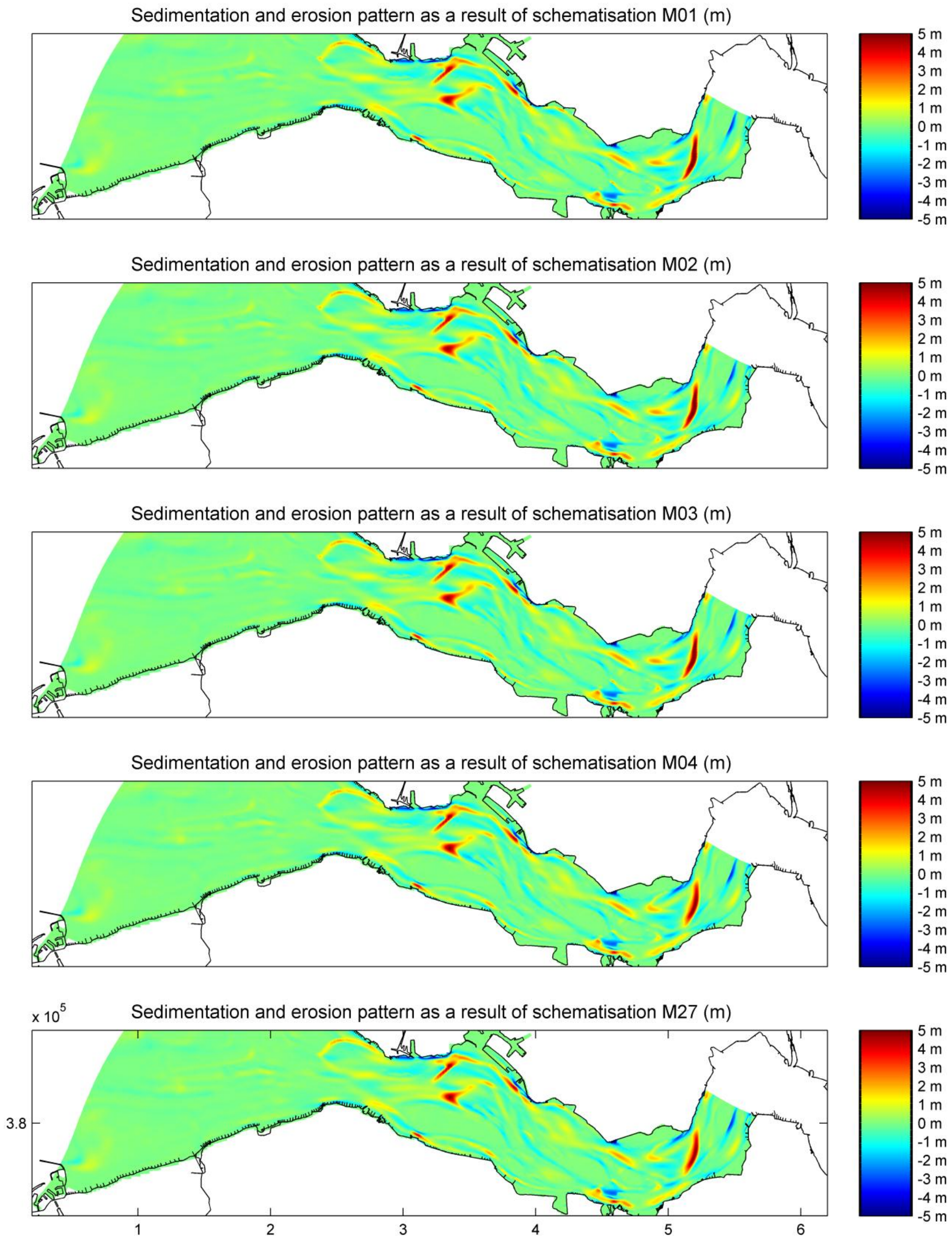

Figure 52. Sedimentation and erosion patterns as function of selected amount of classes: M01 (15 classes), M02 (10 classes), M03 (5 classes), M04 (1 class, Opti method) and M27 (1 class, method of correlation).

From Figure 52 it can be seen that the patterns of sedimentation and erosion are very similar. The reason for decreasing correlation and increasing differences in bottom changes are due to local differences in the patterns. These differences are clearly visible in Figure 53, where the results of simulations with 10 classes, 5 classes and 1 class are compared to the benchmark simulation with 15 classes (subtracted from each other). Within these figures, also the correlation coefficient (*r*) and *relative rms* (rel. rms) between each two compared simulations are presented.

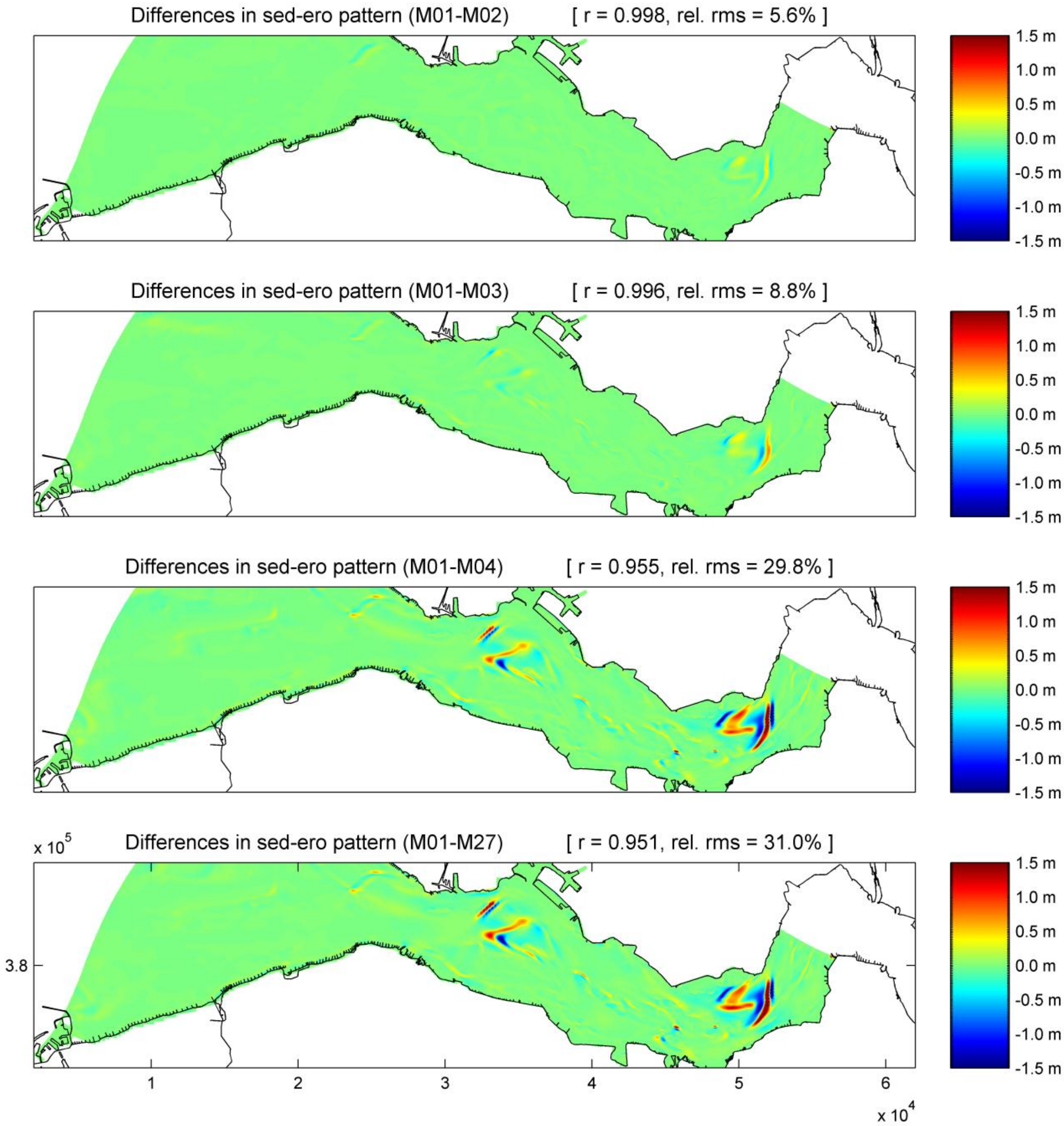

Figure 53. Differences in patterns of sedimentation and erosion between the benchmark simulation (M01) and simulations with 10, 5 and 1 class schematisations. 1st panel: difference between 15 and 10 classes. 2nd panel: difference between 15 and 5 classes. 3rd panel: differences between 15 classes and 1 class (based on Opti). 4th panel: difference between 15 classes and 1 class (based on method of correlation).

From Figure 53 it can be seen that the differences in sedimentation and erosion patterns can directly be linked to the presented *relative rms*. It also appears that the differences are located at the shoals of Spijkerplaat and the shoals south of Everingen. These differences are the main cause for the value of the relative *rms*. In the other parts of the area, the local differences are small (in the order of 0.1 m). It also appears that for the schematisation based on ten classes (M02) and five classes (M03), the found differences are small and mainly occur at the shoals south of Everingen. Here, the differences in sedimentation and erosion are in the same order as the *relative rms.* (e.g.: the difference is about 0.4 m – 0.5 m, where the total sedimentation and erosion is in the order of 5.0 m, hence a relative difference of 8 – 10%, which is of the same order as the *relative rms*). When only one class is selected (M04 and M27), the local differences not only increase around the shoals south of Everingen, but in these cases also large local differences at the shoals of Spijkerplaat occur. Here the differences are in the order of 30% (1.0 m – 1.5 m difference at 5.0 m sedimentation or erosion).

Values in Figure 53 are not exactly in line with Figure 51. In Figure 51 the values are corrected for the influence of the morfac value, in Figure 53 this has not been done. The differences between the simulations as shown in Figure 51 are a result of different amount of classes and different values of the *morfac*. Differences only due to the amount of classes is 5 – 10% smaller. The influence of the morfac for this situation is explained at the end of this section (Figure 51 is relatively easily adjusted to exclude the influence of the morfac, for Figure 53 this is not easily done).

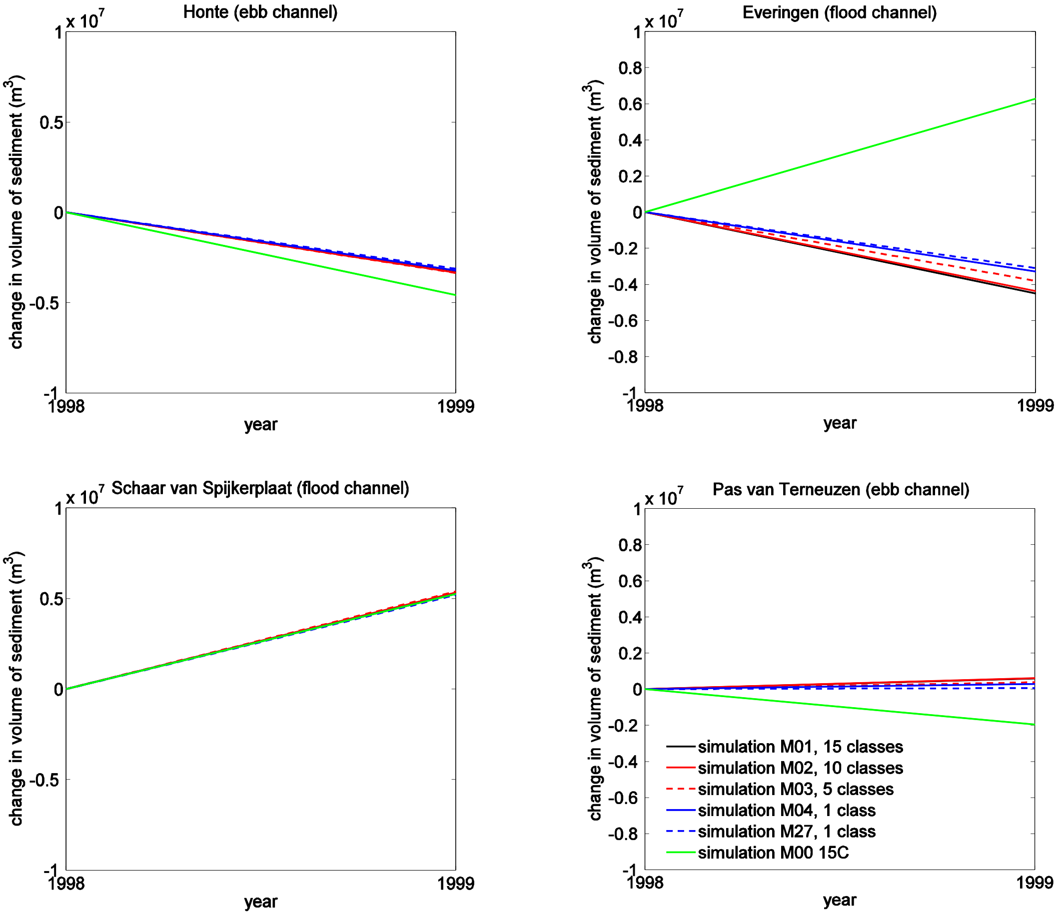

Figure 54. Volume changes in the ebb and flood channels.

It appears that at the channels of Honte and Spijkerplaat the differnce in cganges of volume are negligible. This does not mean that the patterns of sedimentation and erosion are equal as can be seen from Figure 52. At the channels of Everingen and Pas van Terneuzen, the influence of the amount of classes is more visible. The result of the schematisation with ten classes is (at this spatial scale) equal to the result of the schematisation with fifteen classes. For five classes and one class, this differences increases. However, the range between the different schematisations is small compared to the general influence of waves on the volume change.

As mentioned in section Volume changes in current channels of the macro cells6.3.2, volume changes in the channel area can only be interpreted when also spatial information is used. When the pattern of sedimentation and erosion of these simulations are used, the found difference in volume changes can be explained as follows. Different amount of classes within a wave climate schematisation result in differences in bottom changes at the shoals of Spijkerplaat and the shoals south of Everingen. These differences result in a shift of the local pattern compared to the benchmark simulation. When this shift occurs at the boundaries of the defined channels areas, the volume in the channel area can change somewhat. This occurs at the areas of Everingen and Pas van Terneuzen. At Honte and Spijkerplaat these small shifts occur not at the boundary of the defined area and as a consequence no difference in the changes in volume are visible.
From this can be concluded that the amount of classes result in a local shift of the patterns of erosion and sedimentation (local means here the spatial scales of the shoals). A change in volume can thus be interpreted as a shift in the local pattern.

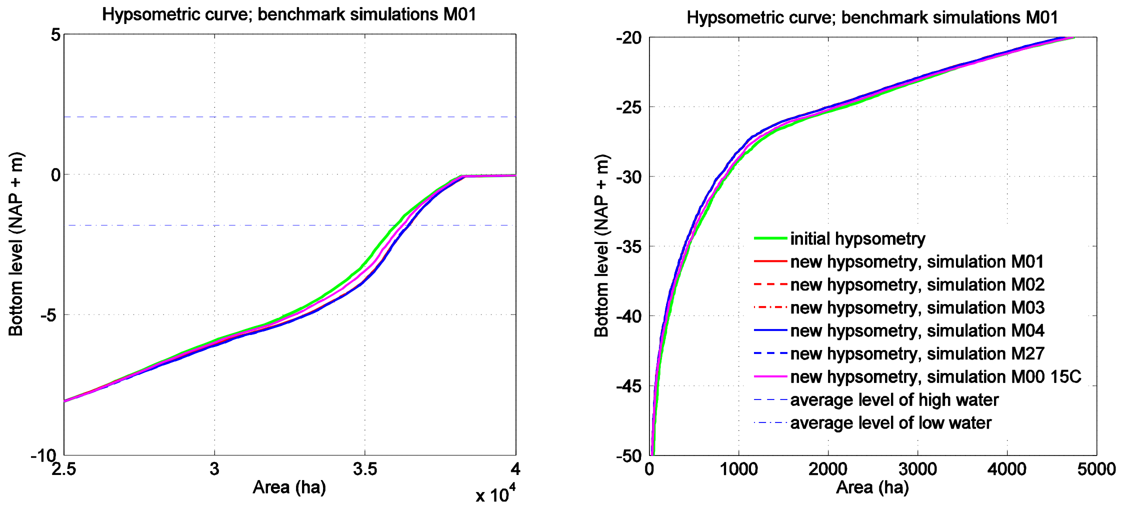

Figure 55. Hypsometric curves to indicate the influence of the amount of classes

On the spatial scale of the whole area, no difference in the hypsometric curve as result of the different amount of classes is visible. The general influence of the waves can again clearly be seen. At the spatial scale of the whole area, the amount of classes within a climate schematisation is subordinate to the general influence of waves.

Implicit error due to applied morfac values

As already mentioned in this section, it is important to appoint the influence of the *morfac* value when different amount of classes are compared. The influence of the *morfac* on the correlation coefficient and *relative rms* can be found when the simulations *without* wind and waves are analysed. It appears that in the situation without wind and waves (the green lines in Figure 56) a decrease of the amount of selected classes results in a *decrease* of the correlation coefficient and an *increase* of the relative rms compared to the simulation with 15 classes. Although no wind and wave classes are imposed in this simulation, the amount of morphological tides is equal the amount of morphological tides in the simulations with imposed classes (section 6.2.4). The imposed flow conditions are constant for all morphological tides. It is therefore expected that the different *morfac values* cause the decrease in the correlation and increase of the relative *rms*: when the number of classes decreases, the morfac value subsequently increases (in order to account for the same specific period of time). Especially when only one class is applied, the morfac value is large: in the order of 350. Apparently, a morfac value in the order of 350 is too high, resulting in deviations from the morphological development compared to the simulations with lower values (70 for 5 classes, 35 for 10 classes, 25 for 15 classes). This *error* is also included in the wave climate schematisations. Hence, for a correct interpretation of the influence of the amount of selected classes within a wave climate schematisation, this error must be removed. This is done by subtracting the absolute rms of the simulations *without* wind and waves from the absolute rms of the simulations *with* wind and waves. The correlation coefficient is corrected by adding the deficit in correlation to the calculated correlation. This is a very practical solution, but results in a better insight in the influence of the wave climate schematisations, without being blurred by an implicit error from a different order. The corrected correlation coefficients and relative rms are presented in Figure 51. It must be stressed that the correction does not change the *trend* of the result, it only changes the absolute values of the correlation coefficient and rms.

In the following sections, the values are not corrected for the influence of the applied morfac. This is not necessary: the influence of the type and location of target are compared at an equal amount of classes and hence all have the same error due to the *morfac*. Since the differences between different schematisations are considered, this error due to the applied *morfac* value is automatically excluded. Only when schematisations with different amount of classes are compared (as is done in this section), the results need to be correct for the error induced by the applied *morfac*, since this error changes per amount of selected classes.

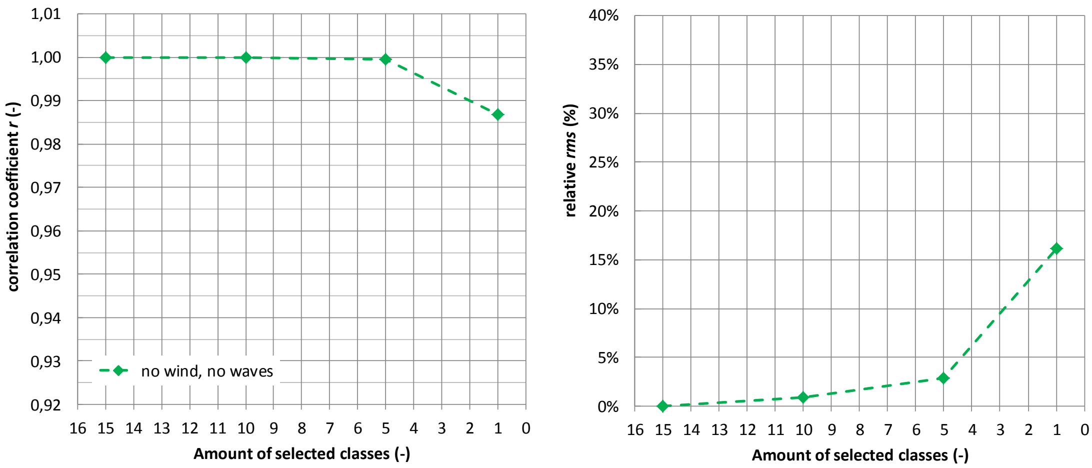

Figure 56. Correlation coefficient *r* (left panel) and relative *rms* (right panel) as a function of the number of selected classes for the simulations *without* imposed wind and wave conditions. Deviation from the benchmark (15 classes) is caused by the applied *morfac* values.

6.4.2 INFLUENCE OF SCHEMATISATION METHOD

The influence of the method of schematisation can only be determined for the climate schematisations which are based on one class. The reason for this is that the method of correlation can only be applied for schematisations based on one class.

From Figure 51 it can be seen that the wave schematisations based on one class based on the method of correlation (section 5.4.4) show the same order of correlation and *relative rms* with the benchmark simulations as the one class schematisations based on the Opti method. This can be explained by the fact that the morphological impact the remaining classes in case of one class schematisation with the Opti method are to a large extent similar (Figure 27 - Figure 29). It is important to state that a wave climate schematisation based on one class is relatively low correlated (around 0.96 – 0.97) with the benchmark simulation and has a relative large *relative rms* (around 20%; Figure 51), regardless the method of schematisation.

Because of the local influence on the wave conditions inside the estuary, a lot of classes are very similar in terms of morphological impact (section 5.6.2) and also have a high correlation with the weighted averaged morphological development. From this it can be concluded that the method used to select one class has only a small influence. Because of the similarity of the classes in terms of morphological impact, the weight of a certain class plays probably an important role. Within the method of correlation only one weight is given to the remaining class (100%), where in the Opti method, the 'ideal' weight is given to the remaining class, with a possible small deviation from 100%. This might explain why the range of correlation coefficient and relative *rms* (as can be seen in Figure 51) with the Opti method is smaller than the range of the same parameters with the method of correlation.

6.4.3 INFLUENCE OF LOCATION OF TARGET

To address the influence of the location of the target, the results of wave climate schematisations based on the **ebb tidal delta** and **estuary** are compared with the results of the schematisations based on the **whole area** (the ebb tidal delta and estuary combined).

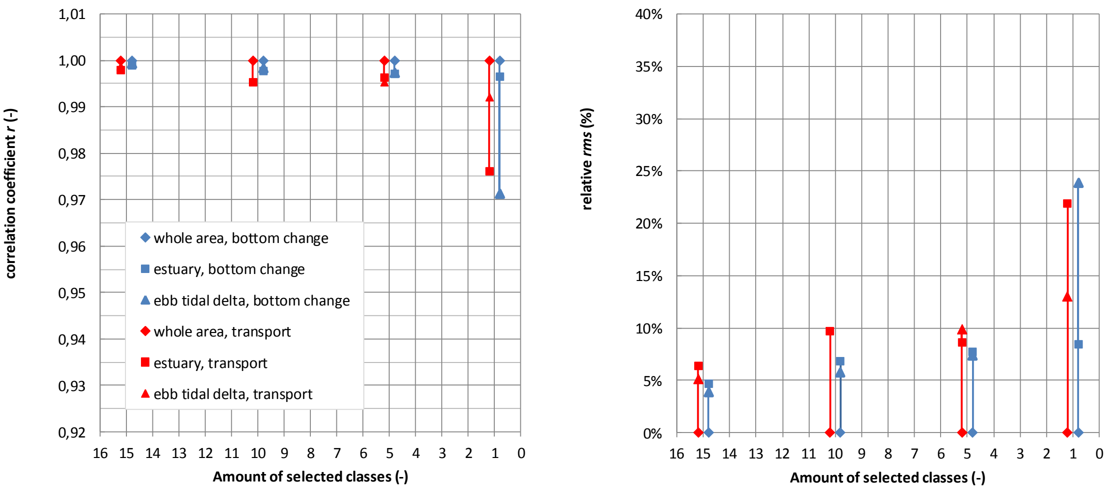

Figure 57. Correlation coefficient (left panel) and relative *rms* (right panel) between the three types of target (whole area, estuary and ebb tidal delta).

Figure 57 presents the correlation coefficient and the relative *rms* between the three types of locations. The diamonds represent the whole area, the squares represent the estuary and the triangles represent the ebb tidal delta. All locations of target are compared with each other for the two types of transport (bottom change (blue symbols) and sediment transport (red symbols)) and for all selected amount of classes. The schematisations based on the whole area are set as reference for the schematisations based on the ebb tidal delta and estuary.

The correlation coefficient between the three locations of target is high (0.999) when 15 class are selected but decreases when less classes are selected for the schematisation. The relative *rms* between the three locations of targets is small (5%) when 15 classes are selected but increases when less classes are selected.

Up to five classes, the correlation is relatively high (0.995) and the relative *rms* is low (10%) (hence small differences in morphological development). Furthermore, the found values are of the same order for both types of target. Only when only one class is selected, the correlation strongly decreases and shows a large range between the different areas (0.995 – 0.955) . The relative *rms* strongly increases and also shows a large range between the different areas (10% – 30%). The decrease of the correlation and increase of the relative *rms* indicates that the difference between morphological developments increase. This is in line with Figure 51, where the range increases as the amount of classes decreases

From these results can be concluded that the increase of difference in simulated morphology is not caused by the location of target, but rather by the decrease of the amount of selected classes. Hence, the influence of the location of target is small (a relative *rms* of about 5% when 15 classes are selected) compared to the influence of the amount of selected classes (which can be as large as about 20%). As long as multiple classes (five or more) are selected, the influence of the location of the target is subordinate to then influence of the amount of classes.

To visualize the presented values, the differences between the locations of target when the schematisations are based on the whole area, ebb tidal delta or estuary are presented. This is done for the schematisations which are based on the bottom change (the blue symbols in Figure 57). Table 20 shows also the codes of the visualized simulations.

Type of target	Location of target	15 classes (benchmarks)	10 classes	5 classes	1 class (opti)
Bottom change	Whole area	M01 ↓	M02 ↓	M03 ↓	M04 ↓
Bottom change	Ebb tidal delta	M05	M06	M07	M08

Table 20. Comparison of schematisations to address influence of the location of target. The red coloured simulations form the references for the simulations in the same red coloured box.

Figure 58 presents the difference between the schematisations based on the whole area and the ebb tidal delta. Also included at the top of the panels are the values for the correlation coefficient (r) and relative *rms* (rel. rms). From this, the meaning of these values in terms of differences in bottom changes can easily be seen.

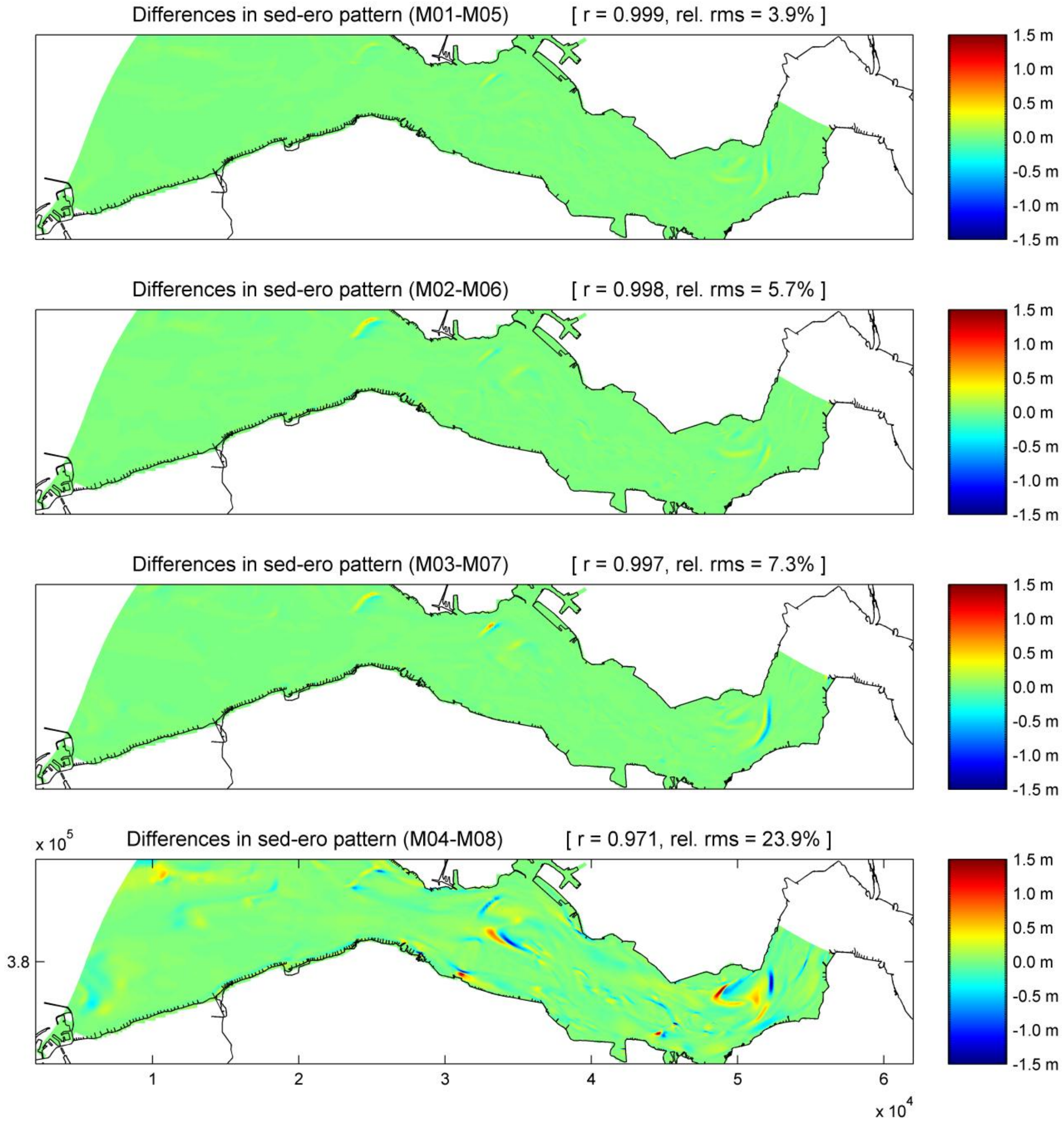

Figure 58. Differences in sedimentation and erosion patterns between schematisations based on the whole area (M01, M02, M03 and M04) and schematisations based on the ebb tidal delta (M05, M06, M07 and M08). 1st panel; difference due to area in case of 15 selected classes. 2nd panel; difference due to area in case of 10 selected classes. 3rd panel; difference due to area in case of 5 selected classes. 4th panel; difference due to area in case of 1 selected class.

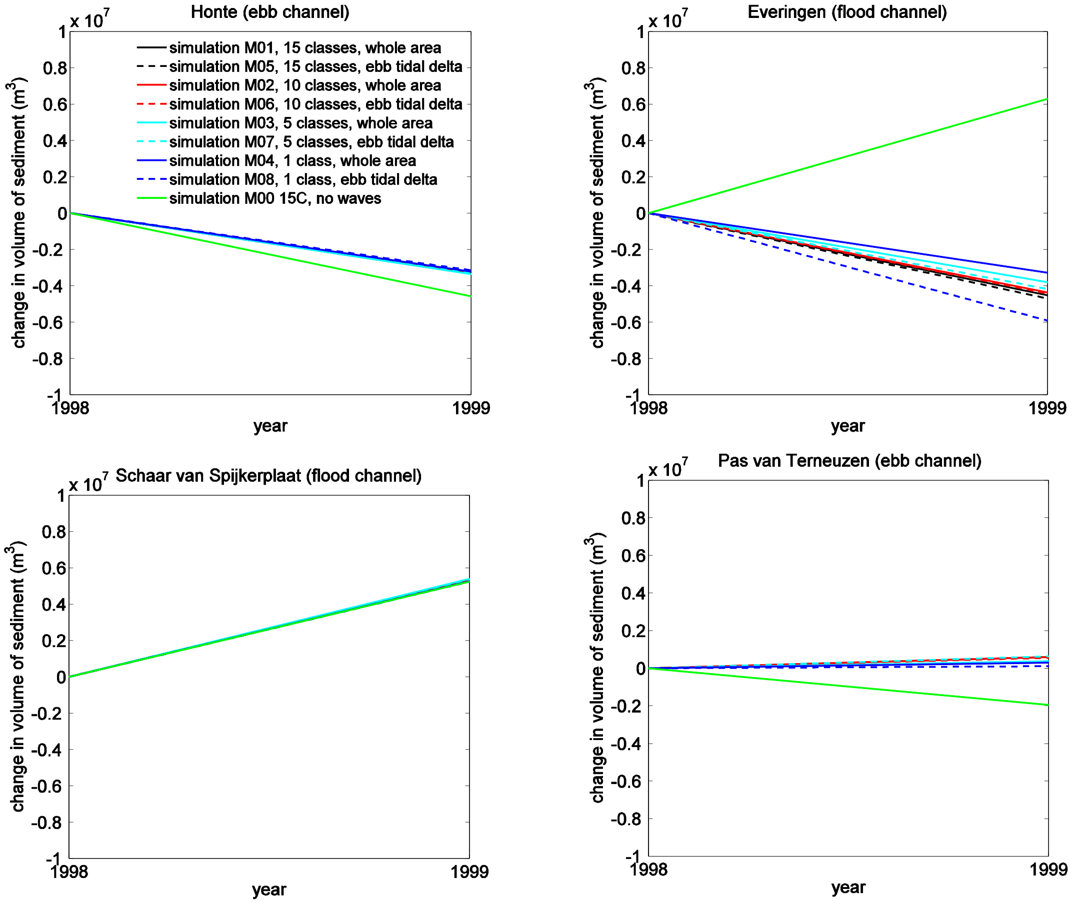

Figure 59. Volume changes in the ebb and flood channels.

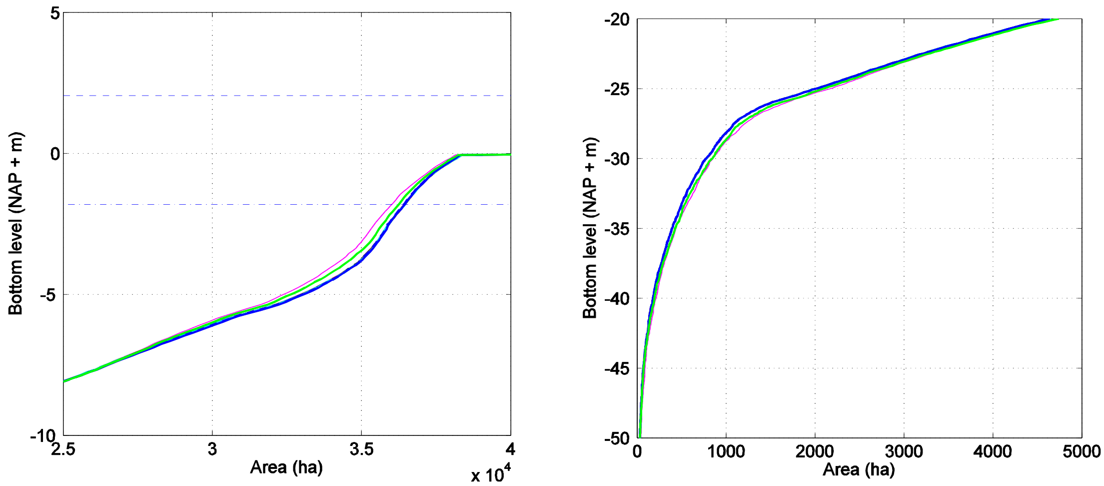

Figure 60. Hypsometric curves.

As described in the previous section, the differences in change in volume is caused from the local differences in sedimentation and erosion on the scale of the shoals. As long as five or more classes are selected, the range of difference between the locations of target remains small. This range increases when only one class is selected: as can more clearly be seen in Figure 58.

Also for the changes in the hypsometric curve due to the location of target, the same applies as for the influence of the amount of classes. No visible differences in the hypsometric curve on the scale of the whole area can be seen.

6.4.4 INFLUENCE OF TYPE OF TARGET

To address the influence of the type of the target, the results of wave climate schematisations based on the **bottom change** are compared with the results of the schematisations based on the **sediment transport**.

From Figure 51 it can already be seen that the wave climate schematisations based on the bottom change (blue lines in the figures) show a slightly higher correlation with their benchmark simulations compared to the schematisations based on transport of sediment (red lines in the figures). When the climate schematisations based on the ebb tidal delta and estuary are compared to schematisations based on the whole area, the following figures can be constructed.

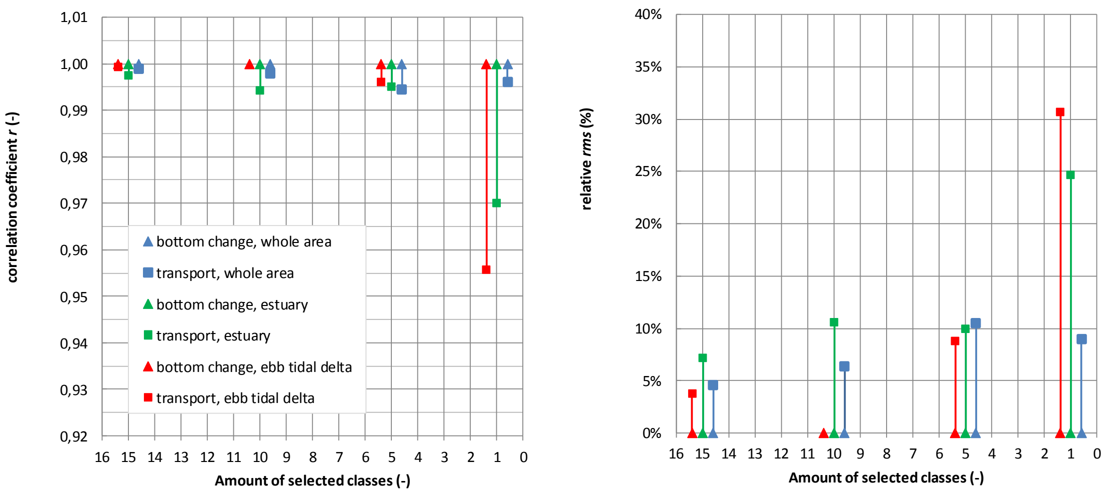

Figure 61. Correlation coefficient (left panel) and relative *rms* (right panel) between the two types of target (bottom change and transport).

Figure 61 presents the correlation coefficient and the relative *rms* between the two types of target, The triangles represents the bottom change, the squares represents the transport of sediment. Both types of target are compared with each other for the three types of area (whole area (blue symbols), estuary (green symbols) and ebb tidal delta (red symbols)) and for all selected amount of classes. Again it can be seen that the range between the different types of target is small as long as multiple classes are selected. This indicates that also the influence of the type of target is subordinate to the influence of the amount of selected classes.

The correlation coefficient between the two types of target is high (0.999) when 15 class are selected but decreases when less classes are selected for the schematisation. The relative *rms* between the two types of targets is small (5%) when 15 classes are selected but increases when less classes are selected. Up to five classes, the correlation is relatively high (0.995) and the relative *rms* is low (10%) (hence small differences in morphological development). Furthermore, the found values are of the same order for all three distinguished areas. Only when only one class is selected, the correlation strongly decreases and shows a large range between the different areas (0.995 – 0.955) . The relative *rms* strongly increases and also shows

a large range between the different areas (10% – 30%). The decrease of the correlation and increase of the relative *rms* indicates that the difference between morphological developments increase.
From these results can be concluded that the increase of difference between the simulations is not caused by the type of target, but rather by the decrease of the amount of selected classes. Hence, the influence of the type of target is small (a relative *rms* of about 5%) compared to the influence of the amount of selected classes (which can be as large as about 20%).

To visualize the presented values, the differences between sedimentation and erosion patterns when the schematisations are based on transport or bottom change are presented. This is done for the schematisations which are based on the estuary location (the green symbols in Figure 61). Table 21 shows also the codes of the visualized simulations.

Type of target	Location of target	15 classes (benchmarks)	10 classes	5 classes	1 class (opti)
Bottom change	Estuary	M09 ↓	M10 ↓	M11 ↓	M12 ↓
Transport	Estuary	M21	M22	M23	M24

Table 21. Comparison of schematisations to address influence of the type of target.

From the differences in sedimentation and erosion patterns in Figure 62, the same results are found as is the case from Figure 53, where the influence of the amount of classes is presented. Most important to recognize is again the direct link between the relative *rms* and the differences in the pattern of sedimentation and erosion. The three upper panel shows that as long as the relative *rms* is low (between 5 – 10%) and the correlation is high (around 0.995), the differences in pattern focusses on the shoals south of Everingen. When the correlation further decreases (lower than 0.995) and the relative *rms* further increases (higher than 10-15%), the differences in sedimentation and erosion pattern increase and also focusses at other locations (shoals of Spijkerplaat). From the statistical parameters of Figure 61 it can be concluded that the differences are mainly caused by the amount of selected classes and not by the type of target.

From the differences in volume changes in Figure 63, it can be concluded that the simulations show similar changes in volumes in the channels Honte, Schaar van Spijkerplaat and Pas van Terneuzen. When only one class is selected, there is a small range in the change of volume between the schematisation based on transport or bottom changes in the ebb channel Pas van Terneuzen. At the flood channel of Everingen, there appears to be a range in results regardless the amount of classes. The range is the largest for the schematisations which are based on one class. The range is the smallest for schematisations based on 15 classes (hardly no range), but large for schematisations based on 1 class (a range of 4 million m^3). Again it can be concluded that the differences are mainly caused by the amount of selected classes rather the type of target: when enough classes are selected (5 or more), the differences are small.

From the hypsometric curves in Figure 64, again it appears that the difference between the different wave climate schematisations are too small to result in different hypsometric curves.

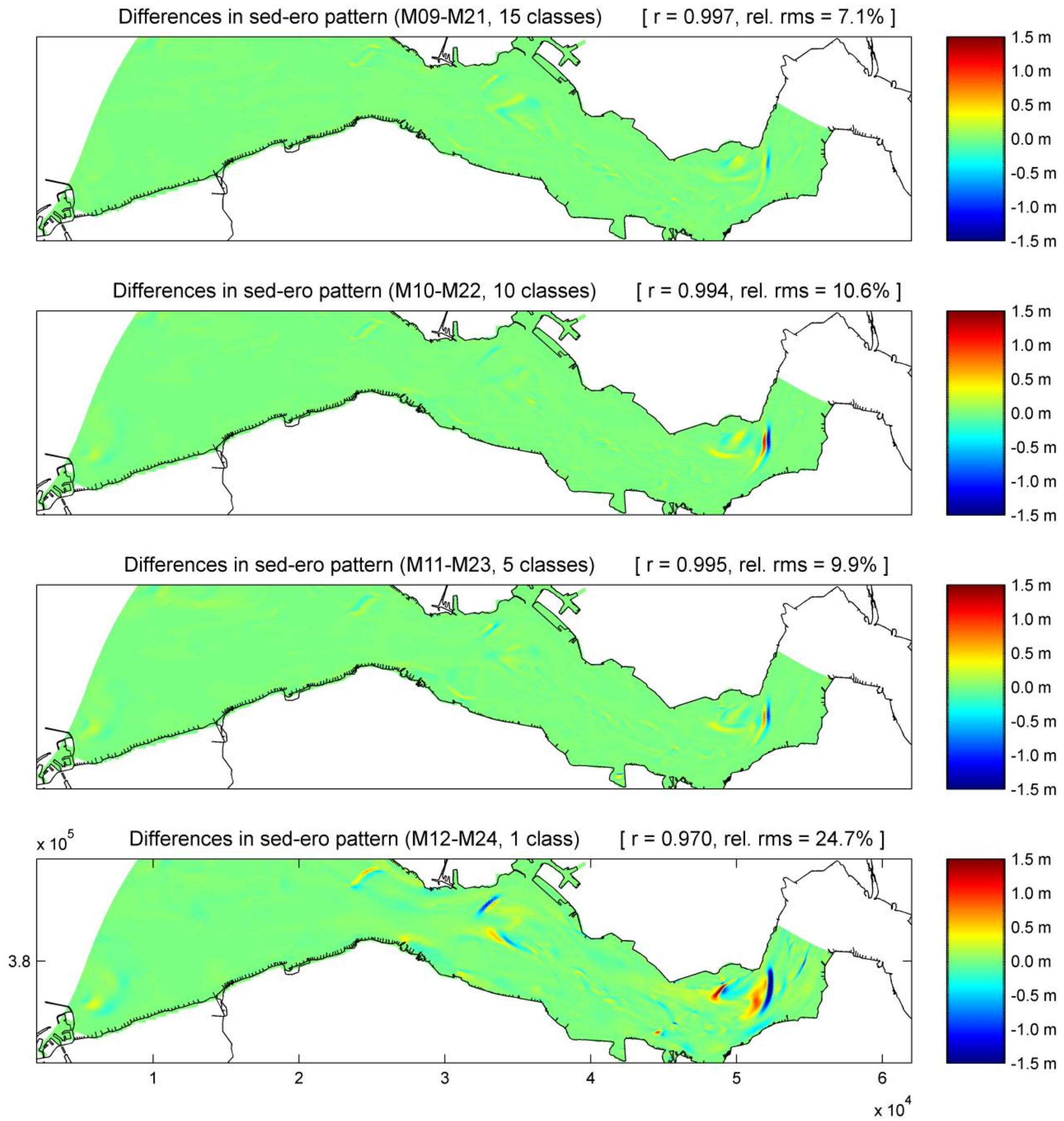

Figure 62. Differences in sedimentation and erosion patterns of schematisations based on bottom change (M09, M10, M11 and M12) and sediment transport (M21, M22, M23 and M24).

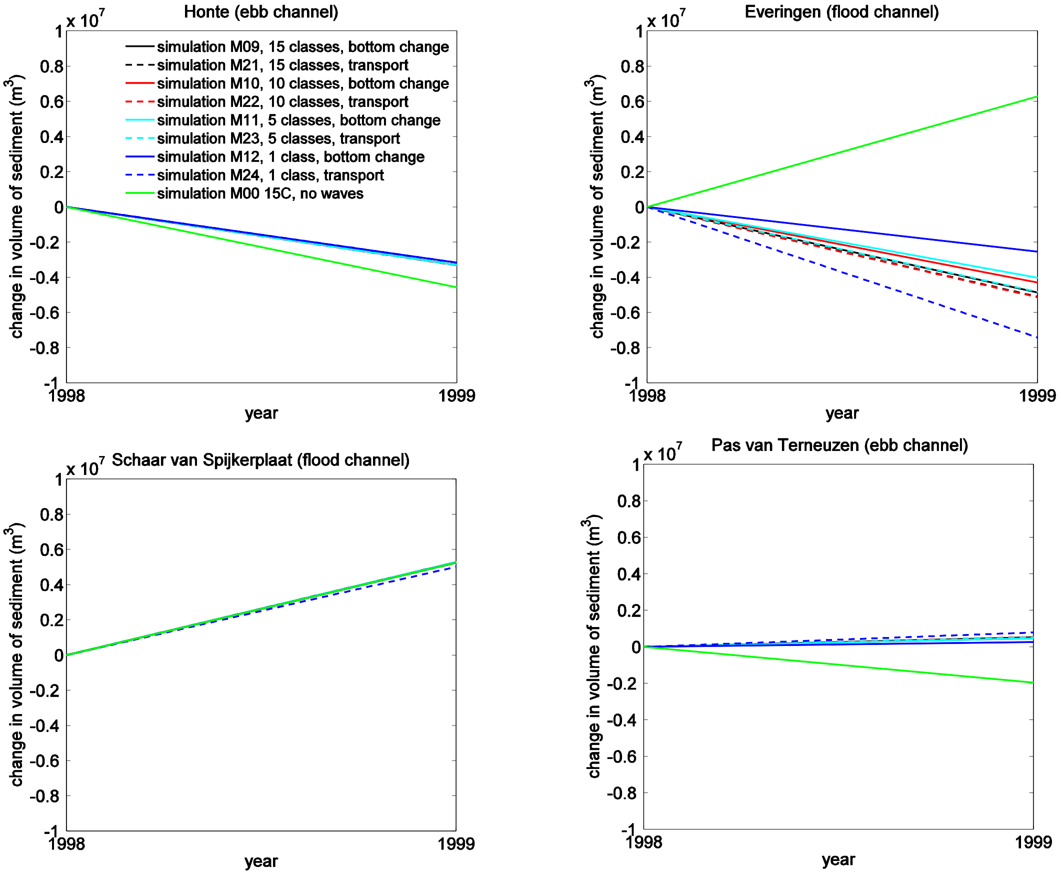

Figure 63. Volume changes in the ebb and flood channels.

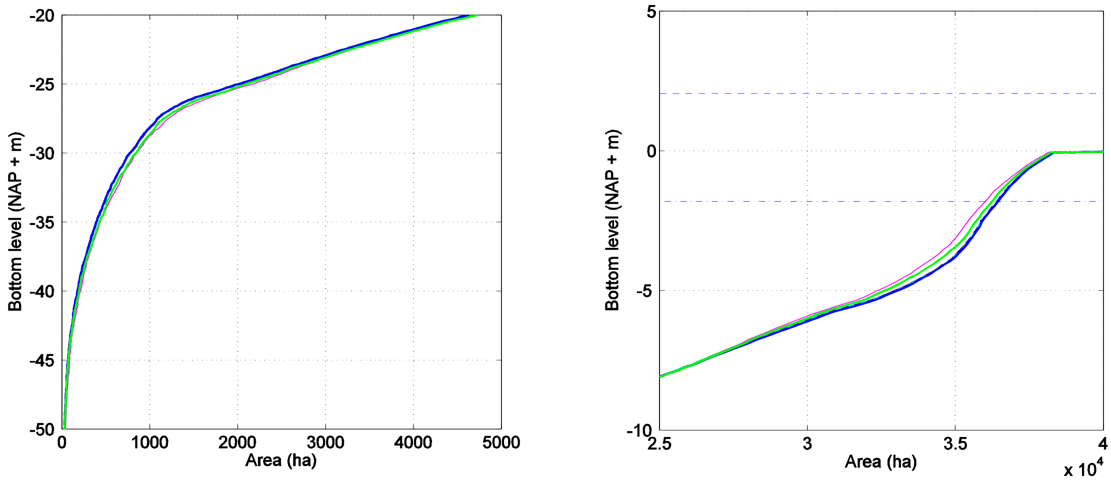

Figure 64. Hypsometric curves.

6.4.5 INFLUENCE OF SEASONALITY AND STORM EVENT

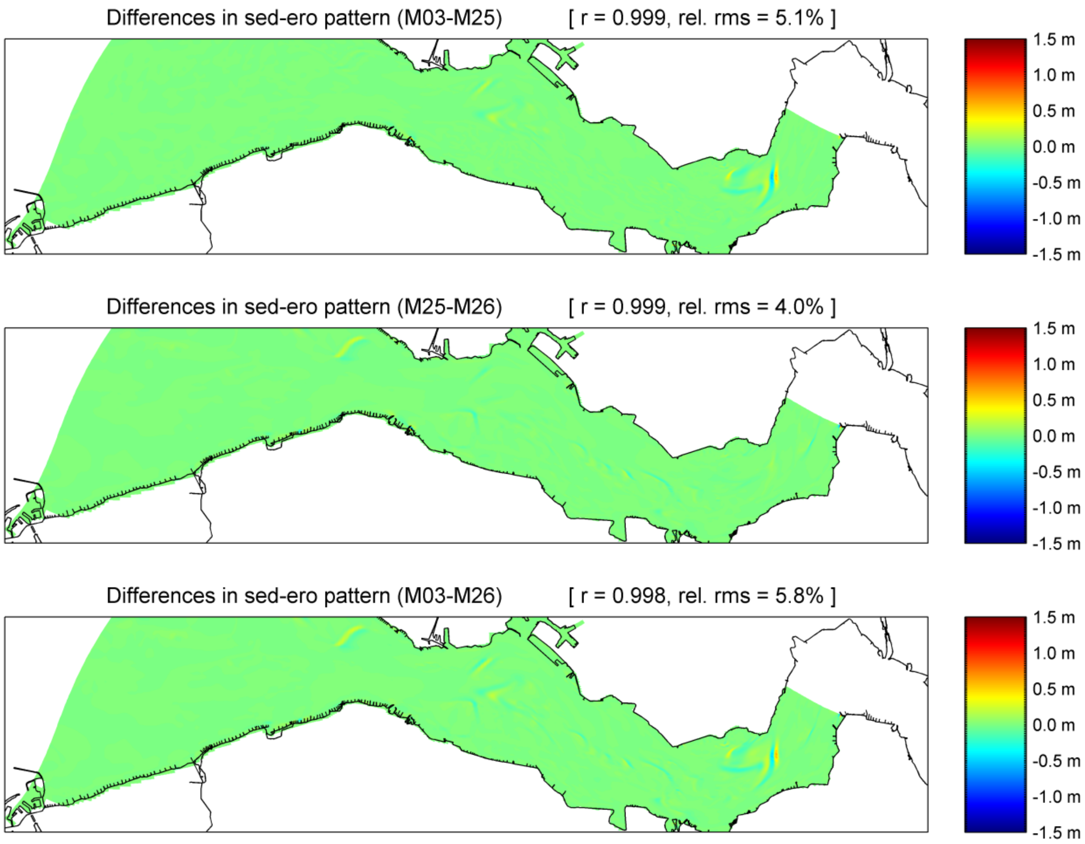

Figure 65. Differences in sedimentation and erosion patterns. Upper panel: influence seasonality, middle panel: influence storm event, lower panel: influence seasonality including storm event.

The influence of seasonality is relatively small (relative *rms* of 5%). From the upper panel in Figure 65 it can be seen that small local differences mainly occur at the shoals south of Everingen. Again, the relative local differences in sedimentation and erosion are of the same order as the relative *rms*: 0.25 m differences on a total sedimentation or erosion of 5.0 m. The influence of seasonality is an order smaller than the influence of the amount of classes. Based on the comparison in Figure 65 including seasonality does not significantly changes the morphological development, but has some small local influences.

The influence of a storm event on the time scale of one year is small. From the middle panel of Figure 65 it can be seen that the main influence occurs at Nolleplaat (slightly westwards of Vlissingen, part of ebb tidal delta). Furthermore some small differences occur along the edges of the shoals. The storm is introduced at the beginning of the simulation. Although the storm event has a short duration in the simulation (25 hours), the influence can still be found in the simulation with a duration of one year. However, no significant changes (switching points) due to the storm event have occurred (this was the main reason to invest the influence of a storm event).

It can be concluded that the storm event has a large impact on a short time scale and can locally and temporarily disturb the morphology. Since no irreversible changes occur, the influence of the storm event is recovered by the often occurring, moderate conditions.

6.4.6 INFLUENCE ON SIMULATION RUN TIME

The morphological simulations are run on two twelve processor computers. The simulations can be divided in running of the FLOW module and the WAVE module. The FLOW module of each simulation uses two of the twelve available processors (it uses two since the domain of the model consists of two subdomains and each subdomain runs at its "own" processor (domain decomposition)). The SWAN wave model in the WAVE module however uses all twelve available processors. Since more simulations are run at the same time, the SWAN wave model slows down all simulations. Since all simulations consist of a FLOW and WAVE part, this occurs almost constantly, resulting in higher simulation runtime of the individual simulation when compared to the situation where only one simulation is run. Performing multiple simulations parallel result in an equal of possible less runtime (averaged per simulation) compared to the situation where simulation are run in series. The presented runtime are therefore not the ideal runtime for a single simulation but are ideal when multiple simulations are run parallel.

- Simulations with a wave climate schematisation of one class: 2 days
- Simulations with a wave climate schematisation of five classes: 7 days
- Simulations with a wave climate schematisation of ten classes: 14 days
- Simulations with a wave climate schematisation of fifteen classes: 21 days

6.5 CONCLUSIONS

The objective of this chapter is to address the influences of the way the wave climate is schematised on the simulated morphological development. Based on these conclusions, the research questions as stated for this thesis can be answered.

General influence of waves on morphological development
From the sedimentation and erosion patterns, the change in volume and the hypsometric curves appears that on a time scale of one year, the waves mainly pronounce the influence of currents. More erosion occurs at the slopes and edges of the shoals, while more sedimentation occurs at the flood channels. This occurs throughout the area along all shoal edges, but is mostly visible at the location of the shoals of Spijkerplaat and the shoals south of Everingen. There, erosion of the edges of shoals and sedimentation in the shallow parts of the flood channels also results in a local shift of the patterns. From this can be concluded that waves move sediment from the edges of the shoals to deeper parts in the estuary (offshore directed transport). The influence of waves can be seen on the scale of the shoals (in the sedimentation and erosion patterns and cross sections), scale of the channels (in the volume changes) and on the scale of the whole area (in the hypsometric curves). Based on these results, it is recommended to take the influence of waves into account in the simulations on medium-term morphological development in the entrance of the Western Scheldt.

Influences of the way the wave climates are schematised
It can be concluded that the result of different climate schematisations for five classes or more, are very similar on the large scale of the whole area and the ebb and flood channels over the time period of one year. On the scale of the shoals, difference in sedimentation and erosion occur between the different schematisations. These differences are an order smaller (5% - 10%) than the general influence of waves in the entrance of the Western Scheldt as long as five classes or more are included in the wave climate schematisation. When only one class is selected in the wave climate schematisation, this difference in sedimentation and erosion pattern can be as large as 20%.

The schematisations are mostly influenced by the amount of wind and wave classes that are included in the schematisations. The influences of the type of target or location of target are subordinate to this. The reason for this is that more or less the same classes are selected in the climate schematisations regardless the type or location of the target. The individual influences of these selected classes on the morphological development is also similar to a large extent. The influence of the type or location of target are especially subordinate when five classes or more are included in the schematisation. This is in line with the conclusions on the different obtained climate schematisations in section 5.6.2; the schematisations based on different areas and different types of target are very similar, as long as multiple classes are selected. The schematisations can differ more when only one class is selected. The reason for this is that when more classes are applied, these classes keep each other in some kind of balance, preventing one class to fully dominate over the others. When only one class is selected, the influence of that class on the morphology is not counteracted.

As a result of the similarity in the climate schematisation, the results the simulations with five, ten or fifteen classes included in the schematisations, are also similar to a great extent. Only locally differences in sedimentation and erosion occur, which are about 5 - 10% of the local changes in bathymetry and mainly occur at the shoals south of Everingen. It can thus be concluded that the influence of the amount of classes is twofold. The more classes are included in the wave climate schematisation, the better the result of the benchmark simulation is reproduced (i.e. more classes result in a higher correlation coefficient with the benchmark and a lower *relative rms* with the benchmark). Second, the amount of classes influences the range of results for different types and locations of targets: as less classes are selected, this range becomes larger. The reason the for the small ranges when five or more classes are selected stems from the fact that the morphological impact of the selected classes are to a large extent similar.

Although the influence of the type and location of the target are an order smaller than the influence of the amount of selected classes, they still have some influence. It can be concluded that the wave climate schematisations based on the bottom change (type of target) in the estuary (location of target) show the highest correlation and lowest deviation (*relative rms*) with their benchmark when less than 15 classes are selected.

One class schematisations based on the method of correlation show the same order of correlation and relative *rms* with the benchmark simulations as one class schematisations based on the Opti method. So, the method of correlation is not an improvement compared to the Opti method. Opti might in this case be even better, since the 'ideal' weight is given to the remaining weight, where in the method of correlation only one weight is given (100%).

The influence of seasonality is an order smaller than the influence of the amount of classes. This also holds for the influence of the imposed storm event. It can be concluded that the storm event has a large impact on a short time scale and can locally and temporarily disturb the morphology. Since no irreversible changes occur, the influence of the storm event is however recovered by the often occurring, moderate conditions.

It can also be concluded that although the area of the western Scheldt is complex, the influence of the benchmark simulations on the large scale morphological development of the macro cells can be approached within the specified range of accuracy ($r > 0.98$, *relative rms* < 10%) by five classes of wind and waves.

Influence morfac

From the simulations without wind and waves, it can be concluded that the morphological acceleration factor (*morfac*) plays an important role in the simulated morphological development as well. The results based on morfac values of 23, 35 and 70 don't show significant differences (applied for the schematisations based on 15, 10 and 5 classes respectively). When a morfac value of 350 is applied (simulation with a climate schematisation based on 1 class), differences in the sedimentation and erosion patterns occur of about 15% compared to the lower mentioned values. This is of the same order as the found differences in simulated morphology between the simulations based on one class schematisation and the benchmark simulations. It is therefore concluded that a *morfac* value is too high. The *morfac* value must be in the order of 70 to prevent additional deviations from benchmark simulations due to the applied *morfac*.

7 Final conclusions and recommendations

7.1 INTRODUCTION

This final chapter answer the research questions as stated for this thesis. This is done on the results and conclusions of the previous chapters. Based on those results and conclusions, also the five hypotheses formulated at the start of this thesis can be verified. Finally, a few recommendations are made, related to further investigation of the wave climate schematisation, preferred wave climate schematisation to be used for the simulations in the Western Scheldt and methodology for other estuary entrances.

7.2 ANSWERS TO RESEARCH QUESTIONS

In section 1.2 (Problem and objective), the research questions for this thesis are stated. Here, these questions are repeated and answered.

Main question

> What is the influence of the way the wave climate is schematised on the predicted medium-term morphological development of the entrance of the Western Scheldt estuary on the scale of shoals and channels.

The way the wave climate is schematised influences the simulated morphological development on the scale of the channels and shoals during one year up to 24%. This means that at theses spatial and time scales, the simulated local bottom change (referred to as sedimentation and erosion pattern) due to currents and waves can deviate 24% between simulations which are based on different wave climate schematisations. These local bottom changes mainly occur at the low-lying shoals of Spijkerplaat and the shoals south of the Everingen flood channel (Figure 6, section 2.2.3). At these locations, the general influence of waves on simulated morphological development is the highest. The local deviations are in the form of magnitude (less or more pronounced patterns of sedimentation and erosion) and location: at the considered locations, waves intend to shift the local patterns compared to the situation where no waves are taken into account. Differences in wave climate schematisation therefore results in local shifts of these patterns.

The general influence of waves compared to the situation where no waves are taken into account result in erosion of the edges and slopes of the shoals around the water line (Figure 41, section 6.3.1). This results in local shifts of the patterns of sedimentation and erosion (Figure 36 - Figure 38, section 6.3.1), especially at the shoals of Spijkerplaat and the shoals south of Everingen. The shift in pattern might be explained by the fact that at these locations, waves locally increase the depth averaged velocity (Figure 26, section 5.3.1), hence increasing the capacity of the current to transport sediment. Next to this location, the depth average velocity is the same as without waves. The pattern is thus only locally shifted due to a locally change in the depth average velocity. The influence of waves focusses around the line of low water. This can be explained by the fact that at times of low water, the shoals are just above or just below the water line. The influence of the waves is for this situation higher compared to the situation at times of high water. The reason that the waves are most effective at the low-lying shoals of Spijkerplaat and the shoals south of Everingen, is the presence of the tidal currents at and over these shoals. The sediment that is brought into suspension by the waves can consequently be transported by the tidal currents. Around other shoals, such as Hooge Platen and Middelplaat, the magnitude of the tidal currents is smaller or absent. Although waves bring more sediment into suspension at the shoals compared to the low-lying shoals of Spijkerplaat and Everingen, this sediment is consequently not transported. At the considered time and spatial scale, only small changes in morphology are simulated compared to the situation where no waves are taken into account. Again, the changes are in the form of erosion of the edges and slopes of the shoals. The eroded sediment is deposited at the channels adjacent to the shoals.

Although the considered spatial scale is the scale of the ebb and flood channels and the shoals in the entrance of the Western Scheldt, waves have influence on the scale of the whole area. This is found form changes in hypsometric curves of the whole area. Also from this curves is found that waves in general erode the area around the line of low water (the edges and slopes of the shoals) and deposit sediment at the lower areas (the ebb and flood channels).

This general influence of waves is based on a benchmark simulation, which acts as a representative for the complete wave climate schematisation. The result of the benchmark simulation is reproduced by different wave climate schematisations within a range of deviation of 24%. The amount of classes that is selected within a specific climate schematisation has the most influence on this deviation. Other influences within the way the wave climate is schematised are subordinate to this. These other influences are the quantity on which the schematisation is based (bottom change or transport of sediment) and the area where this quantity is considered (the ebb tidal delta, estuary, or both areas added). When an amount of fifteen classes are selected, the range of deviation between different climate schematisations is in the order of 5%. The influence of the quantity on which the schematisation is based (the so-called *type of target*) and the influence of the area which is considered (the *location of target*) are thus in the order of 5%. The reason the small influence of the type and location of target is that to a large extent the same wind and wave classes are selected to form the schematised climate (Figure 33 and Figure 34, section 5.6.1). The reason for this is that the *morphological impact* of the selected class is similar to a large extent (Figure 27 - Figure 29, section 5.3.3), i.e. it doesn’t matter much which classes are selected, as long as enough classes are selected. How enough is defined depends on the required accuracy of the result of the schematisation (i.e. the deviation from a certain benchmark)
When less classes than fifteen classes are selected in the wave climate schematisation, the deviation from the result of the benchmark simulation increases. With a decrease of the amount of selected classes, also the influence of the type and location of target seems to slightly increase. This again can be explained by the fact that the small differences in selected classes within a schematised climate become more pronounced when less classes are present to keep the differences small (“keep each other in balance”).

Underlying question 1

> In what manner is the wave climate to be schematised to realistically and efficiently reproduce the total morphological development by the full wave climate.

The morphological development is realistically and efficiently reproduced when the applied wave climate schematisation consists of five classes, based on bottom changes in the estuary. The deviation from the benchmark is in this case 4%. This is explained in the following.

When ten classes are selected, the deviation from the benchmark simulation is around 5%, with a range of plus and minus 2% (Figure 51, section 6.4.1). It is again emphasized that this deviation mainly occurs at the low lying shoals of Spijkerplaat and the shoals south of Everingen. In the remain part of the Western Scheldt entrance the deviations are smaller. When five classes are selected, the deviation from the benchmark increases to around 7%, with a range of plus and minus 3%. When one class is selected, the deviation increases to around 20%, with a range of plus and minus 4%. The correlation of the simulation with the benchmark simulation decreases with a decrease of the amount of selected classes. When ten of five classes are selected, the correlation coefficient is around 0.995 or higher, with a small range for the type or location of target. When only one class is selected, the correlation decreases to 0.96, with a range for the type and location of target of 0.01.

The required accuracy of the result of a certain schematised climate with respect to the benchmark simulation is 1% accuracy for the correlation coefficient (hence in the range 0.99 – 1) and 10% accuracy for the deviation (section 5.4.1). To fulfil this requirement, a climate schematisation should consist of five or more selected classes. Simulations based on climates of ten or fifteen classes reproduce the result of the benchmark better than a simulation based on climate of five classes, but are also more expensive (section 6.4.6). It is therefore recommended to apply a wave climate schematisation based on five selected wind and wave classes.
Although the quantity (bottom change or transport of sediment) on which the schematised climate is based and the area where this quantity is considered is of smaller influence, it still has influence on the result of the simulation. The schematised wave climate based on bottom change in the estuary show the lowest deviation from the benchmark in case of five selected classes compared to other combinations of quantity and area (Figure 51, section 6.4.1).

Underlying question 2

> To which extent is the influence of waves during storm events taken into account.

The influence of waves during storm events is taken into account in two ways. First, the storm classes are represented in the complete climate schematisation (Figure 14, section 4.2.2) and the morphological impact of the storm classes is simulated over a short period of time. Although a storm event has a large impact on the morphology, it contribution to the total morphological development is relatively small. This is caused by the low probability of occurrence of the storm classes. Due to this, the storm classes are the first classes to be left out by the Opti method.
The influence of waves during a storm are again taken into account by manually include a storm class in an existing wave climate schematisation (obtained with the Opti method). By doing so, the possibility of the creation of an irreversible morphology due to a storm event (i.e. a switching point in the system) is investigated. From simulated morphological development is appeared that no irreversible changes due to the storm event occur. The influence of a storm event are visible in the morphology, even after multiple months, but no significant changes occur. The influence of the storm event is recovered by the often occurring, moderate conditions.

7.3 VERIFICATION OF HYPOTHESES

The hypotheses for this thesis are stated in section 1.3. They are shortly repeated and verified.

1. *When waves propagate from the North Sea towards the entrance of the Western Scheldt, a large amount of wave energy is dissipated over the ebb tidal delta. As a result, inside the estuary the wave conditions are mainly locally influenced and the influence of the imposed wave conditions strongly decreases inside the estuary.*

   This hypothesis can be confirmed. Due to the presence of the ebb tidal delta, wave conditions at the North Sea only have a relative small influence on the wave conditions inside the estuary. The wave conditions inside the estuary are dominated by the local wind conditions. The local wind conditions have an influence on the local wave conditions of 60 % - 80% around the shoals of Spijkerplaat. Further towards Terneuzen this influence increases to 80% - 100% (Figure 22, section 4.4.4). This also justifies the approach to classify the wave conditions in wind speed and wind direction classes.

2. *The quality of the reproduction of the morphological development by a schematised wind and wave climate depends on the amount of wind and wave classes within the schematised climate. Increasing the amount of classes improves the reproduction of the morphological development by the full wind and wave climate.*

   This hypothesis can be confirmed. As explained and concluded in the previous section, the amount of classes has the most influence on the quality of the reproduction of the benchmark simulation compared to other influences. By definition the quality of the reproduction increases when more classes are selected, regardless the other choices made for schematisation of the wave climate.

3. *Wind and wave conditions from a westerly direction are expected to have more influence on the morphological development than conditions from a easterly direction.*

   This hypothesis can be confirmed, with a nuance on the time scale. On a medium-term time scale (years), westerly direction have the most influence on the morphological development. The reason for this is that these conditions have the highest probability of occurrence, as explained in section 2.2.1. The influence on a short time scale is to a large extent equal to conditions from an easterly direction, at least up to average wind speed of 15 m/s (Figure 27 - Figure 29, section 5.3.3). Therefore, the probability of occurrence of the westerly direction becomes decisive.

4. *Storms (high wind speeds) have a large influence on the morphological development. Due to the higher water level (during high water and storm surge), waves can travel further into the estuary, where the impact will be larger compared to the situation with lower water levels.*

   This hypothesis can be confirmed, again with a nuance on the time scale. On the time scale of the storm itself the impact is large compared to classes with lower wind speed and smaller waves. On the medium-term time scale, where the probability of occurrence of a certain class plays a role, storms don't have a large influence on the simulated morphology (at least not the investigated storm class).

5. *Influence of waves on sediment transport and morphology mainly focusses at the edges of shoals (ebb tidal delta, shoals of Spijkerplaat, shoals south of Everingen). Due to the influence of waves at the edges, waves contribute to the steepening of the cross shore profiles and consequently influence the hypsometric curves.*

   This final hypothesis can be confirmed as well. In the simulated changes in morphology, the waves erode the edges of the shoals and deposit sediments in the channels (Figure 41, section 6.3.1). As a result, the hypsometric curve of the area is adjusted (Figure 45, section 6.3.3).

7.4 RECOMMENDATIONS

From the results and conclusions of this thesis, the following recommendations are made:

- Include wave conditions when the morphological development in the entrance of the Western Scheldt is simulated. Use a schematisation of the wave climate that consists of five classes, based on the bottom change in the estuary.
- Include multiple wind conditions in the applied climate and apply the correct wind conditions. Since the wave conditions inside the estuary are dominated by the local wind conditions, multiple wind conditions must be included to simulate the wave conditions and hence their influence on the morphology. The recommended climate has five wind classes. This recommendations especially holds for areas further into the estuary: although no influence of the wave conditions at the North Sea influence the wave conditions, waves still influence the morphology, mainly by shifting patterns of sedimentation and erosion.
- Calibrate the model when a wave climate schematisation is applied.
- Compare the influence of waves to a simulation without waves on a longer time scale, e.g. four years. Don't use a morphological acceleration factor higher than an order of 70 to prevent errors in simulated morphology due to this factor. To simulate a longer time scale, use a longer morphological tide.
- Investigate the development of the deviation and correlation coefficient between one and five selected wave classes. It might be possible to obtain a good reproduction of the benchmark simulation with less than five classes. Simulations with less classes are less expensive.
- Check whether a benchmark of 15 classes also is good representative for the complete climate schematisation on a medium-term time scale. This is now assumed based on a short term time scale. It is further recommended to investigate how the benchmark relates to the full time series of wind and wave conditions.
- Increase options of the wave model as it is now implemented. The stand-alone version of the SWAN wave model has more options related to the imposed wave spectrum and physical settings. These might result in a better reproduction of the wave conditions and therefore result (at least in theory) in a better reproduction of the influence of wave on morphology.

Recommended methodology for application in other estuary entrances

The conclusions on the amount of classes to select within a schematised wave climate and the consequences of that choice refer to the situation of the Western Scheldt entrance. This does not apply for other estuary entrances. However, the methodology as described in this thesis can be applied to address the necessity of including waves in morphological simulations and consequently address the necessity to schematise the wave conditions. Before starting to schematise the wave conditions, the following trace should be followed (like the described traces in section 1.4):

1. Analyse the area of consideration: what are the wind, wave and tidal climate, what is the ratio tide over wave influences, what are the characteristics of the area and the influence of that on wave conditions.
2. Schematise the wind and wave climate from available time series on wind and wave conditions.
3. Think of possible influences of waves on the morphology of the area and vice versa, and perform short simulations. Perform one simulation without wind and waves and one simulation with wind and waves. For this last simulation, apply only one wind and wave class, e.g. the condition that occurs most often.
4. Analyse the simulations: compare found influences of waves with expected influences.
5. Based on the found influence of the waves, determine the necessity to include waves in the morphological simulations and determine the necessity to further investigate the influence of the way the waves are schematised. For this last part, follow the traces as described in section 1.4 of this thesis.

Bibliography

Battjes, J.A., 1982. *A case study of wave height variations due to currents in a tidal entrance*. Coastal Engineering, 6, 47-57.

Bosboom, J., Stive, M.J.F., 2011. *Coastal dynamics I*. Lecture notes (version 0.2) for the course 'Coastal dynamics I', Delft University of Technology (course code CIE4309). VSSD.

Carter, R.W.G., 1988. *Coastal environments. An Introduction to the physical ecological and cultural systems of coastlines.* Academic Press Limited. ISBN 0-12-161855-2

Dekking, F.M., Kraaikamp, C., Lopuhaä, H.P., Meester, L.E., 2005. *A modern introduction to probability and statistics*. Springer-Verlag London Limited. ISBN 1852338962.

Delft University of Technology, 2010, *Ocean waves* (course, course code CIE 4325)
Delft University of Technology, 2011, *Coastal dynamics I* (course, course code CIE 4305)
Delft University of Technology, 2012a, *Coastal dynamics II* (course, course code CIE4309)
Delft University of Technology, 2012b, *Breakwaters and Closure dams* (course, course code CIE5308)

Delft University of Technology, 2011, *SWAN user manual*, SWAN Cycle III version 40.85, www.swan.tudelft.nl

Delft University of Technology, 2011, *SWAN Scientific and technical documentation*, SWAN Cycle III version 40.85, www.swan.tudelft.nl

Deltares, 2011a. *Delft3D-FLOW, Simulation of multi-dimensional hydrodynamic flows and transport phenomena, including sediments.* User manual, version 3.15 (revision 18392).

Deltares, 2011b. *Delft3D-WAVE, Simulation of short-crested waves with SWAN.* User manual, version 3.04 (revision 15779)

Grasmeijer, B.T., 2012. *Actualisatie Delft3D model van de Westerschelde, Concept.* ARCADIS.

Holthuijsen, L.H., 2007. *Waves in oceanic and coastal waters*. Cambridge University Press. ISBN-13 978-0-521-86028-4

Kuijper, C., Steijn, R., Roelvink, J.A., Van der Kaaij, T., en Olijslagers, P, 2004. *Morphological modelling of the Western Scheldt*. Report Z3648/A1198. WL | Delft Hydraulics en Alkyon Hydraulic Consultancy & Research.

Kuijper, C., Van der Kaaij, T. en De Goede, E, 2006. *LTV-O&M actieplan voor morfologisch onderzoek modelinstrumentarium*. Report Z3950. WL | Delft Hydraulics.

Lesser, G.R., 2009. *An approach to medium-term coastal morphological modelling*. PhD thesis, UNESCO-IHE & Delft Technical University, Delft. CRC Press/Balkema. ISBN 978-0-415-55668-2.

Mol, A.C.S., 2007. *Reduction of boundary conditions with Opti.* User manual, draft version. H4959.10 WL | Delft Hydraulics.

Pietrzak, J., 2011. *An introduction to oceanography for civil and offshore engineers.* Lecture notes (draft version) for the course 'Physical oceanography', Delft University of Technology (course code CIE 5317).

Pratap, R., 2006. *Getting started with Matlab7*. A quick introduction for scientists and engineers. Oxford University Press, Inc.. ISBN-13 978-0-19-517937-8

Roelvink, J.A. and Reniers, A., 2012. *A guide to modeling coastal morphology*. Advances in Coastal and Ocean Engineering, volume 12. World Scientific Publishing Co. Pte. Ltd. ISBN-13 978-981-4304-25-2, ISBN-10 981-4304-25-5.

Savenije, H.H.G., 2005. *Salinity and tides in alluvial estuaries*. Elsevier BV. ISBN-13 978-0-444-52108-8

Verhagen, H.J., d'Angremond, K. and Van Roode, F., 2012. *Breakwaters and closure dams*. VSSD. ISBN 978-90-6562-173-3

Van Banning, G., Van Vledder, G. Ph., Bliek, A.J., Jansen, M.H.P. and Dam, G., 2000. *De modellering van de hydro-dynamica in het intergetijdengebied.* Report 00327/1165-A647. Alkyon Hydraulic Consultancy & Research and Svašek Hydraulics.

Van der Kaaij, T. Roelvink, J.A., Kuijper, C., 2004. *Morphological modelling of the Western Scheldt. Intermediate report Phase I*. Report Z3648/A1198. WL | Delft Hydraulics and Alkyon Hydraulic Consultancy & Research.

Van Rijn, L.C., 1993. *Principles of sediment transport in rivers, estuaries and coastal seas*. Aqua publications. ISBN 90-800356-2-9.

Van Vledder, G. Ph., 2007. *Hindcast Westerschelde*. Report A1939R1r2. Alkyon Hydraulic Consultancy & Research

Zijlema, M., 2011. *Computational modelling of flow and transport.* Lecture notes for the course 'Computational modelling of flow and transport, Delft University of Technology (course code CIE4340).

List of figures

List of tables

Appendix 1 Nautical charts

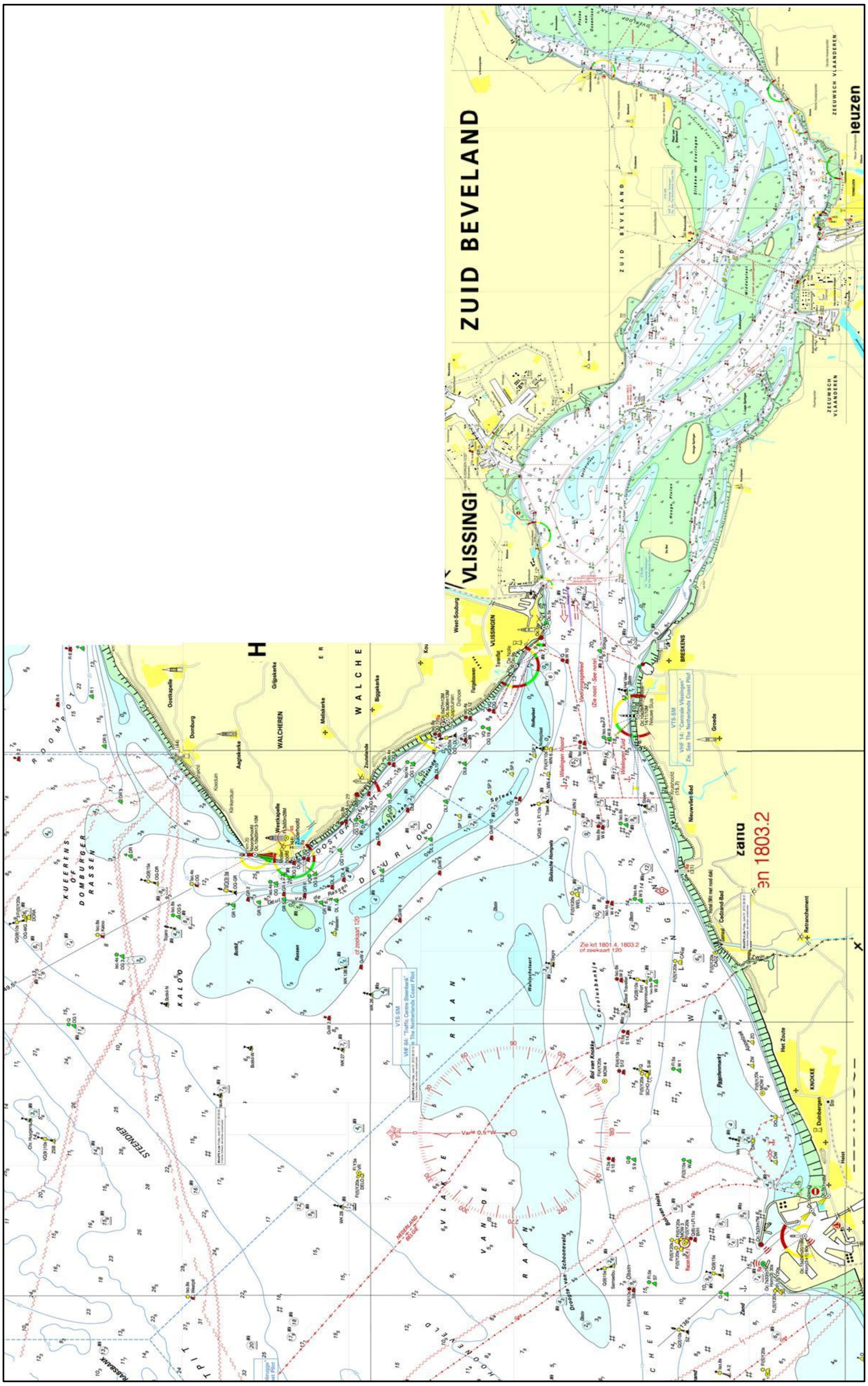

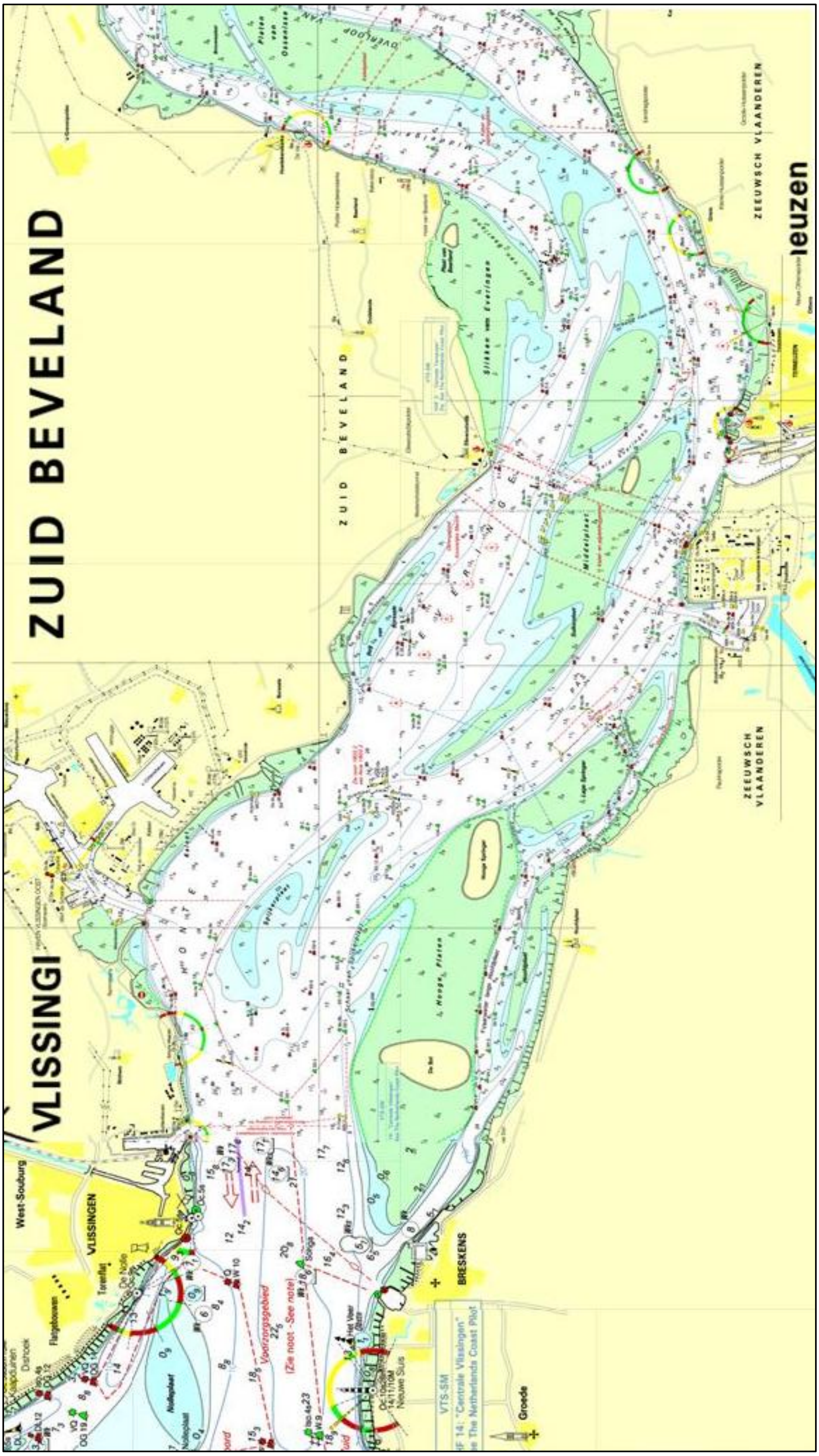
ZUID BEVELAND
VLISSINGEN
BRESKENS
ZEEUWSCH VLAANDEREN
ZUID BEVELAND
ZEEUWSCH VLAANDEREN
West-Souburg
Groede


Westkapelle
Domburg
Oostkapelle
Aagtekerke
WALCHEREN
Zoutelande
Biggekerke
Meliskerke
Grijpskerke
Nieuwvliet-Bad
Groede
Cadzand-Bad
Retranchement
Het Zoute
KNOKKE
Duinbergen
Heist
VLAKTE VAN DE RAAN
RAAN
STEENDIEP
KALOO
Rassen
Walvischstaart
Sluissche Hompels
Bol van Knokke
Paardenmarkt
Droogte van Schooneveld
VTS-SM
VHF 64: "Traffic Centre Steenbank"
VTS-SM
VHF 14: "Centrale Vlissingen"
Zie, See The Netherlands Coast Pilot
zand
1803.2

Appendix 2 Wind and wave climate classes

No.	Wind dir. θ_{wind} (°N)	Wind speed U_{10} (m/s)	Wave height H_{m0} (m)	Wave period T_p (s)	Wave dir. θ_{wave} (°N)	Surge (m)	Weight (%)
1	20.32	3.01	0.61	5.55	353.60	-0.04	2.654
2	21.24	6.52	1.07	5.48	7.45	-0.03	4.307
3	21.54	10.21	2.07	6.54	9.21	0.00	0.902
4	16.47	14.41	3.86	8.33	356.72	0.26	0.029
5	49.45	2.95	0.54	5.42	0.81	-0.06	2.490
6	49.20	6.46	1.01	5.37	23.12	-0.10	3.924
7	49.44	10.53	2.10	6.58	26.60	-0.18	0.799
8	50.00	14.48	3.25	7.72	24.73	-0.35	0.067
9	79.79	2.97	0.55	5.41	9.64	-0.09	2.409
10	79.90	6.37	0.93	5.24	41.01	-0.17	3.581
11	80.25	10.39	1.78	6.12	49.22	-0.38	0.741
12	74.29	14.00	2.66	6.85	42.25	-0.43	0.012
13	110.67	3.04	0.49	5.28	15.85	-0.10	2.722
14	109.55	6.31	0.74	4.74	76.64	-0.19	3.104
15	106.35	10.27	1.46	5.50	87.51	-0.43	0.323
16	100.00	14.22	2.29	6.42	78.60	-0.77	0.009
17	139.53	3.01	0.46	5.23	352.85	-0.08	2.481
18	140.12	6.14	0.61	4.51	139.25	-0.13	2.349
19	142.17	10.15	1.21	5.02	158.75	-0.21	0.197
20	170.35	3.03	0.48	5.19	270.19	-0.06	2.402
21	172.05	6.35	0.75	4.72	201.30	-0.08	3.338
22	174.33	10.27	1.47	5.47	197.67	-0.19	0.719
23	178.13	14.35	2.41	6.54	203.63	-0.40	0.027
24	199.89	3.00	0.51	5.23	277.25	-0.04	2.752
25	200.52	6.73	0.92	5.00	223.91	-0.03	5.796
26	201.69	10.56	1.72	5.92	219.23	-0.03	3.258
27	203.74	14.79	2.71	6.97	221.76	-0.08	0.279
28	206.67	18.97	3.77	7.63	205.05	-0.22	0.005
29	230.29	3.04	0.54	5.23	283.95	-0.02	3.020
30	230.76	6.79	0.99	5.18	242.37	0.03	7.065
31	231.36	10.71	1.88	6.22	231.46	0.10	5.031
32	231.94	14.70	2.90	7.27	229.60	0.16	0.548
33	233.33	19.01	3.89	8.22	227.41	0.22	0.026
34	259.32	3.07	0.60	5.34	297.10	0.01	2.659
35	258.22	6.69	1.07	5.36	262.01	0.08	5.806
36	258.14	10.62	2.04	6.47	249.69	0.23	2.793
37	259.31	15.03	3.26	7.85	247.17	0.47	0.346
38	258.00	18.90	3.78	7.93	223.97	0.78	0.009

No.	Wind dir. θ_{wind} (°N)	Wind speed U_{10} (m/s)	Wave height H_{m0} (m)	Wave period T_p (s)	Wave dir. θ_{wave} (°N)	Surge (m)	Weight (%)
39	260.00	23.40	5.05	9.36	249.00	1.06	0.002
40	289.65	2.93	0.67	5.51	313.99	0.01	2.281
41	289.09	6.72	1.28	5.75	295.03	0.15	3.530
42	289.03	10.78	2.38	6.95	285.37	0.42	2.074
43	288.22	14.84	3.53	8.07	273.98	0.78	0.366
44	281.25	18.75	4.50	8.78	268.50	0.87	0.014
45	319.78	2.95	0.68	5.58	329.39	0.00	2.250
46	320.01	6.74	1.35	5.97	325.46	0.16	2.726
47	319.27	10.67	2.45	7.11	321.08	0.43	1.131
48	316.43	14.65	3.78	8.48	313.84	0.87	0.168
49	320.00	19.38	5.16	9.62	308.93	1.43	0.005
50	350.09	2.96	0.66	5.63	344.11	-0.02	2.360
51	350.09	6.64	1.31	5.92	346.50	0.07	3.078
52	349.61	10.56	2.48	7.17	344.09	0.30	0.960
53	348.64	14.74	3.90	8.58	335.62	0.77	0.075
54	340.00	18.13	4.85	10.27	339.00	1.15	0.002

Table 22. Wind and wave classes.

Appendix 3 Figures chapter 3

Figure 66. Settings FLOW and WAVE module Delft3D

Figure 67. Settings MOR module Delft3D

Appendix 4 Figures chapter 4

Figure 68. Location calculation grid and measurement locations

Figure 69. Wind rose with numbered classes

Figure 70. Winter climate 1981 – 2001, location Schouwenbank

Figure 71. Summer climate 1981 – 2001, location Schouwenbank

Figure 72. Beaufort wind scale

Figure 73. Full time series wind and wave 1981 – 2001

Figure 74. Scatterplot wind and wave conditions 1

Figure 75. Scatterplot wind and wave conditions 2

Figure 76. Scatterplot wind and wave conditions 3

Figure 77. Imposed wind and wave conditions wave modelling

Figure 78. scatterplots and table measured and simulated, Dora

Figure 79. Scatterplots and table measured and simulated, Scheur West

Figure 80.Scatterplots and table measured and simulated, Deurloo

Figure 81. Scatterplots and table measured and simulated, Wielingen

Figure 82. Scatterplots and table measured and simulated, WCT

Figure 83. Scatterplots and table measured and simulated, Hoofdplaat

Figure 84. Scatterplots and table measured and simulated, PVT

Figure 85. Time series influence model choices, outside estuary, H_{m0}

Figure 86. Time series influence model choices, inside estuary, H_{m0}

Figure 87. Time series influence model choices, outside estuary, T_p (T_{m02})

Figure 88. Time series influence model choices, inside estuary, T_p (T_{m02})

Figure 89. Time series influence model choices, outside estuary, T_p ($T_{m-1.0}$)

Figure 90. Time series influence model choices, inside estuary, T_p ($T_{m-1.0}$)

Figure 91. Time series influence physics 15,16,17 outside estuary, H_{m0}

Figure 92. Time series influence physics 15,16,17 inside estuary, H_{m0}

Figure 93.Time series influence physics 15,16,17 outside estuary, T_p

Figure 94. Time series influence physics 15,16,17 inside estuary, T_p

Appendix 5 Figures chapter 5

Appendix 6 Figures chapter 6